PALEOFLOOD HYDROLOGICAL ANALYSIS OF SELECTED SOUTH AFRICAN RIVERS

Peter K Zawada
Johan Hattingh
Dirk van Bladeren

Report to the
WATER RESEARCH COMMISSION
by
COUNCIL FOR GEOSCIENCE
WRC Report No 509/1/96
ISBN 1 86845 240 9

ACKNOWLEDGEMENTS

This study would not have been possible without the cooperation of the following organisations and individuals:

The Council for Geoscience, the Water Research Commission and the Department of Water Affairs and Forestry are gratefully acknowledged for their financial and logistical support for this project.

Many thanks go to Dirk van Bladeren for his assistance in organising and supervising the slope-area surveys across the Orange River which were done in cooperation with the Bloemfontein and south-western Cape regional survey offices of the Department of Water Affairs and Forestry. Dirk's assistance in completing the flood-frequency analysis for the Orange River is gratefully acknowledged.

Dr J. Vogel and his laboratory personnel in providing radiocarbon, thermoluminescence and infra-red stimulated luminescence dates for the Orange River slack-water sediments is much appreciated.

TransHex (Pty) Ltd, Namdeb Diamond Corporation (Pty) Ltd and the landowners in the Prieska region of the Orange River are thanked for their permission to study the palaeoflood sediments on their respective properties.

EXECUTIVE SUMMARY

The development and evolution of palaeoflood hydrology from the status of a research-based technique to an applied one has occurred, mainly in the United States, over a period of nearly 20 years. In contrast, South Africa's geologists, geomorphologists and hydrologists have largely ignored this technique, neither appreciating its applied value in flood forecasting, nor its application to fluvial sedimentology, geomorphology and palaeoclimatology for the Southern African region as a whole. In recognising the need to develop palaeoflood hydrological expertise in Southern Africa, with the objective of establishing it as a complementary applied tool in the important field of water resource management, a three-fold approach has been adopted in this study.

(1) An inventory of the types and characteristics of palaeoflood evidence that exist from differing climatic regions of the country was established in order to show that certain regions of South Africa are well suited to applying palaeoflood hydrology.

(2) Detailed palaeoflood hydrological analysis of the middle and lower reaches of the Orange River has shown that this technique yields flood information which would be overlooked or inaccessible during conventional hydrological investigations.

(3) Palaeoflood records represent an important source of proxy palaeoclimatic data that can be used to verify and refine the Holocene palaeoclimate change models for southern Africa.

A reconnaissance investigation of 67 potential palaeoflood sites for 8 major rivers has identified several types of palaeoflood hydrological evidence. The potential for constructing palaeoflood stratigraphies at 49 slack-water sites was assessed in terms of their biogenic reworking and the mean annual rainfall at the site. The Orange Free State, the Cape Province north of the Cape Mountains, and the Cape Mountains from Port Elizabeth westward to Cape Town and northward to approximately latitude 33° south are most suited for palaeoflood hydrological analysis using slack-water sediments.

A detailed palaeoflood hydrological analysis in bedrock-controlled reaches for the middle (Prieska) and lower reaches (Richtersveld) of the Orange River was completed using 5 sites comprising slack-water sediments in back-flooded tributaries. For each site detailed sedimentological analyses of the slack-water sequences were made, to ensure the confident differentiation between palaeoflood and non-

palaeoflood deposited sediments, and to gain a better understanding of the sedimentation dynamics during slack-water deposition. A total of 43 palaeoflood slack-water units were identified from the 5 sites. For the middle reach of the Orange River (Prieska) the three sites each comprised an average of 6 flood units, whereas the two sites for the lower Orange River (Richtersveld) comprised 9 and 6 flood units.

In addition to detailed outcrop descriptions, the well-established technique of relief peels was applied to the fine- to very fine-grained Orange River slack-water sediments. Detailed examination of 50 relief peels representing an accumulated thickness of approximately 25 m showed that this technique is a useful, and in some cases, indispensable aid in the description and interpretation of palaeoflood deposits. Relief peels represent a new approach to the study of slack-water sediments which assisted the hydrodynamic interpretation of slack-water deposition and the accurate differentiation of palaeoflood-deposited units.

Palaeodischarge estimates based on the maximum elevation of the flood units indicate that the palaeoflood sequences of the middle and lower reaches of the Orange River represent two ranges of palaeodischarge. At Prieska the range varies from 2 660 m^3/s - 13 080 m^3/s whereas the Richtersveld sites record a range of 5 580 m^3/s - 27 870 m^3/s. A total of 39 age determinations of slack-water sediments and several interbedded non-palaeoflood sediments using a combination of radiocarbon TL and IRSL were obtained. The dating results also indicate that the palaeoflood sequences of the middle and lower Orange River cover two ranges of ages. The Prieska sites exhibit a range from 12 400 ±2 480 years (IRSL date) to 120 ±15 years B.P. (radiocarbon date), whereas the Richtersveld sites exhibit an age range from 5 440 ±1 090 years (IRSL date) to 210 ±50 years B.P. (radiocarbon date). In terms of the number of palaeoflood units identified, their respective palaeodischarges and their ages, the palaeoflood sequences of the middle reach of the Orange River are markedly different from those of the lower Orange River.

The lower Orange River has experienced 13 palaeofloods with discharges in the range of approximately 10 200 m^3/s - 14 660 m^3/s during the last 5 500 years. These discharges are considerably larger than the largest historically documented or gauged discharge of 8 330 m^3/s in 1974 at Vioolsdrift and therefore represents additional flood information for the lower Orange River. In addition, slack-water sediments representing a flood with a discharge of approximately 28 000 m^3/s were recorded at both sites. This flood was over three times the discharge of the largest historically recorded or gauged flood and is therefore regarded and termed as a catastrophic flood. Furthermore, this flood is almost twice the discharge of 16 000 m^3/s recorded for the Mfolozi River in 1984, which represents the largest recorded flood in South Africa. Of further importance is that three radiocarbon dates indicate that the catastrophic flood recorded from the lower Orange River occurred relatively recently

in the period after A.D. 1444 - A.D. 1462.

Flood-frequency analysis of the lower Orange River using the systematic gauge record for the period 1933 - 1992 indicates that the return period for the catastrophic flood varies between 200 years to greater than 10 000 years, depending on which probability distribution function is employed. However, flood-frequency analysis using the systematic record and the discharge and date of occurrence of the catastrophic flood yields a more consistent and acceptable return period of approximately 1 000 years using the Log Pearson Type 3 (LP3) probability distribution function. Similarly, incorporating the palaeoflood record that comprises nine palaeofloods with the systematic record yielded a return period of 1 000 years for the catastrophic flood. The minimal effect on the return period of incorporating the palaeoflood record with the systematic record for the catastrophic flood indicates that the systematic record for the lower Orange River is a representative record in terms of discharges and the time span over which flow gauging occurred. A further conclusion is that the inclusion of the smaller palaeofloods does not appreciably influence the return period of the catastrophic flood using the LP3 distribution. This indicates that a knowledge of only the largest palaeoflood is crucial for verifying conventional flood-frequency estimates. Flood-frequency analysis of the lower Orange River has also indicated that the inclusion of only the largest palaeoflood is valuable for assessing and identifying the most appropriate probability distribution function.

The palaeoflood record of the lower Orange River has been interpreted as a series of exceeded thresholds or changing flood thresholds through time. Plotting discharge as an index of magnitude against age of the palaeoflood units indicates that the palaeoflood record of the lower Orange River can be subdivided into 4 palaeoflood periods, each being characterised by a threshold discharge value. Period 1 is approximately 3 650 years long, from 1 800 ±360 years B.P. to 5 450 ±1 090 years B.P., during which the lower Orange River did not experience a flood that exceeded the threshold discharge of 12 800 m^3/s. Of further significance is the occurrence of several floods in relatively quick succession over a period of 650 years from 4 770 ±70 years B.P. to 4 120 ±160 years B.P. Period 2 represents a period of 400 years from A.D. 961 - A.D. 1332, during which the lower Orange River did not exceed the threshold discharge of approximately 14 700 m^3/s. Period 3 includes the catastrophic flood with a discharge of approximately 28 000 m^3/s. During the period A.D. 1453 - A.D. 1785 the lower Orange River did not exceed the maximum threshold discharge of approximately 28 000 m^3/s. Period 4 extends from A.D. 1785 till the present during which the lower Orange River did not exceed the threshold discharge of 9 500 m^3/s.

The lower Orange River palaeoflood record has been interpreted as a series of exceeded thresholds which were hydroclimatically controlled. Four periods of

increased flooding in terms of discharge correlate with periods of increased temperature and rainfall based on other proxy climatic data for southern Africa. Periodic adjustments of the tropical circulation system over the subcontinent is the most likely explanation for this correlation. A partial correlation also exists with the neoglacial episodes recorded in southern South America for the periods 4 500 - 4000 years B.P and for the last 1 000 years. The development of large cyclonic frontal systems over the summer rainfall region during these episodes may have been responsible for producing the catastrophic flood.

It is suggested that the lower Orange River could, in the present hydroclimatic regime, experience a catastrophic flood with a discharge of approximately 28 000 m^3/s. This conclusion is based, firstly, on the similarity of the catastrophic discharge to the discharges calculated using the Francou-Rodier method of regional maximum flood estimation. This indicates that the palaeoflood information supports the accuracy of the RMF method of peak-flood estimation for the Orange River. Secondly, the 1 000 year return period obtained for the catastrophic flood suggests that this flood is not an extremely rare phenomenon and may be significant for high-risk projects such as nuclear power plants or very large dams, where failure would have catastrophic consequences. Thirdly, the correlation between increased flooding and increased temperature during the past 5 500 years with the observation that there has been gradual warming since the end of the Little Ice Age (A.D. 1850), suggests that the present hydroclimate is approaching or has attained conditions that could result in the lower Orange River experiencing a flood with a 28 000 m^3/s discharge.

Palaeoflood hydrological analysis of the Prieska sites has been disappointing when compared with the results obtained from the lower Orange River. For example, the correlation of individual flood units between sites proved difficult due to extensive reworking of several of the basal flood units, possible errors in the surveying of cross sections and the difficulty experienced in collecting sufficient quantities of organic material for radiocarbon dating. IRSL and TL dating of the slack-water sediments was therefore done to augment the radiocarbon dates, but in most cases yielded conflicting results. Palaeodischarge modelling of the flood units at Prieska yielded a range of discharges from approximately 2 660 m^3/s - 13 080 m^3/s. The ranges at the different sites varied from 3 040 m^3/s - 11 260 m^3/s at site 19, 2 480 m^3/s - 13 080 m^3/s at site 9 and 2 760 m^3/s - 9 000 m^3/s at site 14. Although the Prieska palaeoflood record did not record the effect of relatively large floods, even those that were historically recorded, the following conclusions regarding the smaller palaeofloods were made:

(1) The basal portion of the palaeoflood stratigraphy at all three sites indicates that the Orange River experienced a series of floods with discharges of between approximately 2 500 m^3/s - 4 000 m^3/s. Radiocarbon and IRSL dating

indicates that these floods occurred between approximately 7 000 years B.P. - 12 500 years B.P.

(2) A flood with a discharge of approximately 4 440 m^3/s occurred 500 ±90 years B.P., which corresponds to the most probable calibrated age of A.D. 1440 (flood unit F4, site 19). This indicates that the overlying palaeoflood units F5 and F6 with respective discharges of 5 050 m^3/s and 9 030 m^3/s were deposited after A.D. 1440.

Difficulty was experienced in collecting sufficient quantities of uncontaminated organic material from the slack-water sediments for radiocarbon dating. A combination of thermoluminescence (TL), infra-red stimulated luminescence (IRSL) and radiocarbon dating techniques was therefore used. The TL dating yielded older dates than the radiocarbon dates. The IRSL dates followed the stratigraphy, were younger than the TL dates but were still older than the radiocarbon dates. Although IRSL dating of slack-water sediments is more accurate than TL dating, problems still exist with residual luminescence. This is attributed to the very fine-grained texture of the sediments and the insufficient resetting or exposure of the sediment to the sunlight during turbid flood conditions.

A preliminary mineralogical analysis of the Orange River slack-water sediments indicates that they are compositionally similar at any particular site, as well as between sites and between the middle and lower reaches of the Orange River. The predominance of smectite indicates that the large palaeofloods documented for the lower Orange River for the past 5 000 years may have been generated in the upper and middle portions of the Orange River catchment with a minor contribution from the lower reaches.

Recommendations for future palaeoflood hydrological studies include:

(1) The completion of detailed palaeoflood hydrological investigations for the major rivers in Kwa-Zulu/Natal such as the Mzimvubu, Mzimkulu, Mkomazi, Umvoti, Tugela, Mgeni, Mfolozi, Mkuze and the Pongola Rivers.

(2) Completion of detailed palaeoflood hydrological analysis of other major rivers in South Africa such as the Limpopo, the Orange River at proposed dam sites at Vioolsdrift, Boegoeberg and Pella and the larger rivers in the lowveld such as the Komati, Letaba and the Olifants River.

CONTENTS

APPENDICES

FIGURE CAPTIONS

TABLE CAPTIONS

1. INTRODUCTION

This chapter gives an overview of the flood problem both globally and nationally with an evaluation of the common flood-prediction methods employed by hydrologists in South Africa. It will be shown that a need exists to incorporate Holocene palaeoflood records to extend the period of flood observation. The chapter concludes with the aims and objectives of this study.

1.1 The flood problem

> "Estimating the probabilities of extreme floods is an important and challenging problem. It is important because the stakes are high: very large floods kill people and destroy property, and the cost incurred in attempting to avoid these damages can be great. The probabilities that such floods will occur during the life of a particular project are a crucial part of the analytical input for making decisions about that project" (Water Science and Technology Board, p. viii, 1988).

The enormity of the flood problem was acknowledged by the American Meteorological Society (1978) who stated that flash floods now rank as the most destructive weather-related natural hazard in the U.S. This contention is supported by statistics indicating that between 1973 and 1979, 80% of the 193 declared national disasters by the U.S. President were flood related (Lundgren, 1986). In terms of loss of life, U.S. figures show that the annual average death toll from floods since 1968 has risen to approximately 200. This represents a two-fold and three-fold increase when compared to the 1960's and 1940's respectively (Costa and Baker, 1981). Annual average economic costs for the U.S was estimated to be 3,8 billion dollars (Platt, 1979). Worldwide losses as a result of floods are staggering when measured in terms of deaths of which a selection is presented in Table 1.1. Lundgren (1986) reported that during the period 1947 - 1967, 154 000 lives were lost in Asia (excluding Russia) and 10 540 lives lost in Europe (excluding Russia). Shah (1983) also reported that between 1947 - 1980, 194 000 lives were lost due to flooding that was not associated with tropical cyclones, hurricanes and typhoons.

Although South Africa has not experienced major flood disasters on the scale of

those presented in Table 1.1, it has nonetheless experienced severe floods. For example, during the period 1973 - 1988, over 1 000 deaths were flood related (Alexander, 1988). In addition, Van Heerden (1990) in an analysis of flooding for the period 1911 - 1988 found that on average South Africa experienced two destructive floods per annum.

Year	Region	Deaths
1887[1]	Hwang-ho River, China	800 000
1970[2]	Bangladesh	300 000 - 500 000
1642[1]	China	300 000
1939[1]	Northern China	200 000
1911[1]	Yangtze River, China	100 000
1960[1]	East Pakistan	10 000
1963[1]	Vaiont, Italy	2 600
1889[1]	Johnstown, Pennsylvania	2 100
1953[1]	Northern Europe	2 000
1988[3]	Bangladesh	2 000
1988[4]	Southern Thailand	373
1972[1]	Rapid City, South Dakota	232
1987[5]	Natal, South Africa	200
1976[1]	Big Thompson Canyon, Colorado	139
1972[1]	Eastern United States (Hurricane Agnes)	118
1966[1]	Arno Valley, Italy	113
1981[6]	Laingsburg, South Africa	104

Data sources: [1]Costa and Baker (1981); [2]Frank and Husain (1971); [3]Bingham (1989); [4]Nutalaya (1989); [5]Fourie (1990); [6]Marais (1981).

Table 1.1 - A selection of major flood disasters.

It is clear that although floods have always posed a threat to man in terms of loss of life and damage to property, a perception exists amongst the public that floods occur randomly with seemingly little hope of predicting their magnitude both spatially and temporally. Baker (1993) went further to suggest that although much research has

gone into the development of sophisticated techniques, we are still suffering an increasing damage to life and property due to catastrophic floods. Despite the acknowledgment by hydrologists that very real difficulties exist in assessing the risk of large magnitude flood events (Snell, 1990), it is nevertheless a statutory requirement in South Africa that this assessment is done in all cases where development is potentially at risk from flooding. This has placed the hydrologist and practitioners of flood-risk assessment in an unenviable position where estimation of peak-runoff flows and recurrence must be calculated with the knowledge that flood records in South Africa are short and in many instances absent, resulting in predicted peak runoff flows exhibiting high margins of error (see section 1.2 for a detailed discussion of conventional flood-peak estimation methodologies adopted by hydrologists). Increasing development in flood-prone areas has resulted in a need to improve our understanding and predictive abilities with respect to flood-peak estimation. However, it is acknowledged that because of short flood-peak records, great difficulties exist in confidently ascertaining flood-peak estimates upon which floodplain zonation policies can be formulated and employed to mitigate the effects of flood-related damage. Realising these difficulties, this report will contend that an important and untapped source of data from the Holocene stratigraphic record can be used to extend the flood-peak record.

1.2 Current status of flood prediction in South Africa

In South Africa the estimation of flood-peaks has primarily been the concern of the hydrologist. Current estimation techniques fall in one of three methodological categories (Kovács, 1988). In the following three sections, a critical review of the techniques used in South Africa is presented. This will provide an overview or conceptual framework into which the aim of this study namely, justifying the validity of Holocene palaeoflood-hydrological data, can be incorporated.

1.2.1 Deterministic methods

The principal assumption underpinning deterministic methods (chance independent) in flood-peak estimation is that the annual exceedance probability (AEP) of the resultant flood is the same or is dependent on the causative rainfall (Alexander, 1990a). This relationship can be expressed in the following simple equation:

$$Q = C\ I\ A$$

where the variable:

Q represents discharge
C represents the runoff coefficient
I represents the rainfall intensity
A represents the area of the catchment.

Specifically, the magnitude of a flood is a function of the following variables:

- Storm-rainfall properties (variable I) such as the depth-duration-frequency relationship of point rainfall and the relationship between point rainfall and rainfall over the catchment (Alexander, 1990a).
- Catchment characteristics such as area, slope, soil permeability and vegetation cover (variables A and C) .
- Catchment processes which control the conversion of rainfall into runoff such as inception, infiltration and sub-surface movement of water (variable C).
- Antecedent conditions which modify the catchment processes such as antecedent rainfall and antecedent river flow (variable C).

In reality it is difficult to estimate the temporal and spatial variation of storm rainfall across the entire catchment from rainfall gauging data. Therefore the characteristics of a storm rainfall must be derived from what Alexander (1990a) termed a qualitative understanding of the meteorological processes that produce the rain. To calculate the magnitude of a flood for a particular catchment requires therefore, the transposition of a historically recorded storm exhibiting spatial and temporal characteristics over the catchment area exhibiting certain characteristics that modify the conversion of storm rainfall to river discharge.

The major advantage of deterministic methods in flood-peak estimation is in attempting to understand and integrate the many variables that control runoff. It is an attempt to understand the flood-producing system on a holistic level. Kovács (1988), a proponent of empirical methods, stated that although this holistic approach to flood-peak estimation has merit, some of the variables such as the storm rainfall areal reduction factor, transposition of storms, storm loss and the validity of unit-graph principles during extreme flood conditions are either imprecisely known and/or

represent as yet unverified hypotheses. Consequently, the error of flood-peak estimation may even reach the magnitude of the probable maximum flood (PMF) itself (Kovács, 1988). Kovács (1988) supported this claim by referring to a flood-peak estimation study of over 100 dam sites in South Africa by the Department of Water Affairs and Forestry (DWAF) using deterministic methods which yielded grossly unrealistic and inconsistent figures. Alexander (1990b) also recognised these uncertainties, stating that deterministic methods exhibit the problem of dimensionality, where, unless a precise understanding of the interaction between independent variables exists, the inclusion of additional variables will actually decrease the accuracy of the prediction. A further problem associated with deterministic methods is the inability to derive the annual exceedance probability of a flood because the depth-area-duration-frequency of the storm rainfall and the probability characteristics of the storm rainfall-runoff process in unknown (Alexander and Kovács, 1988).

1.2.2 Statistical methods

Fig. 1.1 illustrates the statistical method of flood-peak estimation where an attempt is made to predict the tail of the probability distribution from an annual peak-flood series (normally comprising flow-gauge data). The method involves applying a best-fit probability-distribution curve to the relative cumulative frequencies of the annual peak-flood series. Although a number of probability distributions exist, the log-Pearson type III is the most commonly applied one for hydrological analyses in South Africa as it seems to fit most hydrological data sets (Alexander, 1990a). The log-Pearson type III distribution is also widely adopted by federal agencies in the U.S. (Kochel, 1980) and is recommended by the U.S. Water Resources Council (1976) and the Water Science and Technology Board (1988).

Because the log-Pearson type III probability distribution is a log-normal distribution, it plots on log-probability paper as a straight line. This makes it theoretically possible to extrapolate the distribution line to ascertain the flood exceedance probabilities and discharges of large magnitude flood events. The statistical method is dependent however, on three principal assumptions which are examined in the following section.

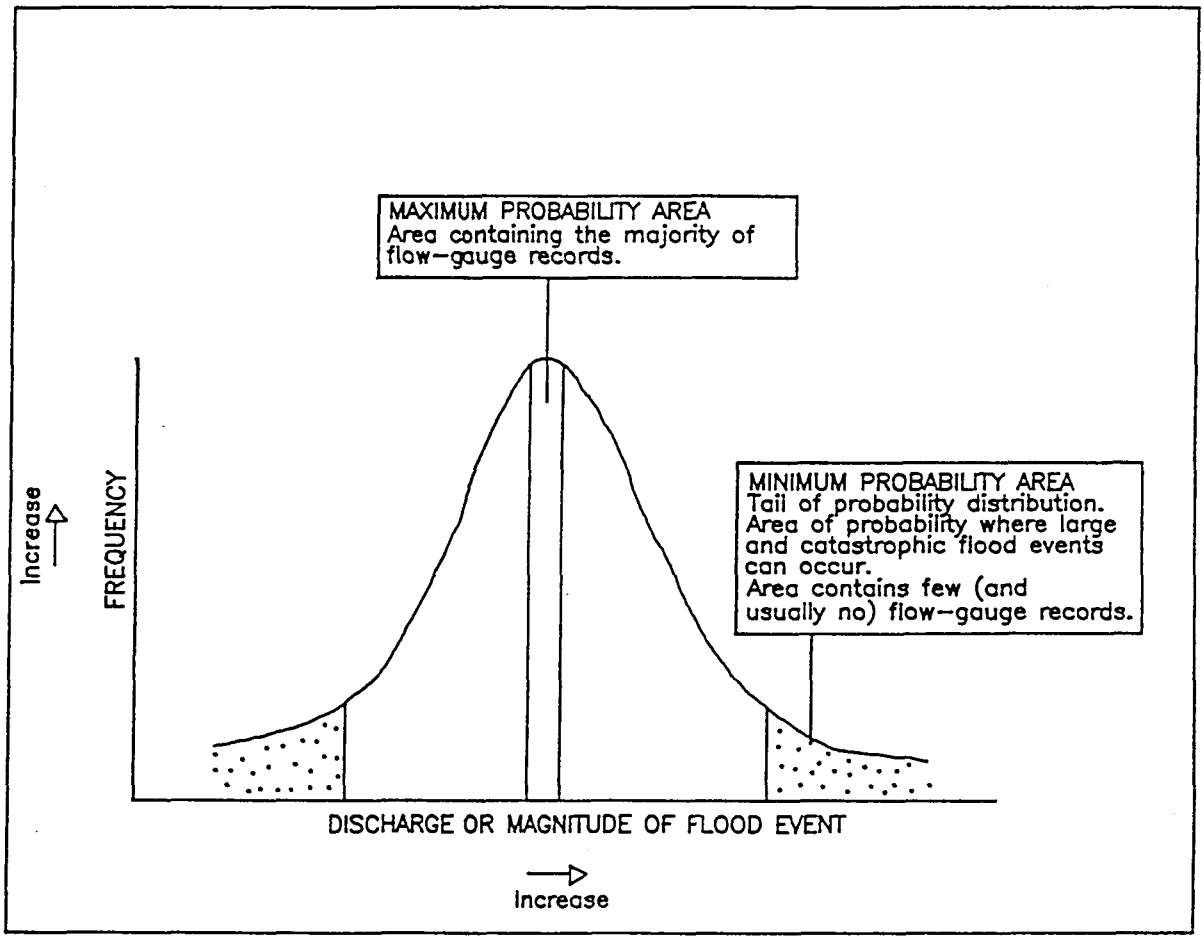

Fig. 1.1 - A typical frequency distribution based on an annual flood-peak series from which the return periods of large or catastrophic floods are calculated. Note that the tail of the probability distribution to the right of the figure is based on in many instances little or no flow-gauge data.

Assumption 1. Each annual flood-peak value in the annual series is independent of the previous and subsequent one. This was alternatively stated by Klemeš (1988, p. 45) that hydrological processes are assumed to be "realizations of an ergodic stochastic process". Although Alexander (1990a) regarded this assumption to be acceptable for annual flood maxima, Klemeš (1988) disagreed, stating that no basis exists for supposing that hydrological phenomena (including annual flood maxima) have a random distribution. He considered it as equally likely that hydrological processes have proceeded in a particular direction and may or may not continue to do so in the future.

Assumption 2. The data are comprehensive and free of measurement error. Currently, most flow-gauge data in South Africa are managed by the DWAF using the Hydrological Information System (Van Wyk et al., 1990). The accuracy of the flow-gauge record is dependent on four main factors (Van Wyk et al., 1990), namely, the continuity of the time series; the range of readings covered by the record; how well the readings have been recorded; and how well the flow-gauge station is calibrated. Van Wyk et al. (1990) observed that most of the gaps existing in the South African flow-gauge records are due to high flood flows. This is attributed to only 27 of the 1 180 gauging stations in the country being calibrated and designed to measure flow stages in excess of 10 m. The range of flow data is, according to Adamson (1975), a critical factor when attempting to establish a reasonable estimate of the mean and variance of an annual flood series. According to Adamson (1975) the range of readings must not be shorter than 50 years. Muller (1978) reached a similar conclusion stating that 40 years is a minimum length of an annual flood series from which reasonable flood forecasts can be made. It is therefore important to note that of the flow gauge stations under the control of the DWAF, 166 stations have flow records longer than 30 years, 127 have flow records of at least 40 years and 39 stations with at least 50 years of record. The longest flow-gauge record is approximately 80 years (Van Wyk et al., 1990). Alexander (1990a) recognised possible data errors in flow-gauge data, stating that it is particularly important to check for systematic errors where the design of a major structure is involved. It is difficult, however, to assess the quality of flow-gauge data because there has never been an in-depth quality analysis of the data in South Africa (Van Wyk et al., 1990).

Assumption 3. The annual flood-peak series is a reliable and representative sample (in time) of random and homogenous events. This is a critical assumption hydrologists have made in order to justify stochastic models as predictors of flood magnitude and frequency (Baker, 1987b). As already stated, Klemeš (1988) has questioned the basis of randomness on which hydrological models are supposed to operate. Further possible violations of assumption 3 can occur in the following two ways:

(1) The conventional flood record may not be representative of all the major flood-producing weather systems. In the case of southern Africa, these would include tropical cyclones, cut-off lows, tropical weather systems, intense cyclonic and mid-latitude as well as mesoscale convective systems. Alexander (1990a) also recognised this violation stating that a strong possibility exists that many of the apparent anomalies in statistical analyses stem from the mixture of differing meteorological conditions. This observation indicates the possibility of serious flood-peak estimation errors where a short and possibly unrepresentative gauging record (South Africa has an average of 30 years; Alexander, 1990a; Kovacs, 1988) is used from which extrapolation to obtain the magnitude of the 1:200 year or greater flood event is made. Kochel (1980) provided an example of the unrepresentativeness of the flood-peak record for the Pecos River, Texas. In 1954 and 1974 catastrophic floods with discharges of 27 400 m^3/s and 16 100 m^3/s were recorded respectively. The 1954 discharge was almost 9 times larger than the largest historically recorded flood and was the result of Hurricane Alice being centred over the Pecos and Devils River catchments. According to Kochel (1980) extrapolation of the 55 year long annual flood-peak series, including the 1954 and 1974 outliers, yielded a 78 year recurrence interval for the 1954 flood, which according to Kochel (1980) is unrealistically low. Conversely, a simple extrapolation excluding the 1954 and 1974 floods yielded a recurrence interval of several tens of thousands of years, which Kochel (1980) interpreted as being absurd. A similar, but less dramatic example illustrating the problems associated with extrapolating from unrepresentative annual flood-peak series is the Domoina floods of Natal which occurred in January-February 1984. The weather system responsible for these floods was the tropical cyclone Domoina that tracked southward through southern Mozambique, Swaziland and north-eastern South

Africa (Alexander and Kovács, 1988). Three weeks later a second cyclone Imboa tracked southwards but further to the east, which also resulted in flooding. Both of these cyclones were unusual, firstly because they resulted in floods that were the largest ever recorded up till that time, and secondly, because of their rarity in a region that had only recorded eight cyclones in the past 34 years. Furthermore, Domoina and Imboa were the only cyclones to have tracked so far southward. Flood-peak frequency analysis by Alexander and Kovacs, (1988) using the log-Pearson distribution based on only the 33 years of flow-gauge data yielded a recurrence interval of 400 years. In contrast, including the flood peaks of Domoina and Imboa reduced the return period to slightly less than 100 years. A similar example which illustrates the dramatic effect that previously unrecorded storm-rainfall events can have on peak flood return-period estimates is the Buffels River, Laingsburg (chapter 4, section 4.3). In this example, the apparently unusual meteorological conditions were due to a cut-off low system centred over a previously saturated catchment.

(2) Climate is not constant through time. Oxygen isotope analysis of speleothems, mollusc remains, foraminiferal studies, palynological and micromammalian research has documented the existence of climate change for the southern African subcontinent for the past 2 000 years (Tyson and Lindesay, 1992). In particular, cooler and drier conditions prevailed from 1300 A.D. to 1850 A.D. (Little Ice Age) with a warm period between 1500 A.D. and 1675 A.D. (Tyson and Lindesay, 1992). Because the hydrological regime varies in response to climate change (Barron et al. 1989), these relatively recent changes of climate would therefore nullify the assumption of representative and homogenous events. This would especially apply where a 30 year-long flow-gauge record is used to extrapolate the recurrence and magnitude of the 1:200 year flood and certainly the 1:1 000 year flood, which according to Klemeš (1988) is a common planning request for certain high-risk projects.

Alexander (1990a), a protagonist of statistical methods, stated that these methods represent the most powerful tools for estimating flood-peak discharges. He acknowledged, however, that because extreme floods are often the product of rare meteorological conditions, the assumption that annual flood peaks form part of a

single population is inappropriate (Alexander and Kovács, 1988). According to Alexander and Kovács (1988) extreme flood prediction should therefore place a greater emphasis on local, regional and world observed flood maxima as guidelines to flood design rather than the statistical and deterministic methods. In a similar vein, Costa and Baker (1981) claimed that because the basin characteristics such as soil, geology, morphology and vegetation affect the flood magnitude and probability both spatially and temporally, there is little reason to believe that a universally applicable stochastic flood forecast model exists.

1.2.3 Empirical methods

Because of limitations in statistical and deterministic methods in flood-peak estimation for long return flood intervals up to the probable maximum flood (PMF), there has been a recent tendency to apply empirical techniques using maximum-recorded flood-envelope curves on a world-wide basis. Kovács (1988; 1990) stated that stochastic models imply that the concept of an absolute maximum flood which is so important to the design of structures, defies an acceptable scientific definition because in theory a catchment area does not exhibit an upper limiting flood. Similarly, Alexander (1990b) concluded that the analyst will never know if a PMF determination is either unrealistically low or high, because in Alexander's words "...thePMF doesn't exist!" (Alexander, 1990b; p. 10). This assumption has, however, been recently challenged by Enzel et al. (1993) using historical and palaeoflood data for the Colorado River catchment. Their study showed that the inclusion of palaeoflood data, which in some cases exhibited discharges far in excess of the historically recorded floods, did not exceed the upper bound of maximum flood discharges as delineated by the maximum flood-envelope curve. This would imply that catchments do indeed exhibit a natural upper bound in terms of flood magnitude.

In view of the stochastic limitations in estimating large or probable maximum floods, Kovács concluded that the merit of a particular flood-estimation method, should not be assessed in terms of its apparent sophistication and "...amount of theory..." but rather by the "...consistency of results and their compatibility with observed values" (Kovács, 1990; p. 2). This led Kovács (1980) to apply empirical techniques in order to establish realistic maximum floods that could occur for the southern African region.

The basis for developing an empirical approach in estimating the regional maximum flood (RMF) is contained in the contrasting definitions of the RMF and the PMF. The RMF is defined as an upper envelope of floods that have occurred in a region. Alexander (1990a) further stated that the RMF is therefore a realistic lower limit of the maximum flood that can be reasonably expected. It is important to note that the RMF is based on observed maximum floods. In contrast, the PMF is an estimate of the largest flood that could occur based on modelling maximum rainfall events over a catchment region. An important advantage of the RMF method is its emphasis on recording and documenting the tail of the peak-flood probability distribution (Fig. 1.1) from which an empirically derived maximum flood limit can be defined.

Francou and Rodier (1967) collected approximately 1 200 maximum recorded floods from most regions of the world. They observed that when plotting the peak-discharge values against catchment area on a log-log scale, an envelope curve for a hydrologically homogenous region was identified. These envelope curves can be defined as a function of a K value which is calculated using the following Francou-Rodier equation:

$$K = 10\{1 - (\log Q - 6)/(\log A - 8)\}$$

where the variable
Q represents the largest flood (m^3/s) observed at a site.
A represents the effective catchment area in km^2.

The envelope curves when approximated as straight lines converge towards a single point where A is equal to 10^8 km^2 and Q is equal to 10^6 m^3/s (Fig. 1.2). These figures represent approximately the total drainage area and the total mean flow of all rivers on the earth respectively. The flood zone in Fig. 1.2 refers to catchments greater than 100 km^2 where maximum flood discharge is dependent on storm rainfall (intensity, area and duration) and catchment characteristics. In contrast, the storm zone (Fig. 1.2) refers to catchment areas of less than 1 km^2 where peak discharge is dependent only on rainfall intensity. The upper limit of the storm zone is set at 800 mm/hour which corresponds to world record rainfall intensities (Kovács, 1988). The lower limit is set at the minimum rainfall intensity that results in runoff. The transition

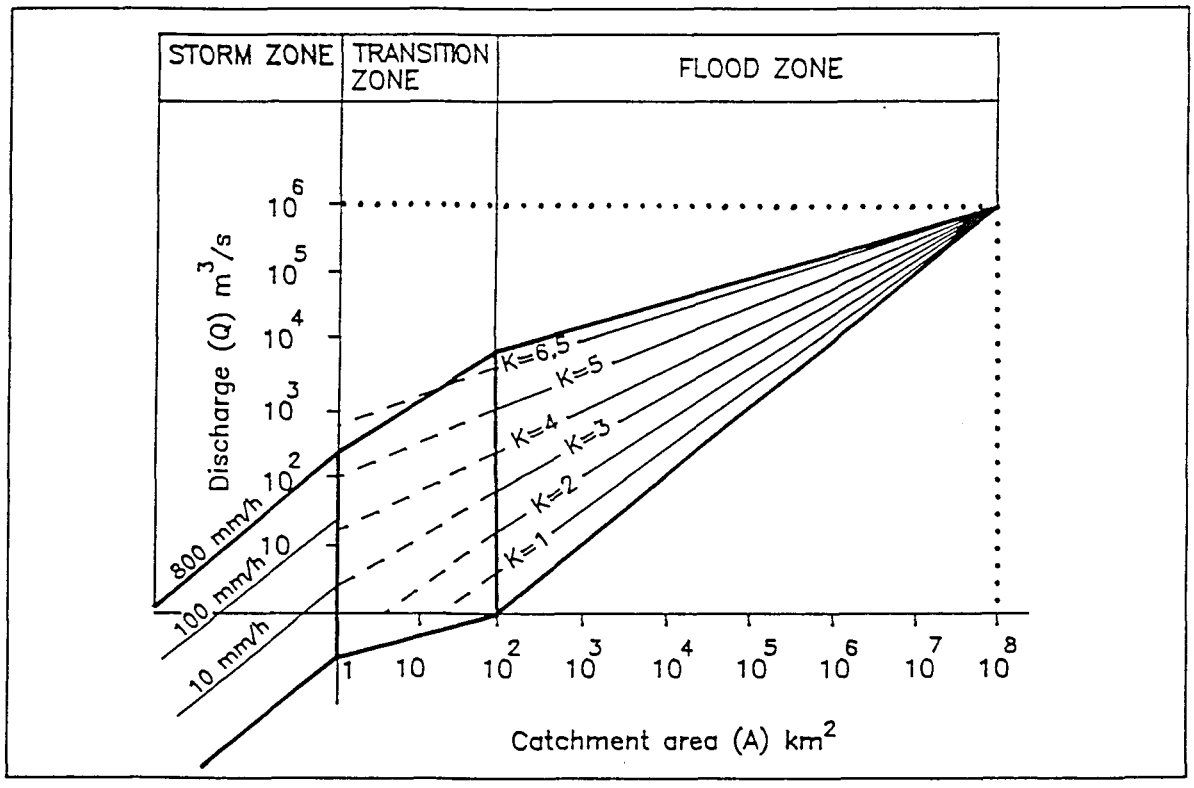

Fig. 1.2 - Francou-Rodier diagram of regional maximum flood-peak classification (modified after Kovács, 1988 and Alexander and Kovács, 1988).

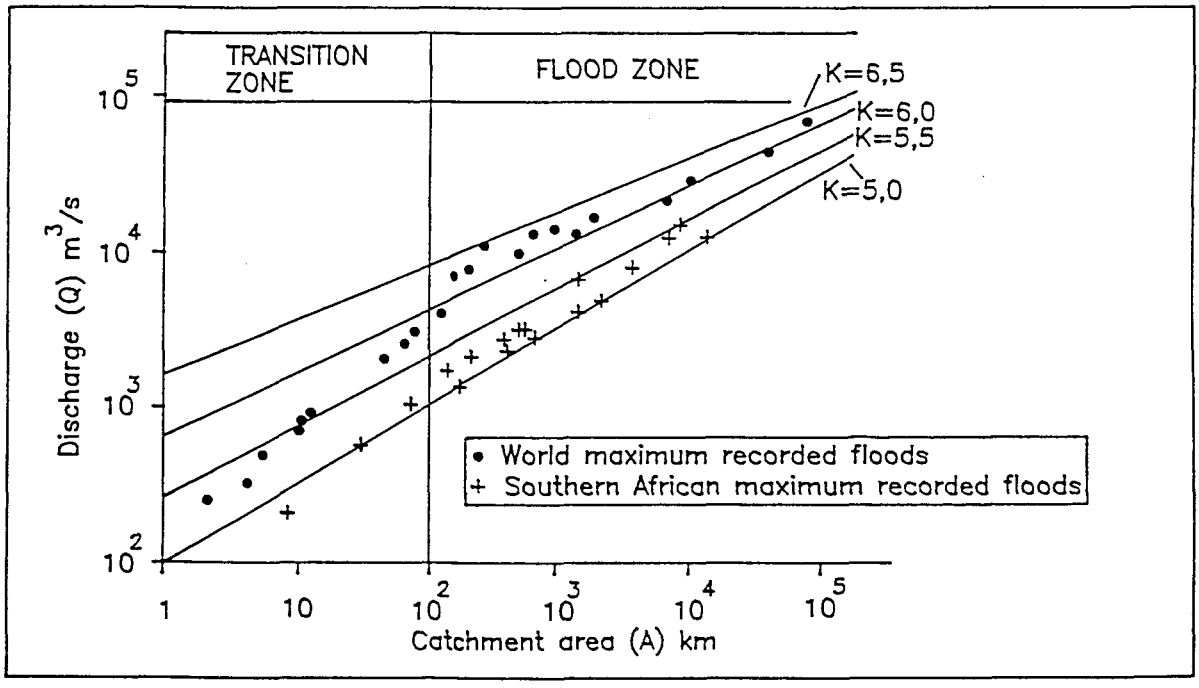

Fig. 1.3 - World and southern African flood peaks plotted on the Francou-Rodier diagram (modified after Kovács, 1988 and Alexander and Kovács, 1988).

zone (Fig. 1.2) refers to catchments in the size range 1 - 500 km^2. According to Kovács (1988) this zone is the transition between the storm zone where runoff is dependent only on rainfall intensity and the flood zone where storm rainfall is modified by catchment characteristics.

In southern Africa the Francou-Rodier method of RMF peak estimation was first applied by Kovács (1980) and later revised (Kovács, 1988). Kovács (1988) plotted the world catalogue of maximum floods, of which some are shown in Fig. 1.3, and 519 southern African maximum floods from South Africa, Lesotho, Swaziland, Namibia, Botswana, Zimbabwe and Mozambique, of which some are presented in Fig. 1.3. Kovács (1988) concluded that the trends for both the global and southern African data sets were similar in both the flood and the transition zones (Fig. 1.3) and the directions of the observed maximum floods were coincident with the K-value envelope curves. This would imply that the southern African maximum flood database is sufficiently comprehensive to enable the application of RMF calculations.

Kovács (1988) further applied the Francou-Rodier method by calculating the K value using the Francou-Rodier equation and plotting the geographical position of each observed maximum flood. This enabled the compilation of a map of southern Africa containing eight regions, each one being characterised by a K-envelope value (Fig. 1.4). Given the K value and the effective catchment area of a site enables the calculation of the RMF using the Francou-Rodier equation. According to Kovács (1988) this method is expected to give the best results for catchment regions in the size range of 300 km^2 -20 000 km^2.

The advantage of this empirical approach is its dependency on a large peak-flood database for the southern African region. Consequently it is independent of an unverifiable probabilistic or stochastic model. Alexander (1990a) stated that the Francou - Rodier equation does describe the upper boundary of maximum floods in South Africa and has been found to be a reliable method in other parts of the world. Its disadvantages, according to Kovács (1988), are uncertainties in defining the homogenous regional maximum flood boundaries and the inapplicability of the method to either very large or very small catchments because of unusual hydrological conditions. A criticism levelled at the RMF method, which is also applicable to the

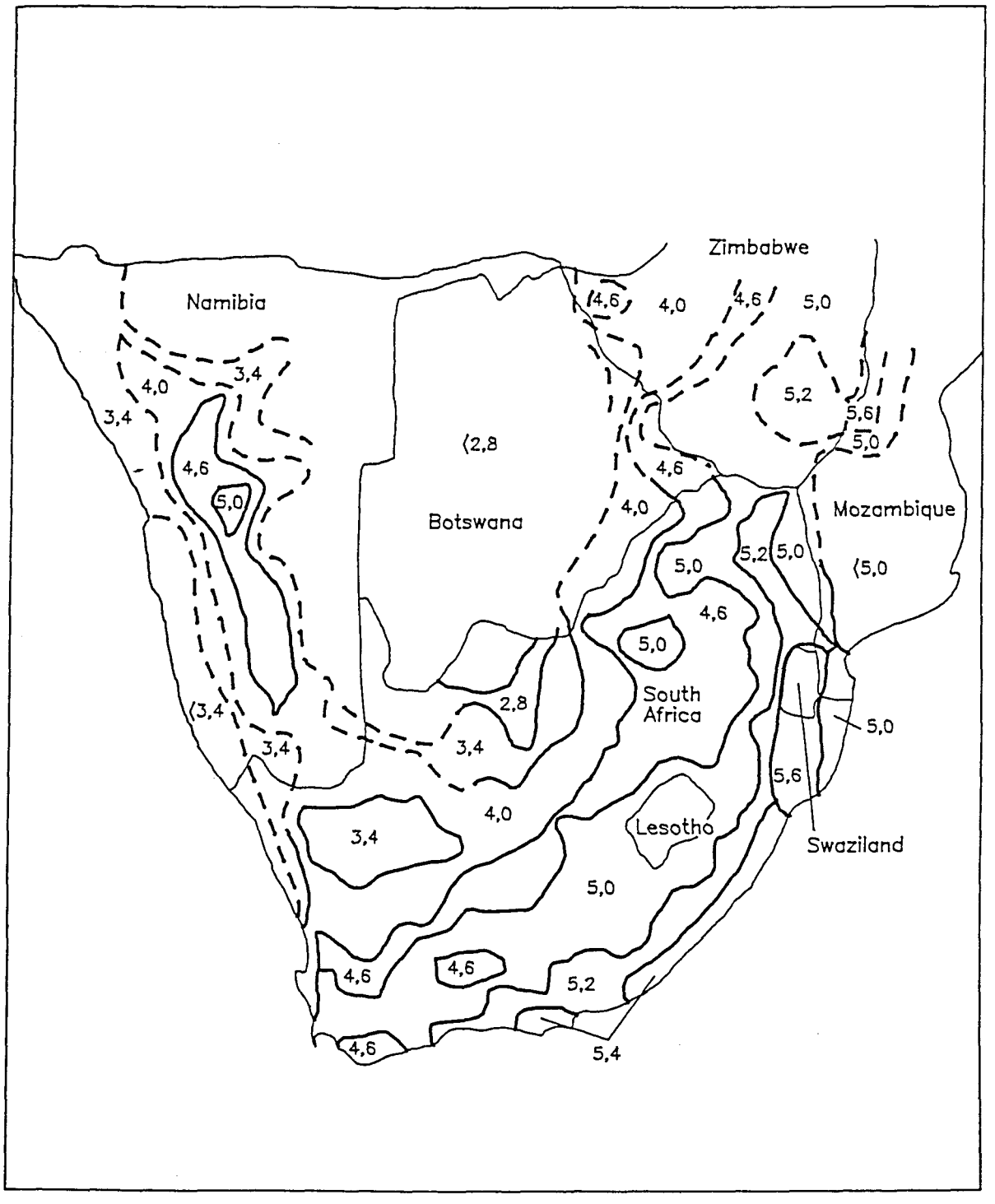

Fig. 1.4 - Regional maximum flood-peak regions in southern Africa. Numbered regions refer to the regional Francou-Rodier K envelope value (modified after Alexander and Kovács, 1988). Note that the highest K value for South Africa extends from Swaziland southward towards the eastern seaboard; a region that experiences tropical cyclones.

deterministic and statistical methods, is its reliance on historical records that will be exceeded with time (Alexander, 1988). However, Kovács (1988) stated that the K-values were only marginally adjusted when further peak flood data for the past decade were incorporated into the Southern African catalogue of maximum floods.

1.3 Palaeoflood hydrology and conventional flood-frequency analysis

In recognising the difficulties associated with conventional flood-frequency analysis such as insufficient or non-continuous data, poor quality data and an uncertainty in applying largely untested flood-prediction models, a shift has occurred towards investigating Holocene stratigraphic records of past floods (Costa, 1978a; Costa, 1986; Stedinger and Baker, 1987). This is primarily attributed to the potential Holocene fluvial sediments have for recording evidence of floods which occurred prior to the time of either direct observation or measurement (Baker et al., 1990a). The identification and analysis of past floods is termed palaeoflood hydrology. The importance of palaeoflood hydrology as a complementary method for flood prediction (Baker et al., 1990a) lies in the following two fundamental differences that set it apart from conventional flood-prediction techniques employed by hydrologists. Firstly, because the method uses physical evidence of past floods, it is independent of unverifiable or imprecisely known stochastic hypotheses (Zawada and Hattingh 1994). Alternatively stated, because the palaeoflood hydrological technique is restricted by the physical constraints of the flood-producing system, it therefore imposes physical limits to the flood-prediction model, which although it may be inaccurate in certain respects (Baker et al., 1990a), is nonetheless preferable to a purely statistical model. Secondly, the method makes the assumption that because a flood has occurred in the recent geological past, it is therefore reasonable to expect a flood of this magnitude to reoccur in the near geological future (Costa, 1978a). Baker et al. (1990a) reiterated this point by stating that because palaeoflood hydrology gives evidence of the largest magnitude palaeofloods to have occurred over long periods of time (Holocene epoch), this provides important data points with regard to the kind of flows that are possible in a fluvial setting.

1.4 Palaeoflood hydrology in South Africa: previous studies

Few palaeoflood investigations with the objective of constructing the flood history have been completed for modern South African rivers. Although Zawada (1991)

recognised that palaeoflood hydrology could provide potentially important data to improve the accuracy of flood probability calculations, South African palaeoflood hydrology was reported as still being in its infancy. An early application of palaeoflood hydrology was that of Smith and Zawada (1990) who calibrated geomorphological features (terrace levels and knick points) and particle-size analysis to the gauged record of the Crocodile River northwest of Pretoria. Using terrace levels and maximum particle-size analysis 4 palaeofloods were identified with discharges of 4 500 m^3/s, 6 000 m^3/s, 7 000 m^3/s and 9 500 m^3/s of which the latter was considered to have occurred in a different hydroclimatic regime. In a palaeoflood hydrological analysis using slack-water sediments deposited on the bedrock valley side of the Umgeni River in Natal Smith (1992a) concluded that they represent four palaeoflood events with discharges of 24 000 m^3/s - 28 000 m^3/s. Although no age was obtained from the slack-water sediments, it was concluded that the palaeofloods predate 1750-1800 A.D. They were possibly the result of tropical cyclonic activity which at that time tracked farther south into the Umgeni River catchment than at present.

Further palaeoflood analysis in South Africa has focused on its application to Holocene palaeoclimatic change models for the southern hemisphere and in particular southern Africa (Smith, 1991; 1992b). Discussion has centred on the issue of climatic non-stationarity which according to Smith (1991) largely nullifies the value of incorporating palaeoflood hydrological information into flood series to improve flood-peak estimation and recurrence calculations. He went further to conclude that in the light of climatic non-stationarity many of the palaeoflood events identified from the Orange River, the Umgeni River and the Crocodile River were unlikely to recur. An alternative view expressed by Zawada (1991) states that by acknowledging the non-stationarity of climate and the potential for palaeoflood analysis to identify this change, this can be used to generate an accurate and complete palaeoflood record to augment modern palaeoflood records. Zawada (1991) stated further that in view of the incompleteness of the palaeoflood record, the absence of testing of the hypothesis of non-stationarity, and the relatively recent use and limited application of palaeoflood hydrology in South Africa, it is premature to conclude, as Smith (1991) did, that palaeoflood hydrology is of dubious value when the intention is to extend the modern flood record.

Palaeoflood hydrology has been recognised as a potentially important technique for flood prediction in South Africa (Alexander, 1990a). This view has been echoed by funding being provided by the Water Research Commission to complete this study. This study represents the first attempt to review the palaeoflood evidence on a national level as well as at a site specific level where detailed palaeoflood hydrological analysis has been done. As yet, palaeoflood hydrology has not been widely adopted as either a research tool or as an application in flood-peak estimation in South Africa. This is despite the overseas experience where the emphasis on palaeoflood hydrology has shifted from a research-based technique to an application that can be used to test the credibility of calculated probable maximum flood values used in the design of high-hazard constructions (Baker et al., 1987).

1.5 Aims and objectives

The aims of the project as set out in annexure A of the memorandum of agreement entered into by and between the Water Research Commission and the Council for Geoscience were as follows:

(1) To elaluate whether palaeoflood hydrology can supply reliable maximum peak-flood estimates for South African Rivers with the aim of placing an upper limit to the peak maximum flood for each river under investigation.

(2) To refine the present peak-flood estimates as calculated using the statistical, deterministic and empirical approaches as applied by the hydrologist and in particular, to test the validity of the probable maximum flood and regional maximum flood figures against palaeoflood hydrological data.

(3) To briefly examine and identify rivers from differing climatic regions in South Africa, that are most suited for palaeoflood hydrological anlaysis.

The above aims were partially modified and made more specific as the project progressed and are listed below.

(1) To document the nature and type of palaeoflood evidence that exists for

South African rivers subject to differing climatic regimes by way of a national reconnaissance investigation. This approach has never before been attempted on a national basis and was motivated out of the need to increase our understanding of the interaction of geological, hydrological, botanical and geomorphological factors that promote the recognition and preservation of palaeoflood records.

(2) To complete detailed palaeoflood hydrological investigations for the middle (Prieska) and the lower (Richtersveld) reaches of the Orange River. The detailed phase of the investigation had the broad aim of assessing palaeoflood hydrological techniques for South African rivers in terms of its scientific, practical, logistical and cost effectiveness as a tool in Southern African flood prediction. In addition, the specific goals of the detailed phase were:

(i) to ascertain if the rivers had experienced floods hundreds to thousands of years ago that were either the same, smaller or greater than those experienced today,
(ii) to test the feasibility of identifying and constructing a dated, flow-modelled palaeoflood stratigraphy,
(iii) to augment the short gauging record with palaeoflood data in an attempt to refine the calculated exceedance probabilities of future floods, and
(iv) to ascertain the probable maximum flood of the river based on its palaeoflood stratigraphic record.

2. A RECONNAISANCE STUDY OF PALAEOFLOOD SITES IN SOUTH AFRICA

This chapter sets out the aims and objectives for initiating a reconnaissance investigation of palaeoflood sites in South Africa. An account of the methodology and criteria used to evaluate the palaeoflood evidence follows with a review of the substantive conclusions arising from the investigation. The chapter concludes with the selection of river and palaeoflood sites for detailed palaeoflood hydrological analysis.

2.1 The need for a reconnaissance investigation

Until 1992 the few instances of palaeoflood analysis completed in South Africa was site specific (Smith and Zawada, 1990; Smith, 1992a; Smith and Zawada (unpubl.) and lacked a holistic view of the potential in applying palaeoflood hydrology on a country-wide basis. For example, little was known of the types of palaeoflood evidence that existed in South African rivers. Although it was known that constructing a flow modelled and dated palaeoflood stratigraphy from temperate - humid regions was generally difficult due to biogenic reworking and contamination by post-flood organic material, no understanding existed as to which areas in South Africa were more suitable than others. For example, the semi-arid - arid regions exhibited a high potential for preserving slack-water sediments compared to the sub-tropical region of KwaZulu/Natal. However, little was known of the feasibility of applying palaeoflood hydrology in regions with an intermediate rainfall and variable vegetation density such as the central Cape Province, eastern portion of the Orange Free State and the temperate - mediterranean climate of the southern Cape. In consultation with the Department of Water Affairs and Forestry and the Water Research Commission, 21 river systems were therefore selected for investigation on a reconnaissance basis with the following objectives (Table 2.1; Fig. 2.1):

(1) to compile a data bank that documents the nature and type of palaeoflood evidence for rivers from different climates in South Africa (section 2.3.1);
(2) to gain a better understanding of the interaction of geological, hydrological, botanical, geomorphological and climatic factors that affect the recognition and preservation of palaeoflood records (section 2.3.2);

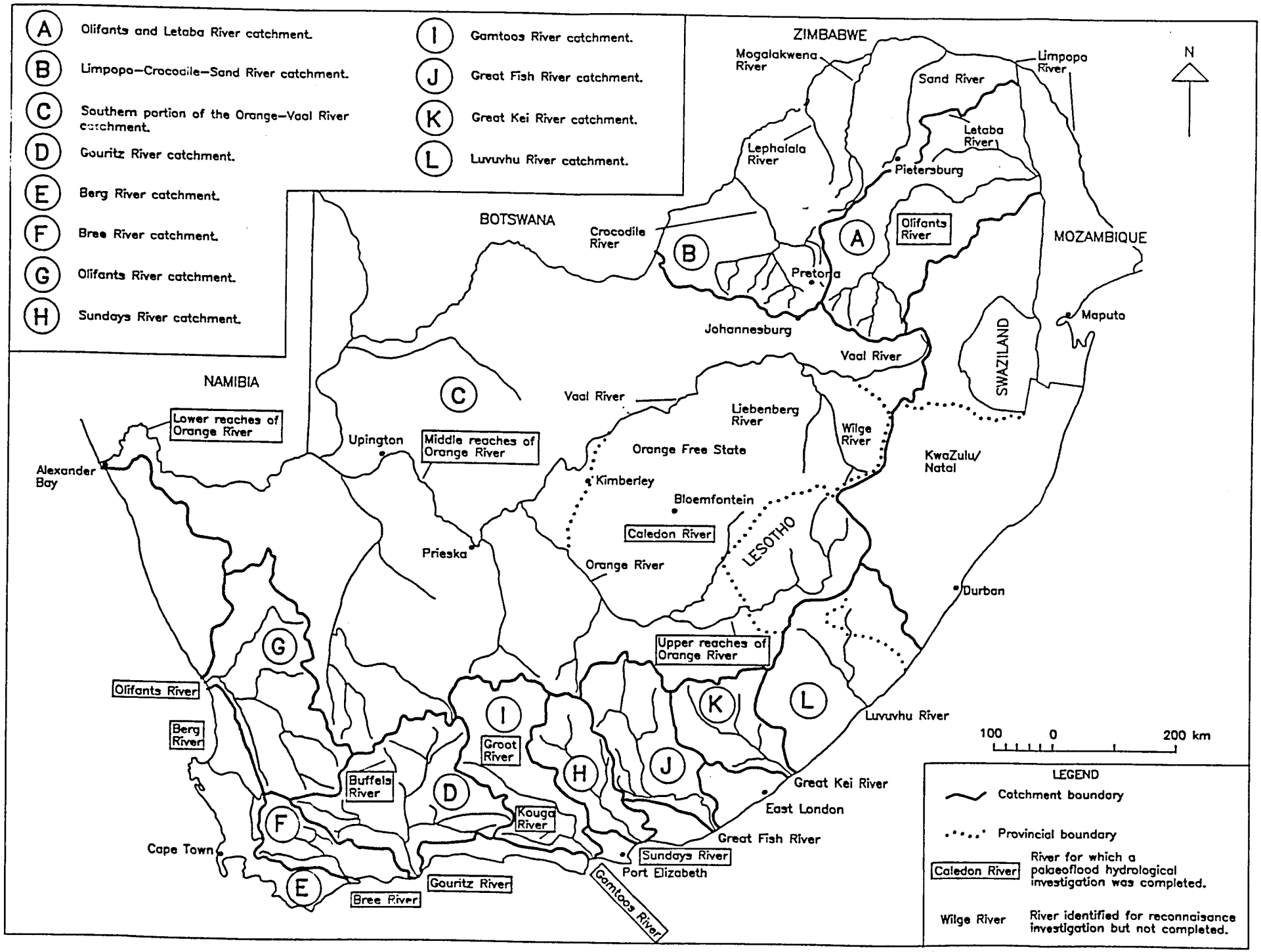

Fig. 2.1 - Map of the rivers and associated catchments that were selected for reconnaisance investigation showing also those rivers that were complet

River	Investigated	Number of sites	Comments
Olifants (Transvaal)	Yes	16	Forms part of the Olifants River system
Klein Olifants (Transvaal)	Yes	1	
Limpopo	Partial	-	A map analysis indicated that few bedrock reaches exist for the Limpopo River. In view of the importance of the Limpopo River, further reconnaissance should be completed.
Crocodile	No	-	A map analysis indicated that no suitable bedrock reaches exist for the Crocodile River.
Lephalala	No	-	
Mogalakwena	No	-	
Sand	Partial	-	It is known that bedrock reaches exist where the river passes through the Soutpansberg Mountains.
Luvuvhu	No	-	
Letaba	No	-	
Upper reaches of Orange	Yes	3	Border security problems between South Africa and the former Transkei did not permit further sites to be investigated. Excellent palaeoflood sites exist for the upper Orange River.
Middle reaches of Orange	Yes	11	Several excellent palaeoflood sites occur in the Prieska area.
Lower reaches of Orange	Yes	3	These sites contain excellent palaeoflood evidence.
Caledon	Yes	5	An important flood-contributing tributary of the upper Orange River catchment.
Wilge	Partial	-	A map analysis indicated that no bedrock reaches exist for the Wilge River.
Liebenberg	Partial	-	A map analysis indicated that no bedrock reaches exist for the Liebenberg River.
Gouritz	Yes	4	Forms part of the Gouritz River catchment. Excellent palaeoflood sites occur in the Buffels River.
Buffels	Yes	6	
Berg	Yes	-	The reconnaissance was based only on an examination of the topocadastral sheets. The Olifants River exhibits regions which may contain palaeoflood evidence.
Breë	Yes	-	
Olifants (Cape)	Yes	-	
Sundays	Yes	9	
Gamtoos Groot	Yes	6	Forms part of the Gamtoos River catchment.
Kouga	Yes	3	
Great Fish	No	-	Border security problems prevented access to the river.
Great Kei	No	-	Border security problems prevented access to the river.

Table 2.1 - List of rivers that were investigated on a reconnaissance basis (Fig. 2.1 and 1993 Water Research Commission Report by Zawada and Hattingh, 1993).

(3) to locate palaeoflood evidence in bedrock-controlled reaches from a variety of hydroclimates (section 2.3.1);
(4) to assess the potential of the palaeoflood site for providing a palaeoflood record (section 2.3.1);
(5) to assess the potential of the palaeoflood site for dating (section 2.3.2);
(6) to briefly investigate, where appropriate, the sedimentological characteristics of the palaeoflood evidence, and
(7) to identify palaeoflood sites that are suitable for detailed palaeoflood hydrological analysis (section 2.4).

2.2 Methodology

Because the best palaeoflood information occurs as slack-water sediments, especially in back-flooded tributary settings, the reconnaissance investigation focused on locating slack-water sediments in reaches of channel stability. For each river investigated the following modus operandi was adhered to.

(1) Pre-field work phase. This involved studying 1:50 000 topocadastral map sheets and 1:10 000 orthophotographs (where available) to locate bedrock-controlled reaches on which potential palaeoflood sites were marked.

(2) Field-work phase. Each potential palaeoflood site was investigated in the field with the following information being recorded:

- river name;
- name of palaeoflood site;
- a description of the type of palaeoflood evidence present with a sketch map showing the geomorphological setting of the site and access to site,
- location of site in degrees, minutes and seconds,
- a description of the type of river; information on the rock type of the channel, degree of sinuosity and any other relevant geological/geomorphological information.
- In the case of slack-water sediments, a brief lithological description documenting the texture, colour, sedimentary structure, thickness and any palaeoflood units that were

identified was produced.

- A qualitative assessment of the type and amount of organic material that can be collected for radio-carbon dating.

(3) Report phase. Each site that contained promising palaeoflood evidence was documented with an evaluation of its potential for future detailed palaeoflood hydrological analysis (Zawada and Hattingh, 1993). Similarly, for each river system the palaeoflood sites were compiled to further evaluate the potential for a detailed palaeoflood hydrological analysis.

2.3 Results of reconnaissance investigation

The reconnaissance investigation examined 67 sites in the Olifants (northern Transvaal province), Orange, Gouritz, Berg, Breë, Olifants (south-western Cape Province), Gamtoos and Sundays River systems (Table 2.1; Fig. 2.1) (Zawada and Hattingh, 1993).

The results of the reconnaissance investigation were compiled into an extensive report to the WRC (Zawada and Hattingh, 1993) of which the substantive conclusions are presented in the following section. The report serves two important functions. Firstly, it represents a valuable data source on a large number of palaeoflood sites countrywide, which can assist future researchers by providing an assessment of the potential of the palaeoflood site in containing a palaeoflood record, or for example, giving information on the likely probable maximum flood (see Zawada and Hattingh, 1993; p. 37, 99, 116, 160, 178 for the tabulated summaries given at the end of each river system). The second function in compiling the reconnaissance report has been to enable a better understanding of the interaction between geology, climate, botany and hydrology in the recognition and preservation of palaeoflood records. These findings are briefly reviewed in sections 2.3.1 - 2.3.2.

2.3.1 Documenting the nature and type of palaeoflood evidence

Reconnaissance field work of the 67 palaeoflood sites revealed 5 types of palaeoflood evidence which are listed and briefly described:

(1) terraces;
(2) knick-line features cut into bedrock;
(3) large in-channel boulders;
(4) slack-water sediments in back-flooded tributaries, and
(5) botanical features.

Terraces. Several promising palaeoflood sites comprising well-developed terraces were identified from the Gouritz River (sites 1 and 4; Zawada and Hattingh, 1993; p. 117 and 123 respectively), the Sundays River (sites 1, 2, 4, 5 and 6; Zawada and Hattingh, 1993; p. 101, 103, 106, 107 and 109 respectively), the Olifants River (sites 1, 12 and 16; Zawada and Hattingh, 1993; p. 8, 26 and 32 respectively) and the Gamtoos River (sites 2, 4, 5 and 9; Zawada and Hattingh, 1993; p. 166, 168, 170 and 175 respectively).

Terraces are sediments located on the channel margin occurring either singly or paired with respect to the channel thalweg. They were found to form in regions of abrupt channel expansion where sudden reductions of flow regime occurred. The terraces usually exhibited a stratigraphy that reflected a palaeoflow record and are in many respects similar to slack-water sediments in back-flooded tributary settings. Terraces represent therefore excellent palaeostage indicators for which accurate palaeodischarge estimates can be made. However, in-channel terraces did not exhibit couplets that reflect the interplay between slack-water deposition and non-flood tributary deposition such as that found in tributary back-flooded settings. It was therefore difficult to differentiate between intra-flood pulses and inter-flood events.

Knick-line features. Knick-line features cut into the valley-wall bedrock were observed at palaeoflood sites from the Olifants River, Transvaal (sites 3 and 5; Zawada and Hattingh, 1995; p. 12 and 15 respectively) and the Gouritz River (sites 3, 7 and 9; Zawada and Hattingh, 1993; p. 121, 138 and 150 respectively).

Caution should be exercised when using this feature as a palaeostage indicator as it is uncertain whether the feature was formed by frequent flood events that occurred in the existing channel geometry or is relict having formed in response to a previous higher elevation of the channel thalweg. A good example of bedrock valley-

wall knick-line features occurs in the Gouritz River at site 3 where prominent paired knick-line features are laterally continuous for up to 1 km at a height of 14,20 m above low water level (Zawada and Hattingh, 1993; p. 121 and Chapter 5, Table 1). The well defined nature and lateral continuity of this feature may indicate a period of frequent large floods which could be used as an indication of the probable maximum flood for the Gouritz River. Although this feature cannot be dated, its value as a palaeostage indictor increases when correlated with other palaeostage indicators such as dated and flow-modelled slack-water sediments.

Large in-channel boulders. Palaeoflood sites that comprised large in-channel boulders were documented for the Olifants River (sites 2, 6 and 14) and the Sundays River (site 8) (Zawada and Hattingh, 1993).

Using maximum particle-size as an indictor of palaeoflow assumes that the catchment of the river can produce clasts of a sufficiently large size which were fluvially transported at a level close to the maximum competence of the flood flow. An example of where this condition was not met was noted in the Sundays River (sites 1 - 5; Zawada and Hattingh, 1993; p. 101 - 107) where the geology of the catchment upstream of Downlington Dam (previously known as Lake Mentz) is extensively fractured along foliation planes. The resultant bed load comprises relatively small clasts that do not reflect a threshold of flow competency. A further required condition when relating maximum particle-size to palaeoflow is ensuring that the particles were fluvially transported. For the reconnaissance investigation, particles were selected where they exhibited the following evidence indicating fluvial transport:

(1) percussion marks on at least two faces;
(2) rounding, and
(3) forming part of an imbrication train.

Although maximum particle size-analysis has limitations and uncertainties, the technique is still of use where it is incorporated with other palaeohydrological techniques such as slack-water sediments.

Slack-water sediments. Because slack-water sediments represent the most accurate palaeoflood evidence to indicate palaeostage and palaeodischarge, the reconnaissance investigation focused on locating slack-water sediments in bedrock-controlled reaches. Of the 67 palaeoflood sites examined, 49 comprised slack-water sediments in back-flooded tributaries, in-channel caves or concave regions of incised meander bends of which eight sites are from the Olifants River (Transvaal) (Zawada and Hattingh, 1993; Chapter 1, Table 6), 20 from the Orange River (Zawada and Hattingh, 1993; Chapter 2, Table 7), 5 from the Sundays River, (Zawada and Hattingh, 1993; Chapter 3, Table 2), 11 from the Gouritz River (Zawada and Hattingh, 1993; Chapter 4, Table 1) and 5 from the Gamtoos River (Zawada and Hattingh, 1993; Chapter 6, Table 1). A discussion on the recognition and preservation of slack-water sediments from different climates is presented in section 2.2.2.

Botanical features. One example of a palaeoflood site comprising flood-affected trees was observed and documented from the Olifants River (site 9; Zawada and Hattingh, 1993; p. 20). Notwithstanding the difficulties in applying dendrochronology to South African tree species, the limited period for which botanical features can be used and the uncertainty with modelling discharges, botanical features can be used in collaboration with more reliable palaeostage indicators. It was noted for example, that the reach of the Olifants around site 9 showed several examples of flood-damaged trees showing multi-phase adventitious sprouting. Correlation of these phases in terms of stage and age with slack-water and/or terrace studies could provide useful information covering the ultra-modern flood record.

2.3.2 Factors that promote the recognition and preservation of palaeoflood records

The preservation of palaeoflood records principally applies to slack-water sediments as they are prone to biogenic and non-biogenic reworking. The reconnaissance investigation showed that the identification, preservation of stratigraphy and radio-carbon dating potential of slack-water sediments is primarily a function of rainfall and consequently density of vegetation. This has enabled a subdivision of the country into four regions based on climate and vegetation and their effect on the preservation and radio-carbon dating potential of slack-water sediments (Fig. 2.2) (Zawada and Hattingh, 1994). This information could be of value where palaeoflood hydrology is being considered for inclusion in a flood-prediction model. For example,

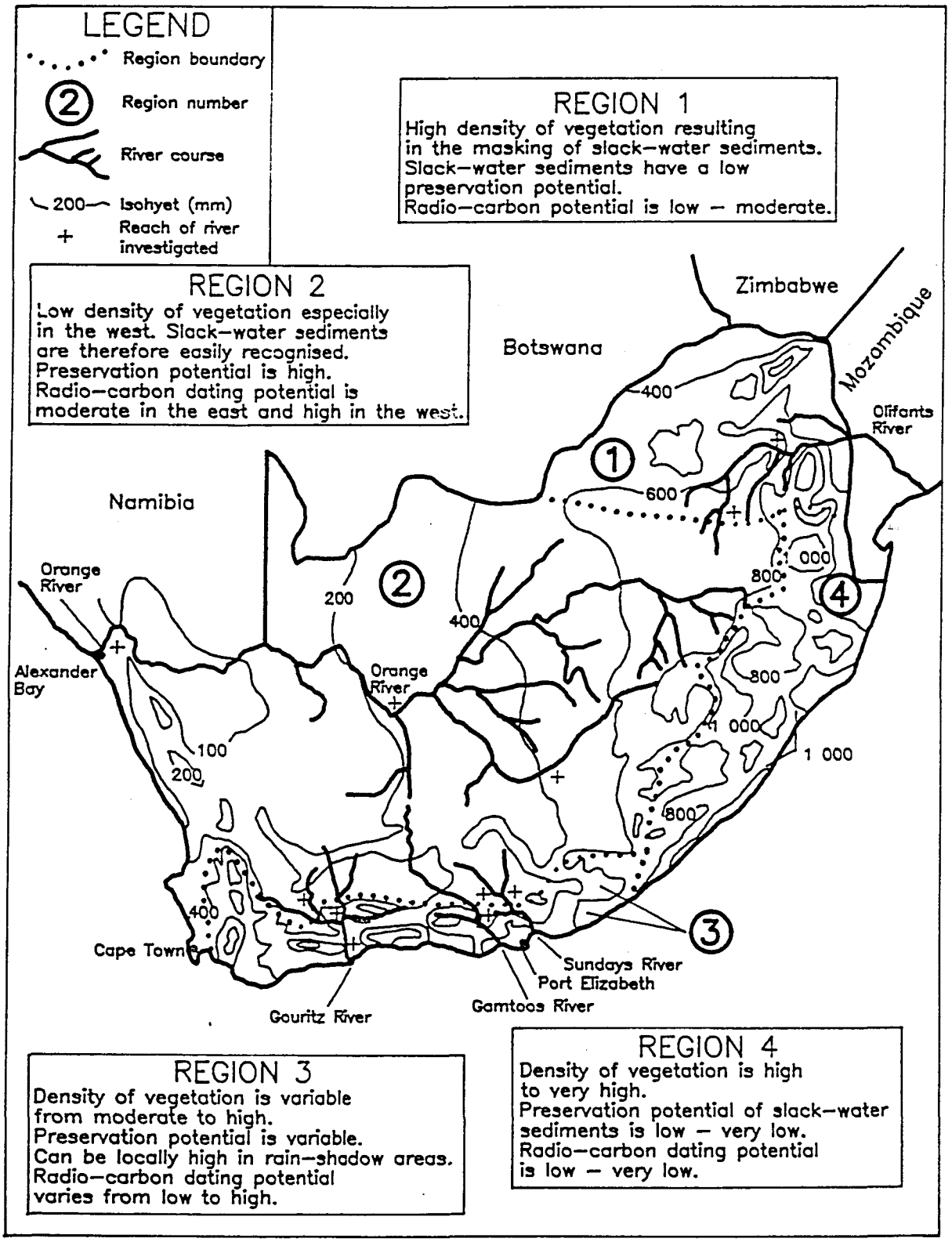

Fig. 2.2 - Mean annual rainfall for South Africa (modified after Tyson, 1986). Characterization of regions is based on density of vegetation, preservability of slack-water sediments and radiocarbon dating potential.

out of the four regions, regions 2 and 3 probably contain the best palaeoflood evidence in terms of slack-water sediments.

Region 1. This region includes much of the northern Transvaal with a mean annual rainfall varying from approximately 1 000 mm in the east to 600 mm - 500 mm in the central portion through to 400 mm in the far northern portion of the province (Fig. 2.2). Investigation of 8 slack-water sites for the upper and lower reaches of the Olifants River (sites 4, 7, 8, 10, 11, 13, 15 and 17; Zawada and Hattingh, 1993; chapter 1, Table 6) indicates that the slack-water sediments are affected by a high vegetation density which results in difficulty in locating slack-water sediments. In addition, the sediments were extensively bioturbated exhibiting few contacts and sedimentary structures. Due to contamination of the sediment by post-depositional vegetation, the radio-carbon dating potential is low - moderate (Fig. 2.2). This, together with the low preservation potential, suggests that future studies in this region should focus on identifying in-channel palaeoflood evidence such as large, fluvially transported boulders and valley-wall knick line features (Zawada and Hattingh, 1994).

Region 2. This region includes much of the central interior of the country namely the Orange Free State and the Cape Province north of the Cape Fold Mountains. The mean annual rainfall varies from 800 mm - 900 mm in the east, declining westward to 200 mm - 400 mm in the central Karoo through to 100 mm - 200 mm along the west coast, Namaqualand and the Richtersveld area of the far north-western Cape (Fig. 2.2). Investigation of the Orange River from its upper reaches in the east to the lower reaches in the west (sites 1, 3 - 23; Zawada and Hattingh, 1993; chapter 3, Table 7) indicates that the slack-water sediments in region 2 are affected by a low - moderate density of vegetation cover which decreases from east to west. Much of the region exhibits well preserved slack-water sediments, with excellent examples occurring in the Richtersveld area (Fig. 2.2). The radio-carbon dating potential varies from moderate in the east to high in the west (Fig. 2.2).

Region 3. This region includes the Cape Fold Mountains from Port Elizabeth which has a mean annual rainfall of approximately 600 mm, westward to Cape Town and north of Cape Town up to around Porterville, which receives on average 600 mm - 800 mm rain per year (Fig. 2.2). Investigation of slack-water sediments in region 3

from the Gouritz River system, (sites 1, 2, 5 - 10A; Zawada and Hattingh, 1993; chapter 4, Table 11), the Gamtoos River system (sites 1, 3, 6 - 8; Zawada and Hattingh, 1993; chapter 6, Table 1) and the Sundays River system (sites 2, 3, 5, 7, and 9; Zawada and Hattingh, 1993; chapter 3, Table 2) indicates that much of the region has a high but variable vegetation density. For example, orographic rainfall is common resulting in rain-shadow areas and an increase in the preservation potential of slack-water sediments (Fig. 2.2). The radio-carbon dating potential therefore varies from low to high (Fig. 2.2).

Region 4. This region includes the subtropical portions of Natal which have a mean annual rainfall of 800 mm - 1 000 mm (Fig. 2.2). Although no specific rivers were investigated as part of the reconnaissance study, experience in region 1 with preliminary field work in the uMgeni River immediately downstream of Inanda Dam, indicates that slack-water sediments from region 4 are affected by a very high vegetation density. This leads to extensive if not total reworking of the sediment and contamination by ultra-modern vegetation. Accordingly, the index of preservation and radio-carbon dating potential is low (Fig. 2.2). Of all the regions in the country, region 4 is considered to be least likely for providing comprehensive palaeoflood catalogues.

2.4 Selection of sites for detailed palaeoflood hydrological analysis

The middle and lower reaches of the Orange River were selected for detailed palaeoflood hydrological analysis on the basis of well preserved slack-water sequences occurring in bed-controlled reaches of the river. A further consideration was the large size of the Orange River catchment (nearly 900 000 km^2) and the influence that the major flood-producing rivers such as the Vaal River, the Caledon River, the Molopo River and the Fish River have on generating large or catastrophic floods that have not been historically recorded. Because flood magnitude and frequency are primarily a function of hydroclimate (Wells, 1990; Ely et al., 1993; Knox, 1984; 1993), a significant change of climate that affected the Orange River catchment may have been recorded in the palaeoflood stratigraphy of the lower reaches of the Orange River. It is therefore possible to incorporate the palaeoflood record of the Orange River as proxy evidence of climate change into Holocene palaeoclimate change models. The reconnaissance investigation for sites 21, 22 and 23 from the lower reaches of the Orange River (Zawada and Hattingh, 1993; p. 76 - 88) showed evidence of extremely

large and possibly catastrophic flooding with flood stages being almost 3 times higher than the 1988 Orange River flood. A flood of such catastrophic size carries important hydroclimatic implications, of which one is the possibility that such a flood could occur in the present hydroclimatic regime. A detailed palaeoflood hydrological analysis of the lower reach of the Orange River would not only furnish a palaeoflood history for the Orange River, but would also verify the existence, magnitude and age of the catastrophic flood in order to ascertain its likelihood of recurrence.

3. PALAEOFLOOD HYDROLOGY OF THE ORANGE RIVER

This chapter gives an introduction to the Orange River-Vaal drainage basin, followed by a listing of the palaeoflood sites used in the study. A detailed account of the sedimentology and stratigraphy of each site is presented giving particular attention to the differentiation of palaeoflood from non-palaeoflood-deposited sediments. An evaluation of the palaeodischarge estimates and dating results obtained for the palaeoflood units is presented. An attempt to correlate the palaeoflood sites follows. It will be shown that the application of palaeoflood hydrology has identified a series of large floods and a flood of catastrophic magnitude occurred in the lower reach of the Orange River which have not been previously recorded. A flood-peak analysis of the lower Orange River using the palaeoflood and systematic record is presented. This is followed by a discussion on incorporating the palaeoflood hydrological results obtained from the lower reach of the Orange River into a Holocene palaeoclimate change model for southern Africa. A discussion assessing the possibility of the catastrophic flood recurring in the present climatic regime is presented. A preliminary mineralogical investigation of the Orange River slack-water sediments follows in an attempt to identify possible changes of subcatchment contributions (provenance changes) of flood-transported sediment to the Orange River through time.

3.1 Introduction

The Orange River was named after the Dutch House of Orange by the explorer Robert Jacob Gordon (circa. 1777) and not from its colour as is popularly believed. The catchment area of the Orange River is approximately 891 780 km^2 comprising the subcatchment regions of the Vaal River (193 780 km^2) (Perry, 1988), the Orange River (356 230 km^2) (Perry, 1988), the Molopo River (233 200 km^2) (Kokot, 1965) and the Fish River (108 780 km^2) (Kokot, 1965). Within South Africa, the Orange River drains 45 % of the surface area of the country (Bremner et al., 1990). The Orange River can be subdivided into an upper reach which extends upstream from the Vaal-Orange River confluence, a middle reach from the confluence downstream to the Augrabies Falls and a lower reach from the Falls to the mouth at Alexander Bay (Fig. 3.1) (Wellington, 1958).

According to Bremner et al. (1990) the Orange River is classified as one of the worlds major rivers as it exhibits a mean annual runoff of approximately 11,9 km^3. This represents approximately 22 % of the total runoff of South African Rivers (Noble and

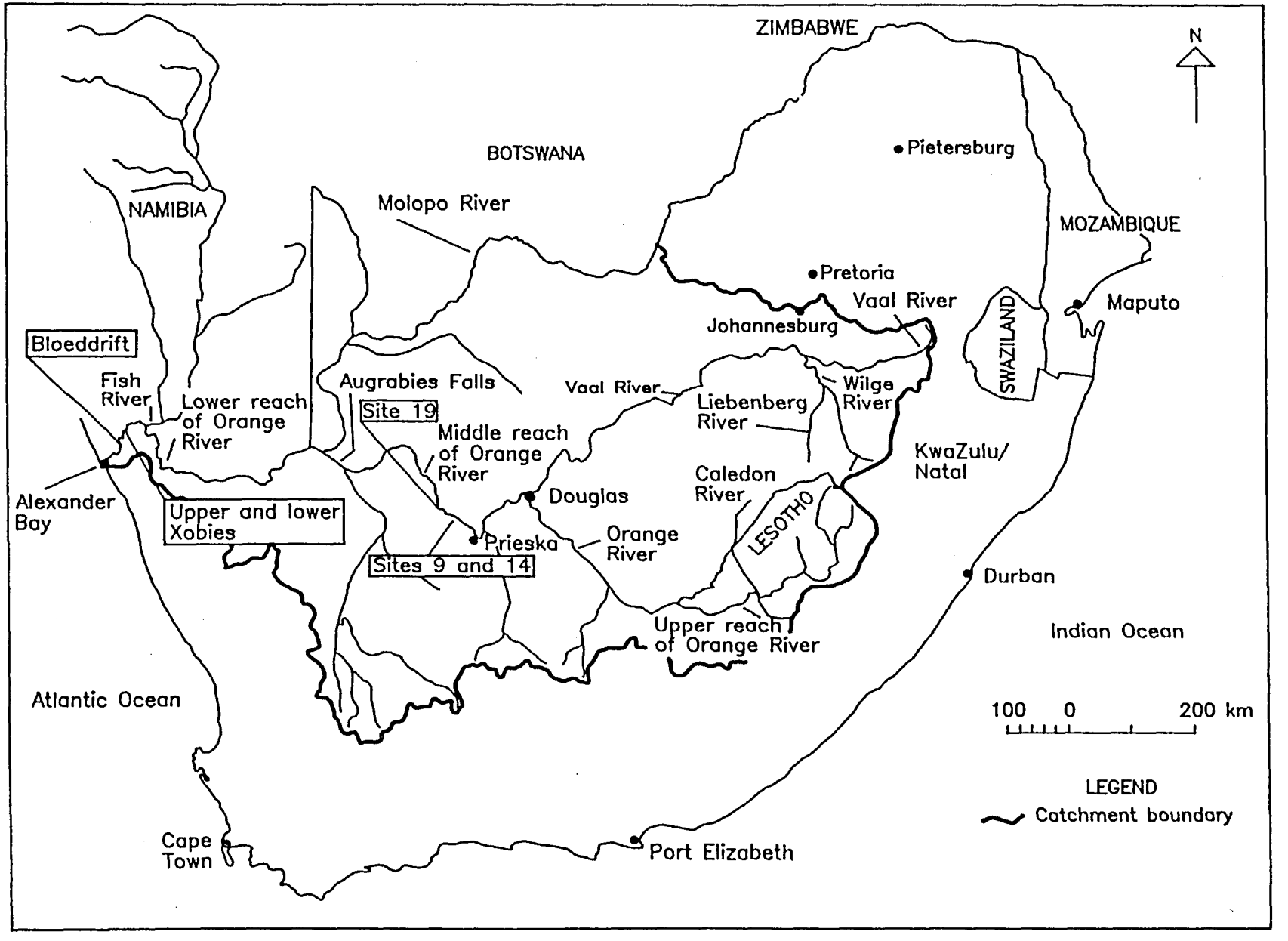

Fig. 3.1 - Map showing the Orange River catchment in South Africa and Namibia. The positions of the palaeoflood sites that were used for detailed palaeoflood hydrological analysis are indicated.

Hemens, 1978). The major proportion of this runoff is derived from the Orange River catchment with only 0,21 km^3 being contributed from the dry western portion below the Vaal-Orange River confluence.

The Orange River has a thalweg length of 2 173 km (Perry, 1988) from its headwaters in Lesotho through to its mouth at Alexander Bay (Fig. 3.1). It crosses a number of rainfall regions ranging from over a 1 000 mm annual rainfall in Lesotho to approximately 400 mm at the Vaal-Orange River confluence to less than 100 mm in the west near its mouth (Zawada and Smith, 1991). The river traverses a wide variety of rock types. From the headwaters to approximately 40 km upstream of the Vaal-Orange River confluence the river flows across progressively younger strata of the Karoo Supergroup (Jurassic - Carboniferous) from the easily erodible Drakensberg basalt to the sandstone, siltstone, mudstone and shale of the Clarens, Elliot and Molteno Formations through to fine- to medium-grained sandstones, mudstones, dark-coloured shales and tillite of the Beaufort Group, the Ecca Group and the Dwyka Formation. From 40 km upstream of the confluence to 80 km west of Prieska, the Orange River flows across Vaalian age (2 600 Ma) andesitic lavas of the Ventersdorp Supergroup and dolomite, limestone, chert, banded iron formation and jaspilite of the Vaalian age (2 300 Ma) Griqualand West Sequence. Further downstream to approximately 75 km from the mouth, the Orange River traverses the central zone of the Namaqua Metamorphic Province (2 100 Ma) comprising a succession of complexly deformed medium- to high-grade metamorphosed gneisses (Tankard et al., 1982). The lower-most reaches of the Orange River comprises a succession of phyllite, quartz-chlorite schist, dolomite, acid volcanics, basaltic and andesitic lava, very coarse-grained quartzite and arkose of the Gariep Group (920 - 550 Ma) (Tankard et al., 1982).

In documenting the historical or pre-gauge flood record (prior to 1910) for the Orange River, Van Bladeren (1995) showed that the earliest recorded Orange River flood was in 1804 at Prieska where a discharge of 12 470 m^3/s was calculated using historically recorded flood levels. Additional flood events in 1860, 1873 and 1896 with discharges of 7 290 m^3/s, 13 970 m^3/s and 11 940 m^3/s respectively, were identified (Van Bladeren, 1995). In another account of Orange River flooding, Bremner et al., (1990) in quoting Burchell (1822, p. 390) described an Orange River flood in 1811 as follows:

"...Ibeheld the mouth of the Nu-gariep (Orange River) rolling into the Great River (Vaal River), a rapid and agitated tide of muddy water, swelled to a terrific height, overwhelming the trees on its banks, and thrown into waves by the force of its own impetuous current..."

The start of systematic flow gauging of the Orange River was in 1910 at Prieska. The flood record shows that the Orange River has flooded on several occasions of which the more notable where the floods of 1925 (12 040 m^3/s), 1934 (9 100 m^3/s), 1954 (6 170 m^3/s), 1966 (7 500 m^3/s), 1974 (10 460 m^3/s) and most recently in 1988 (8 760 m^3/s). According to Bremner et al. (1990) and Van Bladeren (1995) the return period of these floods is in the range of 1 in 12 - 1 in 20 years.

In developing a palaeoflood stratigraphy for the Orange River six sites were identified during the reconnaisance phase of this project. Three palaeoflood sites (sites 9, 14 and 19; Zawada and Hattingh, 1993; p. 57, 64 and 74 respectively) were located in the middle reach of the Orange River in a bedrock-controlled reach approximately 27 km downstream of Prieska (referred to as the Prieska palaeoflood sites) (Fig. 3.1). Three further palaeoflood sites (sites upper Xobies, Bloeddrift and lower Xobies; Zawada and Hattingh, 1993; p. 88 and p. 76 refer to the former two sites) were located from the lower reach of the Orange during the reconnaisance phase of the project (referred to as the Richtersveld sites. These sites are bedrock controlled in a 33 km long section of the river situated approximately 70 km from its mouth (Fig. 3.1).

In the following section, the palaeoflood hydrology of the Prieska sites is presented followed by the Richtersveld sites (section 3.3).

3.2 Palaeoflood hydrology of the Prieska palaeoflood sites

3.2.1 Palaeoflood site 9

3.2.1.1 Geological and geomorphological setting

Site 9 is located at longitude 22°38'06" and latitude 29°29'10" on the topocadastral sheet number 2922BC Bloubosfontein (Fig. 3.2) (Zawada and Hattingh, 1993; p. 57). The Orange River at site 9 is steeply incised, flowing in a low-gradient, single low-sinuosity channel across steeply dipping folded strata of the Ghaap Plateau

and Asbestos Hills Formations of the Griqualand West Sequence. The predominant rock types are dolomite, limestone, chert, banded iron formation (BIF) and jaspilite. The Orange River is approximately 100 m - 150 m wide exhibiting in-channel and side-attached sand bars. The density of vegetation is low on the valley sides increasing only on areas immediately adjacent to the river course.

Site 9 is located on the left hand bank (looking downstream in the tributary) in a steeply incised, high gradient (0,036 m/m) unnamed tributary of the Orange River. The catchment area of the tributary is approximately 20 km^2, is bedrock controlled and flows from the Asbestos Hill Plateau cutting through steeply dipping folded strata of the Asbestos Hills Formation of the Griquatown Group which forms part of the Vaalian age Griqualand West Sequence (Geological Map of South Africa, 1984) (Fig. 3.2). The dominant lithology in the tributary catchment is BIF and jaspilite with subordinate dolomite, limestone and chert.

The tributary enters the Orange River at an angle of approximately 90° with the confluence comprising a low lying outwash gravel derived from the tributary catchment. The tributary is approximately 40 m wide comprising a single active channel 5 m - 10 m wide situated on the far left hand side of the tributary (looking downstream) which has incised the tributary gravel infill to a depth of 0,5 m - 0,75 m. Lateral migration of this channel has resulted in exposing a 150 m laterally continuous exposure of interbedded Orange River slack-water sediments and tributary-deposited gravel. The exposure rests on the tributary thalweg which in places, comprises a calcretised gravel containing 2 cm - 20 cm-long clasts. The tributary infill comprises angular - subangular BIF gravel 10 cm - 20 cm in length with some clasts being 40 cm long. Downstream-orientated imbrication was observed where the active channel had incised and exposed vertical sections of the infill.

3.2.1.2 Description and interpretation of the palaeoflood stratigraphy

Site 9 exhibits two major stratigraphic elements. With reference to Fig. 3.3, the one element is situated in a distal position (in relation to the Orange River-tributary confluence) comprising horizontally interbedded gravel and fine- to very fine-grained sand. The second and proximal element exhibits inclined fine-grained sand that onlaps the underlying portion of the horizontally-bedded stratigraphy (Fig. 3.3). These

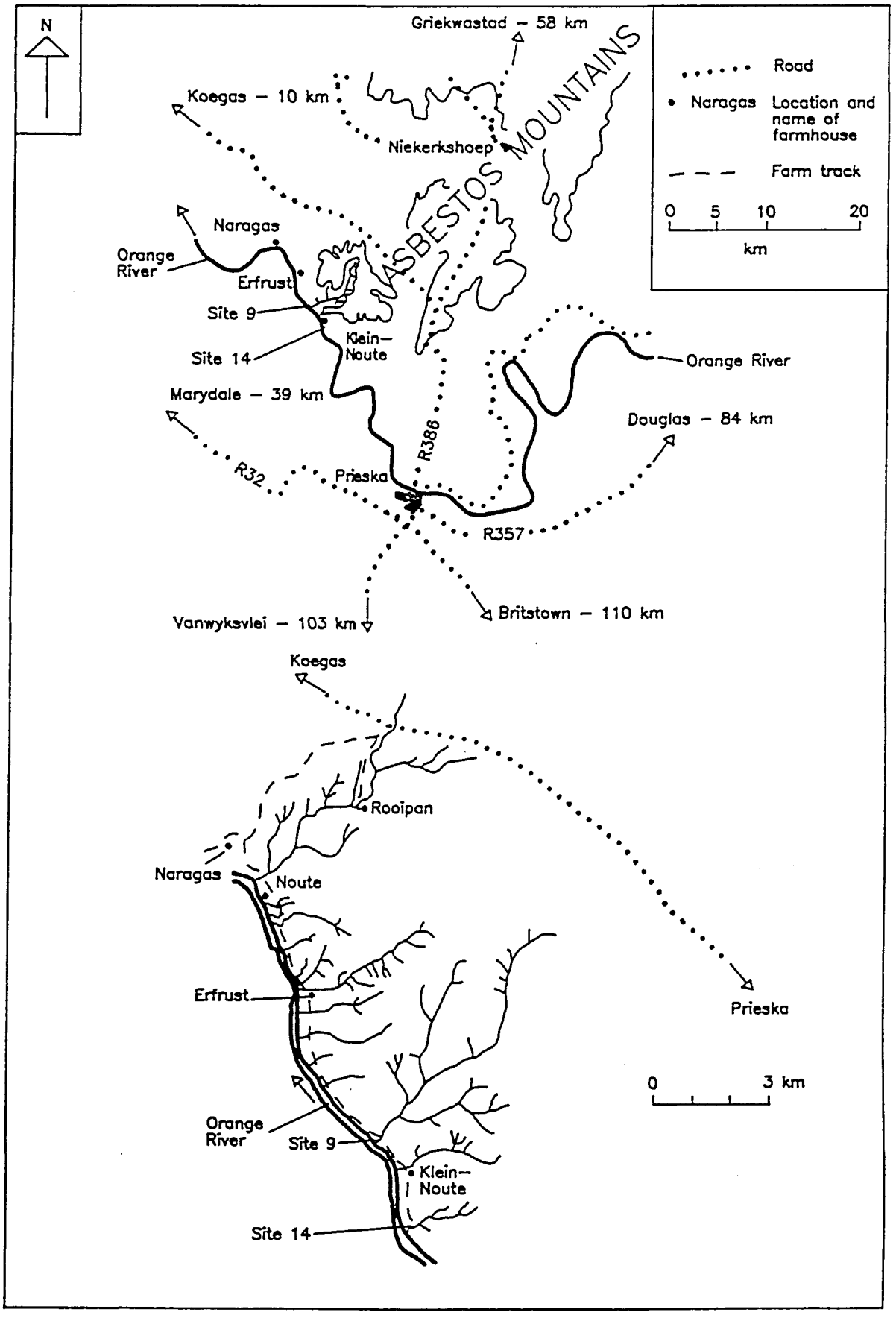

Fig. 3.2 - Location of the Prieska palaeoflood sites 9 and 14.

stratigraphic elements are also distinguished in the field with the proximal sediments exhibiting a darker colour than the distal sediments. Accordingly, site 9 was examined using two sections; namely section 1 and section 2 from which detailed lithological descriptions were recorded (Fig. 3.3). Further sedimentological information was collected and examined using relief peels, of which over 5 m were made primarily from the fine- to very fine-grained sediments. This technique was especially valuable in firstly, confirming the vertical lithological changes recorded in the field and, secondly, in providing information on the nature of bounding contacts, inter-flood hiatuses such as burnt horizons, thin soils and bioturbated units and intra-flood pulses and/or surges which were not readily observed directly from the exposure. Relief peels were also valuable in confirming whether the fine-grained slack-water sediments examined in the field were truly massive. Because the Orange River slack-water sediments are very fine grained and apparently massive in outcrop, relief peels of slack-water sediments is a useful technique in ensuring their comprehensive description and hydrodynamic interpretation.

Section 2. The position of section 2 at site 9 is shown in Fig. 3.3. The total thickness of the section from the base of the tributary thalweg to the point where the very fine-grained sediments pinch out against the valley side of the tributary is 10,80 m. The basal 5 m is best exposed exhibiting a sequence of interbedded gravel and fine- to very fine-grained sand. The overlying 5,80 m comprises mainly fine-grained sand but is poorly exposed. Section 2 exhibits two predominant lithologies, namely angular-subangular gravel with a total thickness of 1,60 m and is compositionally and texturally indistinguishable from the gravel infill of the present day tributary channel. The other dominant lithology is fine- to very fine-grained light-grey brown - tan sand which is texturally similar to sand adjacent to the Orange River channel. Section 2 was examined in detail in order to document the interaction between tributary-deposited gravel and fine-grained slack-water sediments deposited during several phases of Orange River tributary back-flooding. Sedimentological analysis indicates that at least six Orange River palaeofloods have back-flooded the tributary. These are numbered F1 - F6 and are described and interpreted in the following section.

Flood unit F1 is an 8 cm-thick, creamy grey, massive very fine-grained sand

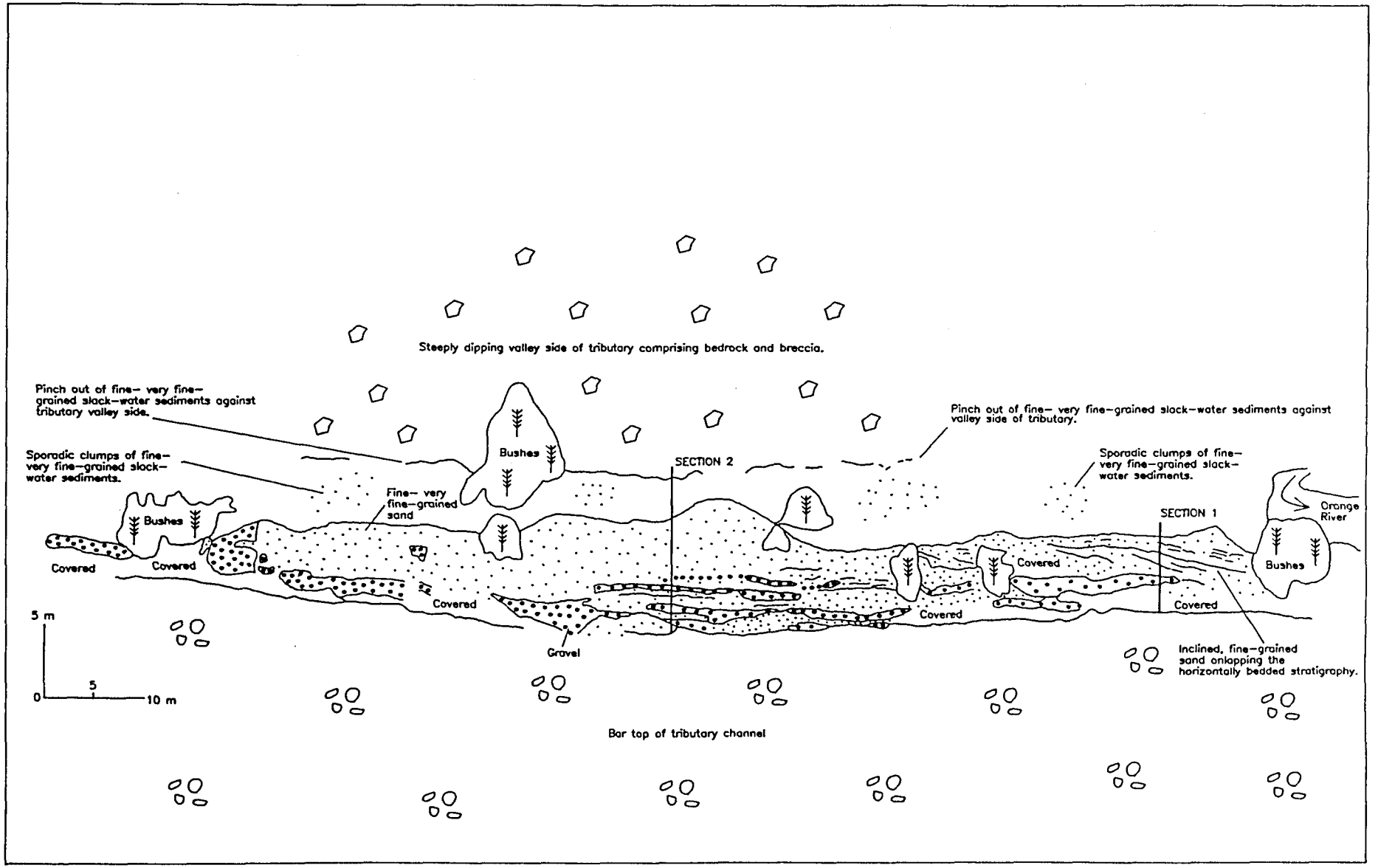

Fig. 3.3 - Sketch from a photo-mosaic illustrating the broad vertical and lateral relationships of the tributary-deposited gravel and the fine- very fine-grained slack-water sediments deposited by back flooding into the tributary during Orange River flooding. Note the positions of sections 1 and 2 for which detailed sedimentary profiles were recorded. Note the onlapping slack-water sediments at section 1.

(unit B; Figs 3.4 and 3.5). Flood unit F1 is stratigraphically situated between two gravel units 50 cm and 44 cm thick (units A and C respectively; Fig. 3.4) both of which exhibit sharp, planar upper and lower contacts (Fig. 3.4). The gravel units contain angular - subangular BIF clasts 0,5 cm - 22 cm in length exhibiting downstream-orientated imbrication with respect to the tributary channel. The gravel units A and C are laterally continuous for a distance of approximately 30 m.

The interpretation of unit B as a palaeoflood slack-water deposit is justified on the basis of its very fine-grained texture which is similar to the present day Orange River sediments and its interbedded position between the gravel units A and C which were deposited by tributary-related flow (Fig. 3.5). The basis for interpreting the gravel units as tributary-deposited sediments is firstly their compositional and textural similarity to the present day infill of the tributary, the downstream-orientated imbrication of clasts and secondly, their angularity suggesting a local source where minimal fluvial transport occurred. The sharp basal and upper contacts of the gravel units, the lack of upward-fining grading indicates that the onset of tributary flow was sudden followed by a rapid waning of flow-regime (Fig. 3.5). Flow was however, sufficiently competent and of a duration to enable the entrainment and imbrication of the clasts.

Flood unit F2 is a 30 cm-thick, brown-grey very fine-grained sand exhibiting either flat-laminated, tan silt lenses (unit D; Figs 3.4 and 3.5) or irregularly-shaped patches of tan silt. The basal 3 cm of unit D is predominantly a fine-grained sand with scattered or floating grains of very coarse-grained sand - angular gravel 0,2 cm - 0,4 cm in length (Fig. 3.4) fining upward into a very fine-grained sand. Overlying unit D is unit E comprising a 6 cm thick, medium-grained reddish-brown sand with angular tan silt clasts 1 cm in length (Fig. 3.4). Unit E is variable grading laterally over centimetres into a gravel.

Flood unit F2 was deposited by the settling out of suspended very fine-grained sand punctuated by intervals during which silt was deposited. Periods of increased flow competency where partial reworking of silt beds and the entrainment of small silt clasts occurred (Fig. 3.5). Further evidence of increased flow regime is observed from the basal 3 cm of unit D where scattered very-coarse-grained sand and gravel were

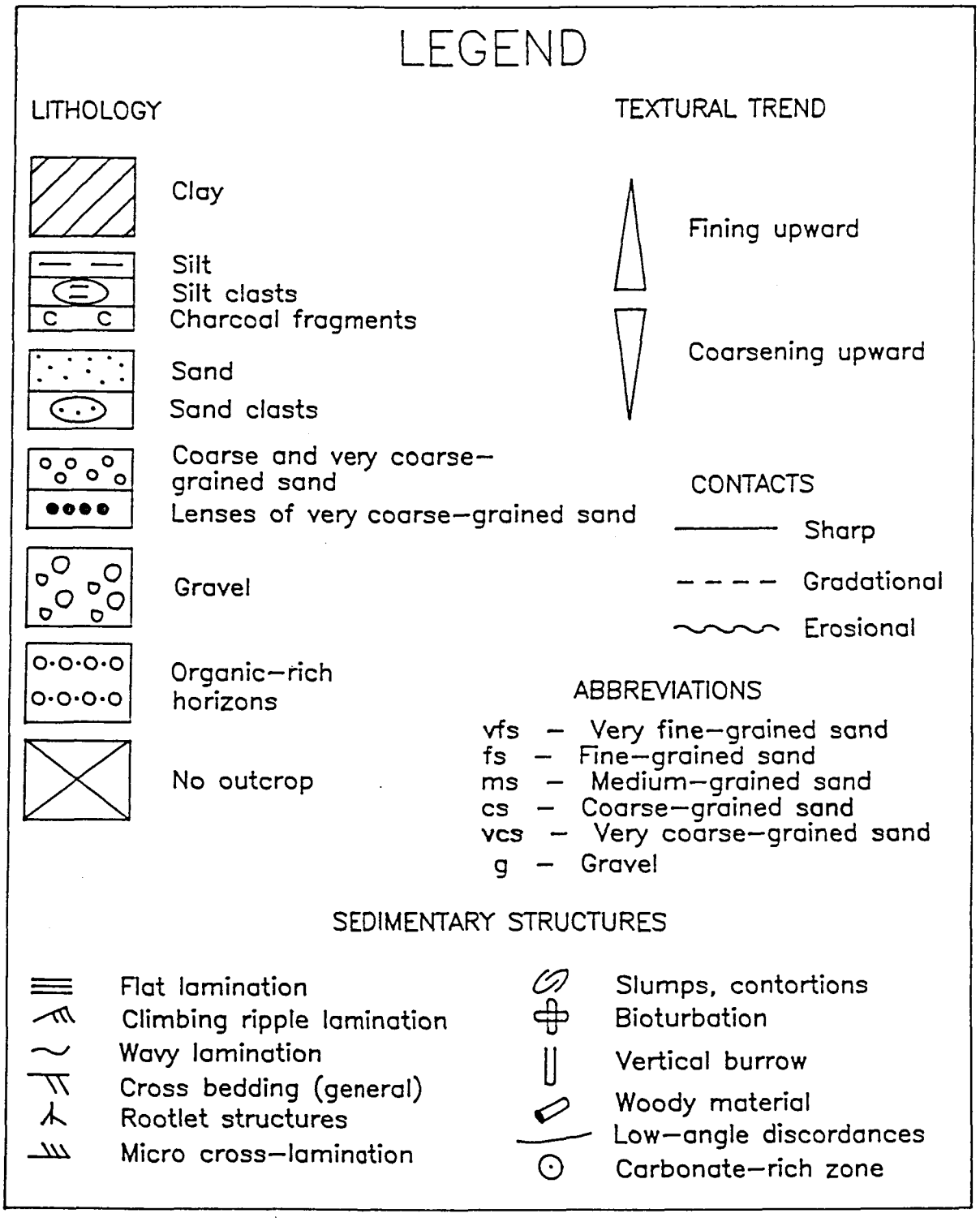

List of symbols used in Figs 3.4 - 3.8, 3.12, 3.15, 3.16, 3.19, 3.20 and 3.21.

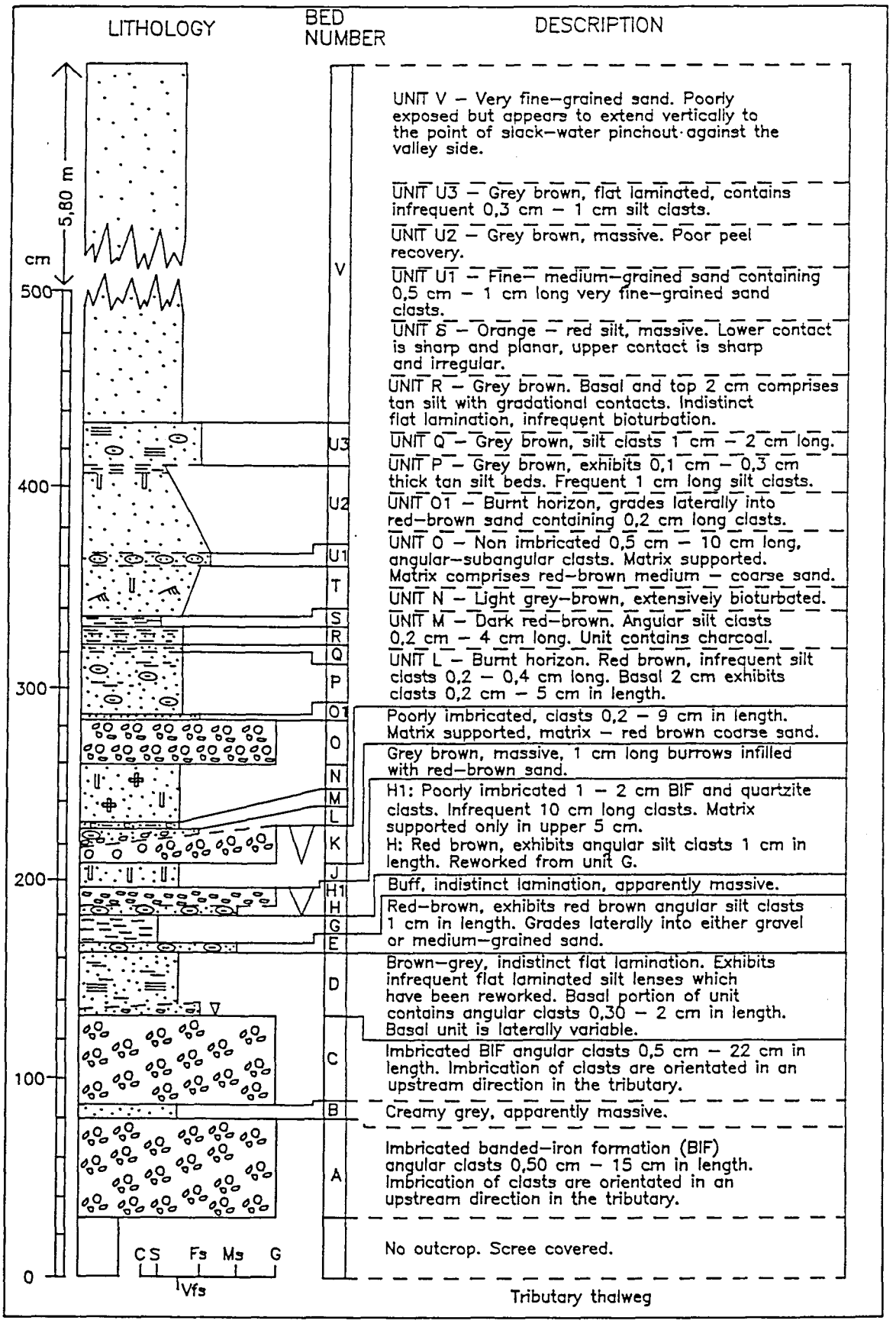

Fig. 3.4 - Lithological description of the slack-water sediments at section 2, site 9 (see legend on page 40).

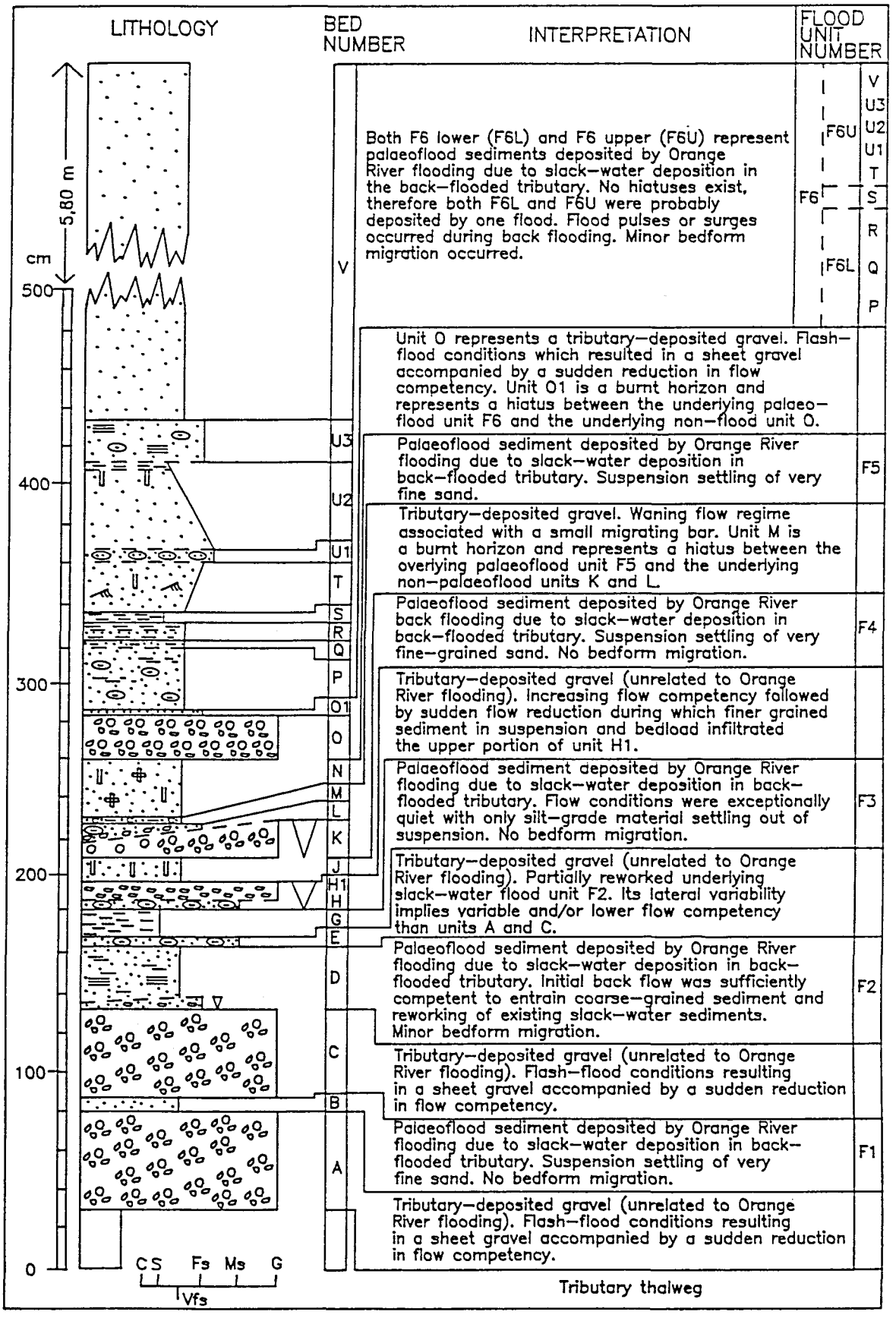

Fig. 3.5 - Hydrodynamic interpretation of the sequence at section 2, site 9 and the subdivision of the stratigraphy into palaeoflood and non-palaeoflood deposited units (see legend on page 40).

entrained, transported and deposited contemporaneously with the very fine-grained sand (Fig. 3.5). Flood unit F2 is interpreted as a slack-water sediment deposited during back flooding in the tributary (Fig. 3.5). This interpretation is justified on the basis of the fine-grained texture of unit D in contrast to the underlying tributary-deposited gravel of unit C (Figs 3.4 and 3.5). A similar contrast is noted between unit D and the overlying coarse-grained sediment of unit E which was also deposited by tributary-related flow. A relief peel taken across the contact between units D and E showed that the contact is gradational. This indicates that unit E had partially reworked unit D resulting in an amalgamation of flood (unit D) and the non-flood deposited unit (unit E). Similar amalgamation was described by Smith (1993) from the Missoula flood slack-water deposits. However, as with flood unit 2, Smith (1993) noted that such amalgamation is local and invariably it was possible by following the contact laterally, to observe a sharp contact between the flood and non-flood deposited sediments.

A significant feature of flood unit F2 and one common to many of the palaeoflood units at site 9, is the significant amount of reworking observed. Attempts to locate examples in the literature of intra-flood reworking from slack-water sediments indicates that this feature has not been previously documented. Even the detailed sedimentological analysis of slack-water sediments by Smith (1993) where some of the slack-water deposits were interpreted to have been deposited from "rapidly moving currents" (Smith 1993, p. 97), did not record evidence of intra-flood reworking. In attempting to explain this feature, consideration was given to reworking by subsequent non-flood processes such as tributary flow. However, in all cases of tributary flow-related deposition from site 9, the reddish-brown colour and coarser-grained texture of the sediments is conspicuous. No evidence of this sediment type was found in any of the partially-reworked palaeoflood units. A more plausible explanation is that reworking was the result of either back-flood flow, during which pulses or surges occurred or was the result of the return back-flow from the tributary as flood-waters in the Orange River subsided.

Flood unit F3 is a 14 cm thick, buff mainly massive silt exhibiting infrequent and indistinct flat lamination and vertical burrows (unit G; Figs 3.4 and 3.5). Unit G is interbedded between the underlying reddish-brown, medium- coarse-grained sand (unit E; Fig. 3.4) and overlying coarse-grained sand and gravel (units H and H1

respectively) (Fig. 3.4).

Flood unit F3 represents a slack-water sediment deposited by suspension settling of silt-grade sediment in quiet-water conditions during tributary back-flooding and subsequent ponding. Both the overlying and underlying units E and H-H1 respectively, represent non-trunk stream flood events deposited during tributary flow.

Flood unit F4 is a 12 cm thick, grey brown, mainly massive very fine-grained sand with infrequent 1 cm long vertical burrows (unit J; Figs 3.4 and 3.5). Flood unit F4 is situated between the underlying gravel units H and H1 and the overlying gravel units K, L and M (Fig. 3.4). Units H and H1 total 14 cm thick of which the basal unit (unit H) is 4 cm thick comprising reddish-brown medium- to coarse-grained sand exhibiting indistinct flat bedding and tan-coloured angular silt clasts 0,5 cm - 1 cm long. In the basal portion of unit H, the silt clasts are preferentially orientated parallel to bedding, progressing upward into a more chaotic orientation at or close to the gradational contact with the overlying unit H1. Unit H coarsens upward into unit H1, comprising angular-subangular, BIF gravel 1 cm - 2 cm in length increasing up to 10 cm with a weakly-developed imbrication. The upper 7 cm of unit H1 contains a finer grained matrix similar to that described and termed by Church et al. (1987) as a filled gravel. The gravel unit (unit K) overlying flood unit F4 is approximately 10 cm thick, comprising angular-subangular BIF, limestone and quartzite clasts up to 9 cm long decreasing upwards to 3 cm. Overlying unit K is a 4 cm - 10 cm-thick, reddish-brown fine- to medium-grained sand with angular gravel clasts 0,2 cm - 5 cm long (unit L; Fig. 3.4). Unit L fines upward into a 4 cm thick, reddish-brown fine-grained sand containing infrequent tan-coloured silt clasts 0,3 cm long and 0,1 cm in diameter carbonate concretions (unit M; Fig. 3.4).

Flood unit F4 (unit J; Fig. 3.5) is interpreted in the light of its stratigraphic position and contrasting lithological characteristics between the underlying units H and H1 and the overlying units K, L and M (Fig. 3.5). The upward-coarsening sequence H-H1 was deposited by tributary flow characterised by an increasing flow regime. Although the basal portion of unit H indicates that flow was not competent to entrain clasts of centimetre size, it was able to entrain silt clasts from the underlying slack-water sediments of flood unit F3. The upward change from preferentially to chaotically

orientated clasts, accompanied by an upward increase in grain size also testifies to an increasing flow regime. The filled gravel feature exhibited in the uppermost portion of unit H1 reflects a waning-flow regime during which suspended and bed-load material infiltrated the gravel (Frostick et al., 1984).

The upward-fining sequence K-L-M (Fig. 3.4) reflects a sudden onset of tributary flow with sufficient competence to entrain and imbricate clasts up to 9 cm long. Gradual flow reduction followed (units L and M) during which fine- to very fine-grained sand settled out of suspension. Units K, L and M together forms a motif similar to that of in-channel tributary bars observed in the present day tributary.

Flood unit F4 represents a slack-water sediment deposited during Orange River flooding and associated tributary back-flow characterised by suspension settling of very fine-grained sand with negligible bedform migration.

Flood unit F5 is a 31 cm thick, light-grey brown, very fine-grained bioturbated sand (unit N; Fig. 3.4). Flood unit F5 is interbedded between the underlying units M, L and K and the overlying gravel unit O (Fig. 3.4). Unit O is a 22 cm thick, matrix supported non-imbricated gravel with 0,5 cm - 10 cm long angular-subangular clasts. The matrix comprises reddish-brown medium- to coarse-grained sand similar to that of units K and H1.

The interbedded position of unit N between the coarse-grained tributary deposited units M, L and K and the overlying unit O indicates that it was deposited as a slack-water sediment characterised by suspension settling of very fine-grained sand during tributary back flooding (Fig. 3.5). Unit O represents a tributary flow-deposited sediment unrelated to Orange River flooding (Fig. 3.5).

Flood unit F6 is approximately 7,30 m thick of which the basal 1,48 m was examined in detail. The remainder was only partially investigated because of poor outcrop. Flood unit F6 was subdivided into a number of lithological units namely, units P, Q, R, S, T, U and V (Figs 3.4 and 3.5). This sequence was then grouped into a lower subsequence (F6L) comprising units P, Q and R and an upper subsequence (F6U) comprising units T, U and V (Figs 3.4 and 3.5). The intervening unit S is

discussed separately to establish its significance as representing a flood hiatus.

Subsequence F6L is 46 cm thick, grey brown, very fine-grained mostly massive sand containing frequent tan-coloured silt clasts and silt beds 0,1 cm - 0,3 cm thick. The silt beds from the basal portion of the subsequence F6L are continuous, whereas in the upper portion are discontinuous having a broken-up appearance. Unit R exhibits gradual upward coarsening from very fine-grained sand to silt followed by gradual fining into silt (Fig. 3.4).

Although detailed description of subsequence F6U could only be obtained from the basal 1 m due to poor outcrop, several upward-coarsening and upward-fining sequences were observed (Fig. 3.4). Much of subsequence F6U comprises fine- to very fine-grained sand with infrequently developed inclined lamination. Because of poor peel recovery it was not possible to identify the lamination as climbing ripple-lamination or contorted lamination due to possibly slumping. Units U1 and U3 (Figs 3.4 and 3.5) contain 0,5 cm - 1 cm long, subrounded very fine-grained - silt clasts.

Unit S is a conspicuous 3 cm thick orangy-red massive silt, interbedded between subsequences F6L and F6U exhibiting a sharp, planar basal contact and a sharp, irregular upper contact (Figs 3.4 and 3.5).

Flood unit F6 is interpreted as a slack-water sediment deposited by tributary back-flow during Orange River flooding. Much of the unit was deposited by suspension settling of fine- to very fine-grained sediment with minor bedform migration. The many upward-fining and upward-coarsening motifs, the partially reworked silt beds and the intraformational silt clasts indicates that flow conditions during back flooding were unsteady. No evidence of tributary-related flow exists either laterally or vertically to account for the reworking. It is therefore suggested that back flooding was characterised by pulses or surges.

Flood unit F6 does not exhibit clear flood hiatuses and is therefore interpreted as representing one flood event. However, attention was given to the possibility that the intervening unit (unit S) between the subsequences F6L and F6U, represents a flood hiatus. Superficially, unit S is similar to the tributary-deposited units in terms of

colour and sharp basal and upper contacts. However, the colour of unit S is intermediate between the reddish-brown sand associated with the non-flood units (i.e units E and H) and the greyish light-brown of the slack-water sediments, implying a mixing of tributary- and trunk-stream derived sediment. Unit S being a silt is considerably finer grained than the tributary-deposited units implying it was deposited by trunk-stream back flooding despite the observation that neither the adjacent or in-channel sediments of the Orange River exhibit a similar colouration. A possible explanation to account for the deposition of unit S is that it was deposited by a back-flow event during which winnowing of silt-grade sediment from the tributary channel and mixing with the suspended sediment derived from the Orange River occurred. This explanation does not account however, for the absence of similar units being present in flood units F1 - F5 which were also deposited by tributary back-flooding.

Section 1. Section 1 is located approximately 40 m downstream in the tributary from section 2 (Fig. 3.3) in a proximal position relative to the tributary-Orange River confluence. As previously mentioned, the sequence of sediments at section 1 were observed to onlap the horizontally-bedded sediments recorded from section 2 with a 20° angle of repose. This clearly indicates that the sediments from section 1 are younger than the horizontally-bedded sediments of section 2. A further indication of possible age differences between sections 1 and 2 is the sediments comprising section 2 are more indurated than those from section 1. These possible chronostratigraphic differences are discussed further in section 3.2.4.

The total thickness of section 1 is approximately 5 m of which 90 cm comprises a gravel, 154 cm a fine- to very fine-grained sand and 256 cm as no outcrop (Fig. 3.6). One flood unit was identified from section 1 (F7) which is described and interpreted below (Figs 3.6 and 3.7).

Flood unit F7 is a dark-grey, fine- to very fine-grained sand with a minimum thickness of 154 cm exhibiting several upward-fining and upward-coarsening motifs (units B1-B4; Fig. 3.6). Although much of the flood unit was noted to be apparently massive when observed in outcrop, the relief peels revealed a number of sharp and gradational contacts that bound units of differing lithological characteristics such as units B2, B3 and B4 (Fig. 3.6). Unit B2 is a 66 cm thick, upward-coarsening, very fine-

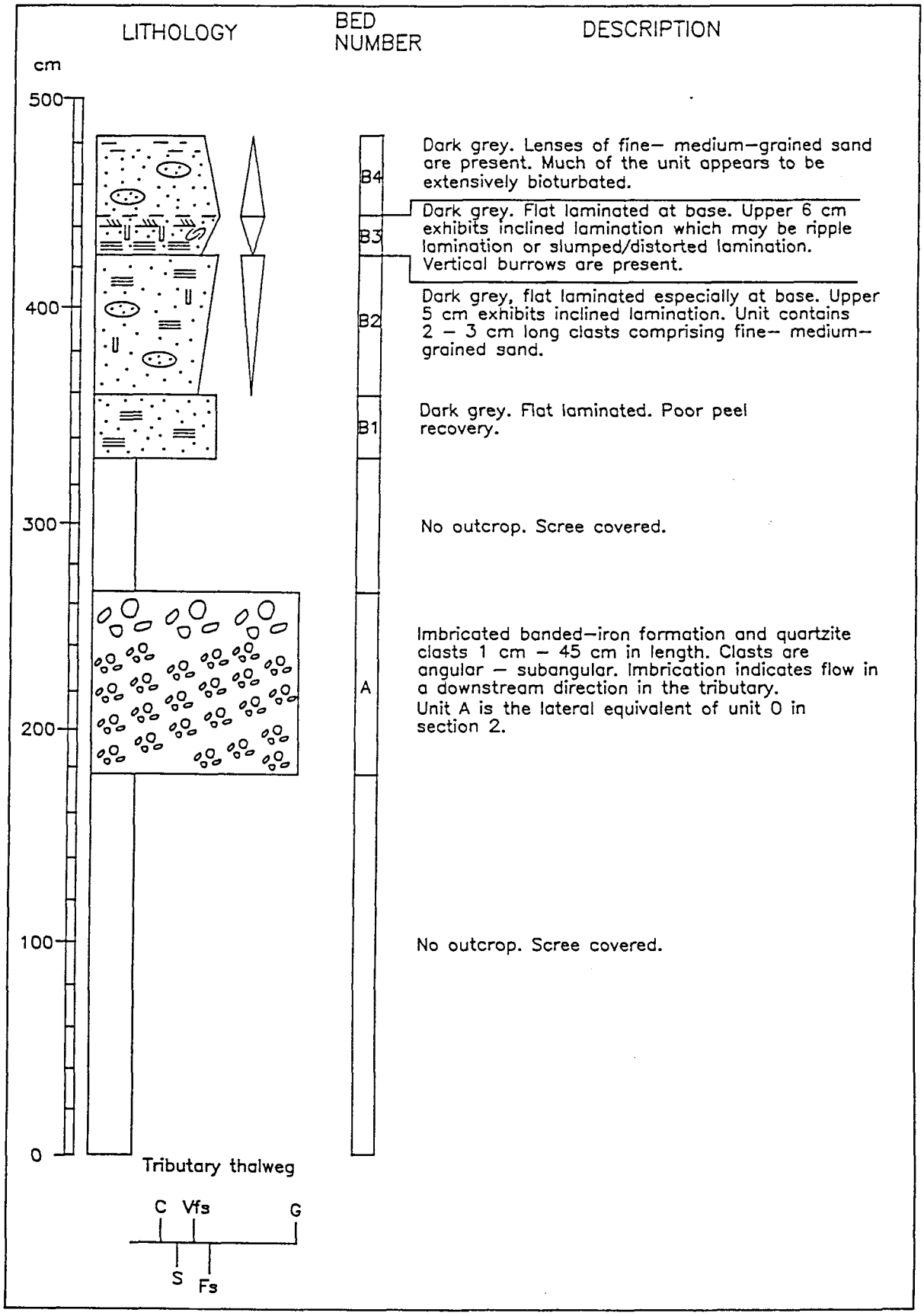

Fig. 3.6 - Lithological description of the slack-water sediments at section 1, site 9 (see legend on page 40).

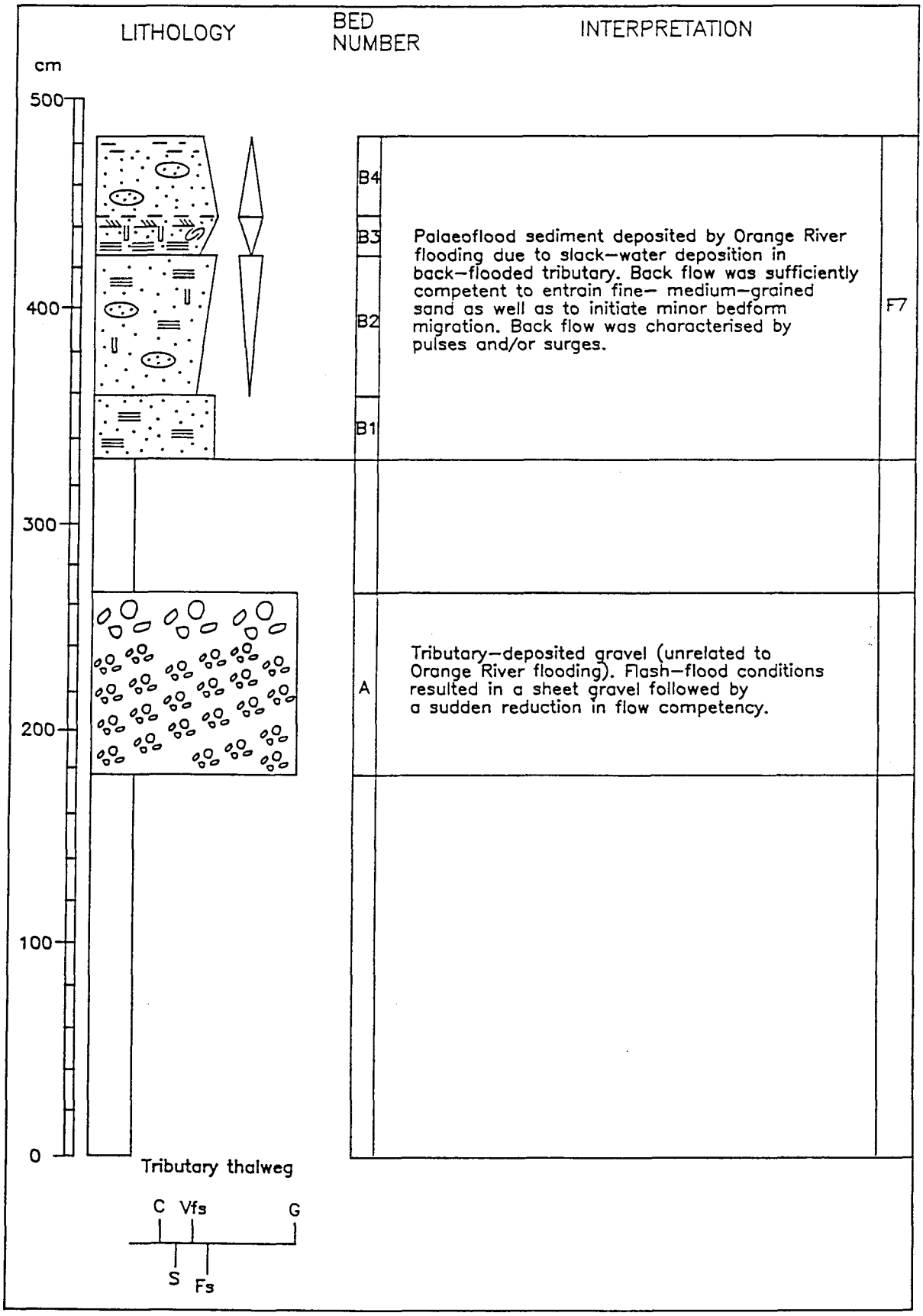

Fig. 3.7 - Hydrodynamic interpretation of the sequence at section 2, site 9 and the subdivision of the stratigraphy into palaeoflood and non-palaeoflood deposited units (see legend on page 40).

grained flat-laminated sand containing 2 cm - 3 cm long fine- to medium-grained clasts. B3 is a 20 cm thick upward-coarsening, very fine-grained sand showing an upward change from flat to cross lamination. Unit B3 has a gradational upper contact with unit B4 which is a 39 cm thick upward-fining very fine-grained sand containing fine- to medium-grained sand lenses. The top 9 cm of unit B4 comprises a light-grey massive silt.

The base of flood unit F7 is covered but in places overlies the gravel unit A (Fig. 3.6). Unit A is a 90 cm thick, imbricated gravel containing 1 cm - 45 cm long, angular-subangular BIF and quartzite clasts with the top exhibiting larger clasts. The orientation of the imbrication indicates a downstream flow direction in the tributary. Unit A was traced in an upstream direction and found to be correlatable with unit O recorded from section 2. This does not imply however, that the overlying flood unit (F7) is therefore correlatable with flood unit F6 at section 2. Unit A is a tributary-deposited unit formed during an increasing flow regime after which flow suddenly ceased.

Units B1-B4 represent slack-water sediments deposited by tributary back flooding during Orange River flooding (Fig. 3.7). Although flood unit F7 does not contain evidence of flood hiatuses, it does however, show changes of sedimentology, reflecting variable stream-power changes during back flow. For example, the gradual upward change from unit B3 to B4 testifies to initial suspension settling through to an increased flow regime where small bedform migration and the entrainment of fine- to medium-grained sand occurred. This was followed by a waning of flow regime during which suspended silt-grade sediment settled out of suspension.

3.2.2 Palaeoflood site 14

3.2.2.1 Geological and geomorphological setting

Site 14 is located at longitude 22°38'37" and latitude 29°30'24" on the topocadastral sheet number 2922DA Prieska (west) (Zawada and Hattingh, 1993; p. 64) approximately 1,5 km upstream of site 9 along the Orange River (Fig. 3.2). Accordingly, the geological and geomorphological characteristics of the Orange River are similar to those described for site 9.

The palaeoflood stratigraphy at site 14 is exposed in a high-gradient, unnamed bedrock-controlled tributary with a catchment size of approximately 1,6 km^2. The tributary enters the Orange River at an angle of approximately 90° with the confluence comprising reworked remnants of an outwash gravel. The tributary thalweg varies between 3 m - 5 m in width comprising angular - subangular BIF, jaspilite, dolomite, limestone and chert clasts 2 cm - 20 cm in length. Above the point of slack-water pinch out, the tributary exhibits a low-sinuosity becoming more sinuous as it passes through the slack-water sediments closer to the tributary - Orange River confluence. This is ascribed to sedimentary infilling of the tributary by Orange River flood(s) followed by episodic tributary flow during which, the thalweg course was established in response to the varying lithologies of the slack-water sediments. Two major exposures (sections 1 and 2) are present at site 14 for which detailed sedimentological descriptions and interpretations were made.

3.2.2.2 Description and interpretation of the palaeoflood stratigraphy

Section 1. Section 1 is approximately 6,6 m thick being exposed over a lateral distance of approximately 20 m. It is situated 100 m - 150 m from the Orange River - tributary confluence. Nine relief peels covering the basal 4 m of the section were made.

Section 1 exhibits seven palaeoflood units deposited by Orange River slack-water deposition (F1 - F7). These units are interbedded with coarse-grained sand and gravel originating from the tributary catchment and deposited during tributary flow. The palaeoflood stratigraphy rests on a 24 cm thick, light-grey, calcretised fine-grained sand (unit B; Fig. 3.8). A relief peel through the upper portion of unit B indicates it is extensively bioturbated with a distinctive mottled appearance. Lighter-coloured areas are present where infiltration and precipitation of calcium carbonate occurred. Unit B lies directly on the tributary channel thalweg comprising angular clasts up to 25 cm in length.

Flood unit F1 is 60 cm thick comprising units C, D, E, F and G (Fig. 3.8). The upper bounding surface of flood unit F1 is marked by unit H (Fig. 3.8) comprising either a 2 cm - 6 cm thick gravel with angular clasts 1 cm - 3 cm in length, or a very coarse-grained sand. Flood unit F1 is a grey fine-grained sand that fines upwards into

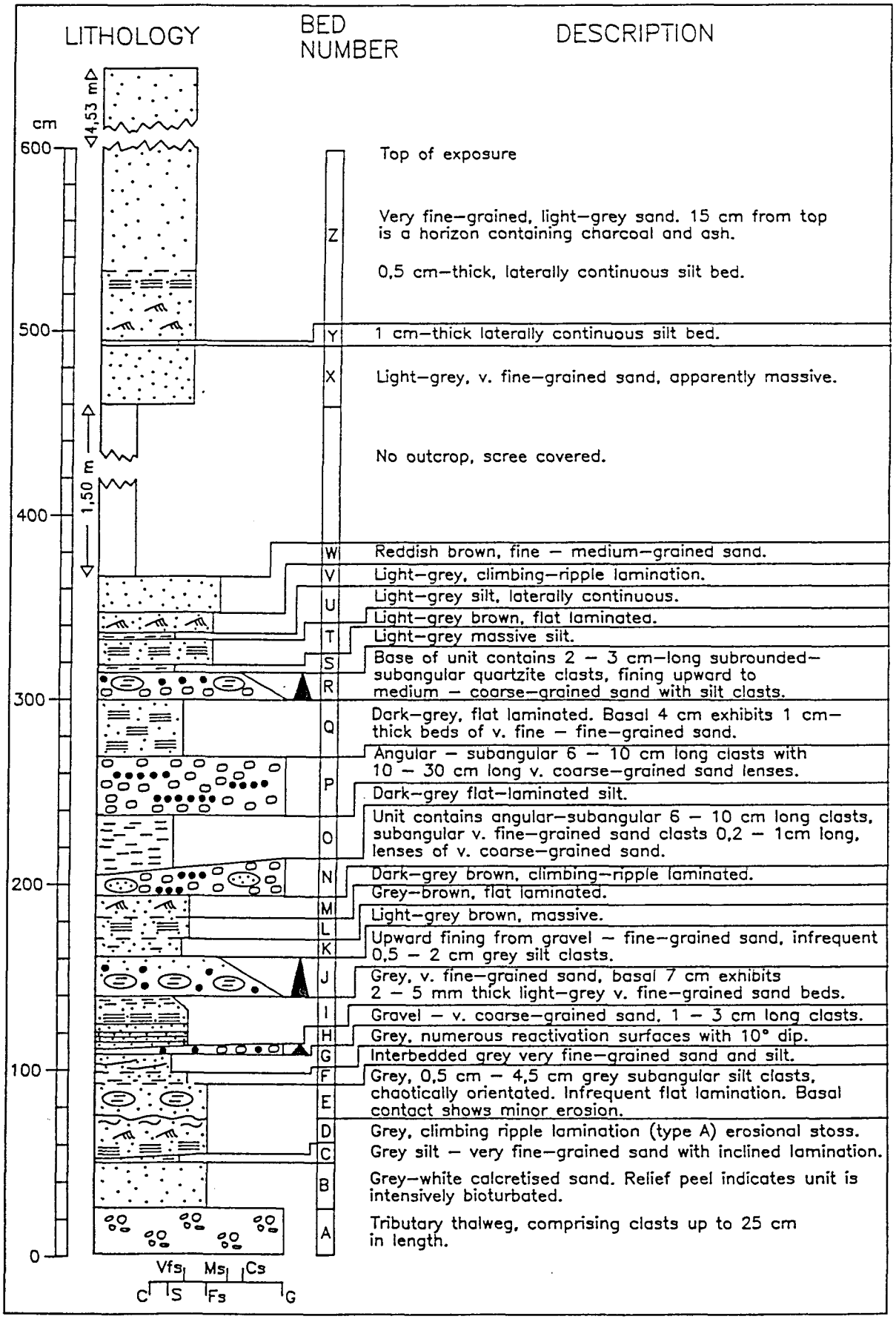

Fig. 3.8 - Lithological description of the slack-water sediments at section 1, site 14 (see legend on page 40).

a very fine-grained sand - silt. The basal portion of flood unit F1 (units C and D; Fig. 3.8) exhibits flat lamination abruptly changing to climbing-ripple lamination of the type described by Ashley et al (1982) as type A erosional stoss climbing-ripple lamination (Fig. 3.9). The climbing ripple sets are between 3 cm - 7 cm thick and are orientated in an upstream direction in the tributary. The angle of climb is variable between 5° - 15°. The climbing-ripple lamination passes into wavy lamination through to flat lamination. The upper 4 cm of unit D exhibits broken or disarticulated laminae

Fig. 3.9 - Relief peel of climbing-ripple lamination from flood unit F1 at site 14. Note the abrupt change from inclined lamination to climbing-ripple lamination. This reflects a sudden increase in rates of suspension settling and flow regime during which small ripples migrated from right to left. The detail exhibited by the relief peel was not observed in outcrop.

Fig. 3.10 - Relief peel of intraformational angular - subangular silt clasts set in a matrix of fine-grained sand from flood unit 1 at site 14 (bed E; Fig. 3.8). Back flooding was characterised by pulses during which partial reworking of existing slack-water sediments occurred. Note that the detail exhibited by the relief peel was not observed in outcrop.

Fig. 3.11 - Relief peel of moderately shallow reactivation surfaces from the top of flood unit F1 at site 14 (bed G; Fig. 3.12). Note the overlying angular quartzite gravel (bed H) which represents tributary flow deposition followed by slack-water deposition of fine-grained sand during backflooding of the tributary as the Orange River flooded (flood unit F2). The reactivation surfaces reflect periodic increases of flow regime during back flooding.

grading upwards into unit E (Fig. 3.8) comprising a 16 cm-thick fine-grained sand containing subangular silt clasts 0,2 cm - 4 cm in length (Fig. 3.10).

Unit E is gradationally overlain by a 4 cm thick bed (unit F) exhibiting interbedded silt and very fine-grained sand with the 1 cm thick silt beds being partially broken. Unit F fines upward into a 10 cm thick very fine-grained sand - silt (unit G) exhibiting flat lamination traversed by numerous low-angle (10°) reactivation surfaces (Fig. 3.11).

Flood unit F1 is interpreted as a slack-water deposited unit in view of its fine-grained texture, its interbedded position between the basal tributary thalweg sediments and unit H which were deposited during tributary flow (Fig. 3.12). In addition, the orientation of the climbing ripples indicates that back flow occurred in an upstream direction in the tributary. Relief peels through flood unit F1 indicate that hydrodynamic conditions were variable. For example, the change from flat lamination (unit C) to climbing-ripple lamination to wavy lamination through to flat lamination (unit D), indicates an upward increase in flow regime from suspension settling with negligible bedform migration, through to bedform migration with suspension settling. This was followed by a gradual decrease in flow regime where only suspension settling occurred (Fig. 3.12). Unit E indicates that back flooding was sufficiently competent to entrain silt clasts probably from an existing palaeoflood unit. An alternative explanation is that unit E was deposited by tributary flow unrelated to Orange River back-flooding. However, unit E does not contain any tributary-derived sediment as well as the observation, that the basal contact with the underlying unit D is gradational. A further indication of back-flow pulses or increased flow competency during slack-water deposition, are the shallow dipping reactivation surfaces present in unit G.

Flood unit F2 is approximately 29 cm thick (unit I; Fig. 3.8) comprising grey, very fine-grained sand - silt. The basal 7 cm exhibits 0,2 cm - 0,5 cm thick light-grey fine-grained sand beds decreasing in frequency upwards. A relief peel through unit I indicates that the basal portion is flat laminated with the remainder being massive. Flood unit F2 is overlain by a sharply-based 20 cm thick gravel fining upwards into a poorly sorted coarse- to very coarse-grained sand (unit J; Fig. 3.8). The basal 4 cm of

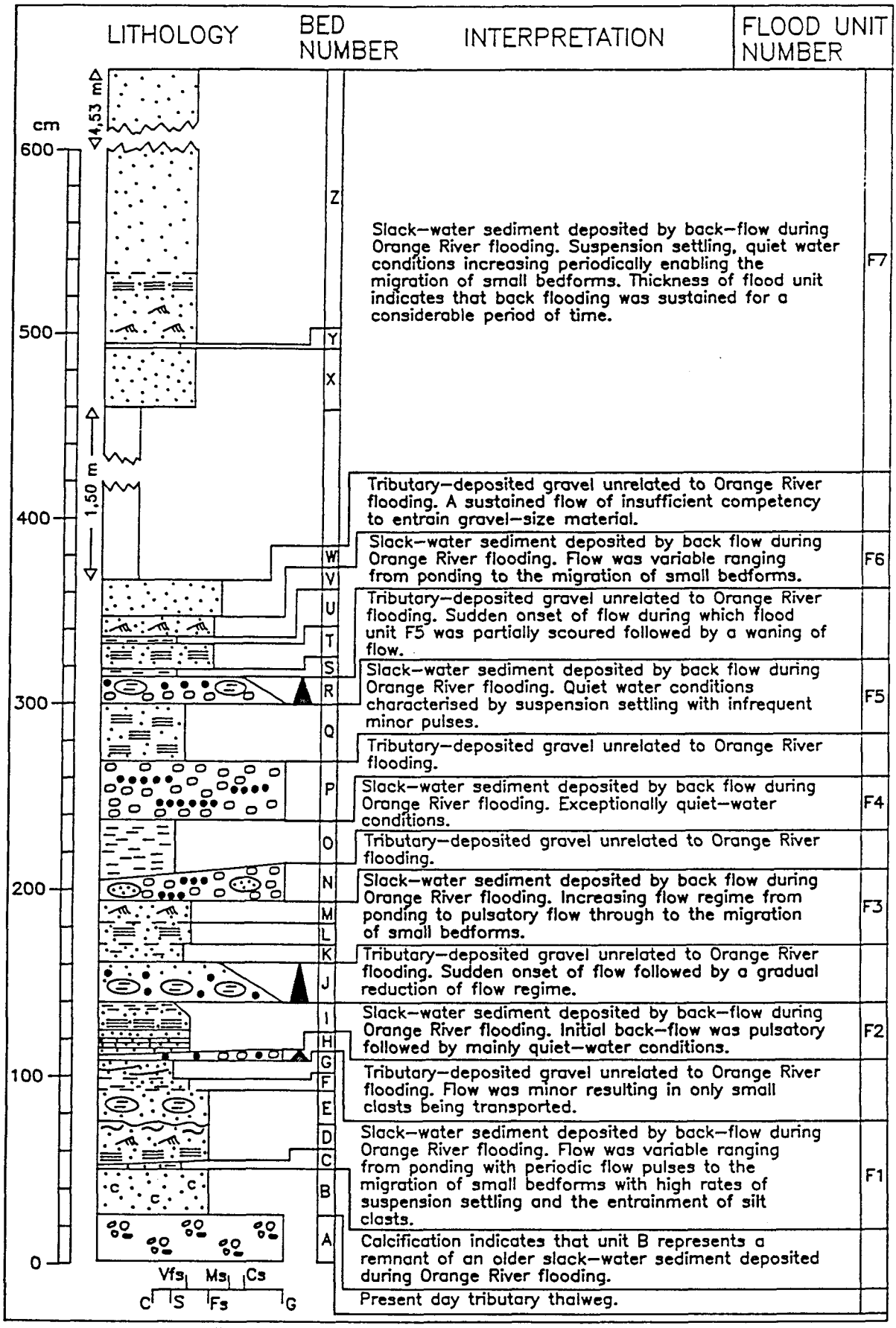

Fig. 3.12 - Hydrodynamic interpretation of the sequence at section 1, site 14 and the subdivision of the stratigraphy into palaeoflood and non-palaeoflood deposited units (see legend on page 40).

unit J contains 0,5 cm - 1 cm long angular clasts grading upwards into a very coarse-grained sand containing infrequent 0,2 cm - 0,5 cm long, grey fine-grained sand clasts.

The fine-grained texture of flood unit F2 and its interbedded position between the overlying and underlying coarse-grained units J and H respectively, indicates that it was deposited by suspension settling of very fine-grained sand - silt during back flow of the tributary as the Orange River increased in stage (Fig. 3.12). The basal portion of flood unit F2 indicates that initial back flow was pulsatory followed by exceptionally quiet water conditions during which rapid suspension settling occurred (Fig. 3.12). The coarse-grained units overlying and underlying flood unit F2 (units J and H respectively) represent deposition by tributary flow (Fig. 3.12). This interpretation is based upon their contrasting texture compared to flood unit F2 and their compositional similarity to the present day sediment found in the tributary thalweg. The reduced size of clasts in units J and H compared to the present day tributary thalweg clasts suggests that tributary flow was relatively small in terms of competence.

Flood unit F3 is a 34 cm thick, grey, very fine-grained sand - silt coarsening upward into a dark-grey fine-grained sand (units K, L and M; Fig. 3.8). The basal contact of flood unit F3 is sharp with the underlying gravel unit J (Fig. 3.8) as well as the upper contact with the overlying gravel unit (unit N; Fig. 3.8). A relief peel through flood unit F3 shows that the basal portion of flood unit F3 (unit K) is a massive very fine-grained sand - silt coarsening upwards into a tan, flat laminated very-fine grained sand (unit L) through to a dark-grey brown, climbing-ripple laminated fine-grained sand (unit M) (Fig. 3.8). The overlying gravel unit (unit N), is 10 cm - 20 cm thick comprising angular - subangular limestone and BIF clasts 6 cm - 10 cm in length. The unit also contains subangular very fine-grained sand clasts 0,2 cm - 1 cm in length and very coarse-grained sand lenses.

Flood unit F3 represents a slack-water sediment deposited by tributary back-flow during Orange River flooding (Fig. 3.12). This interpretation is justified on the basis of its interbedded position and contrasting textural characteristics between the overlying and underlying gravel units N and J respectively. Depositional conditions during back flow were characterised by a gradually increasing flow regime. Initial back flow was dominated by suspension settling of silt-grade material changing to pulsatory

flow (flat lamination; unit L) through to an increase in flow regime where migration of small bedforms together with rapid suspension settling of fine-grained sand occurred (unit M; Fig. 3.12).

Flood unit F4 is a 33 cm-thick, dark-grey brown flat-laminated silt (unit O; Figs 3.8 and 3.13). Flood unit F4 differs markedly from flood units F1, F2, F3, F5, F6 and F7 as it exhibits a finer grain size. The overlying unit (unit P) is a 30 cm-thick gravel containing angular-subangular clasts 1 cm - 13 cm in length and 10 cm - 30 cm long lenses of very coarse-grained sand. The basal contact of unit P is sharp. The base of flood unit F4 is sharp being underlain by gravel unit N (Figs 3.8 and 3.13).

Fig. 3.13 - Relief peel of flood unit F4 at site 14 comprising dark-grey flat-laminated slack-water-deposited silt interbedded between the underlying and overlying non palaeoflood-deposited gravels (beds N and P; Fig. 3.12). The basal gravel comprises intraformational silt - very fine-grained sand clasts and angular - subangular limestone and BIF pebbles.

Flood unit F4 is interpreted as a slack-water sediment deposited by tributary back-flow during Orange River flooding (Fig. 3.12). As with flood units F1, F2 and F3, this interpretation is justified on the basis of its interbedded position and contrasting textural characteristics between the overlying and underlying tributary-deposited gravel units P and N respectively. Depositional conditions during back flow were characterised by suspension settling of silt-grade material.

Flood unit F5 is a 33 cm thick, dark-grey brown, mainly massive silt - very fine-grained sand (unit Q; Fig. 3.8). Unit Q has a sharp lower contact with the gravel unit P and a sharp upper contact with the gravel unit R (Fig. 3.8). A relief peel through unit Q shows that the basal 4 cm of unit Q exhibits 1 cm-thick beds of interbedded very fine-grained sand and flat laminated fine-grained sand. The remaining portion of unit Q is mainly massive with infrequent faint flat lamination. The upper contact of flood unit F5 is sharp and locally erosive. Unit R is a 14 cm thick, poorly sorted upward-fining gravel (Fig. 3.8). The basal portion of unit R contains 2 cm - 3 cm long subangular - subrounded quartzite clasts fining upward into medium- to coarse-grained sand with frequent 2 cm - 7 cm long dark-grey, fine-grained, sub-rounded - rounded sand clasts. Of particular significance is an in situ 8 cm thick by 4 cm wide flat laminated, dark-grey, fine-grained flat laminated sand occurring in unit R (Fig. 3.14).

Flood unit F5 is interpreted as a slack-water sediment deposited by tributary back-flow during Orange River flooding (Fig. 3.12). Flow conditions were characterised by ponding where suspension settling of silt and very fine-grained sand occurred. The massive and homogenous nature of flood unit F5 with infrequent flat lamination, indicates that any pulsatory or unsteady flow was minimal during back flooding. A relief peel through unit Q and the overlying gravel (unit R) suggests that erosion or reworking of the upper portion of flood unit F5 occurred during periodic tributary-flow (unit R). This is supported on the basis of numerous large silt - very fine-grained sand clasts, the erosive nature of the upper contact of unit Q and the presence of an in-situ remnant of sediment similar to that of unit Q in the overlying gravel (Fig. 3.14). Because an unknown thickness of flood unit F5 may have been removed by tributary flow, the palaeoflood stage indicated by the top of flood unit F5 represents therefore, an absolute minimum value.

Flood unit F6 is a 32 cm thick mainly light-grey, fine-grained sand comprising units T, U and V (Fig. 3.8). The basal 3 cm of flood unit F6 comprises a light-grey silt coarsening upwards into a bioturbated and flat-laminated fine-grained sand (unit T).

This in turn is overlain by a light-grey laterally continuous silt (unit U; Fig. 3.8). Overlying unit U is a 12 cm thick, light-grey, fine-grained cross-laminated sand (unit V; Fig. 3.8). Flood unit F6 is overlain by a 20 cm thick, laterally continuous, reddish-brown fine- to medium-grained sand similar to that noted from site 9.

Fig. 3.14 - Relief peel of the non-palaeoflood deposited gravel (bed R; Fig. 3.12) comprising medium- to coarse-grained sand and very fine-grained intraformational sand clasts up to 7 cm long. Note the large, flat-laminated fine-grained sand clast in the bottom right of the peel. This indicates that significant reworking of existing slack-water sediments occurred during the deposition of bed R.

Flood unit F6 is interpreted as a slack-water sediment deposited by back flow during Orange River flooding (Fig. 3.12). This interpretation is based upon the fine-grained texture of units T, U and V which are interbedded between the tributary deposited overlying reddish-brown sand of unit W and the underlying gravel unit R. The tributary-deposited unit capping flood unit F6 (unit W) is different to the

underlying tributary deposited units in terms of colour and a finer-grained texture. However, similar sediments were positively identified as tributary-derived sediment representing the waning stage of a tributary flow from site 9, unit L (Fig. 3.4). Flow conditions for flood unit F6 were variable ranging from suspension settling of primarily silt-grade material through to increased flow competency resulting in the development and migration of small bed forms. The pulsatory nature of flood unit F6 is indicated by the two light-grey silt units at the base of unit T and unit U (Fig. 3.12).

Flood unit F7 is a light-grey very fine-grained sand with a minimum thickness of 5,95 m (units X, Y and Z; Fig. 3.8). Although the basal contact of flood unit F7 was not observed because of poor outcrop, it was inferred that flood unit F7 immediately overlies the reddish-brown tributary-deposited sand of unit W. Approximately 1,42 m of flood unit F7 exhibited sufficient outcrop for examination. The overlying 4,53 m was however, poorly exposed, occurring as isolated clumps of sediment with little vertical and lateral continuity. Although portions of flood unit F7 exhibits climbing ripple and flat lamination, much of the unit appeared to be massive. Approximately 15 cm from the top of the main exposure is a laterally persistent 1 cm - 2 cm thick bed containing charcoal and ash. In addition, two distinctive laterally persistent clay beds were observed from flood unit F7 (Fig. 3.8).

The textural similarity of flood unit F7 to that of sediments closer to the Orange River and its contrasting textural characteristics to that of the underlying tributary-deposited gravel (unit W; Fig. 3.8) indicates that flood unit F7 represents a slack-water sediment deposited by tributary back-flow during Orange River flooding Fig. 3.12). Of significance is that flood unit F7 is the thickest of all the palaeoflood units described and interpreted at site 14. Specifically, it is 16 times thicker than the average thickness of 37 cm for flood units F1 - F6. The limited sedimentological data available from this flood unit indicates that flow was variable characterised by mainly suspension settling of very fine-grained sand, punctuated by periods of small bedform migration and ponding where only silt-grade material was deposited. Because flood unit F7 extends vertically to the point of slack-water pinch out against the bedrock of the Orange River valley, it represents the highest palaeoflood stage for site 14.

Section 2 is a 7,19 m thick sequence of mainly very fine-grained sand located

approximately 30 m downstream from section 1. Section 2 is therefore situated in a more proximal position with respect to the tributary - Orange River confluence than section 1. Section 2 differs to that of section 1 as it does not exhibit interbedded, tributary-deposited coarse-grained sand and/or gravel which were interpreted in section 1 as palaeoflood hiatuses. The absence of non-flood, tributary deposited sediment does not imply however, that section 2 contains no palaeoflood stratigraphy comprising one or more palaeoflood events. An equally likely explanation is that section 2 was located in a position outside or distal to active tributary deposition. A detailed sedimentological investigation was therefore done for section 2 in order to identify possible palaeoflood slack-water deposited sediments.

The entire exposure at section 2 is interpreted as being deposited by slack-water deposition during tributary back flow as the flood stage of the Orange River increased. This interpretation is justified on the similarity in texture and colour of the sediments to that of flood-deposited sediments found immediately adjacent to the Orange River thalweg and those examined and interpreted as slack-water sediments in section 1 and at site 14. Two flood units (F1 and F2) were identified from section 2 and are described and interpreted in the following section.

Flood unit F1 is inferred to be 3,90 m thick with the basal 1,40 m being covered by scree (Fig. 3.15). The flood unit is a grey, flat laminated, very fine-grained sand exhibiting laterally continuous sharp and non-channelised planar contacts (units A, B, C, D, E and F; Fig. 3.15). At none of the contacts was there any evidence of either non-flood sediments such as coarse-grained sand and/or gravel or mudcracks and intense bioturbation.

Flood unit F2 was deposited by mainly suspension settling of very fine-grained sand during slack-water flow conditions punctuated by slight increases of flow regime (Fig. 3.16). The numerous sharp contacts denote sudden cessation of suspension settling during back-flow followed by the equally sudden onset of suspension settling.

Flood unit F2 is a 3,29 thick, buff, mainly very fine-grained sand exhibiting flat and wavy lamination and climbing-ripple lamination and subordinate, laterally continuous silt beds and partings (units F, G, H, I, J, K, L, M, O, P, Q, R and S; Fig.

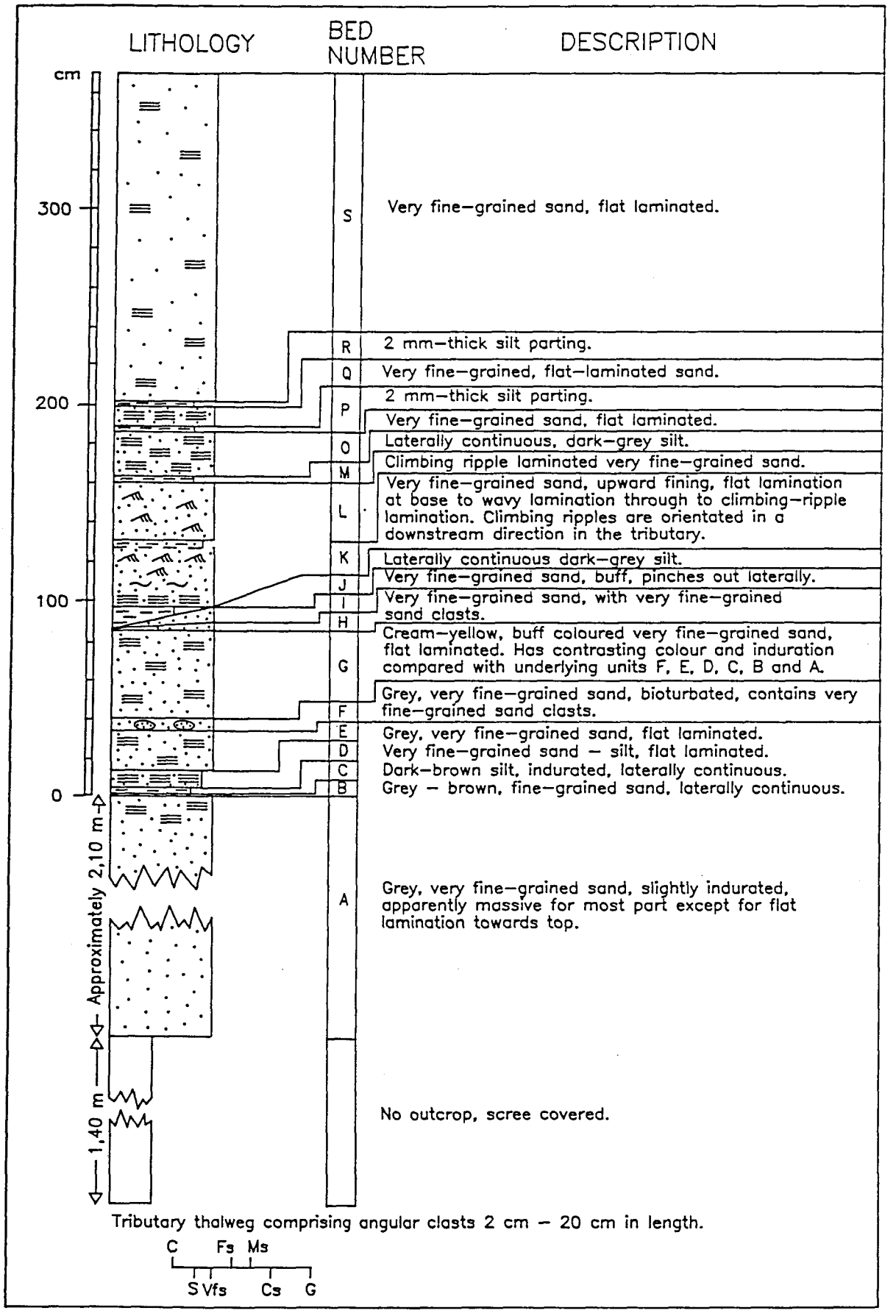

Fig. 3.15 - Lithological description of the slack-water sediments at section 2, site 14 (see legend on page 40).

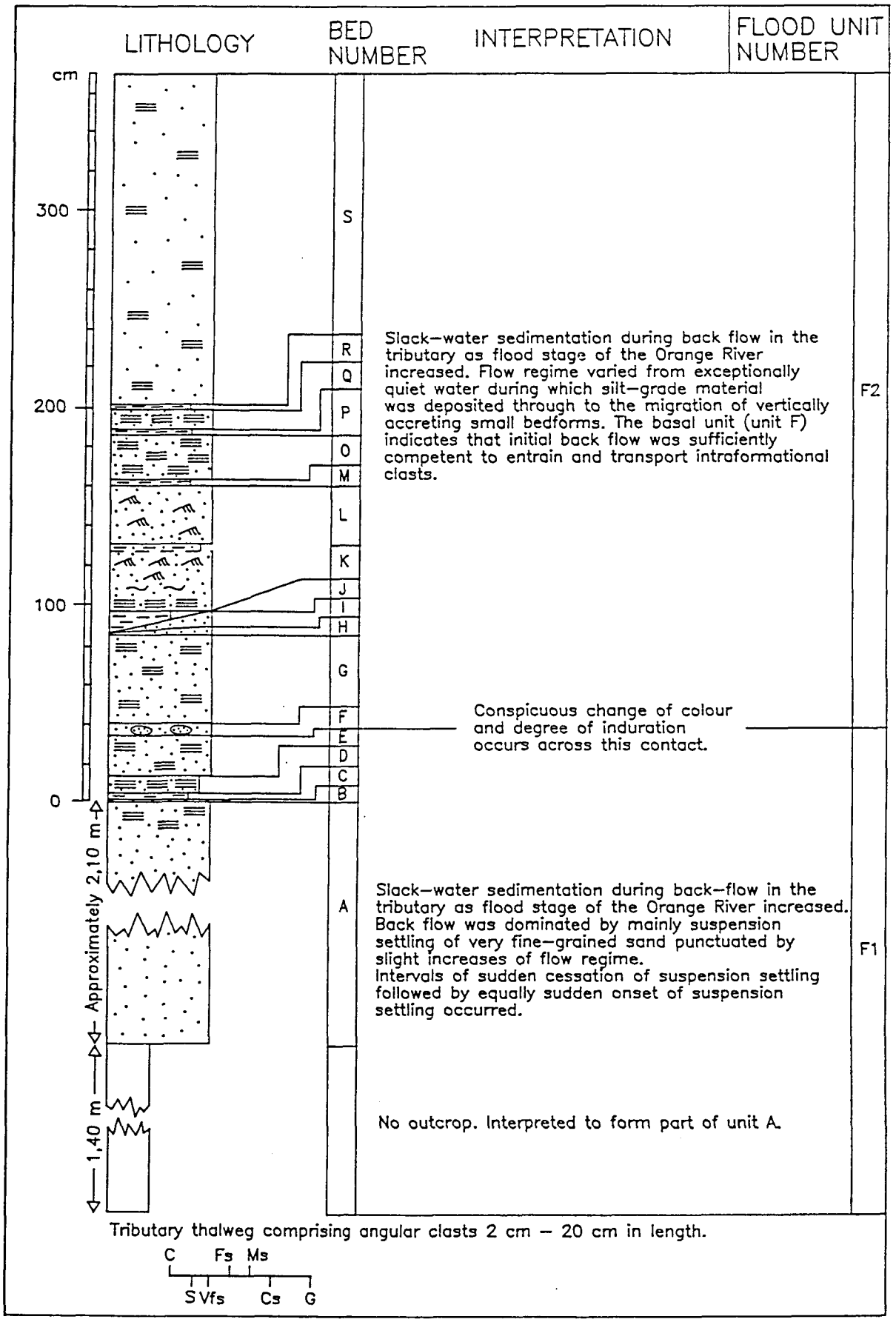

Fig. 3.16 - Hydrodynamic interpretation of the sequence at section 2, site 14 and the subdivision of the stratigraphy into palaeoflood and non-palaeoflood deposited units (see legend on page 40).

3.15). The base of flood unit F2 was taken at the base of unit F (Fig. 3.15) which is a very fine-grained sand containing numerous 0,20 cm - 0,5 cm-long angular very fine-grained sand clasts. Although unit S forms the top of flood unit F2 at section 2, its thickness as measured and illustrated in Fig. 3.15 (1,65 m), represents a minimum thickness. Unit S appears to be similar to the thick slack-water flood unit F7 (units X, Y and Z; Fig. 3.8) documented from section 1. It is therefore likely that unit S from section 2 has a greater thickness and, as with flood unit F7, also extends vertically to the point of slack-water pinch out against the bedrock valley side of the Orange River.

Although flow conditions during the deposition of flood unit F2 was characterised by mainly suspension settling of very fine-grained sand, it differed to that of flood unit F1 in that the flow regime was more variable and of a higher competence. Evidence of variable flow regime is exhibited in unit K where the gradual change from flat to wavy lamination through to climbing ripple lamination indicates a gradual increase of flow regime. Specifically, the basal flat-laminated zone of unit K indicates suspension settling of very fine-grained sand punctuated by slight increases of flow competency. This was followed by an increase of flow regime to form wavy lamination, which in turn was overlain by climbing ripple lamination as flow increased still further resulting in the formation and migration of small vertically accreting bedforms. Further indications of sudden flow change are given in units J, M, P and R that represent deposition in exceptionally quiet water conditions where only silt-grade material settled out of suspension.

The subdivision of section 2 into flood units F1 and F2 was made on the basis of a distinctive colour change at the top of unit F from a grey to a buff colour and the conspicuous difference in induration between the two flood units. Flood unit F1 is considerably more indurated that flood unit F2, so much so that swallows have exploited this difference making their nesting holes only in flood unit F2. The change of induration at the top of unit F1 (Fig. 3.15) is interpreted to reflect a difference in age between flood units F1 and F2. Further evidence supporting the subdivision of section 2 into two flood units, is the presence of intraformational very fine-grained sand clasts from unit F (Fig. 3.15). The single occurrence of these clasts in section 2 and the hydrodynamic implication that the overlying flood unit F2, back-flowed into the tributary with sufficient competency to entrain and transport these clasts from the

underlying slack-water unit, indicates that the bedding plane between unit E and F represents a flood hiatus (Fig. 3.16). Although the outcrop at section 2 was not sufficiently extensive to observe a possible onlapping relationship between flood units F1 and F2, the colour change and difference of induration at the top of unit F1 is similar to that observed at site 14 where the sediments at section 1 were observed to onlap a horizontally bedded palaeoflood stratigraphy (Fig. 3.3). It is tentatively suggested that on the basis of sedimentary features, a correlation of flood units F1 and F2 between section 2 at site 14 and section 1 at site 9 can be made.

3.2.3 Palaeoflood site 19

3.2.3.1 Geological and geomorphological setting

Site 19 is located at longitude 22°24'39" and latitude 29°24'37" on the topocadastral sheet 2922AD Koegasbrug (Zawada and Hattingh, 1993; p. 74) approximately 29 km downstream of site 9 (Fig. 3.17). Although site 19 is located on the outside bank of a broad meander, the river for the most part exhibits a low sinuosity (Fig. 3.17). The river is approximately 250 m wide with gently sloping valley sides comprising scattered outcrops of shale, siltstone and subordinate lenses of sandstone and riebeckitic jaspilite of the Vaalian age (2 620 - 2 070 Ma) Naragas Formation of the Ghaap Group (Griqualand West Supergroup) (Prieska geological map, in press). Between and overlying basement outcrops occur extensive deposits of terrace gravel extending in places from the margin of the Orange River to approximately 100 m above the present water level. Although these terrace gravels were inferred to be of Quaternary age according to the Prieska geological map, De Wit (1993) in citing Partridge and Brink (1967), stated that the oldest and highest terrace gravels (90 m above the Orange River) in the lower reaches of the Vaal River catchment are of Pliocene age.

The density of vegetation is low on the valley sides comprising infrequent small 10 cm - 20 cm high bushes increasing in areas immediately adjacent to the Orange River thalweg to large bushes and trees up to 5 m high.

The palaeoflood stratigraphy at site 19 is located in a high gradient (0,019 m/m), 40 m-wide, single channelled, low sinuosity, unnamed tributary of the Orange River. The tributary enters the Orange River with a junction angle of

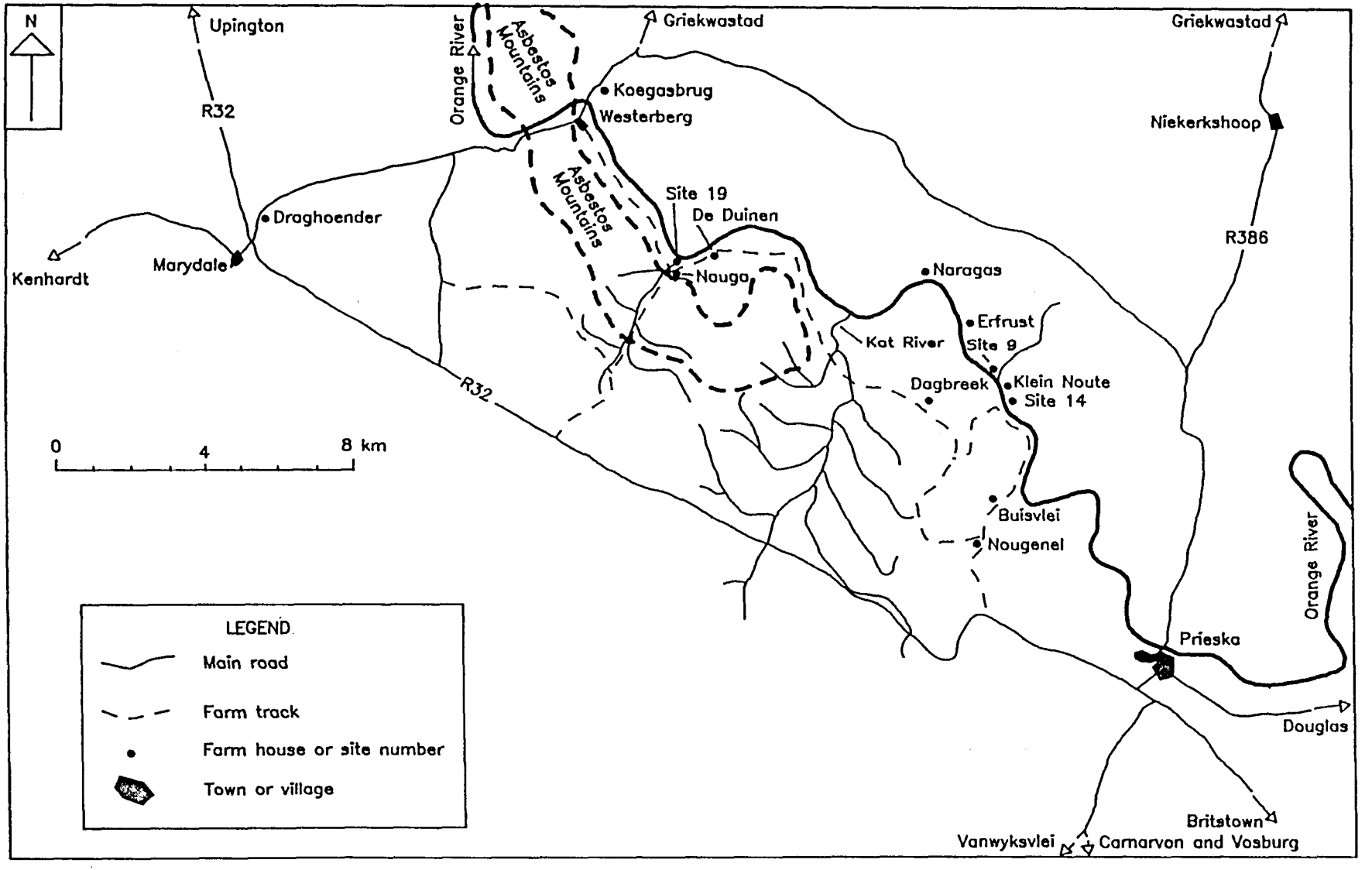

Fig. 3.17 - Location map showing the position of site 19 in relation to sites 9 and 14 and Prieska.

approximately 90°. The catchment area of the tributary is approximately 75 km^2 draining a portion of the north-west - south-east striking Asbestos Mountains. These mountains comprise steeply dipping interbedded dolomite and limestone with interbedded chert, banded ironstone, brown jaspilite, diabase, shale and siltstone of the Vaalian age Griqualand West and Olifantshoek Supergroups (Prieska geological map, in press). The uppermost reaches of the tributary drainage basin flows across red, wind-blown sand of the Quaternary age Gordonia Formation (Kalahari Group) (Prieska geological map, in press). The tributary is ephemeral, bedrock controlled for the most part with the thalweg containing subangular - subrounded 3 cm - 30 cm-long clasts. The tributary channel for the most part is devoid of vegetation and flat. However, closer to the tributary - Orange River confluence, longitudinal bars 20 m - 30 m long and 60 cm thick are present comprising a basal gravel overlain by a 10 cm - 20 cm thick coarse-grained reddish-brown sand.

3.2.3.2 Description and interpretation of the palaeoflood stratigraphy

Two profiles, located 130 m and 80 m from the tributary - Orange River confluence (sections 1 and 2 respectively) were examined and are presented in the following section.

Section 1. Section 1 is located on the right hand bank of the tributary (looking downstream in the tributary) comprising a 7,62 m thick sequence of interbedded gravel, reddish-brown coarse- to very coarse-grained sand and light-grey fine- to very fine-grained sand (Fig. 3.18). This sequence overlies a patchily developed, calcified, grey, fine grained sand that rests on the base of the tributary channel. The exposure is approximately 30 m long enabling the differentiation and tracing of the individual sedimentary units in an upstream direction in the tributary. Six relief peels totalling 3,24 m were made mainly from the finer grained sediments. A description of the exposure and the relief peels from section 1 indicated the existence of five palaeoflood units (F1 - F5).

Flood unit F1 in outcrop appears to be a 12 cm thick very fine-grained grey sand (unit C; Fig. 3.19), similar in colour and texture to previously described slack-water sediments from sites 9 and 14. However, a relief peel of unit C shows that although patches of grey very fine-grained sand occurs, much of the unit contains fine-

grained reddish-brown sand with frequent 0,1 cm - 0,2 cm-long angular shale clasts (Fig. 3.19). In other areas of the outcrop, unit C comprises exclusively grey, apparently massive very fine-grained sand. Although unit C is lithologically variable when traced laterally, it can be traced throughout the entire exposure exhibiting no stratigraphic change with respect to its underlying and overlying sedimentary units. Underlying unit C is a 1,20 m-thick sequence (units A and B; Fig. 3.19) of imbricated, subrounded BIF

Fig. 3.18 - Sequence of interbedded slack-water deposited light-grey fine- to very fine-grained sand and non-palaeoflood tributary-deposited gravel at section 1, site 19. Shovel for scale is approximately 90 cm long.

and limestone gravel clasts 0,5 cm - 15 cm long (unit A). The imbrication direction of clasts from unit A indicate a consistent down-stream direction in the tributary. Unit A also exhibits 10 cm thick, reddish-brown very coarse-grained sand beds with 1 cm-long clasts (Fig. 3.19). Unit A fines upward into a 14 cm thick, poorly sorted, reddish-brown fine- to medium-grained sand with 0,1 cm - 3 cm long, angular shale and limestone clasts (unit B; Fig. 3.19). Light-grey, 5 cm long calcareous nodules are also

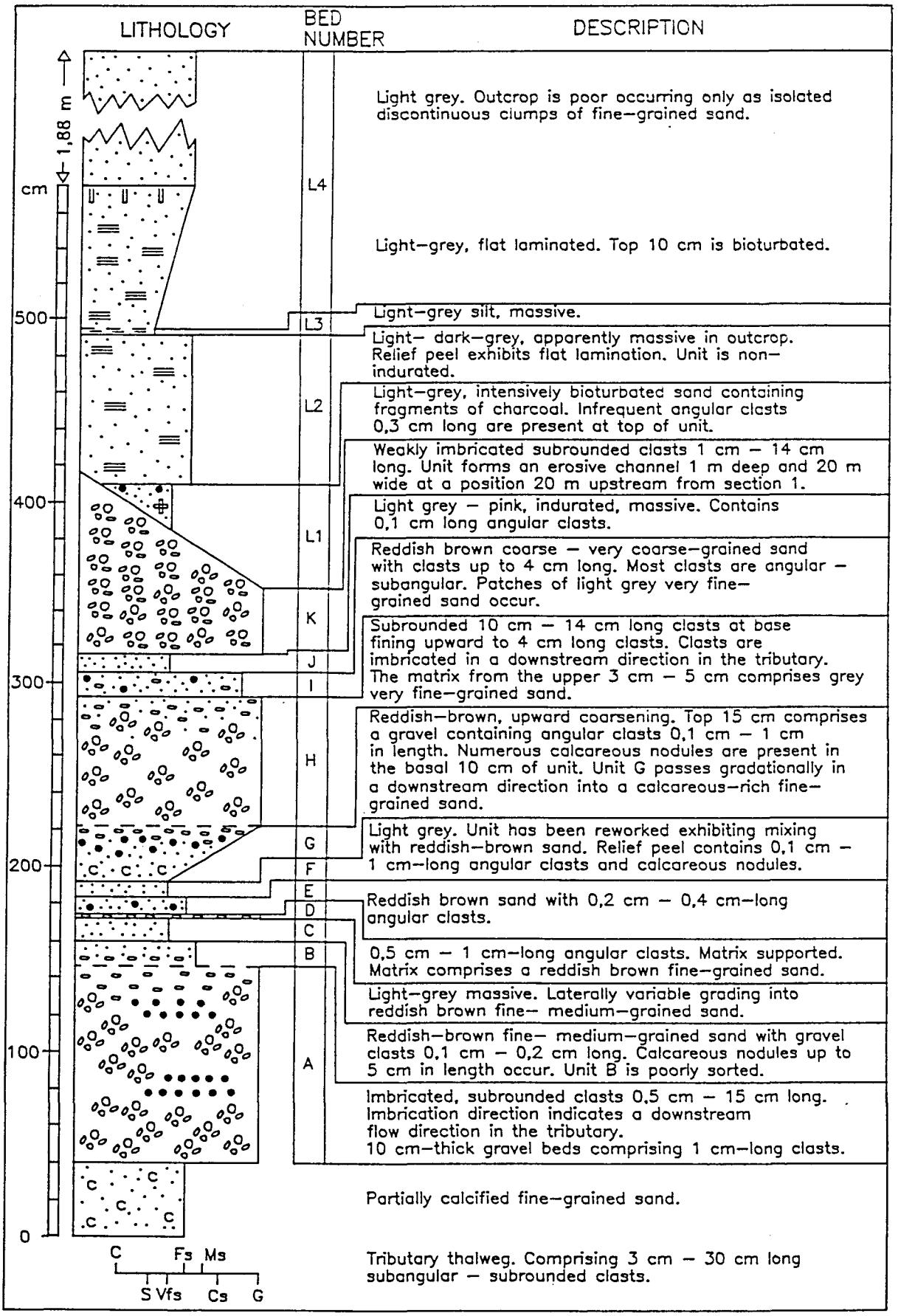

Fig. 3.19 - Lithological description of the slack-water sediments at section 1, site 19 (see legend on page 40).

present. Both the nodules and the clasts are matrix supported. Overlying unit C with a sharp basal and upper contact is a 2 cm thick matrix-supported gravel where the matrix comprises reddish-brown fine-grained sand containing 0,5 cm - 1 cm long angular clasts (unit D; Fig. 3.19). Unit D is overlain by a 10 cm thick, reddish-brown fine-grained sand containing 0,2 cm - 0,4 cm long angular clasts (unit E; Fig. 3.19).

The interpretation of unit C as a possible palaeoflood slack-water sediment deposited by tributary back flooding is problematic as it exhibits features indicative of both back-flooding and deposition by tributary-related flow. In establishing the depositional environment of unit C requires, therefore, the interpretation of the underlying and overlying units A - B and D - E respectively. The gravel texture, its upward-fining motif and downstream-directed imbrication of clasts in units A - B indicates the formation and migration of a bar as a result of tributary-related flow (Fig. 3.20). Further confirmation of this interpretation is the upward fining motif and the reddish-brown fine- to medium-grained sand of unit B which was also noted from in-channel longitudinal bars from the present day tributary-channel thalweg. The reddish-brown sand from unit B allied to the upward fining direction from unit A to B indicates a gradual waning of flow regime. The source of the reddish brown sand is from the headwaters of the tributary catchment comprising red wind-blown sand of the Gordonia Formation. Temporary storage of this sediment may have occurred as a pore filling matrix in the upper portions of the tributary gravel which was entrained during tributary flow. Units D - E are also interpreted as having been deposited during tributary-related flow similar to the interpretation suggested for units A - B, except that units D - E were deposited in lower flow-regime conditions perhaps of a shorter duration than units A - B (Fig. 3.20).

The interbedded position of unit C between the tributary-deposited units A - B and D - E, the presence of patchily developed grey, very fine-grained sand which does not occur as a tributary flow-deposited sediment, suggests that it was deposited as a slack-water sediment during tributary back flooding as the stage of the Orange River increased (Fig. 3.20). The patchily developed, very-fine-grained slack-water deposits is not thought to be a primary depositional feature of slack-water deposition, but rather the result of post-depositional erosion by tributary-flow, possibly related to the formation and deposition of the overlying units D - E. Because an unknown

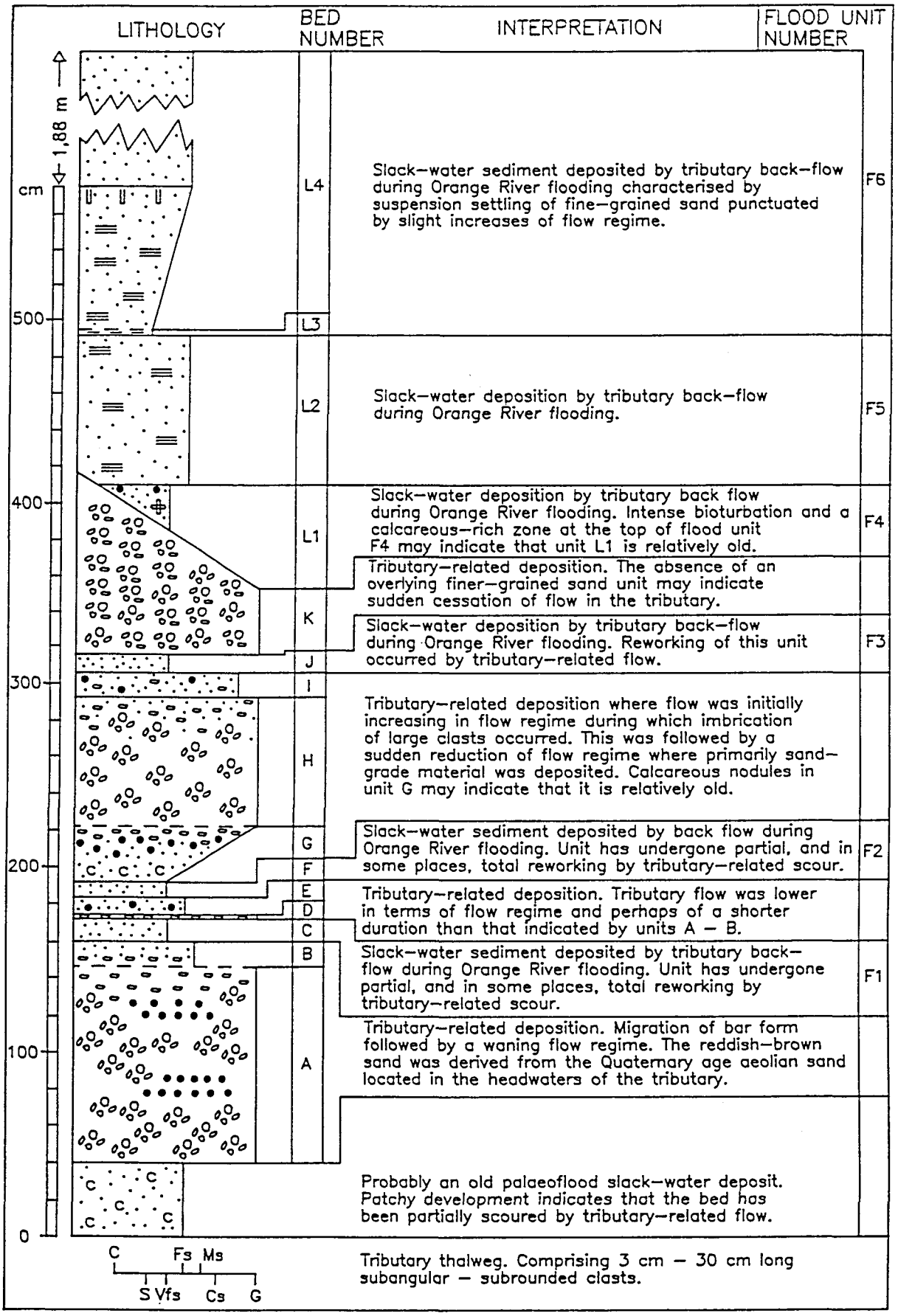

Fig. 3.20 - Hydrodynamic interpretation of the sequence at section 1, site 19 and the subdivision of the stratigraphy into palaeoflood and non-palaeoflood deposited units (see legend on page 40).

thickness of unit C was removed by scour, it can therefore only represent a minimum palaeoflood stage.

Flood unit F2 is an 8 cm thick, light-grey patchily developed fine-grained sand (unit F; Fig. 3.19) underlain by units D - E and overlain by units G, H and I. A relief peel through unit F indicates that the unit can also comprise a reddish-brown fine- to medium-grained sand containing 0,1 cm - 0,3 cm long angular shale clasts and 0,2 cm - 0,4 cm-long calcareous nodules. The overlying unit G is a 30 cm thick reddish-brown fine-grained sand that coarsens upward into a gravel containing angular clasts up to 1 cm long (Fig. 3.19). The basal 10 cm of unit G contains calcareous nodules up to 1 cm long. Unit G exhibits an upper gradational contact with the overlying unit H which is a 70 cm thick, clast supported, upward-fining gravel containing imbricated, 10 cm - 14 cm long subrounded clasts at the base decreasing upwards to 2 cm - 5 cm (Fig. 3.19). Unit H is overlain by a 14 cm-thick, mainly reddish brown, very coarse-grained sand with subordinate angular - subangular clasts up to 4 cm long (Fig. 3.19).

The interpretation of flood unit F2 (unit F) as a palaeoflood slack-water sediment deposited by tributary back-flooding is justified on the basis of its contrasting colour and textural differences to that of the overlying and underlying units (units D - E and G - I respectively) (Fig. 3.20) and its similarity with flood-deposited sediments located immediately adjacent to the Orange River. The patchily developed nature of flood unit F2 as with flood unit F1 is ascribed to tributary-related scour. Consequently, flood unit F2 can only be used to provide an absolute minimum palaeoflood stage for the palaeoflood concerned. The overlying sequence (units G - I) testifies to deposition by tributary-related flow that was initially increasing in flow regime (unit G) to a point where large clasts were transported and became imbricated (unit H), followed by a reduction of flow regime where mainly coarse-grained sand material was deposited (Fig. 3.20). The occurrence of calcareous nodules in unit G may indicate either a period or ongoing process of calcrete formation indicating that the underlying flood unit F2 is of a considerable age.

Flood unit F3 is a 10 cm thick, light-grey - pink, apparently massive fine-grained sand (unit J; Fig. 3.19). During the preparation and study of a relief peel through unit J showed that in some locations, unit J is indurated containing 0,1 cm long angular

clasts. Unit J is stratigraphically located between the underlying sequence of units G - I, and the overlying unit K comprising a 10 cm - 37 cm thick imbricated upward-fining gravel exhibiting subrounded clasts 1 cm - 14 cm long (Fig. 3.19). The imbrication direction of clasts was noted to be downstream orientated in the tributary. Unit K when traced 20 m laterally in an upstream direction in the tributary was observed to form a channel shape with a maximum depth and width of 1 m and 20 m respectively.

Flood unit F3 is interpreted as a palaeoflood slack-water deposit due to tributary back flooding with the same justification to that used for flood units F1 and F2 (Fig. 3.20). As with flood units F1 and F2, flood unit F3 is also patchily developed and in some cases has been almost totally reworked by tributary-related flow as indicated by the pinkish colour of the unit (Fig. 3.19) and the presence of coarser-grained sediment. Because of evidence indicating reworking and therefore the possibility that an unknown thickness of unit J was removed, the palaeoflood stage indicated by unit J represents therefore, a minimum value.

Flood unit F4 is a 26 cm thick light-grey, intensively bioturbated, mottled very fine-grained sand containing fragments of charcoal (unit L1; Fig. 3.19). Unit L1 exhibits a sharp basal and upper contact and is stratigraphically positioned between the underlying tributary-deposited gravel unit, unit K and the overlying light - dark-grey, flat-laminated, infrequently bioturbated fine-grained sand unit, unit L2 (Fig. 3.19). A relief peel through units L1 and L2 shows that a calcareous-rich horizon together with infrequent angular clasts up to 0,3 cm occurs at or next to the contact between units L1 and L2.

The differentiation of unit L1 as a palaeoflood slack-water deposited sediment is based firstly on its contrasting colour and textural characteristics with the underlying tributary-deposited gravel unit, unit K (Fig. 3.20). Secondly, the contrasting colour, the finer texture and intense bioturbation of unit L1 to that of the overlying unit, unit L2, and the presence of rare angular clasts at the top of unit L1 indicates that L1 represents a discrete palaeoflood-deposited sediment (Fig. 3.20). It is important to note that the differentiation of flood unit L1 from the apparently similar overlying similar sediments of unit L2 could not have been made without a relief peel through units L1 and L2. In particular, the subtle difference in colour, the contrasting degree

of bioturbation, and the existence of a sedimentary contact between these two units would not have been identified from inspection of the exposure alone.

Flood unit F5 comprises an 81 cm thick, light - dark-grey, flat-laminated non-indurated fine-grained sand (unit L2; Fig. 3.19). The upper and basal contacts of unit L2 are sharp and although not readily observable in outcrop, can be easily recognised using a relief peel. The unit overlying unit L2 is a distinctive 2 cm thick light-grey massive silt (unit L3; Fig. 3.19) that coarsens upward into a light-grey fine-grained sand (unit L4; Fig. 3.19).

The interpretation of unit L2 as a flood unit is justified on the basis of firstly its basal contact with the palaeoflood hiatus comprising a sharp planar contact with rare angular clasts and, secondly, its upper contact which is sharp with the overlying silt unit, unit L3. Although no unequivocal evidence exists at the base of unit L3 of a palaeoflood hiatus such as a gravel or reddish-brown sand-grade material, the overlying sediments of unit L4 are sufficiently different in terms of texture and upward-coarsening motif to indicate that both units L2 and L4 represent discrete palaeoflood events (Figs 3.19 and 3.20). Flood unit F5 was deposited as a slack-water sediment during tributary back flooding as the stage of the Orange River increased. The predominant flat lamination indicates that suspension settling was the dominant depositional process punctuated by slight increase of flow regime.

Flood unit F6 comprises a 2,70 m thick sequence of light-grey mainly flat laminated fine-grained sand (unit L4; Fig. 3.19). The basal 82 cm were examined in outcrop as well as with a relief peel. The remaining 1,88 m of unit L4 occurs as poorly exposed isolated clumps of sediment extending vertically to the point of pinch out against the side of the bedrock-controlled tributary valley side.

Unit L4 is interpreted as a slack-water palaeoflood sediment deposited during tributary back flooding as the stage of the Orange River increased (Fig. 3.20). The dominant mode of deposition was suspension settling of fine-grained sand punctuated by slight increases of flow regime. Flood unit F6 is the thickest palaeoflood unit observed at site 19 being 10 times thicker than the palaeoflood units F1 - F5. Since flood unit F6 extends to the point of slack-water pinch out above which no further

palaeoflood sediments occur, it represents the highest palaeoflood stage for site 19.

Section 2. Section 2 is located approximately 80 m from the tributary - Orange River confluence on the right-hand side of the tributary looking downstream. The section overlies the tributary thalweg gravel of which the basal metre is poorly exposed. The overlying unit comprises a gravel exhibiting 1 cm - 13 cm long, subangular - subrounded quartzite, diabase and BIF clasts which are infrequently imbricated (unit A; Fig. 3.21). The clasts are imbricated in a downstream direction in the tributary. Unit A can be traced laterally in an upstream direction in the tributary and was observed to be correlatable with unit A described from section 1 (Fig. 3.19). The overlying unit (unit B; Fig. 3.21) is a 60 cm - 150 cm thick, very fine-grained, indurated sand, although no evidence of calcification was noted. Unit B was noted to thin progressively from 150 cm close to the tributary - Orange River confluence to approximately 60 cm at the location of section 2. The unit further thins when laterally traced towards section 1 where it was observed to be correlatable with unit C described from section 1 (Fig. 3.19). Overlying unit B is a 20 cm thick, fine- to medium-grained red-pink sand which although could not be continually traced laterally in an upstream direction due to poor exposure is equivalent to units D - E described from section 1 (Fig. 3.19).

The interbedded position of unit B between the underlying and overlying tributary-deposited sediments of units A and C respectively, its contrasting finer grained texture and its upstream-thinning motif, indicates that unit B represents a palaeoflood slack-water sediment deposited during conditions of tributary back flooding (flood unit F1; Fig. 3.21). The progressive thinning from 150 cm close to the confluence, to 60 cm at section 2 through to 12 cm at section 1 reflects the decreasing depth of the back-flooded water in the tributary. It was stated when describing section 1 that unit C contains evidence of reworking and therefore could not be used as an accurate indication of maximum palaeoflood stage. However, the absence of evidence indicating reworking in unit B at section 2, implies that the reworking observed from unit C at section 1 is probably minimal and therefore, the top of unit B (section 2) and unit C (section 1) represent accurate palaeoflood stages.

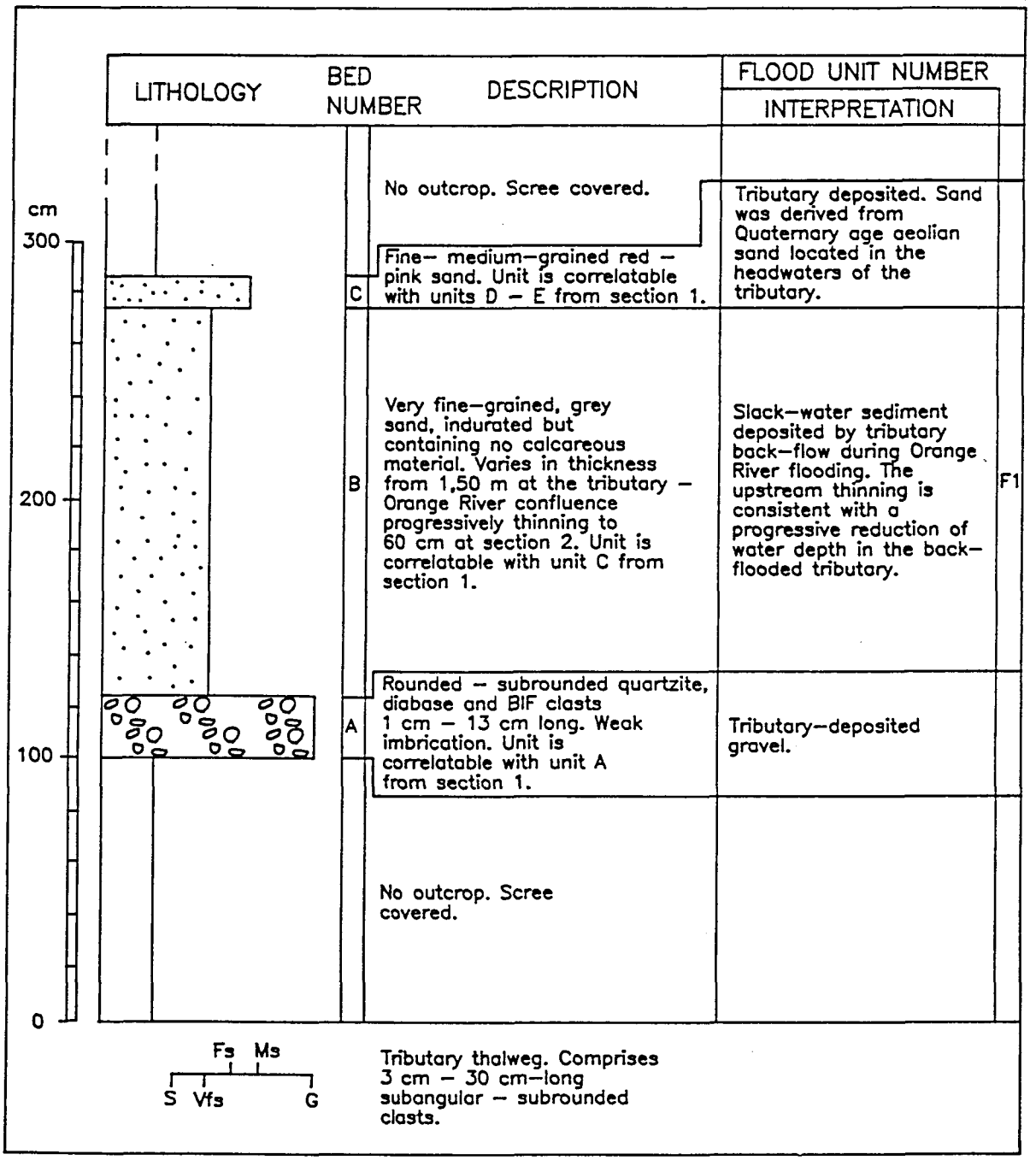

Fig. 3.21 - Lithological description and hydrodynamic interpretation and subdivision of the stratigraphy into palaeoflood and non-palaeoflood deposited units at section 1, site 19 (see legend on page 40).

3.2.4Palaeoflood hydrology and dating of slack-water sediments for sites 9, 14 and 19

The elevations of the slack-water sediments for sites 9, 14 and 19 were surveyed in relation to the elevation of the Orange River thalweg by the Department of Water Affairs and Forestry. In addition, five cross sections of the Orange River were surveyed in relation to the South African co-ordinate system using total station theodolites.

Fifteen dates were obtained from the slack-water sediments of which 4 were radiocarbon dated, 5 were dated using thermoluminescence (TL) and 6 were dated using infra-red stimulated luminescence (IRSL). The majority of dates (13) were obtained from site 9. The low number of radiocarbon dates is ascribed to the difficulty experienced in obtaining sufficient quantities of organic material. For example, no organic material was found in the slack-water sediments from the basal 3 m - 4 m of the palaeoflood stratigraphies at all three sites. Although a combination of TL and IRSL dating was used to augment the dating of the palaeoflood sequences, the dates obtained are largely unverified because of the lack of sufficient radiocarbon dates. The IRSL and TL dating concentrated on the slack-water sediments at site 9. This approach was adopted in consultation with J. Vogel of the luminescence dating laboratory for two reasons. Firstly, it was considered that by combining radiocarbon, IRSL and TL dating procedures for one palaeoflood site would lead to verification of the dates and therefore a more accurate chronostratigraphic subdivision of the palaeoflood sequence. This approach was considered to be more appropriate than obtaining one or two largely unverifiable IRSL and TL dates from each palaeoflood site. Secondly, because expertise in IRSL and TL dating in South Africa is comparatively low especially in dating fine- to very fine-grained fluvial sediments, the costs in preparing, dating and redating the samples proved to be high compared to commercial dating laboratories. Consequently, only 11 of the 18 samples collected for IRSL and TL dating were analysed. All samples were dated by the Quaternary Dating Research Unit (QUADRU) of the CSIR in Pretoria.

In the following account, the palaeoflood stratigraphy of each site is discussed in terms of the surveyed palaeoflood stages, the calculated palaeodischarges followed by an assessment of the accuracy of the radiocarbon, IRSL and TL dates obtained for certain slack-water sediments. This is followed by an attempt to correlate the

palaeoflood sequences at sites 9, 14 and 19 in order to obtain a representative palaeoflood stratigraphy for the Prieska reach of the Orange River (section 3.2.5).

Site 9. Two cross sections situated approximately 250 m apart and immediately upstream and downstream of the tributary-Orange River confluence were surveyed (Fig. 3.22). For each slack-water palaeoflood unit, the maximum elevation was surveyed, plotted on the cross sections (Fig. 3.22) and converted to metres above channel base which was used in slope-area calculations by the Department of Water Affairs and Forestry to derive the corresponding discharges.

Palaeoflood units F1 - F5 exhibit a range of palaeoflood stages from 12,42 m - 14,19 m (Fig. 3.23; Table 3.1). These stages correspond to a range of discharges of 3 850 m^3/s - 5 500 m^3/s (Fig. 3.23; Table 3.1). The overlying palaeoflood unit F6 exhibits the highest elevation of slack-water sediments at site 9 (20,37 m stage) that corresponds to a discharge of 13 080 m^3/s (Fig. 3.23; Table 3.1). Surveying and flow estimation of the onlapping palaeoflood sediments at section 2 shows that the position of pinchout of palaeoflood unit F7 represents a flood stage of 15,14 m with a corresponding discharge of 6 540 m^3/s (Fig. 3.24; Table 3.1).

Two radiocarbon dates, 5 TL dates and 6 IRSL dates were obtained from sections 1 and 2 at site 9 (Figs 3.23 and 3.24). The TL dates at section 2 appear to follow the stratigraphy with flood unit F1 yielding an age of 26 000 ±4 000 years; flood unit F3 (22 500 ±4 500 years); and a TL date of 10 900 ±2 180 years for the basal part of flood unit F6 (Fig. 3.23; Table 3.1). However, TL dating of the top of flood unit F6 yielded an age of 17 800 ±3 560 years. It is likely that both the ages for the base and top of flood unit F6 are anomalously old when considering that a radiocarbon age of 7 060 ±90 years was obtained for the non-palaeoflood sediments (bed O1) underlying flood unit F6. A similar anomaly between the radiocarbon age and the TL date is observed for the top of flood unit F7 at section 1 (Fig. 3.24) where a radiocarbon age of 150 ±45 years B.P was obtained, in contrast the TL age was 6 030 ±1 210 years. Although the basal three TL ages at site 9 are in stratigraphic order, the disparity between the radiocarbon and TL dates indicates that the TL dates yield consistently older ages. This is ascribed to insufficient bleaching or partial emptying of the electron traps (resetting) that leads to a residual luminescence signal

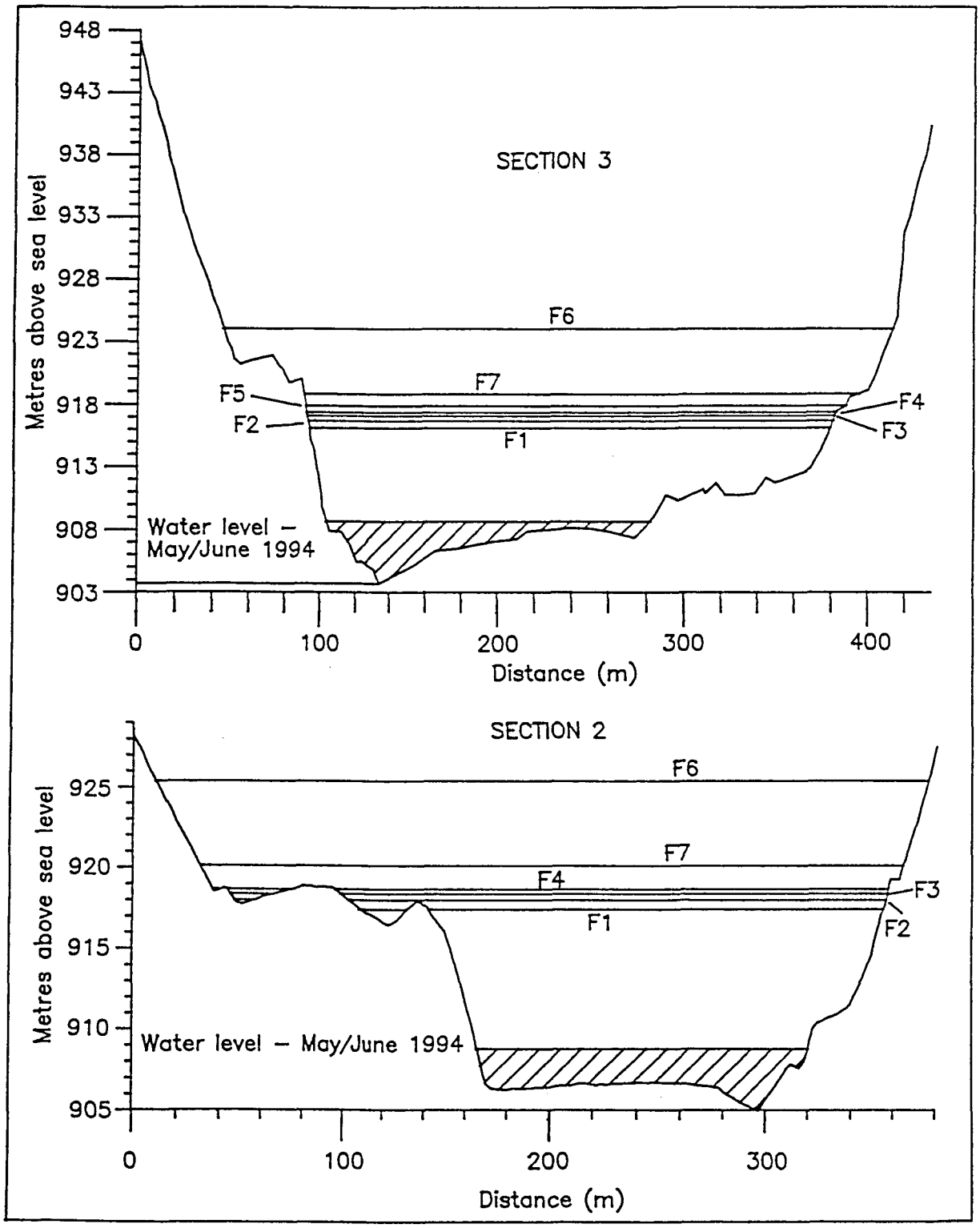

Fig. 3.22 - Cross-sections 2 and 3 of the Orange River which are 250 m apart and situated immediately upstream (section 2) and downstream (section 3) of the Orange River-tributary confluence. The stages of the palaeoflood sediments at site 9 are plotted with respect to the lowest recorded elevation of the Orange River channel base (903,80 m.a.s.l.;section 3).

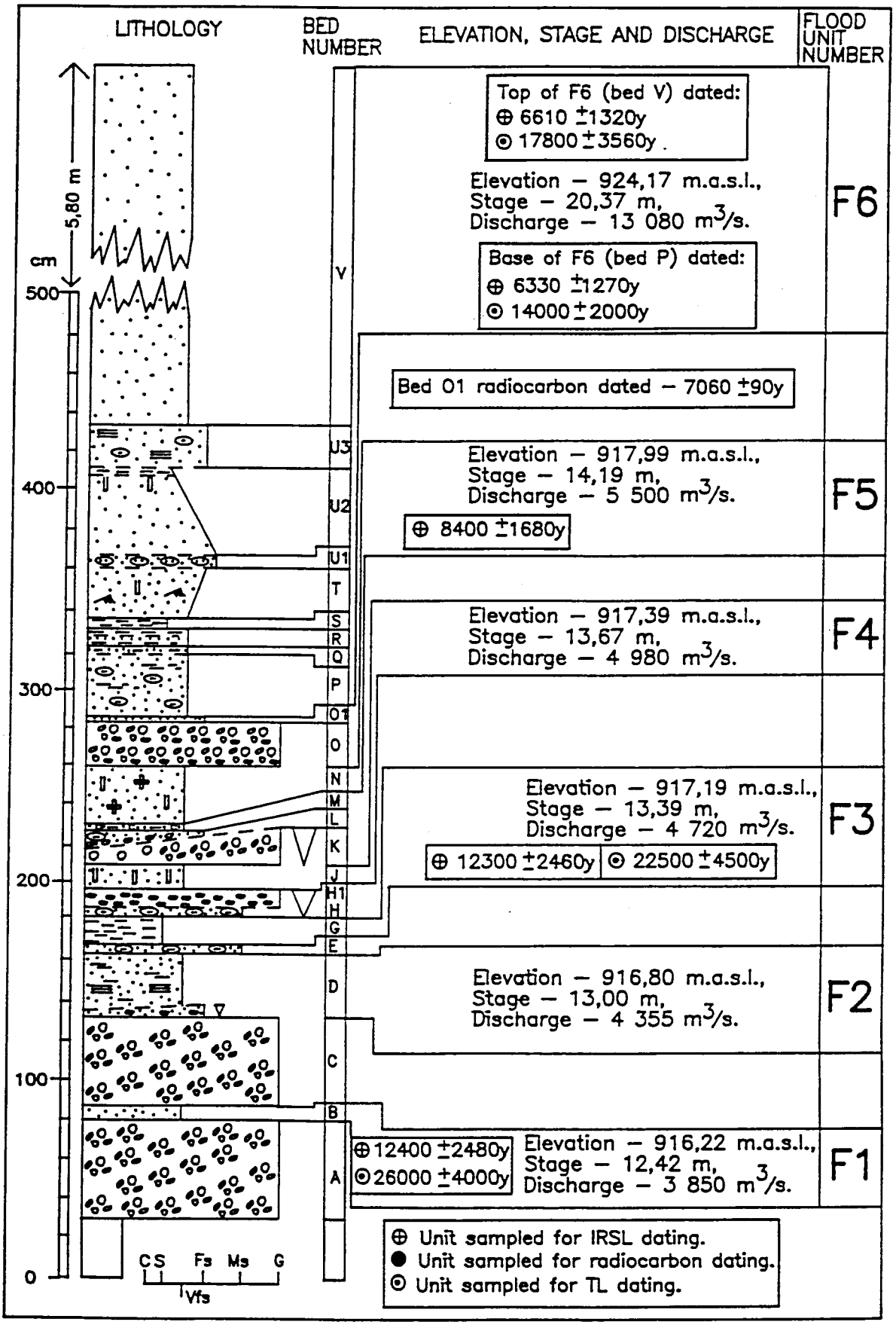

Fig. 3.23 - Elevation (m.a.s.l.),stage, palaeodischarge estimates and dating results (radiocarbon, TL and IRSL) for the palaeoflood units F1 - F6 at section 2, site 9.

Palaeo-flood unit	Height m.a.s.l.	Palaeoflood stage in metres above Orange River channel base[a]	Palaeo-discharge (Q) m^3/s	Radio-carbon sample no.	Type of material dated	Radio-carbon age (years B.P.)[b] or ^{14}C content	Calibrated date[c]	IRSL sample no.	IRSL age (years)	TL sample no.	TL age (years)	Comments
Site 9 section 2												
F6 (Fig. 3.17)	924,17	20,37	13 080	-	-	-	-	Pta-5248 --- Pta-5246	Top of F6 6 610 ±1 320 --- Bottom of F6 6 330 ±1 270	Pta-5248 --- Pta-5246	Top of F6 17 800 ±3 560 --- Bottom of F6 10 900 ±2 180	IRSL age is considered more accurate than TL date. Similarity in age between top and bottom confirms the sedimentology that F6 comprises one flood event. Archaeological remains indicate that F6 exhibits a minimum age of 1650 ± 50 years.
Non-palaeoflood interval	N.A.	N.A.	N.A.	Pta-6519	Organic material from soil horizon	7 060 ±90	-	-	-	-	-	Considered to be an accurate age. Indicates that F6 is younger than approximately 7 000 years B.P.
F5 (Fig. 3.17)	917,99	14,19	5 500	-	-	-	-	Pta-5212	8 400 ±1 680	-	-	
F4 (Fig. 3.17)	917,39	13,67	4 980	-	-	-	-	-	-	-	-	Exhibits an age between the IRSL ages 8 400 ±1 680 years and 12 300 ±2 460 years.
F3 (Fig. 3.17)	917,19	13,39	4 720	-	-	-	-	Pta-5250	12 300 ±2 460	Pta-5250	22 500 ±4 500	Significant difference in age between IRSL and TL dating procedures.
F2 (Fig. 3.17)	916,80	13,00	4 355	-	-	-	-	-	-	-	-	
F1 (Fig. 3.17)	916,22	12,42	3 850	-	-	-	-	Pta-5247	12 400 ±2 480	PKZ-7	26 000 ±4 000	
Site 9 section 1												
F7 (Fig. 3.18)	918,94	15,14	6 540	Pta-6506	Charcoal	150 ±45	A.D. 1924 or 1850	Pta-5245	2 760 ±550	Pta-5245	6 030 ±1 210	Considerable discrepancy exists between the radiocarbon, IRSL and TL dating procedures. The radiocarbon date is considered the more accurate one since a similar age of 120 ±15 years B.P. was obtained from a slack-water sediment at approximately the same stratigraphic position at site 14.

[a] The base of the Orange River channel was surveyed to an elevation of 903,80 m a.s.l.
[b] Radiocarbon years is expressed as years before present i.e. before A.D. 1950. Ages are corrected for variations in isotopic fractionation.
[c] Age calibrated for the southern hemisphere based on data presented by Stuiver and Pearson (1993).

Table 3.1 - Combined palaeoflood stratigraphy (section 1 and section 2) of the Orange River at site 9 comprising stage, palaeo-discharge, radiocarbon and IRSL dating information arranged with increasing palaeoflood magnitude.

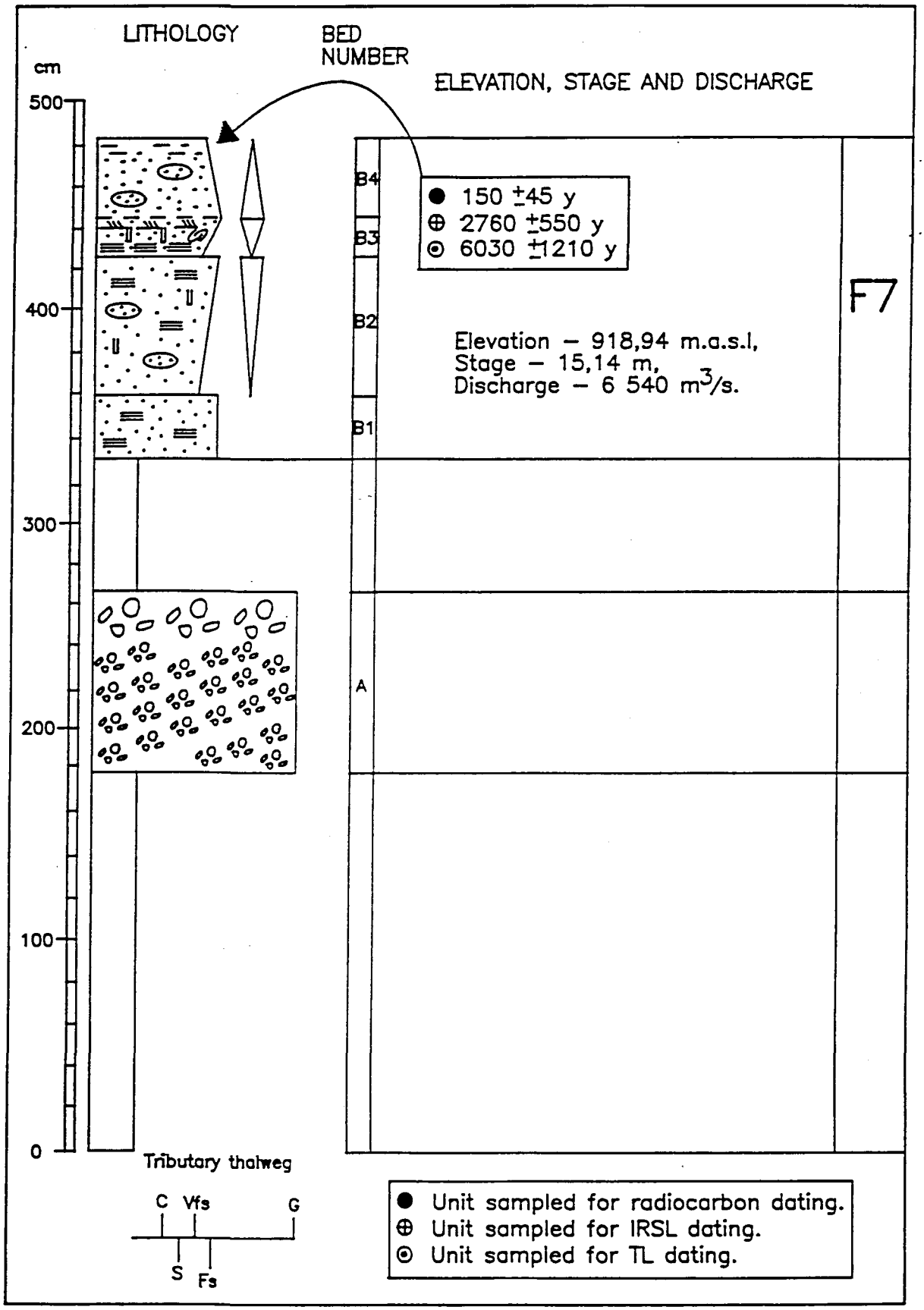

Fig. 3.24 - Elevation (m.a.s.l.),stage, palaeodischarge estimates and dating results (radiocarbon, TL and IRSL) for the palaeoflood unit F7 at section 1, site 9.

due to insufficient exposure to sunlight under turbid flood conditions. A similar observation and conclusion was made by Forman and Ennis (1992) where TL dates from glacial marine sediments which were deposited under high turbidity conditions, yielded ages that were approximately 10 times the known age. They ascribed this to the grains receiving limited exposure to the sun resulting in a variable and elevated residual luminescence signal.

Infra-red stimulated luminescence dating was applied to the palaeoflood units that were TL dated as well as to flood unit F5 in order obtain more realistic ages. The IRSL technique has an advantage over TL dating as it uses light for the stimulation of the dating signal. According to Aitken (1992), the "easy-to-bleach" electron traps are sampled which largely overcomes the problem of a residual luminescence signal even for water-deposited sediments that experience brief exposure to sunlight. The sequence of IRSL ages from F1 - F6 appear to be more reliable than the TL ages as they are firstly in stratigraphic order (Fig. 3.23) and secondly, the same IRSL ages was obtained for the base (6 330 ±1 270 years) and the top (6 610 ±1 320 years) of flood unit F6 (Fig. 3.23). This confirms the sedimentological study that beds P - V were deposited during one flood event. The IRSL ages appear to be more realistic since they are on average less than half the age of the TL dates. In addition, the IRSL date for the base of flood unit F6 (6 330 ±1 270 years) is similar to the radiocarbon age of 7 060 ±90 years B.P. obtained for the underlying bed (bed O1) (Fig. 3.23). Although the IRSL ages for site 9 appear more realistic than the TL results, a disparity in age exists between the IRSL age of 2 760 ±550 years and the radiocarbon age of 150 ±45 years B.P. for flood unit F7 at section 1 (Fig. 3.24). The radiocarbon age is considered to be more accurate because a similar radiocarbon age of 120 ±15 years B.P. was obtained from approximately the same stratigraphic interval at site 14. This suggests that although IRSL dating yields more accurate ages than the TL dating, the dates are still consistently too old especially for the younger slack-water sediments. A similar observation was noted at the lower Xobies and Bloeddrift sites of the lower Orange River where 4 radiocarbon dates for flood unit F9 (lower Xobies) and F6 (Bloeddrift) ranged in age from 450 ±20 years B.P. - 710 ±40 years B.P. In contrast, three IRSL ages for the same flood units ranged in age from 1 110 ±220 years - 1 980 ±400 years.

Although IRSL dating of fluvially-deposited sediments is favoured over TL dating (Aitken, 1992), there still exist problems of resetting and residual luminescence that results in over-estimates of age. A similar observation was noted by Lang and Wagner (1995) when IRSL dating modern flood-deposited sediments in Germany. They suggested that under flood conditions, coagulation or flocculation of grains during transport results in insufficient exposure to sunlight and therefore only partial zeroing of the luminescence signal. This, together with the likely turbid conditions during flood flow, further decreases the opportunity for exposing the sediment to sunlight.

Although a comparatively large number of dates have been obtained for site 9 using a combination of TL, IRSL and radiocarbon dating techniques, the results are disappointing. For example, chronstratigraphic uncertainty still exists for flood units F6 (section 2) and F7 (section 1). A further factor that has impeded the chronostratigraphic interpretation of site 9 is the relatively high error margins associated with the IRSL ages (approximately 20 % of the age). For example, the IRSL age of 8 400 ±1 680 years for flood unit F5 and the overlying IRSL age for the base of F6 (6 330 ±1 270 years) indicates that for approximately 2 100 years the Orange River did not flood with a discharge that exceeded 5 500 m^3/s (Fig. 3.23). However, the associated error margins of these dates indicates that the IRSL ages are identical. The IRSL and the radiocarbon date for bed O1 indicates that the basal 2,86 m of the palaeoflood stratigraphy at site 9 is relatively old ranging in age from approximately 12 400 ±2 480 years - 7 060 ±90 years B.P.. During this interval (approximately 5 300 years) 5 palaeoflood events were recorded ranging in discharge between 3 850 m^3/s - 5 500 m^3/s (Fig. 3.23; Table 3.1).

Constraining the age of flood unit F6 is problematic but is probably younger than the radiocarbon age of 7 060 ±90 years B.P. which was obtained for the underlying non-palaeoflood unit (bed O1) (Fig. 3.23). It is also older than the radiocarbon date of 150 ±45 years B.P. for flood unit F7 at section 1 because the slack-water sediments at section 1 onlap the palaeoflood stratigraphy of section 2 but do not extend up to the point of pinchout of flood unit F6 at section 2. The IRSL ages for the base and the top of flood unit F6 (6 330 ±1 270 years and 6 610 ±1 320 years respectively) suggests that the flood unit is approximately 6 500 years old. However,

the non-indurated nature of flood unit F6 and the problem of residual luminescence observed at section 1 and from IRSL dating in the lower reaches of the Orange River suggests that this age is over estimated. Archaeological artifacts found at the surface that forms part of flood unit F6 was identified by D. Morris of the McGregor Museum, Kimberley to comprise a mixture of Khoi and Korana-type ceramics of which similar Khoi pottery was radiocarbon dated at a site 20 km downstream of site 9 to be 1 650 ±50 years B.P. (Beaumont and Morris, 1990). The Korana artifacts represent younger habitation with a minimum age of A.D. 1780 (Morris, pers comm.). Since the older artifacts form part of the slackwater sediments of flood unit F6, the flood unit exhibits a minimum age of approximately 1 600 years B.P. and a maximum age of approximately 6 500 years based on the IRSL dating.

Site 14. Site 14 is located approximately 1,5 km upstream of site 9 along the Orange River. One cross section (section 1) across the Orange River was surveyed on which the stage elevations of the slack-water sediments were plotted with respect to the elevation of the Orange River thalweg (906,07 m.a.s.l.)(Fig. 3.25).

Palaeoflood units F1 - F6 vary in stage from 8,00 m - 9,78 m (Fig. 3.26; Table 3.2). These stages correspond to a range of discharges from 2 760 m^3/s - 4 095 m^3/s. The overlying palaeoflood unit F7 exhibits the highest elevation at site 14 with a stage of 16,41 m and a corresponding discharge of 9 000 m^3/s (Fig. 3.26; Table 3.2). A further palaeoflood unit at section 2 exhibits a flood stage of 8,90 m with a corresponding discharge of 3 480 m^3/s (Fig. 3.27).

Due to insufficient quantities of uncontaminated organic material from the slack-water sediments at site 14, only one date of 120 ±15 years B.P. was obtained for flood unit F7. This corresponds to several calibrated ages of A.D. 1893, 1900 and 1911 of which A.D. 1900 is regarded as the most accurate (Vogel, pers comm.) (Fig. 3.26; Table 3.2). Although this age could not be verified with other dates at site 14, the slack-water sediments are non-indurated indicating a possibly young age. In addition, this age is identical in terms of radiocarbon years and the associated error margin to the date of 150 ±45 years obtained for stratigraphically similar sediments at section 1, site 9 (Fig. 3.24; Table 3.1).

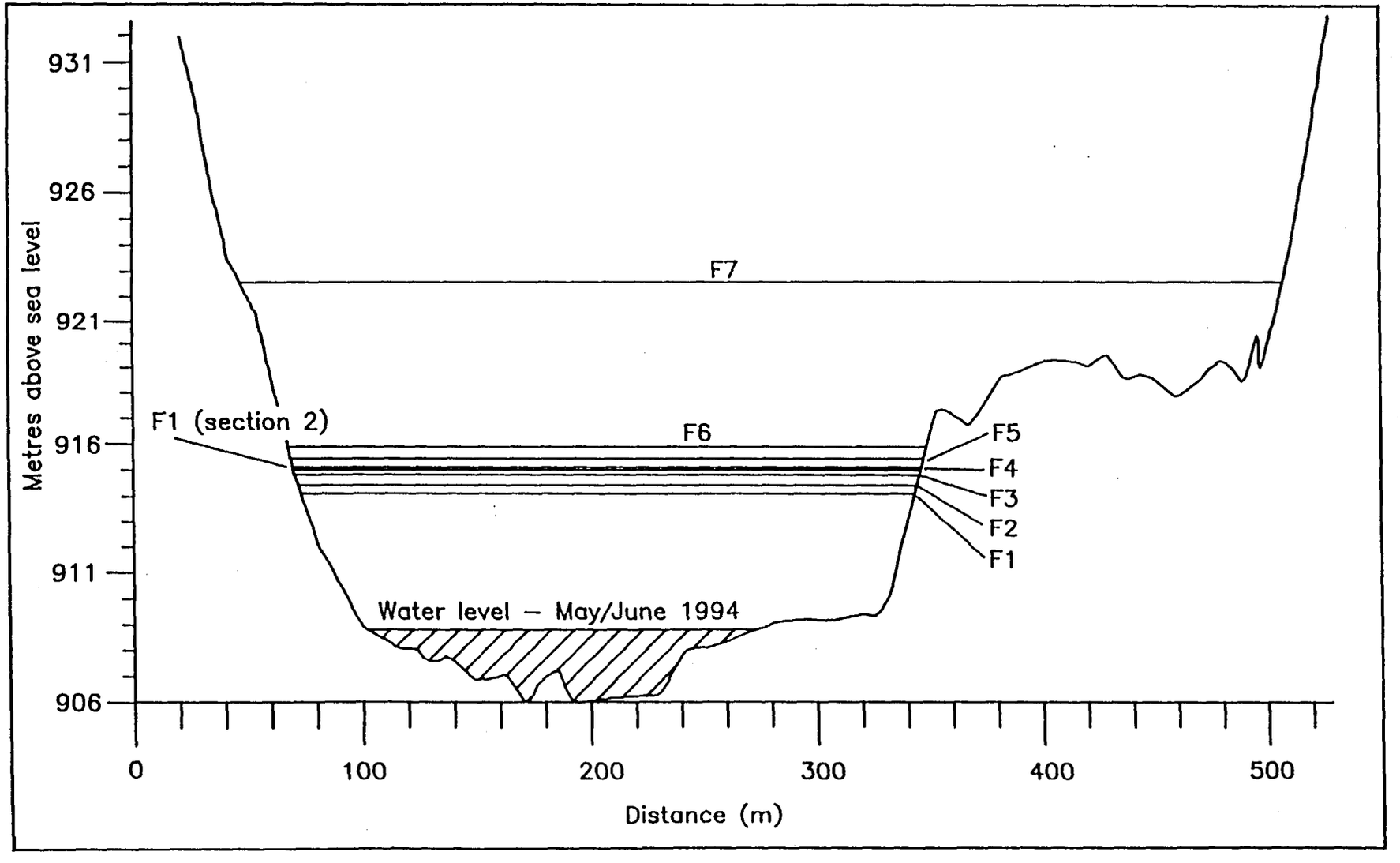

Fig. 3.25 - Cross-section 1 across the Orange River on which are plotted the elevations of the palaeoflood slack-water units F1 - F7 at site 14 with respect to the elevation of the Orange River thalweg (906,07 m.a.s.l.).

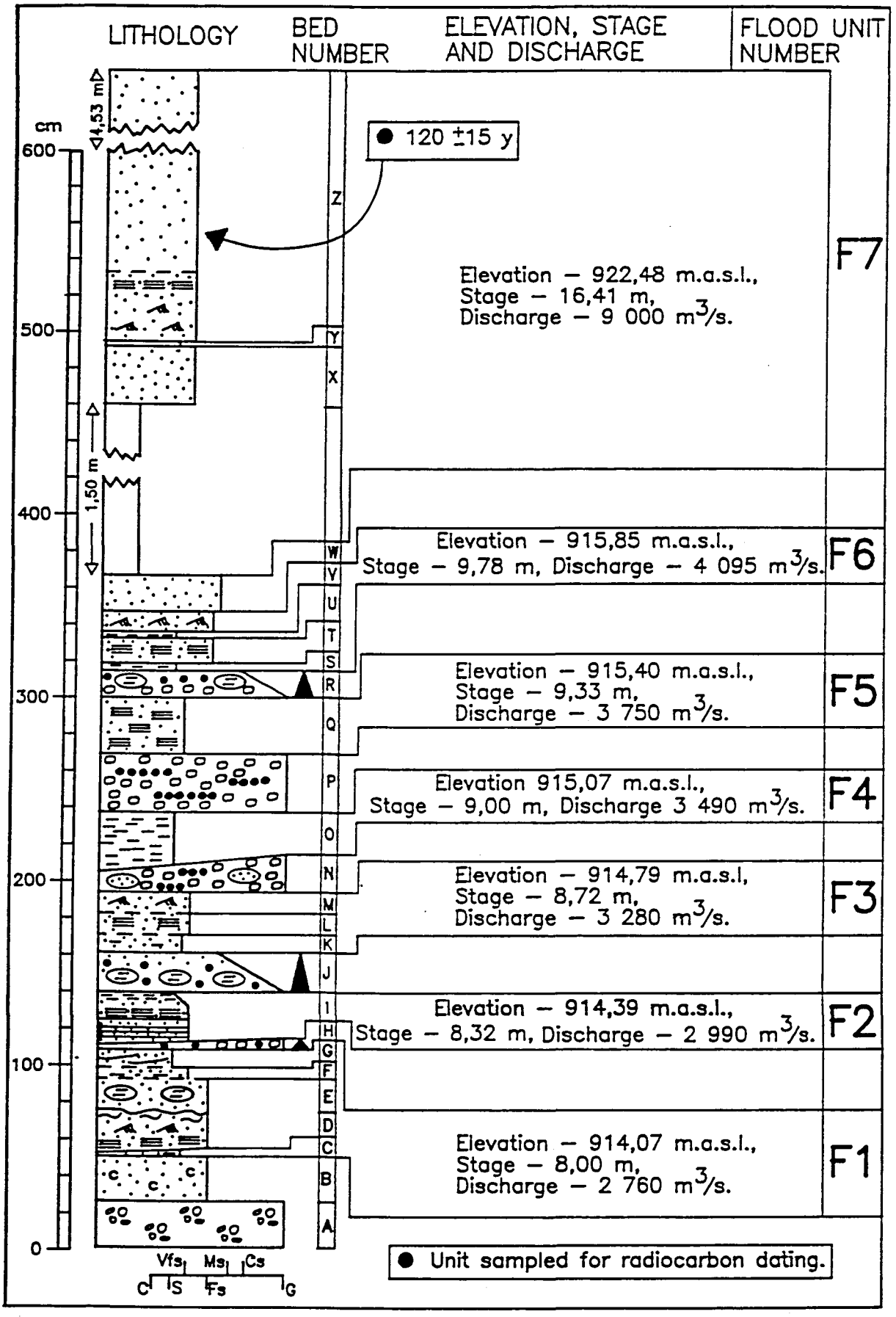

Fig. 3.26 - Elevation (m.a.s.l.), stage, palaeodischarge estimates and dating results (radiocarbon) for the palaeoflood units F1 - F7 at section 2, site 14.

Palaeoflood unit	Height m.a.s.l.	Palaeoflood stage in metres above Orange River channel base[a]	Palaeo-discharge (Q) m^3/s	Radio-carbon sample no.	Type of material dated	Radio-carbon age (years B.P.)[b] or ^{14}C content	Calibrated date[c]	IRSL sample no.	IRSL age (years)	TL sample no.	TL age (years)	Comments
Site 14 section 1												
F7 (Fig. 3.20)	922,48	16,41	9 000	Pta-6509	Charcoal	120 ±15	A.D. 1893(1900))1911	-	-	-	-	Date verifies the age of 150 ±45 years B.P. obtained for F7 from approximately the same stratigraphic interval at section 1, site 9.
F6 (Fig. 3.20)	915,85	9,78	4 095	-	-	-	-	-	-	-	-	
F5 (Fig. 3.20)	915,40	9,33	3 750	-	-	-	-	-	-	-	-	
F4 (Fig. 3.20)	915,07	9,00	3 490	-	-	-	-	-	-	-	-	
F3 (Fig. 3.20)	914,79	8,72	3 280	-	-	-	-	-	-	-	-	
F2 (Fig. 3.20)	914,39	8,32	2 990	-	-	-	-	-	-	-	-	
F1 (Fig. 3.20)	914,07	8,00	2 760	-	-	-	-	-	-	-	-	
Site 14, section 2												
F1 (Fig. 3.21)	914,97	8,90	3 480	-	-	-	-	-	-	-	-	Unit is indurated and is overlain by non-indurated slack-water sediments that are correlatable with flood unit F7 from section 1.

[a] The base of the Orange River channel was surveyed to an elevation of 906,07 m.a.s.l

[b] Radiocarbon years is expressed as years before present i.e. before A.D. 1950. Ages are corrected for variations in isotopic fractionation. Most probable calibrated or calendar date is given in brackets.

[c] Age calibrated for the southern hemisphere based on data presented by Stuiver and Pearson (1993).

Table 3.2 - Combined palaeoflood stratigraphy (section 1 and section 2) of the Orange River at site 14 comprising stage, palaeo-discharge and radiocarbon dating information arranged with increasing palaeoflood magnitude.

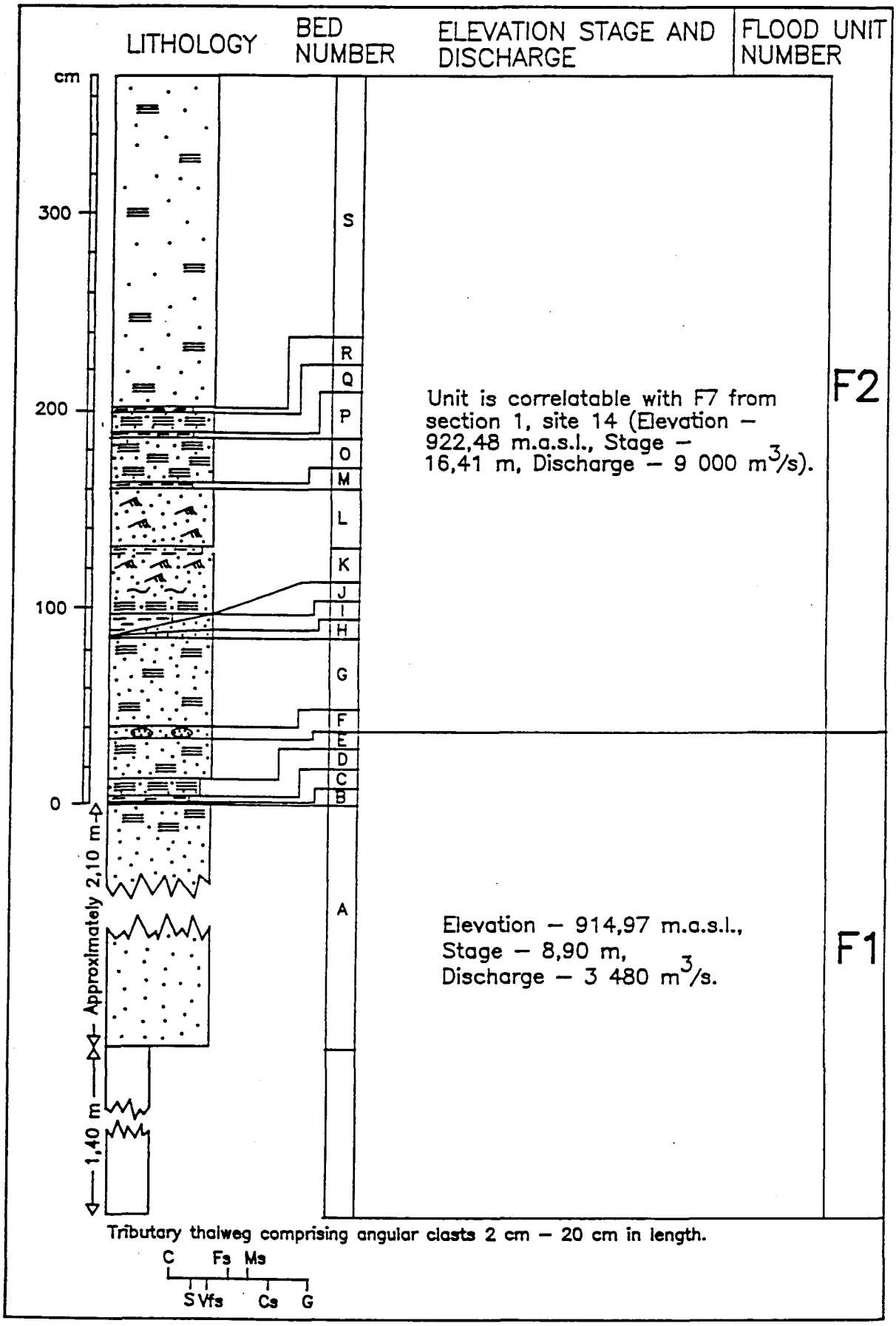

Fig. 3.27 - Elevation (m.a.s.l.),stage and palaeodischarge estimates and dating for the palaeoflood unit F1 at section 2, site 14.

Site 19. Two cross sections of the Orange River (cross-sections 4 and 5) located 100 m and 350 m downstream of the Orange River - tributary confluence were surveyed by the Department of Water Affairs and Forestry. The stage elevations of the flood units F1 - F6 were plotted on cross-section 5 with respect to the thalweg elevation of the Orange River (893,03 m.a.s.l.)(Fig. 3.28).

Palaeoflood units F1 - F5 vary in stage from 10,12 m - 13,18 m (Fig. 3.29; Table 3.3). These stages correspond to a range of discharges from 3 040 m^3/s - 6 290 m^3/s (Fig. 3.29; Table 3.3). The overlying palaeoflood unit F6 exhibits the maximum elevation of slack-water sediments at site 19 with a stage of 16,28 m and a corresponding discharge of 11 260 m^3/s (Fig. 3.23; Table 3.3).

As with site 14, finding sufficient and suitable organic material for radiocarbon dating proved to be difficult. Consequently only one radiocarbon age of 500 ±90 years B.P. was obtained for flood unit F4 (Fig. 3.29). This represents several calibrated ages of A.D. 1411, A.D. 1440 and A.D. 1497, of which the A.D. 1440 date is considered the most accurate (Vogel, pers comm.).

3.2.5 Correlation of the palaeoflood sequences between sites 9, 14 and 19

Correlation of the palaeoflood stratigraphies of sites 9, 14 and 19 was based on the following observations and objectives:

(1) Examination of the palaeoflood sites indicates that they are lithostratigraphically similar. Specifically, each site is characterised by a basal portion (3 m - 4 m thick) comprising a sequence of non-flood deposited interbedded coarse-grained sand - gravel with thin (approximately 10 cm - 50 cm thick) fine- to very fine-grained palaeoflood-deposited slack-water sediments (Fig. 3.30). A closer examination of the basal stratigraphy shows also that the number of non-palaeoflood deposited units is similar varying between 4 - 6. The overlying stratigraphy is also comparable between sites comprising a sequence of fine- to very fine-grained slack-water sediments 3,6 m - 6,70 m thick (Fig. 3.30). Consideration was therefore given to assessing the feasibility of correlating the palaeoflood and non-palaeoflood sediments between sites in order to develop as complete a palaeoflood stratigraphy as possible for this

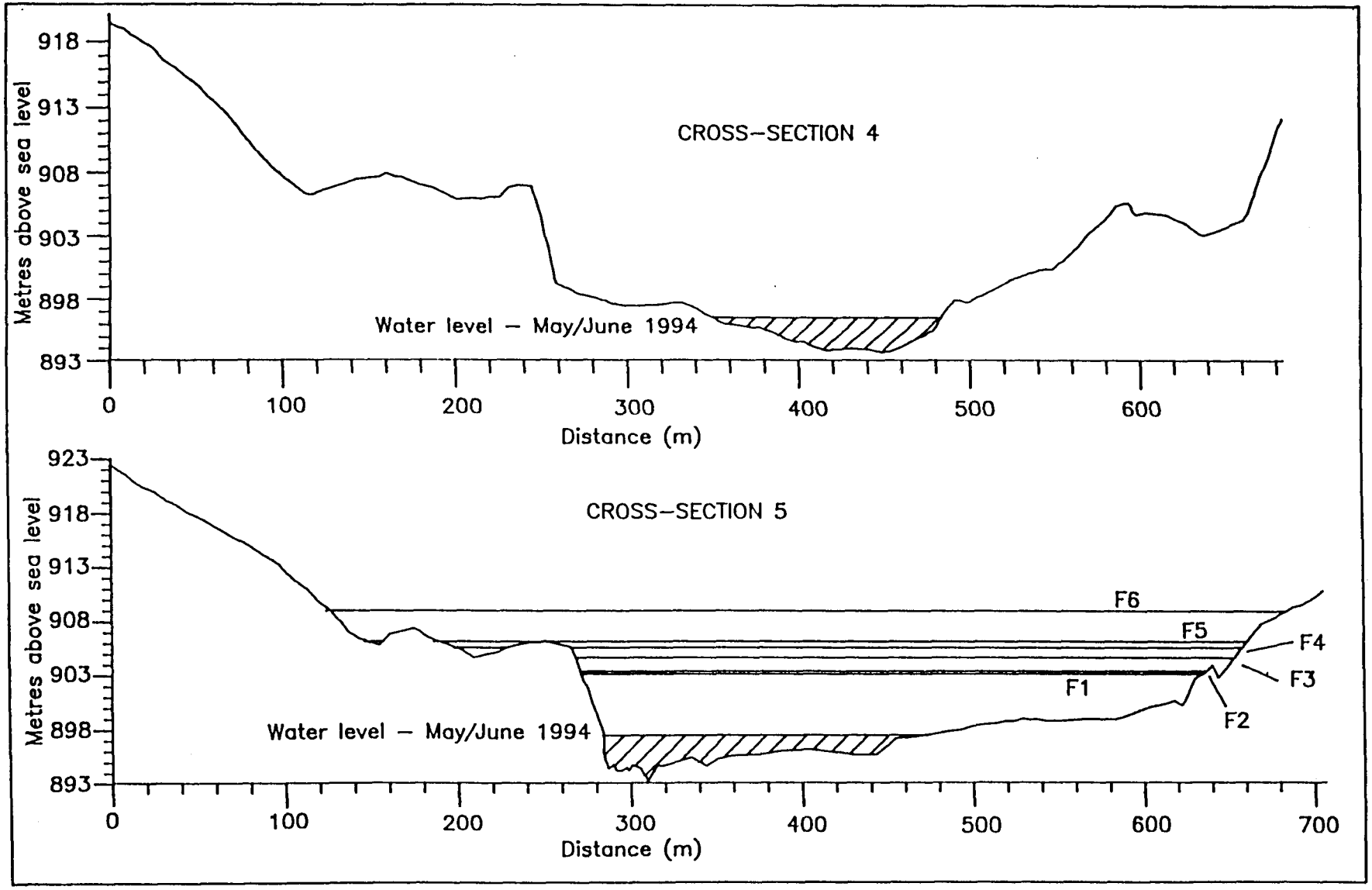

Fig. 3.28 - Cross-sections 4 and 5 across the Orange River on which are plotted (cross-section 5) the elevations of the palaeoflood slack-water units F1 - F6 at site 19 with respect to the elevation of the Orange River thalweg (893,03 m.a.s.l.).

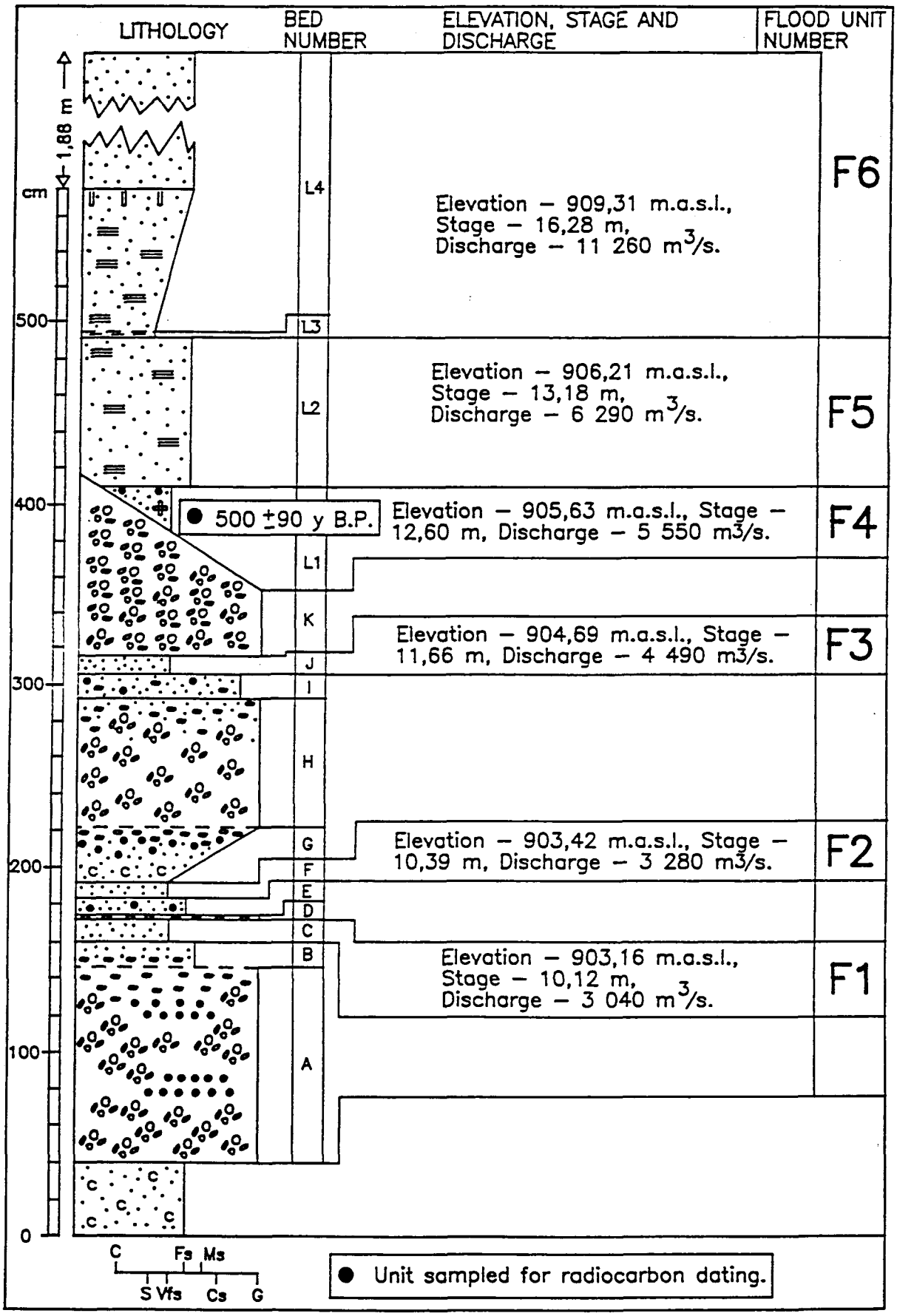

Fig. 3.29 - Elevation (m.a.s.l.), stage, palaeodischarge estimates and dating result (radiocarbon) for the palaeoflood units F1 - F6 at site 19.

Palaeoflood unit	Height m.a.s.l.	Palaeoflood stage in metres above Orange River channel base[a]	Palaeo-discharge (Q) m^3/s	Radio-carbon sample no.	Type of material dated	Radio-carbon age (years B.P.)[b] or ^{14}C content	Calibrated date[c]	IRSL sample no.	IRSL age (years)	TL sample no.	TL age (years)	Comments
F6 (Fig. 3.23)	909,31	16,28	11 260	-	-	-	-	-	-	-	-	Represents the largest magnitude palaeoflood unit at site 19.
F5 (Fig. 3.23)	906,21	13,18	6 290	-	-	-	-	-	-	-	-	
F4 (Fig. 3.23)	905,63	12,60	5 550	Pta-6507	Charcoal	500 ±90	A.D. 1411(1440)1497	-	-	-	-	
F3 (Fig. 3.23)	904,69	11,66	4 490	-	-	-	-	-	-	-	-	
F2 (Fig. 3.23)	903,42	10,39	3 280	-	-	-	-	-	-	-	-	
F1 (Fig. 3.23)	903,16	10,12	3 040	-	-	-	-	-	-	-	-	

[a] The base of the Orange River channel was surveyed to an elevation of 893,03 m.a.s.l.
[b] Radiocarbon years is expressed as years before present i.e. before A.D. 1950. Ages are corrected for variations in isotopic fractionation. Most probable calibrated or calendar date is given in brackets.
[c] Age calibrated for the southern hemisphere based on data presented by Stuiver and Pearson (1993)

Table 3.3 - Combined palaeoflood stratigraphy of the Orange River at site 19 comprising stage, palaeodischarge and radiocarbon dating information arranged with increasing palaeoflood magnitude.

reach of the Orange River.

(2) In discussing the chronstratigraphy of sites 9, 14 and 19 (section 3.2.4) it was shown that the dates obtained from radiocarbon, IRSL and TL dating was largely disappointing. For example, even for site 9 where 11 age determinations were made, the different dating methods yielded often conflicting results with many of the IRSL and TL dates exhibiting high error margins. In addition, the luminescence dates were largely unverified due to an insufficient number of radiocarbon dates. An attempt to combine the chronostratigraphic and lithostratigraphic features by correlating sites 9, 14 and 19 was therefore attempted in order to gain a more accurate chronostratigraphic subdivision for especially sites 14 and 19 where only two age determinations were obtained.

(3) In examining the palaeodischarge estimates of the palaeoflood units in section 3.2.4showed that despite the broad lithostratigraphic similarity between the sites, a considerable difference of discharges exists between sites. For example, the basal palaeoflood stratigraphy at site 9 shows a range of palaeodischarge from 3 850 m^3/s - 5 500 m^3/s (units F1 - F5), whereas site 14 exhibits a range of 2 760 m^3/s - 3 750 m^3/s (units F1 -F5) (Fig. 3.30). Correlation between the sites in terms of lithostratigraphy and palaeodischarge estimates was therefore done in order to account and possibly apply palaeodischarge correction factors where necessary.

In correlating the lithostratigraphy between sites 9, 14 and 19, it was assumed that because a similarity in number and thickness of the tributary-deposited gravel units exists especially between sites 9 and 14, these non-flood units are broadly correlatable with each other (Fig. 3.30). Therefore, the interbedded slack-water sediments are also correlates of each other. Similarly, the stratigraphy above the basal portion of the palaeoflood sequence is comparable in terms of thickness and sedimentology. Accordingly, the palaeodischarge estimates between for example, sites 9 and 14 was expected to also be comparable. However, there is a considerable disparity in the range of discharges for the basal flood units (F1 - F5) (Fig. 3.30). In addition, the discharge corresponding to the maximum elevation of the slack-water sediments between both sites differs by 31 % (site 9, F6, 13 080 m^3/s; site 14, F7

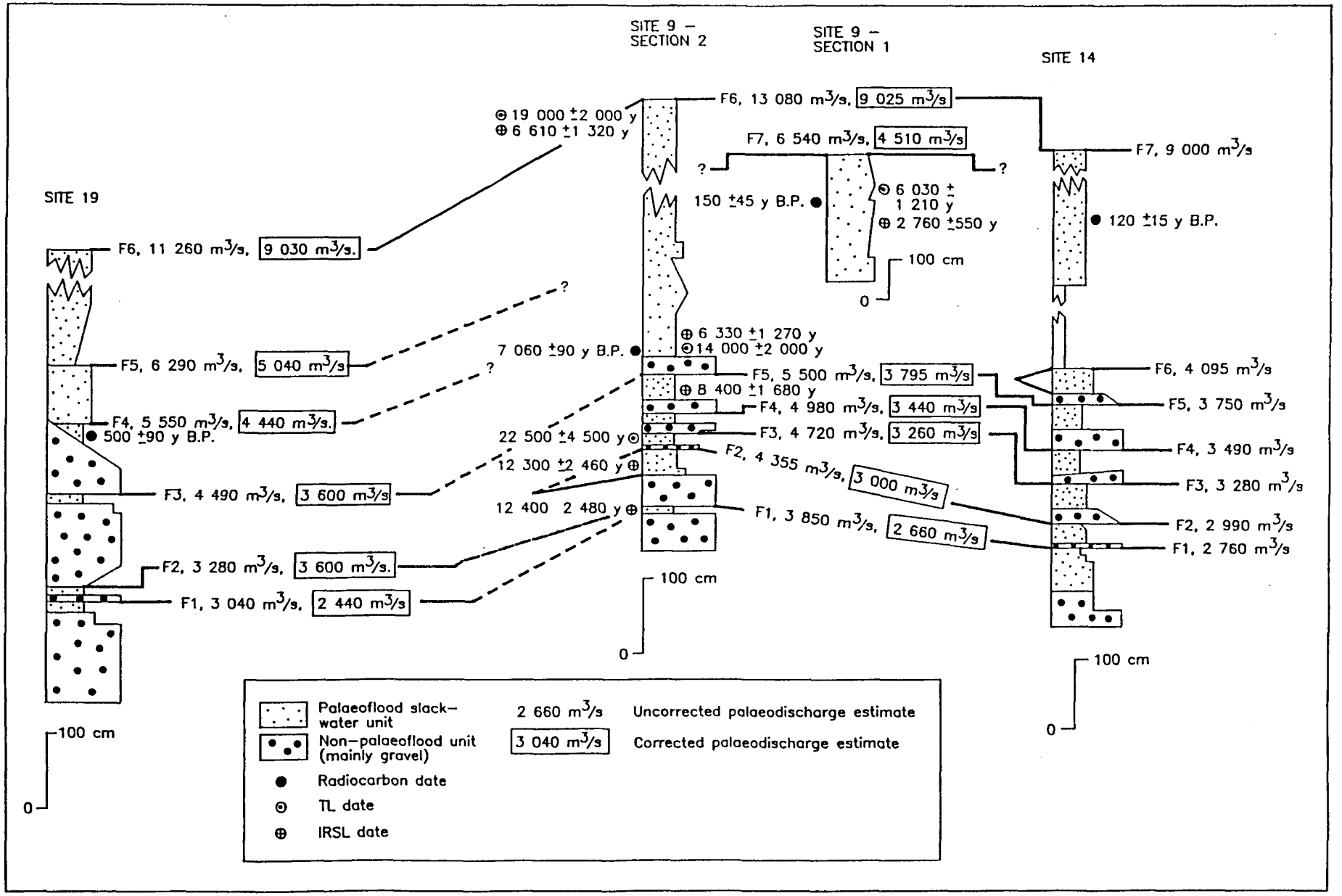

Fig. 3.30 - Correlation of palaeoflood sequences of sites 9, 14 and 19 at Prieska. Note the similarity in lithostratigraphy in the basal portion of the sequences. Note also that the corrected discharge estimates at site 9 compare with those at site 14. This indicates that a systematic error in the palaeodischarge estimates exist. The poor correlation especially from the basal portion of the sequence between sites 19 and 9 is ascribed to reworking of the palaeoflood stratigraphy at site 19.

9 000 m^3/s) (Fig. 3.30). In accounting for this difference, a correction factor of 31 % of the discharge was subtracted from the palaeodischarge estimates of flood units F1 - F6 at site 9. This resulted in all the palaeodischarge estimates for flood units F1 - F6 at site 9 being comparable to those at site 14 (Fig. 3.30). This indicates that although the palaeoflood units and non-palaeoflood units are correlatable between sites 9 and 14, there is a systematic error of 31 % in the palaeodischarge estimates between the sites. Consultation with the Department of Water Affairs and Forestry indicates that the most likely reason for this discrepancy is that hydraulically non-representative cross sections were used in calculating the discharges.

A similar discrepancy in palaeodischarge exists between sites 9 and 19 (Fig. 3.30). For example, the maximum elevation of flood unit F6 at site 19 is approximately 20 % greater than that recorded at site 9 for flood unit F6 (Fig. 3.30). In subtracting 20 % from each palaeoflood unit at site 19 resulted in only a partial agreement of discharges between site 19 and site 9 (Fig. 3.30). A further complication in the lithostratigraphic correlation between sites 9 and 19 is the absence of several flood units at site 19. This is ascribed to erosion and removal of slack-water sediments by non-flood tributary related processes. This conclusion is supported with evidence of reworking found in units F1, F2 and F3 at site 19 described in section 3.2.3.2.

Chronostratigraphic correlation indicates that the basal portion of the palaeoflood stratigraphy at the three sites that extends to the top of the uppermost gravel ranges in age from approximately 7 000 years (radiocarbon date determination) to a minimum age of 12 500 years (IRSL determination) (Fig. 3.30). The upper portion of the palaeoflood stratigraphy is less clear however. For example, there is no correlate of the flood unit F4 at site 19 which was dated to be 500 ±90 years B.P. with either sites 9 and 14. In addition, conflicting discharge estimates exist between flood unit F7 at site 9 (section 1) and flood unit F7 at site 14 even though similar radiocarbon ages of 150 ±45 years B.P. and 120 ±15 years B.P. was obtained for them respectively. It is possible that the radiocarbon date of 120 ±15 years B.P from site 14 refers to also onlapping sediments similar to flood unit F7 (section 1) but the nature of the onlapping was not observed in the field due to poor outcrop and its almost horizontal attitude close to its point of pinch out. Because flood unit F7 at site 9 (section 1) onlaps the palaeoflood stratigraphy at site 9 (section 2) and is not

continuous with the flood unit F6 at site 9, flood unit F6 is older than 150 ±45 years B.P. and possibly younger than 500 ±90 years B.P. It is therefore concluded that either flood unit F5 or F6 at site 19, flood unit F6 at site 9 and the uppermost portion of F7 at site 14 are correlatable and deposited between A.D. 1850 and A.D. 1440.

Correlation of the palaeoflood stratigraphies also exist on the basis of the relative difference in discharge between succeeding palaeofloods. Of further significance is that a similar observation was made for the palaeoflood sequences examined in the lower reaches of the Orange River. Calculation of the relative difference in palaeodischarge as a percentage of the total difference in discharge between the smallest and largest palaeoflood events for sites 9, 14 and 19 reveals two aspects. Firstly, the difference between the largest and second largest palaeodischarge at the three sites is similar, varying between 82 % at site 9, 78,6 % at site 14 and 60 % at site 19 (Table 3.4). This difference is always observed from the upper portion of the palaeoflood stratigraphy i.e. the palaeoflood sequence overlying the last non-palaeoflood deposited gravel. Similar values of 75,5 % at lower Xobies and 82,5 % at Bloeddrift were observed for the lower Orange River. Secondly, the basal portion of the palaeoflood sequence at sites 9, 14 and 19 exhibit average palaeodischarge estimates differences of 4,5 % (site 9), 4,3 % (site 14) and 10 % (site 19) (Table 3.4). Similar average values of 3,6 % and 4,4 % were obtained from the basal portions of the palaeoflood sequences at lower Xobies and Bloeddrift respectively.

The similar pattern of relative difference in palaeodischarge noted between sites 9, 14 and 19 is not fully understood. The change in average palaeodischarge observed from the basal to the upper portion of the palaeoflood sequences indicates a dramatic change of flood regime in terms of magnitude and possibly recurrence. Although the results of dating the palaeoflood units is largely unverified, it is tentatively suggested that between approximately 7 000 years B.P. (radiocarbon date determination) to a minimum age of 12 500 years (IRSL determination) (Fig. 3.30), the Orange River at Prieska experienced a succession of relatively small flood events. From approximately 500 ±90 years B.P. (Fig. 3.30) the Orange River experienced flood events which were over twice the palaeodischarges observed from the basal palaeoflood stratigraphy. The similarity of difference in palaeodischarge between the largest and second largest flood at the Prieska sites and the lower Orange River sites

may indicate that the Orange River at Prieska, experienced a large flood whose discharge contributed to the catastrophic flood discharge recorded for the lower Orange River. No chronostratigraphic confirmation exists however, to substantiate this conclusion since the dating results from Prieska are largely unverified. Consequently, this conclusion should be regarded as tentative.

SITE 9		SITE 14		SITE 19	
Palaeoflood unit change of adjacent palaeofloods.	**Percentage change in discharge as a proportion of the total difference in discharge between units F1 and F6.**	**Palaeoflood unit change of adjacent palaeo-floods.**	**Percentage change in discharge as a proportion of the total difference in discharge between units F1 and F7.**	**Palaeoflood unit change of adjacent palaeo-floods.**	**Percentage change in discharge as a proportion of the total difference in discharge between units F1 and F6.**
F5 to F6	82,0	F6 to F7	78,5	F5 to F6	60,0
F4 to F5	5,5	F5 to F6	5,5	F4 to F5	9,0
F3 to F4	3,0	F4 to F5	4,0	F3 to F4	13,0
F2 to F3	4,0	F3 to F4	3,5	F2 to F3	15,0
F1 to F2	5,5	F2 to F3	4,5	F1 to F2	3,0
		F1 to F2	4,0		

Table 3.4 - Percentage difference in discharge as a proportion of the total difference in discharge between adjacent palaeoflood units at sites 9, 14 and 19. Note the similar difference in discharge between the largest and second largest palaeoflood (upper portion of palaeoflood sequence) and the similar differences in discharges from the basal portion of the palaeoflood sequence.

3.2.6 The palaeoflood record and the historical and flow-gauge record at Prieska

The historical and flow gauge record for the Orange River at Prieska shows that the five largest floods had discharges of 12 470 m^3/s (1804), 13 070 m^3/s (1873), 12 040 m^3/s (1924), 11 940 m^3/s (1897) and 10 460 m^3/s (1973) (Fig. 3.31). The most recent flood was recorded in 1988 with a gauged discharge of 8 760 m^3/s. Relating the palaeoflood record of sites 9, 14 and 19 to the historical and flow-gauge record (modern record) is problematic because of chronostratigraphic uncertainty and possible discharge estimate errors at sites 9 and 14 (section 3.2.5). For example, the maximum palaeoflood recorded at site 9 (flood unit F6) corresponds to an uncorrected discharge of 13 080 m^3/s (Fig. 3.30) which could be correlated with either the 1804 flood (12 470 m^3/s) or the 1873 flood (13 970 m^3/s). However, the IRSL dating (6 610 ±1 320 years), allowing even for the likely overestimate in age due to residual luminescence, indicates that flood unit F6 cannot be related to the modern flood record of the Orange River. This conclusion is surprising as one would have expected evidence of slack-water sedimentation to have occurred by the large floods of 1804,

1873 and 1924. Calibration of the radiocarbon age obtained for flood unit F7 at site 9, section 1 indicates that a flood of approximately 6 030 m^3/s (uncorrected discharge) occurred in 1924 or 1850. Although the modern record does not indicate a flood occurring in 1850, a flood with a discharge of 12 040 m^3/s did occur in 1924 (Fig. 3.31). This difference in discharge may be accounted for by the onlapping sediments of flood unit F7 at section 2 being continuous and extending to the maximum point of slack-water pinchout at section 2. Consequently, flood unit F6 at section 2 and flood unit F7 at section 1 records slack-water deposition by the 1924 Orange River flood. This conclusion is not supported however by the IRSL date of 6 610 ±1 320 years obtained for flood unit F6 at section 2 (Fig. 3.30).

Site 14 also exhibits problems in relating the palaeoflood stratigraphy to the modern flow record. The calibrated radiocarbon date for flood unit F7 indicates that a flood with a discharge of approximately 9 000 m^3/s occurred in either 1893, 1900 or 1911, of which the 1900 date is the most probable date. The flow gauge record shows that no notable floods occurred in 1893 or 1900 (Fig. 3.31). A flood did, however, occur in 1911 but its discharge was only 1 720 m^3/s. The disparity between the palaeoflood discharge and the modern flow record may be ascribed to the incomplete nature of the historical flow record (1804 - 1909).

No flood-frequency analysis using the systematic flow-gauge record and the palaeoflood record was done because of two reasons. Firstly, the palaeoflood record does not contain evidence of floods with magnitudes greater than those recorded in the historical and flow-gauge record. Consequently, the palaeoflood record would not have a significant influence on the flood-frequency analysis. Secondly, the gauge record covers the period 1910 - 1989 with 4 historical peaks that extends the Prieska flood record back to 1804. The inclusion of the relatively small magnitude palaeoflood events in a historical and gauge record that is 185 years long would have a negligible effect if any on the flood-frequency analysis.

Although the palaeoflood record has not recorded the effect of relatively large floods that were recorded in the modern flow record, the following conclusions regarding the smaller palaeofloods can be made:

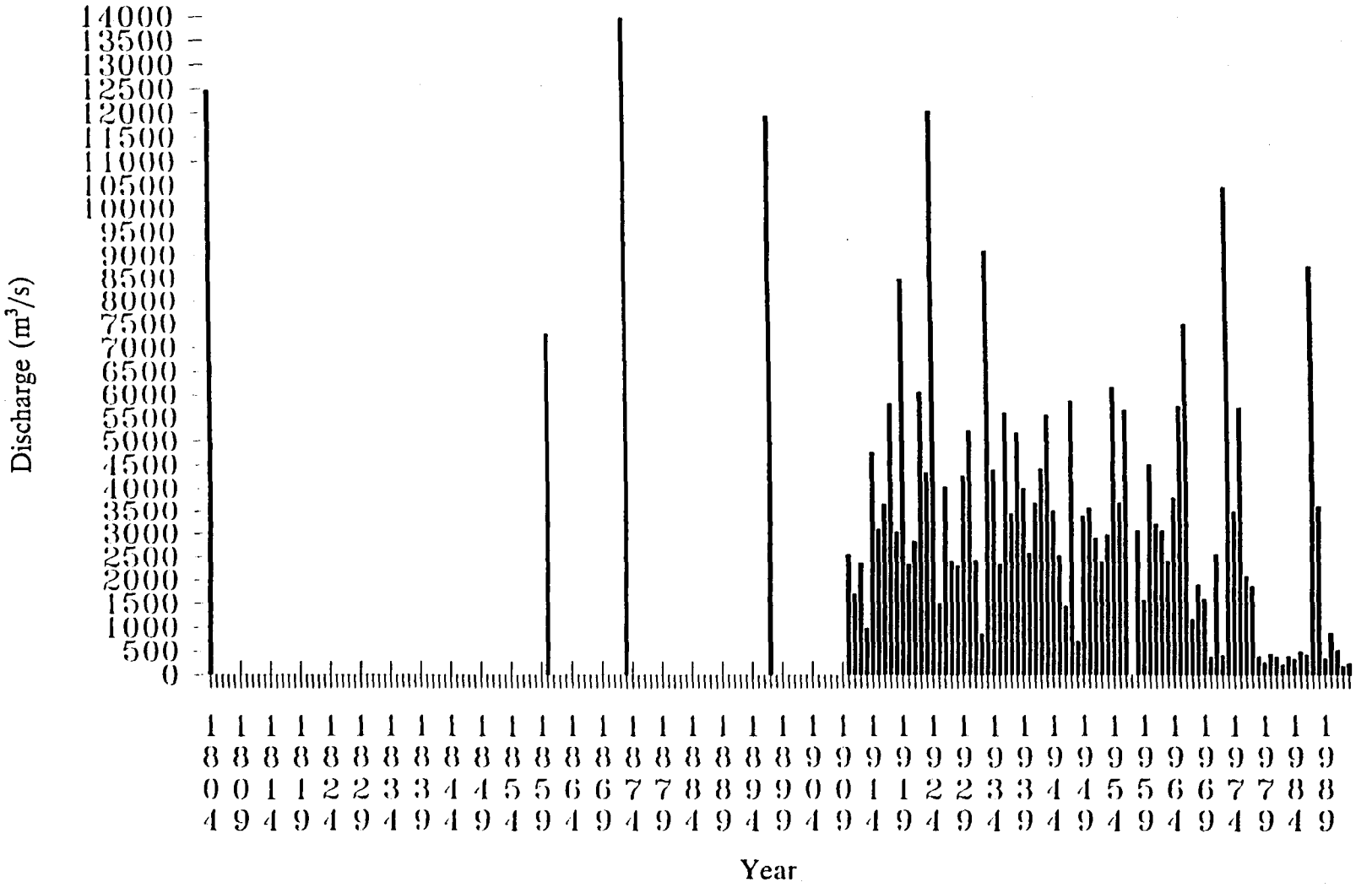

Fig. 3.31 - Historical (1804 - 1909) and annual peak-flow gauge record (1910 - 1993) (Department of Water Affairs and Forestry gauge station D7H002) for the Orange River at Prieska. The discharges for the period 1804 - 1909 were calculated from historically recorded flood levels (Van Bladeren, 1995).

(1) The basal portion of the palaeoflood stratigraphy at all three sites indicates that the Orange River experienced a series of floods with discharges of between approximately 2 500 m^3/s - 4 000 m^3/s (Fig. 3.30). Radiocarbon and IRSL dating indicates that these floods occurred between approximately 7 000 years B.P. - 12 500 years B.P.

(2) A flood with a discharge of approximately 4 440 m^3/s occurred 500 ±90 years B.P. which corresponds to the most probable calibrated age of A.D. 1440 (flood unit F4, site 19) (Fig. 3.30). This indicates that the overlying palaeoflood units F5 and F6 with respective discharges of 5 050 m^3/s and 9 030 m^3/s were deposited after A.D. 1440 (Fig. 3.30).

3.3 Palaeoflood hydrology of the lower Orange River (Richtersveld sites)

The palaeoflood hydrology of the lower Orange River was completed using the palaeoflood sites upper Xobies, lower Xobies and Bloeddrift which were discovered during the reconnaissance phase of this project (Zawada and Hattingh, 1993) (Fig. 3.32). The name Xobies does not occur on the 1:50 000 topocadastral sheet for the area but is used by the Nama people of the region for an abandoned livestock stand on the southern bank of the Orange River (Reck, 1994). The sites are located in a 34 km long reach of the river which is situated approximately 57 km - 91 km from the Orange River mouth (Fig. 3.32).

3.3.1 Lower Xobies palaeoflood site

The lower Xobies palaeoflood site comprises two sections that were examined in detail. Section 1 represents the main exposure which is located approximately 200 m upstream in the tributary from the confluence with the Orange River. Section 2 is a smaller exposure located approximately 50 m from the confluence.

3.3.1.1. Geological and geomorphological setting

The lower Xobies palaeoflood site is situated at latitude 28°13'20" and longitude 16°50'43" on the 1:50 000 topocadastral sheet 2816BB Sendelingsdrif (Fig. 3.32). The Orange River at lower Xobies is a single channelled, high sinuosity 600 m wide river. During low flow, the flow width is 100 m - 150 m during which large longitudinal in-channel bars 500 m long and side-attached sand bars up to 1 800 m long are exposed. The valley sides of the Orange River comprise north - south striking, moderate - steeply dipping beds of small-pebble conglomerate with arkose, schist, limestone dolomite and marble (Geological map of the Richtersveld, 1958) which mainly outcrop on the South African side of the River. Miocene - lower Pleistocene diamondiferous terrace gravels of the Arriesdrift Gravel Formation occur on the South African and Namibian portions of the river valley (Van Wyk and Pienaar, 1986). The terraces range in elevation from 3 m - 51 m above the present level of the Orange River and are best exposed on the Namibian side of the river valley (Van Wyk and Pienaar, 1986). The terraces comprise mainly well rounded - subangular cobble- and boulder-sized quartzite clasts set in a pebbly - sand matrix (Van Wyk and Pienaar, 1986). The banks of the Orange River are densely vegetated across a width of 10 m - 50 m decreasing rapidly away from the river to almost no vegetation.

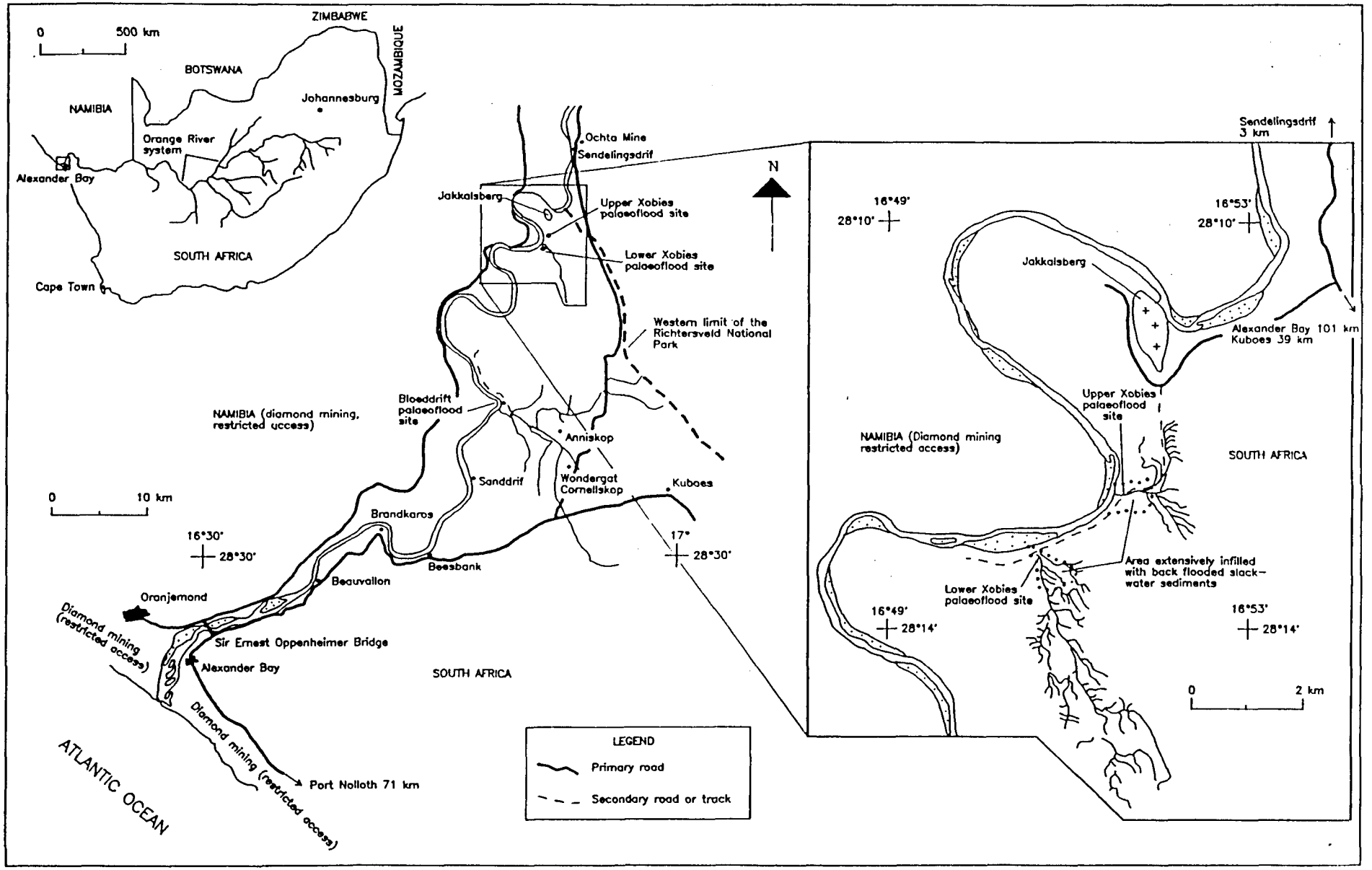

Fig. 3.32 - Location map of the lower Xobies, upper Xobies and Bloeddrift palaeoflood sites examined for the lower Orange River.

The tributary in which the palaeoflood sediments are situated flows in a south - north direction along the strike of exposed limestone, dolomite, conglomerate and schist. The tributary catchment is elongated and approximately 5,0 km^2 in size (Fig. 3.32). The tributary is ephemeral, of a low sinuosity exhibiting a high-gradient (0,011 m/m) with the thalweg comprising subangular dolomite and limestone clasts 0,5 cm - 15 cm long. The tributary is 100 m - 150 m wide at its mouth decreasing rapidly upstream to less than 50 m.

3.3.1.2 Description and interpretation of the palaeoflood stratigraphy at section 1

The palaeoflood stratigraphy at lower Xobies occurs as a blanket cover of mainly buff very fine-grained sand which infills much of the tributary for approximately 500 m in an upstream direction from the tributary-Orange River confluence. Its thickest development occurs close to the confluence progressively thinning and pinching out in an upstream direction in the tributary and towards the tributary valley sides (Fig. 3.33).

The main exposure is situated approximately 200 m upstream from the confluence. This exposure comprises a 5,60 m thick by 40 m - 150 m long sequence of interbedded buff very fine-grained sand and gravel (Fig. 3.33). The exposure was examined and described in the field and in further detail using relief peels totalling 5 m in length. Nine palaeoflood slack-water-deposited units were identified (F1 - F9) which are described and interpreted in the following section.

Flood unit F1 is a 66 cm-thick very fine-grained sand overlying the tributary thalweg gravel that comprises angular, dark-grey schist and limestone clasts 1 cm - 12 cm long (unit A; Fig. 3.34). In outcrop, unit A is apparently massive. A relief peel indicates however, it is flat laminated and extensively bioturbated. The bioturbation comprises vertical - horizontal meniscate burrows up to 10 cm long and 1 cm wide. Approximately 45 cm from the base is a zone of deformed laminae. Although much of unit A lacks grading, the top 1 cm - 2 cm fines upward into a tan very fine-grained sand - silt (Fig. 3.34). Overlying unit A is a 2 cm-thick, laterally continuous gravel comprising chaotically orientated angular schist clasts (unit B; Fig. 3.34).

Fig. 3.33 - The lower Xobies palaeoflood site exhibiting slack-water sediments deposited by Orange River flood waters that back flooded into the tributary. The Orange River flows towards the left of the photograph within the belt of vegetation. Note the upstream thinning and pinchout of the slack-water sediments in the tributary and towards the tributary valley side. The position of sections 1 and 2 are shown. Note the vehicle in the tributary thalweg for scale.

Unit A is interpreted as a palaeoflood slack-water sediment deposited by mainly suspension settling of very fine-grained sand in quiet water conditions due to tributary back flooding. Periodic slight increases of flow regime occurred as the flood stage of the Orange River increased (Fig. 3.35). This interpretation is justified firstly on its interbedded position between the underlying and overlying tributary deposited gravel (Fig. 3.35) and secondly, its contrasting textural characteristics to the adjacent beds. The presence of contorted lamination indicates high rates of suspension settling. The laterally continuous and thin nature of the non-slack-water bed (unit B) suggests deposition by an aerially extensive tributary-related sheet flow (Fig. 3.35).

Flood unit F2 is an 80 cm - 170 cm thick dark-brown, mainly massive, upward fining fine- to very fine-grained sand with a distinctive flat-bedded appearance in

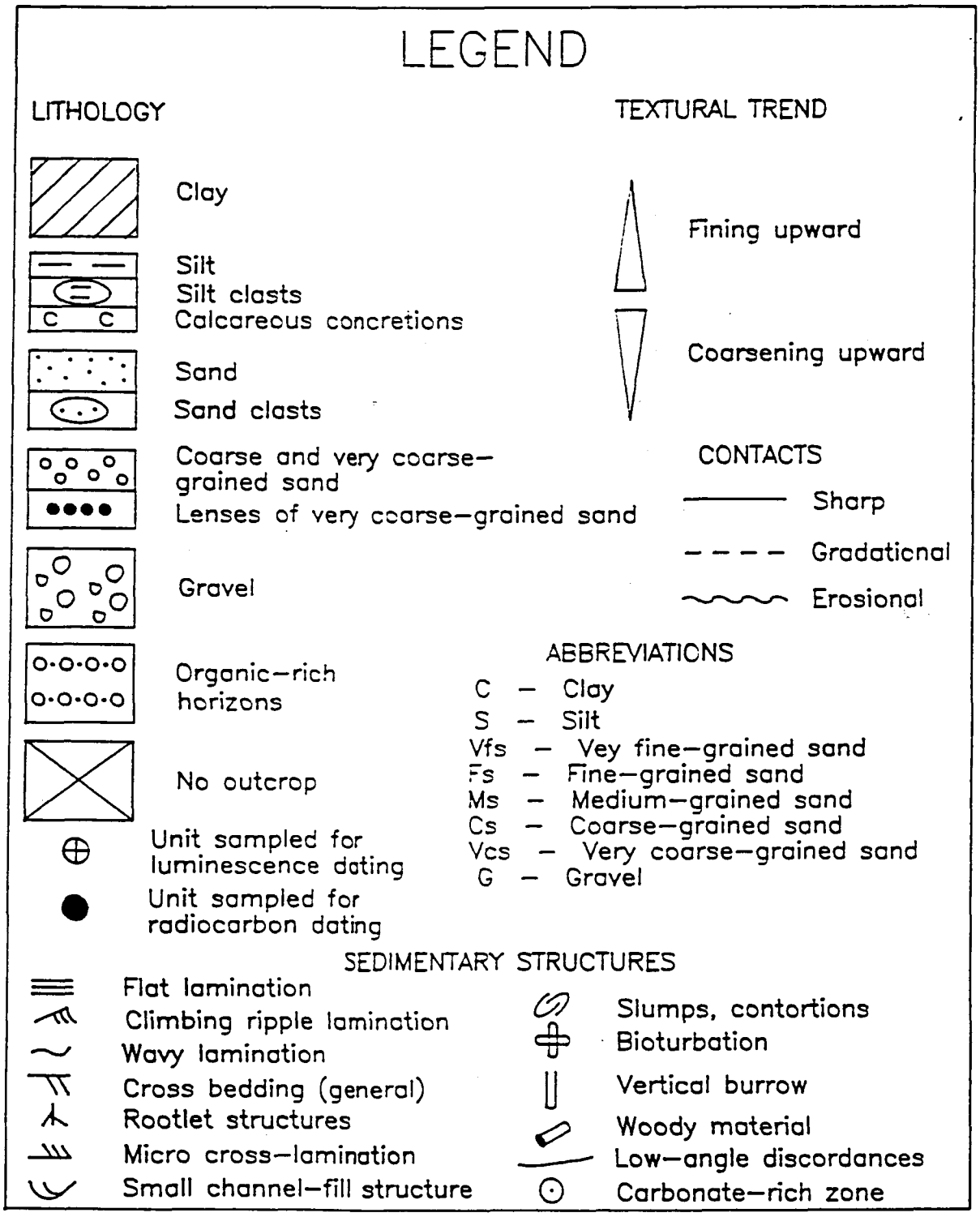

List of symbols used in Figs 3.34, 3.35, 3.47, 3.49, 3.50 and 3.60

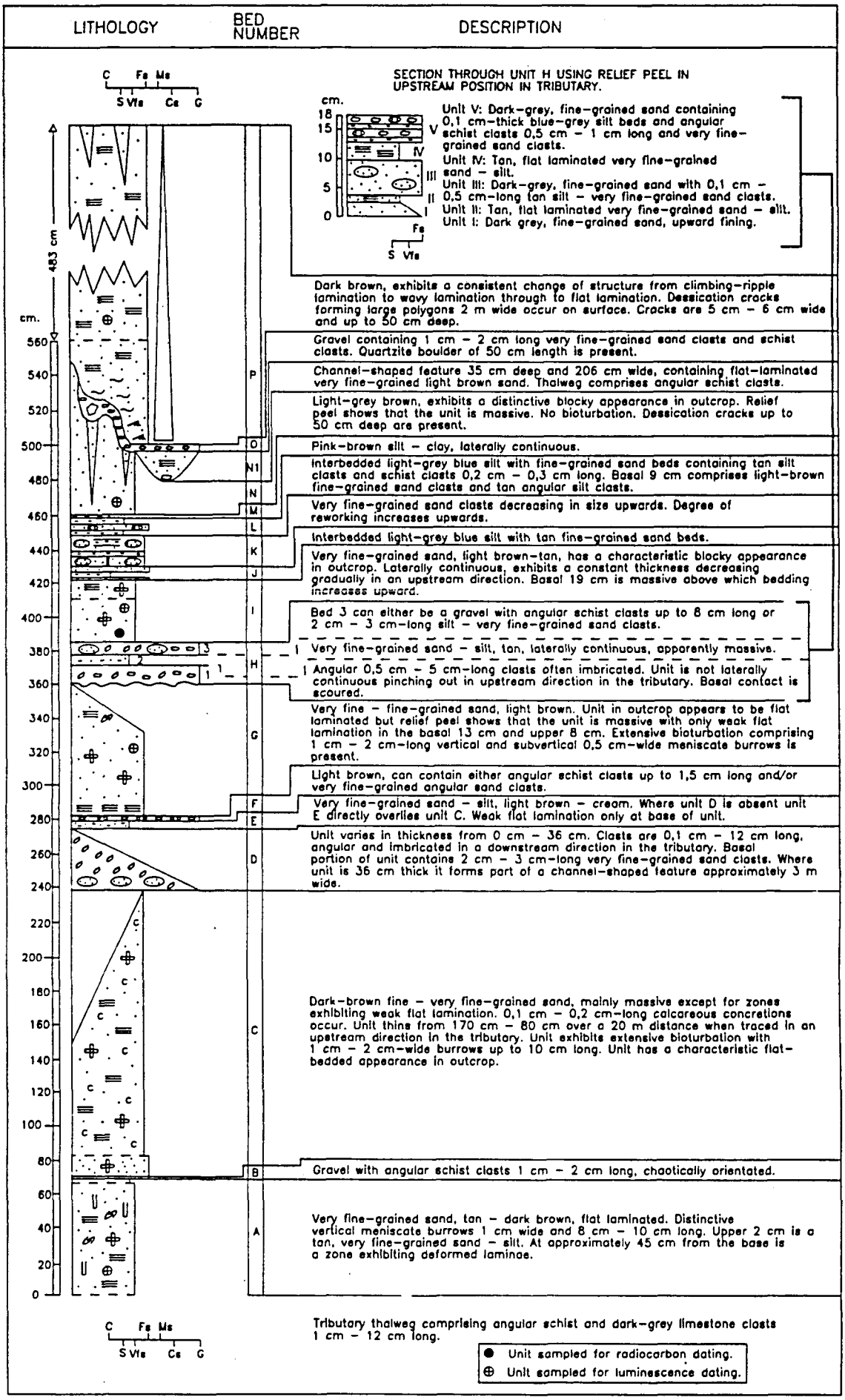

Fig. 3.34 - Lithological description of the palaeoflood stratigraphy at section 1 (lower Xobies (see legend on page 107).

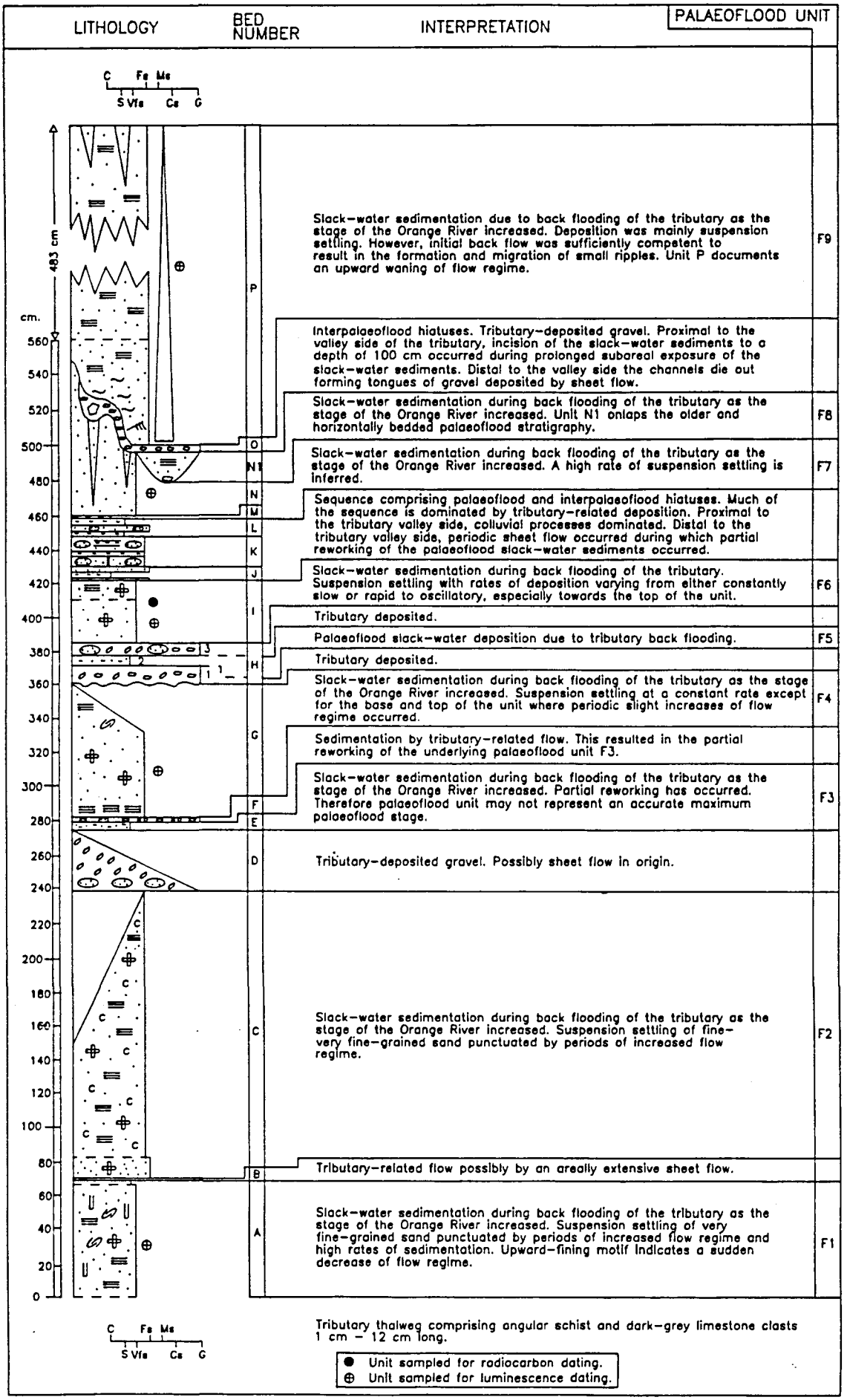

Fig. 3.35 - Sedimentological and hydrodynamic interpretation of the palaeoflood stratigraphy at section 1 (lower Xobies) (see legend on page 107).

outcrop (unit C; Fig. 3.34). Unit C thins progressively from 170 cm - 80 cm in an upstream direction in the tributary over a distance of 20 m. A relief peel shows it is mainly massive except for infrequent and weakly developed flat-laminated zones that increase in frequency upwards. The unit is extensively bioturbated by 1 cm - 2 cm wide and up to 10 cm long vertical - horizontal meniscate burrows. Frequent calcareous nodules 0,1 cm - 0,2 cm in diameter occur. Unit C is overlain by a 0 cm - 36 cm thick gravel comprising 0,3 cm - 12 cm long angular clasts that are imbricated with a downstream flow direction in the tributary (unit D; Fig. 3.34). The base of unit D exhibits 2 cm - 3 cm long very fine-grained sand clasts. Although unit D can be locally absent in which case unit E directly overlies unit C, it can dramatically increase in thickness to form a 36 cm thick and 300 cm wide channel-shaped feature (Fig. 3.36).

Fig. 3.36 - Lenticular gravel-filled channel (bottom left of exposure) in unit D at section 1 (lower Xobies) interbedded between very fine-grained slack-water sediments.

Otherwise the base of unit D is sharp and planar. A detailed discussion on the significance of the gravel-filled channel is given in the section describing and interpreting flood units F7 and F8.

Unit C is interpreted as a palaeoflood slack-water sediment deposited by tributary back flooding during Orange River flooding (Fig. 3.35). This interpretation is based on its interbedded position between the underlying and overlying tributary-deposited gravel units (units B and D respectively) and its progressive upstream thinning, which is ascribed to the progressive decrease of water depth as back-flooding of the tributary occurred. The justification for interpreting unit D as a tributary flow-deposited unit, is its downstream-directed imbrication and its textural and compositional similarity to the gravel forming the present-day tributary thalweg Fig. 3.35). The very fine-grained sand clasts at the base of unit D indicates sufficiently competent flow that partially reworked the upper portion of unit C. The mainly sharp and planar basal contact of unit D probably indicates sheet flow. Flow conditions during back flooding were characterised by suspension settling of mainly very fine-grained sand. The interbedded flat-laminated and massive sand beds may indicate an alternation between pulsatory flow and either rapid or slow continuous rates of sedimentation. The frequent calcareous nodules suggests that flood unit F2 is relatively old.

Flood unit F3 is a 5 cm thick light-brown - cream very fine-grained sand - silt exhibiting weakly developed flat lamination from the basal 1 cm - 2 cm (unit E; Fig. 3.34). Where the underlying unit D is absent, unit E directly overlies unit C (Fig. 3.34). Unit E is reworked containing patches of medium-grained sand. Overlying unit E with a sharp basal contact is a 4 cm thick laterally continuous gravel comprising either angular schist clasts up to 1,5 cm long and/or very fine-grained sand clasts 0,1 cm - 1 cm long (unit F; Fig. 3.34).

The interbedded position of unit E between the gravel-deposited units D and F and its contrasting texture, indicates that it represents a slack-water sediment deposited during tributary back-flooding (Fig. 3.35). Unit F3 has been partially reworked as indicated by the numerous very fine-grained sand clasts at the base of the overlying unit F as well as the patchy distribution of medium-grained sediment in unit E. It is therefore possible that an unknown thickness of unit E has been removed and may not represent an accurate peak palaeostage. However, because the overlying unit F is relatively thin (4 cm) with its basal contact being sharp and not obviously erosive, may suggest that reworking of flood unit F2 was probably minimal.

Flood unit F4 is a laterally continuous 50 cm - 78 cm thick, light-brown fine - very fine-grained sand exhibiting a sharp, basal planar contact and an upper planar - erosive contact (unit G; Fig. 3.34). Unit G in outcrop is apparently flat laminated. A relief peel showed however, that much of the unit is extensively bioturbated exhibiting 1 cm-wide meniscate vertical - horizontal burrows up to 4 cm - 5 cm long with only the basal 13 cm and upper 8 cm exhibiting weakly developed flat lamination. The infilling of the burrows is lithologically identical to the surrounding sediment. However, towards the top of unit G, the burrow infill comprises coarser grained sand. Unit G is homogenous exhibiting neither a visible change of grain size or colour when vertically or laterally traced. Overlying unit G is the basal bed of the overlying unit H comprising an 11 cm thick imbricated - chaotically orientated gravel with clasts 0,5 cm - 5 cm long (bed 1, unit H; Fig. 3.34). This bed thins in an upstream direction in the tributary to a dark-grey upward-fining fine-grained sand (see bed I where unit H was examined using a relief peel; Fig. 3.34).

The fine- to very fine-grained texture of unit G and its interbedded position between the coarser-grained units F and bed 1 of unit H respectively, suggests it was deposited as a slack-water sediment during back-flooding of the tributary (flood unit F4; Fig. 3.34). Unit F and bed 1 of unit H represent hiatuses during which tributary related deposition occurred. The textural homogeneity of flood unit F4, the lack of bedding except for weak lamination at the base and the top of the unit and the absence of soft-sediment deformation features, suggests constant rates of suspension settling of fine- to very fine-grained sand in quiet water conditions. Periodic slight increases of flow regime only occurred at the onset and end of the deposition of unit G.

Flood unit F5 is a thin very fine-grained sand stratigraphically located in unit H (Fig. 3.34). However, unit H varies lithologically depending upon its position with respect to the tributary - Orange River confluence. Nearer the confluence, unit H comprises a basal 11 cm thick gravel bed with a sharp and either planar or undulating contact (bed 1, unit H; Fig. 3.34). Overlying bed 1 is a 6 cm thick very fine-grained, laterally continuous, apparently massive very fine-grained sand - silt (bed 2, unit H; Fig. 3.34). Overlying bed 2 is a 5 cm - 7 cm thick gravel containing either angular schist clasts up to 8 cm long or 2 cm - 3 cm long angular silt - very fine-grained sand

clasts (Fig. 3.34). Tracing unit H in an upstream direction in outcrop and using relief peels showed that it becomes progressively finer with distance from the confluence. In a distal position, unit H is 18 cm thick, comprising an interbedded sequence of dark-grey fine-grained sand with either tan very fine-grained sand - silt or sand containing 0,1 cm long very fine-grained sand clasts (Figs 3.34 and 3.37). Beds III and V contain angular very fine-grained sand clasts with bed V exhibiting containing

Fig. 3.37 - Relief peel of unit H in a distal position with respect to the tributary Orange River confluence at lower Xobies, comprising an interbedded sequence of dark-grey fine-grained sand and tan very fine-grained sand. Note the partially reworked tan very fine-grained sand in the middle and left of the relief peel.

conspicuous 0,2 cm - 0,4 cm-thick blue-grey, laterally continuous silt - clay beds. Underlying bed V (Fig. 3.34), is a 4 cm-thick, tan, flat laminated very fine-grained sand - silt exhibiting sharp, planar upper and basal contacts.

Although beds 2 and IV of unit H could not be continuously traced in the tributary they are correlates of each other. These beds are interpreted as slack-water

sediments deposited during tributary back-flooding as the stage of the Orange River increased. This interpretation is justified on the basis of their fine-grain size which is in contrast to the coarser-grained texture of the underlying and overlying beds. However, for the stratigraphy underlying and overlying bed IV, the interpretation is less clear (Fig. 3.34) because of uncertainty in identifying and interpreting interflood hiatuses.

The identification of interflood hiatuses at lower Xobies is based primarily on interpreting angular coarse-grained sand - gravel size sediment as being deposited by tributary-related flow processes which were either channelised or non-channelised. Other less certain interflood hiatuses comprise sharply based blue-grey silt - clay beds interbedded with tan - light brown very fine-grained sand. Although this type of sequence was observed from unit H at the lower Xobies site, it was best observed in outcrop (Fig. 3.38) from which a relief peel was made (Fig. 3.39) from the upper Xobies palaeoflood site located approximately 1 400 m north of lower Xobies (Fig. 3.32). This outcrop is discussed in detail in order to highlight the importance and difficulty in differentiating palaeoflood from non-palaeoflood events.

Two hypotheses are presented to account for the sedimentary motif shown in Figs 3.38 and 3.39. **Hypothesis 1** is the most favoured one and states that each very fine grained sand bed (beds 1, 3, 5, 7 and 9; Fig. 3.39) represents a discrete tributary back-flood incursion during periodic Orange River flooding. The inter-flood hiatuses are therefore represented by the blue-grey silt - clay beds which were deposited by tributary flow unrelated to Orange River flooding. This interpretation is justified on the basis of the following observations:

(1) the blue-grey colour and clay - silt lithology occurs in the thalweg of the present day tributary at the upper Xobies site. The source of the silt - clay was traced to the dark blue - black highly-weathered schist forming the bedrock of the tributary headwaters.

(2) The blue-grey silt - clay beds grade laterally downstream in the tributary into angular gravel similar to the gravel in the present tributary thalweg. This shows that the blue-grey silt - clay bed represents not only a lateral facies change of tributary-related flow, but also a correlatable

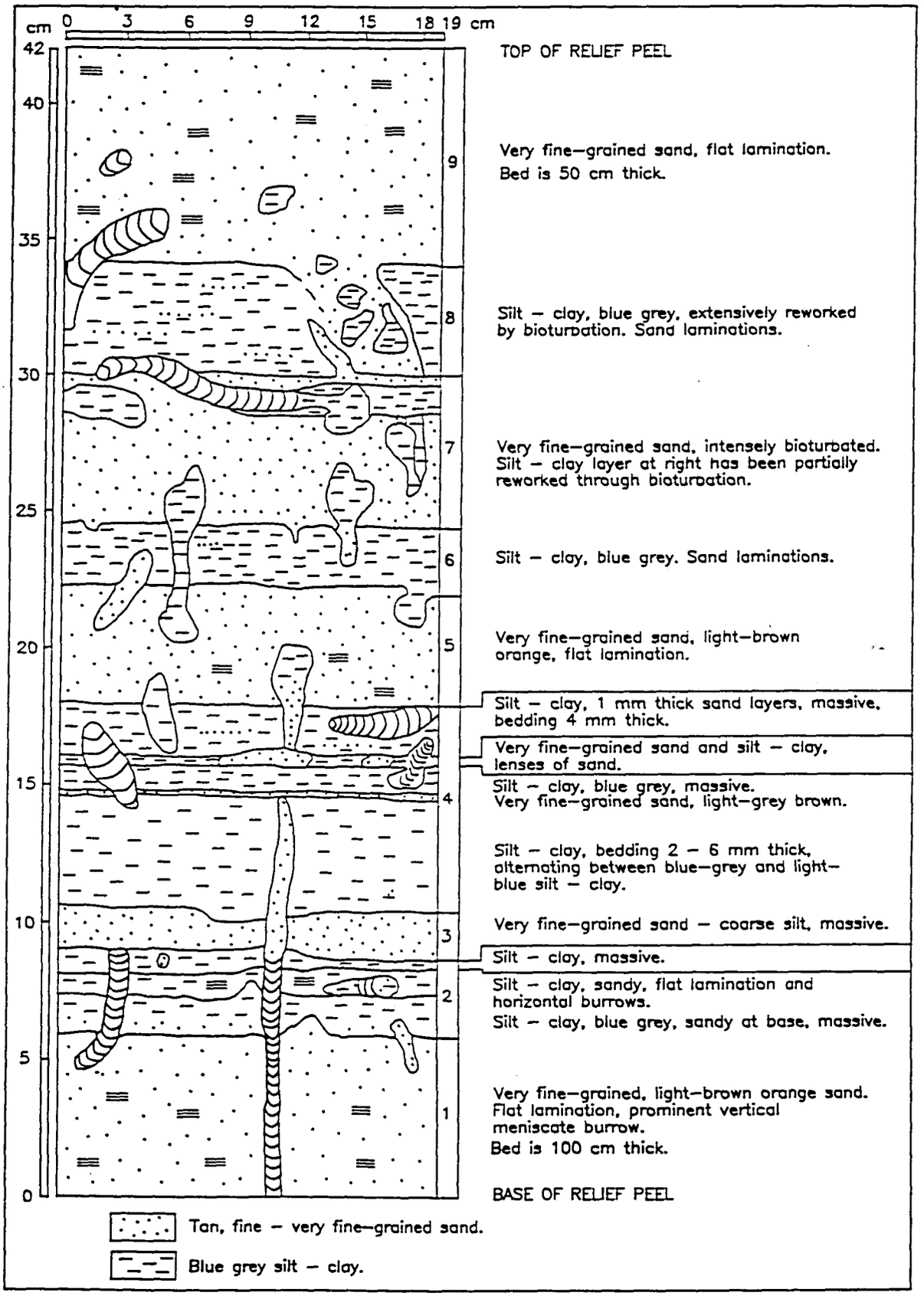

Fig. 3.38 - Sketch of Fig. 3.39 illustrating the sharp lithological contacts between the palaeoflood slack-water sediments (tan very fine-grained sand beds) and the non-palaeoflood tributary flow-related sediments (silt - clay beds) at upper Xobies.

chronostratigraphic horizon.

(3) No evidence exists for the blue-grey silt-clay lithology being associated with Orange River sediments. This suggests that the Orange River does not transport sedimentary material of this type indicating its source as being the tributary catchment. Acknowledging that the blue-grey beds represent non-trunk stream flood deposits, indicates that they represent inter-flood hiatuses. Therefore, the interbedded fine- very fine-grained sand beds are palaeoflood slack-water sediments deposited during tributary back flooding. Furthermore, the interbedded units are thin and non-erosive with the tops of the blue-grey beds not being intensively bioturbated. This indicates that the deposition of the palaeoflood and non-palaeoflood beds shown in Figs 3.38 and 3.39 occurred in rapid succession during which subaerial exposure of the interbedded units was minimal.

An unresolved issue is the deposition of a laterally continuous (across relief peel and outcrop), thin (0,1 cm - 0,2 cm thick), tan silt - very fine grained sand beds (bed; Fig. 3.38) within the framework of hypothesis 1. According to the hypothesis, the bed is a slack-water sediment. However, it is difficult to envisage deposition of such a thin aerially extensive bed during flood conditions. An alternative explanation takes into account its stratigraphic position in the middle of the blue-grey bed (bed 4; Figs. 3.38 and 3.39). The blue-grey bed exhibits distinctive bedding planes across which slight changes of colour and texture occur. This suggests that the light-brown very fine-grained sand was deposited by small very shallow, non-erosive sheet-wash flows generated in the tributary catchment.

Hypothesis 2 postulates that although the sediment comprising the blue-grey beds originated from the weathering of schists exposed in the headwaters of the tributary, the sequence shown in Figures 3.38 and 3.39 was deposited by one back-flood event characterised by pulses or surges. During tributary back flooding, the blue-grey silt - clay fraction which was residing in the pore space of the coarser grained tributary alluvium, became entrained to form part of the larger flood derived suspension load of the Orange River. Ponding between flood surges or a decrease of flow competency resulted in the settling out of the fine- to very fine-grained sand

fraction followed by suspension settling of the blue-grey silt - clay beds. The hydrodynamic difference in settling velocity between the silt - clay and the fine- to very fine-grained sand would account for the sharp upper and lower contacts between the blue-grey silt - clay beds and the fine- to very fine-grained sand. This hypothesis accounts better for the thin sand beds and lenses than hypothesis 1. However, it does not adequately explain the sharp nature of the contacts. If entrainment and suspension of the silt - clay material occurred during back flooding, it is likely that subsequent sedimentation, even taking into account sorting differences between the clay - silt fraction and the fine- to very fine-grained sand would result in partial mixing and simultaneous deposition of the suspended sediment loads resulting in graded contacts. The lack of gradational sedimentary contacts in unit H (Fig. 3.38) indicates that little mixing of Orange River and tributary derived sediment occurred.

Fig. 3.39 - Relief peel of unit H from upper Xobies comprising a sequence of bioturbated blue-grey silt - clay beds which were deposited by tributary related flow, interbedded with light-grey, very fine-grained sand beds which were deposited as slack-water sediments during ponding of water in the back-flooded tributary (see Fig. 3.38 for sketch of relief peel).

Flood unit F6 is a 38 cm thick, very fine-grained tan sand (unit I; Fig. 3.34). In outcrop the unit thins gradually in an upstream direction in the tributary. It has a sharp, inclined basal contact whereas the upper contact is sharp and planar. Unit I in outcrop is apparently massive exhibiting a conspicuous blocky appearance. A relief peel shows that it is lithologically homogenous, displaying neither textural or vertical colour trends. However, at approximately 12 cm from the top, flat lamination occurs abruptly that decreases in thickness upwards until the laminations are almost paper thin. The basal contact of unit I overlies a gravel comprising schist and/or very fine-grained angular sand clasts (bed 3, unit H; Fig. 3.34). Overlying flood unit F6 is a 38 cm thick sequence comprising a basal light - grey blue, bioturbated silt (unit J, 8 cm thick, Fig. 3.34) overlain by a bed comprising chaotically orientated, tan, very fine-grained sand clasts (unit K, 18 cm thick; Fig. 3.34) which in turn is overlain by light-dark-grey, bioturbated, flat-bedded silt (unit L, 12 cm thick, Fig. 3.34). In outcrop, units J, K and L appear genetically related and together can be traced from a distal position with respect to the tributary valley side to a proximal position where units J, K and L gradually coarsen to a 10 cm thick gravel containing angular schist clasts 3 cm - 10 cm long. A relief peel of units J, K and L (Fig. 3.40) shows that units J and L are texturally similar to the blue grey silt - clay beds described from the upper Xobies site (Figs 3.38 and 3.39).

The finer-grained texture of unit I compared to the overlying and underlying units (units J and H respectively; Fig. 3.34), its sharp upper and lower contacts and the thinning of unit I in an upstream direction in the tributary, suggests it was deposited as a slack-water sediment during tributary back flooding (Fig. 3.35). Flow conditions during tributary back flooding were quiet, characterised by suspension settling of very fine-grained sand. Rates of deposition varied however, from either constant or rapid (massive portion of unit I; Fig. 3.34), to periodic changes of depositional rates that increased in frequency upwards (flat-laminated portion of unit I; Fig. 3.34).

The overlying and underlying units (units J, K, L and unit H respectively), represent interpalaeoflood hiatuses. The nature of the hiatuses depends on their position in the tributary with respect to the dominant source of sediment. For example, units J, K and L where observed to comprise only gravel comprising angular

schist clasts 3 cm - 10 cm long close to the bedrock valley side of the tributary. In contrast, a facies change into silt - clay interbedded with abundant intraformational clasts indicates that distal to the tributary valley side, deposition was not influenced by colluvial processes. Instead, the dominant sediment source was weathered schists in the tributary catchment, similar to that observed at the upper Xobies site with the intraformational sediment being derived from partial reworking of the slack-water sediments during periodic sheet flow (Fig. 3.35).

Fig. 3.40 - Relief peel of units J, K and L in a distal position to the tributary valley side at lower Xobies. The sequence comprises light-grey very fine-grained sand - silt interbedded with tan very fine-grained sand beds showing varying degrees of reworking. Although the tan beds may have originally represented slack-water sediments, they were extensively reworked by tributary related flow.

Flood unit F7 is a 34 cm - 90 cm thick tan, apparently massive, very fine-

grained sand with a characteristic blocky appearance in outcrop (units M and N; Fig. 3.34). Although flood unit F7 thins in an upstream direction in the tributary, at any one point, its thickness is variable due to incision from the overlying unit (unit O; Fig. 3.34). The top of flood unit F7 exhibits desiccation cracks 1 cm - 3 cm wide and 50 cm deep. A relief peel through flood unit F7 shows that it is massive displaying neither textural or vertical colour changes except for the base of the unit which comprises a light tan, very fine-grained sand - silt (unit M; Fig. 3.34). A conspicuous feature of unit N (Fig. 3.34) is the absence of bioturbation. The basal contact of flood unit F7 is sharp and planar whereas the upper contact with the overlying unit O is sharp and steeply incised (Fig. 3.34). Unit O is 1 cm - 100 cm thick, has an erratic lower erosional contact in the shape of channel features 2 m - 4 m wide extending to a maximum depth of approximately 180 cm or to the top of unit G (Fig. 3.41). Unit O contains mainly angular schist and intraformational very fine-grained sand clasts up to 2 cm long with one example of a 50 cm-long angular rose quartz clast being noted (Fig. 3.41). Where unit O occurs adjacent to the bedrock valley side of the tributary, its thickness increases to approximately 100 cm with the clasts being up to 30 cm in length.

The very fine-grained texture, the interbedded position of units M and N between the underlying and overlying coarser grained units L and O respectively, their upstream-thinning direction in the tributary and sharp basal and upper contacts, indicates that they represent slack-water sediments deposited by tributary back-flooding. Depositional conditions were predominantly suspension settling of very fine-grained sand under either very high rates of deposition or, a constant rate of deposition where sediment influx from the Orange River into the tributary was constant. Very high rates of deposition is favoured however, because of the massive appearance of unit N together with the absence of escape burrows and other bioturbation.

The underlying and overlying units (units L and O respectively) represent interpalaeoflood hiatuses during which, in the case of unit O, localised channel erosion scoured a portion of the palaeoflood stratigraphy (Fig. 3.34). The scouring observed in unit N (Fig. 3.42) is explained with reference to similar scouring observed in the overlying palaeoflood unit F8 (unit P). Because unit P exhibits the highest palaeoflood

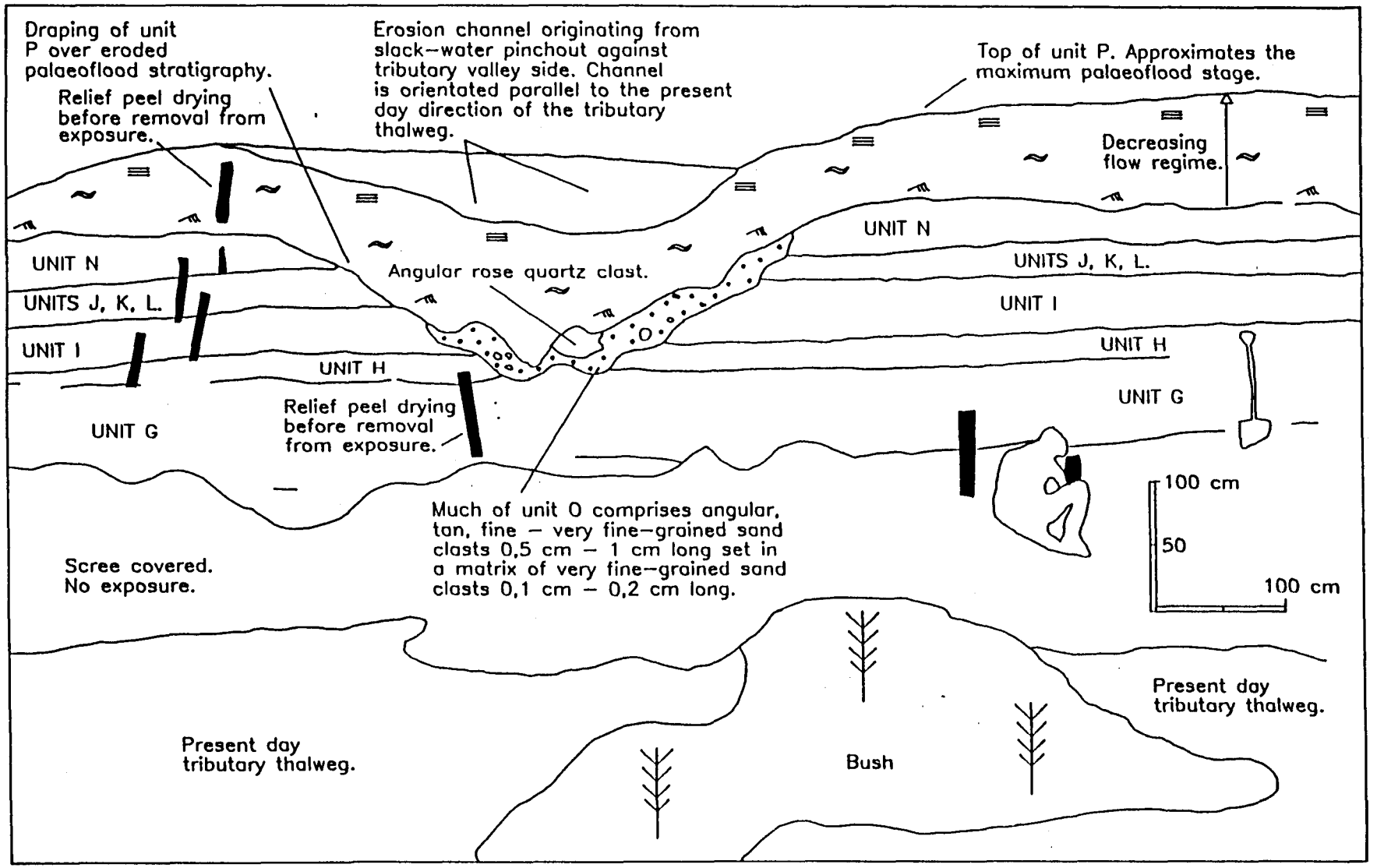

Fig. 3.41 - Sketch of photograph illustrating the incision of units N, J, K, L, I, H and G by unit O at lower Xobies. Note the 50 cm angular rose quartz clast at the base of unit O and the draping of the slack-water sediments of unit P over the palaeoflood hiatus surface of unit O.

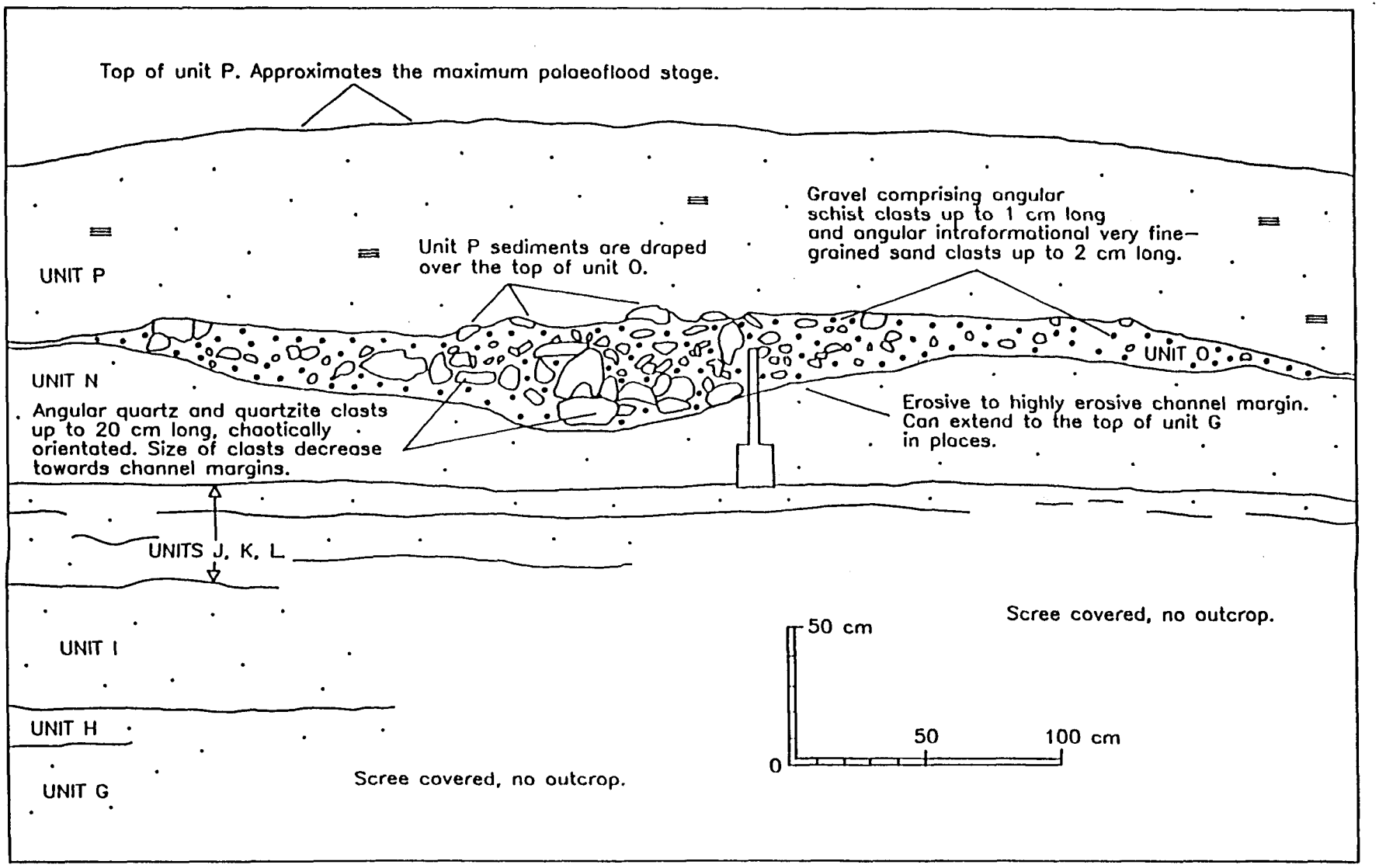

Fig. 3.42 - Sketch of photograph illustrating the dimension of a gravel-filled channel (unit O) that has incised the slack-water sediments of unit N at lower Xobies. Note that the gravel comprises reworked intraformational slack-water deposited sand clasts and extraformational schist clasts derived from the tributary valley side. The chaotic orientation of gravel clasts is attributed to infrequent ephemeral and short-lived flow occurring in the channel.

stage at lower Xobies, its upper surface is exposed revealing several V-shaped channels which are more numerous closer to the pinchout of the slack-water sediments against the bedrock of the tributary valley side (Fig. 3.43). At this position, the channel fill comprises chaotically orientated angular gravel clasts 20 cm - 30 cm long. Tracing the channels in a distal direction from the valley side they become shallower and eventually peter out, leaving only tongues of finer grained gravel comprising angular clasts 2 cm - 3 cm long. The channels formed in response to prolonged subaerial exposure and colluviation on the tributary valley side. Distal to colluviation, flow competency was reduced characterised by sheet-flow processes which led to the entrainment and deposition of finer-grained tongues of gravel.

Flood unit F8 comprises a channel-shaped feature 35 cm deep and 206 cm wide comprising flat laminated, very fine-grained light-brown sand (unit N1; Figs. 3.34 and 3.44). The base of flood unit F8 is erosive incising the underlying unit N and contains a 5 cm - 7 cm thick gravel bed with angular schist clasts (Fig. 3.44). The top of flood unit F8 is truncated by unit P. No further outcrop of unit N1 was observed in an upstream direction in the tributary. However, approximately 100 m downstream from the main exposure, an outcrop of unit N1 underlying unit P occurs. Unit N1 onlaps the horizontally bedded palaeoflood stratigraphy and thins to eventually pinch out at a point close to the top of unit N (Fig. 3.45). Both the upper and basal contacts of unit N1 are sharp with frequent lenses comprising angular, very fine-grained sand and schist clasts up to 1 cm long (Fig. 3.45).

The interpretation of unit N1 as a palaeoflood slack-water deposit is justified on the basis of its very fine-grained texture, its sharp basal and upper contacts which also contain evidence of interflood hiatuses and its onlapping relationship with the older and horizontally-bedded slack-water sediments (Fig. 3.45). The isolated occurrence of flood unit F8 as a channel-shaped feature from the main exposure indicates that its position is close to its point of pinchout or maximum palaeoflood stage. This would account for the absence of unit N1 further upstream in the tributary. Conversely, flood unit F8 is well developed in a downstream direction in the tributary where it was thicker and found to onlap the older palaeoflood stratigraphy. Corroboration of unit N1's point of pinchout is provided by the surveying data, showing that the level at which unit N1 pinches out in the downstream exposure

(40,83 m.a.s.l.), is similar to the palaeoflood stage obtained for the top of unit N1 (40,87 m.a.s.l.) measured approximately 100 m in an upstream direction in the tributary (Figs 3.44 and 3.45).

Fig. 3.43 - Channelised erosion of proximal slack-water sediments by tributary valley side colluviation at lower Xobies. Note the large polygonal structures (approximately 2 m wide) that are bound by desiccation cracks 5 cm - 6 cm wide and up to 50 cm deep.

Flood unit F9 is a 483 cm thick dark brown - light brown fine-grained sand (unit P; Fig. 3.34) of which the basal 60 cm could be examined in detail. The basal contact of unit P is draped over the variable and scoured unit O (Fig. 3.41). The unit thins gradually in an upstream direction in the tributary to eventually pinchout. Because unit P represents the largest slack-water deposit in terms of stage, large areas of its upper surface is subaerially exposed revealing 2 m wide polygonal structures that are bound by desiccation cracks 5 cm - 6 cm wide and up to 50 cm deep (Fig. 3.43). The upper surface of unit P is traversed by small 10 cm - 100 cm wide channels which in places are either partially infilled with gravel derived from the tributary valley side or incised to the depth of the tributary thalweg. Both outcrop and the relief peel

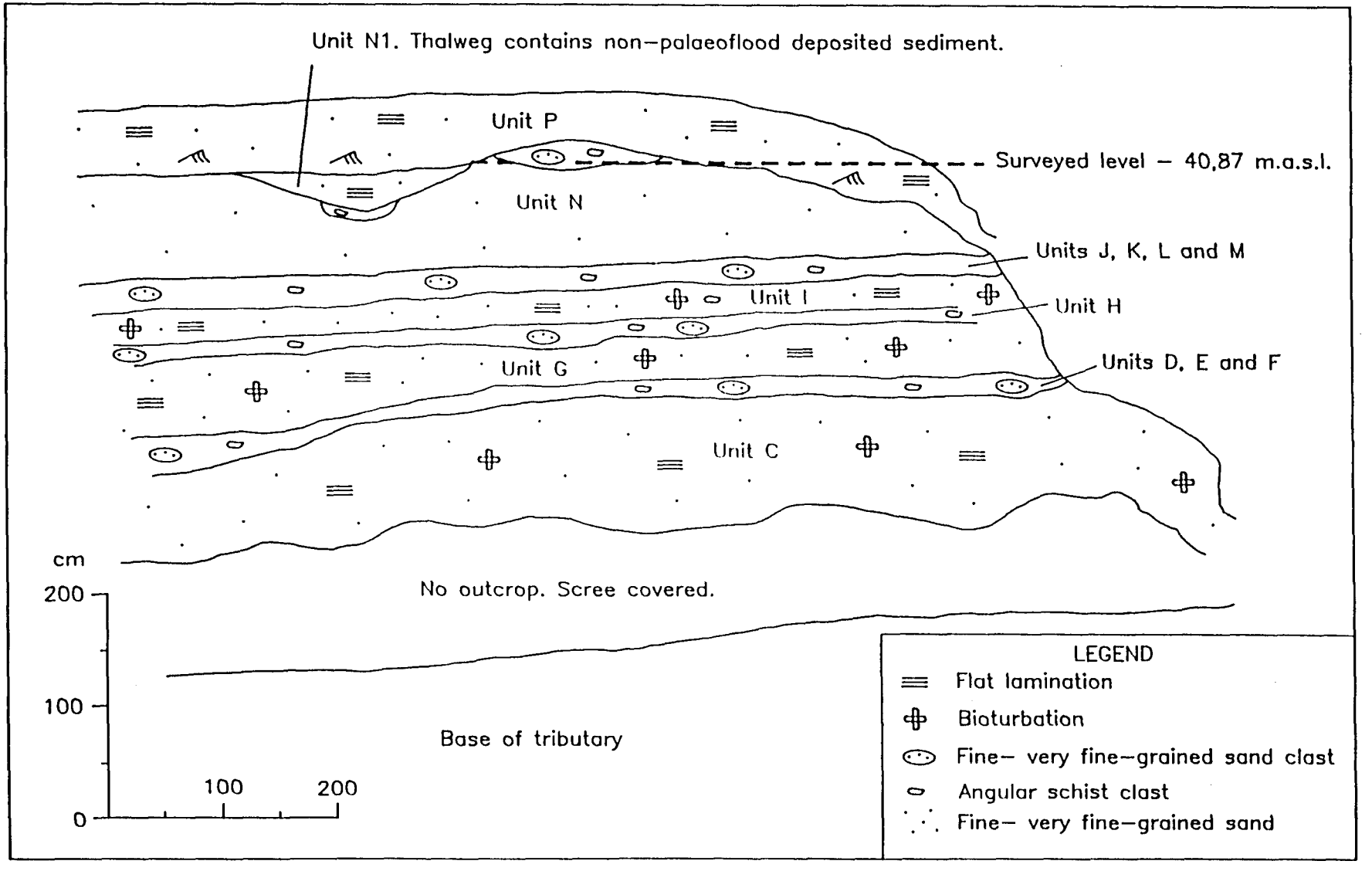

Fig. 3.44 - Sketch from photograph of flood unit F8 (unit N1) occurring as a channel feature between the slack-water units N and P at lower Xobies. Unit F8 does not occur in an upstream direction in the tributary and therefore the surveyed height of its upper surface (40,87 m.a.s.l.)is close to its point of pinchout.

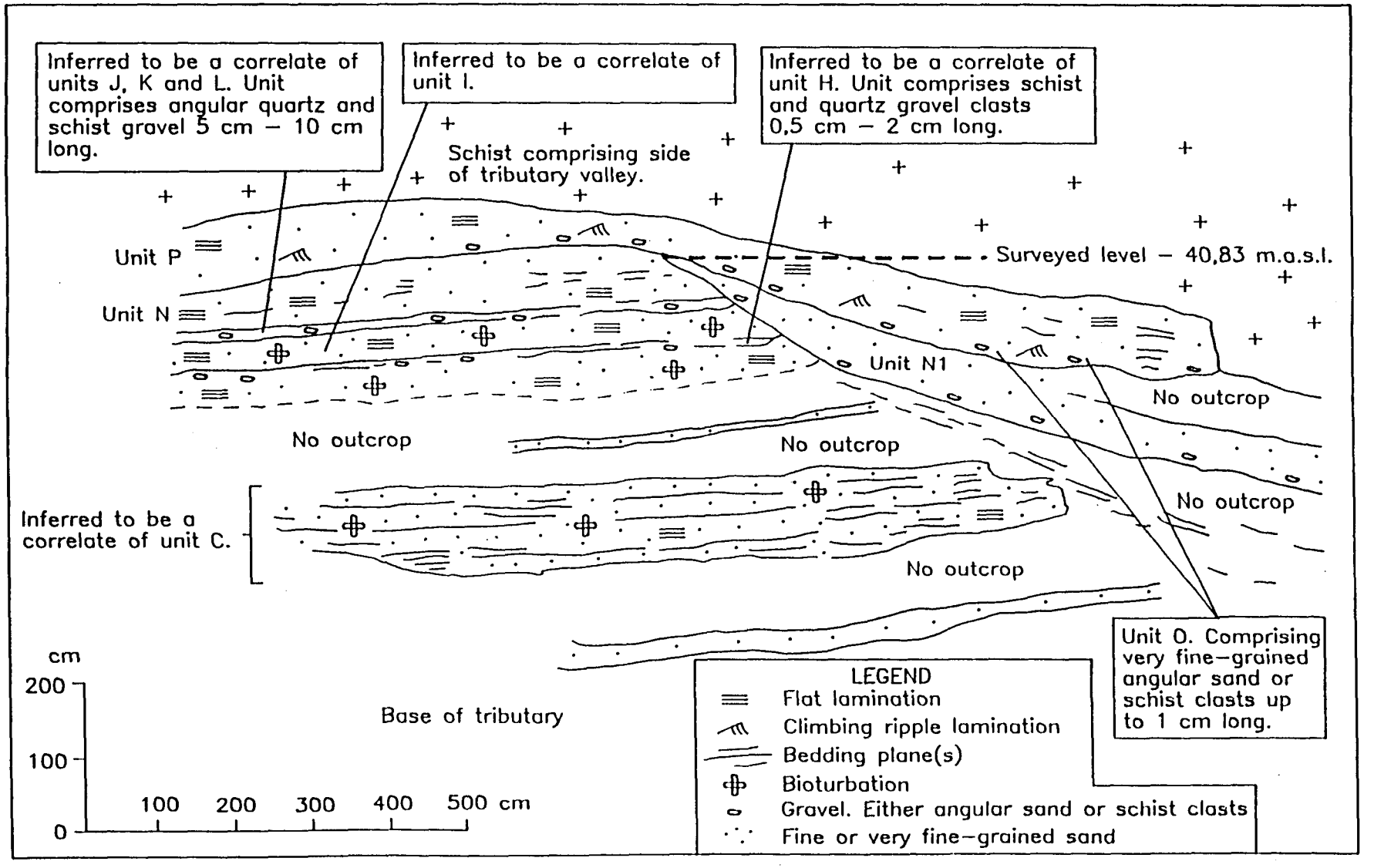

Fig. 3.45 - Sketch from photograph illustrating a sequence of onlapping slack-water sediments approximately 100 m downstream of the exposure shown in Fig. 5.44 at lower Xobies. At this position, flood unit F8 or unit N1 is thicker and pinches out at a height of 40,83 m.a.s.l.which is similar to the height of pinchout (40,87 m.a.s.l.)of the channel feature shown in Fig. 3.44.

showed that unit P has a consistent motif (Fig. 3.46). The basal 10 cm - 15 cm exhibits climbing-ripple lamination with the direction of climb orientated in an upstream direction in the tributary. This direction can also be perpendicular to the tributary thalweg direction in areas where back flooding of a side tributary of the main tributary has occurred. The climbing ripple laminated interval grades upward into an approximately 20 cm thick interval of wavy lamination through to the remaining portion of unit P which is flat laminated (Figs 3.34 and 3.46).

The fine-grained texture of unit P, its stratigraphic position overlying unit O, its thinning in an upstream direction in the tributary and desiccation cracks on its upper surface indicates it was deposited as a slack-water deposit during tributary back flooding as the Orange River flood stage increased (Fig. 3.35). After the inter-flood hiatus of unit O during which incision and partial scour of the older palaeoflood stratigraphy occurred, the upper surface of unit O was uneven and in some places channelised. The subsequent deposition of unit P resulted in the draping of sediment over this subaerially exposed hiatus surface. Flow conditions during back-flooding were predominantly suspension settling except for initial back-flow where flow regime was sufficiently competent to result in the migration of small bedforms under conditions of high rates of suspension settling. Flow regime gradually decreased to form wavy lamination through to flat lamination where only suspension settling of fine-grained sand occurred. The large polygonal desiccation cracks formed in response to the lowering of flood stage and subaerial exposure.

3.3.1.3Description and interpretation of the palaeoflood stratigraphy at section 2

Section 2 at lower Xobies is located approximately 169 m downstream in the tributary and 37 m east of the main exposure at section 1. The section differs from section 1 as it is proximal to the tributary - Orange River confluence and distal to either of the bedrock valley sides of the tributary. It has therefore been unaffected by valley side colluvial or mass-transport processes. The stratigraphic position of section 2 is immediately below unit P (palaeoflood F9; Fig. 3.34).

Section 2 comprises a 90 cm thick sequence of five interbedded light-brown - tan, very fine - fine-grained, flat-laminated sand units (units A, B, C, D and E; Fig. 3.47) with four thin (2 cm - 3 cm thick), chocolate brown, charcoal- and ash-rich beds

(C1, C2, C3 and C4; Fig. 3.47). The charcoal beds C1, C2 and C3 contain small fragments (less than 1 cm long) of an orange-red, low density baked clay-rich bed. Larger examples (2 cm - 3 cm long) with leaf and stem imprints on one side occur at the foot of the exposure.

Fig. 3.46 - Basal 60 cm of unit P (flood unit F9) at lower Xobies comprising fine-grained sand. Note the change from climbing ripple lamination at the base to wavy lamination through to lower-regime flat lamination. This sequence records a progressive waning of flow regime and reduction in rates of suspension settling after initial back flooding of the tributary. Lens cap for scale is 5 cm in diameter.

Section 2 represents a sequence of 5 palaeoflood events deposited during tributary back-flooding by the Orange River (F1A - F5A). This interpretation is justified on the basis of the interpalaeoflood hiatuses represented by the intervening charcoal and ash-rich beds C1 - C4 which formed after the deposition of each slack-water unit (Fig. 3.47). The presence of baked clay from three of the four charcoal beds indicates that sufficient vegetation was available to result in high enough temperatures enabling the partial firing or baking of the clay-rich unit. Although the lower Xobies site is presently devoid of vegetation except for infrequent small shrubs, it is likely that

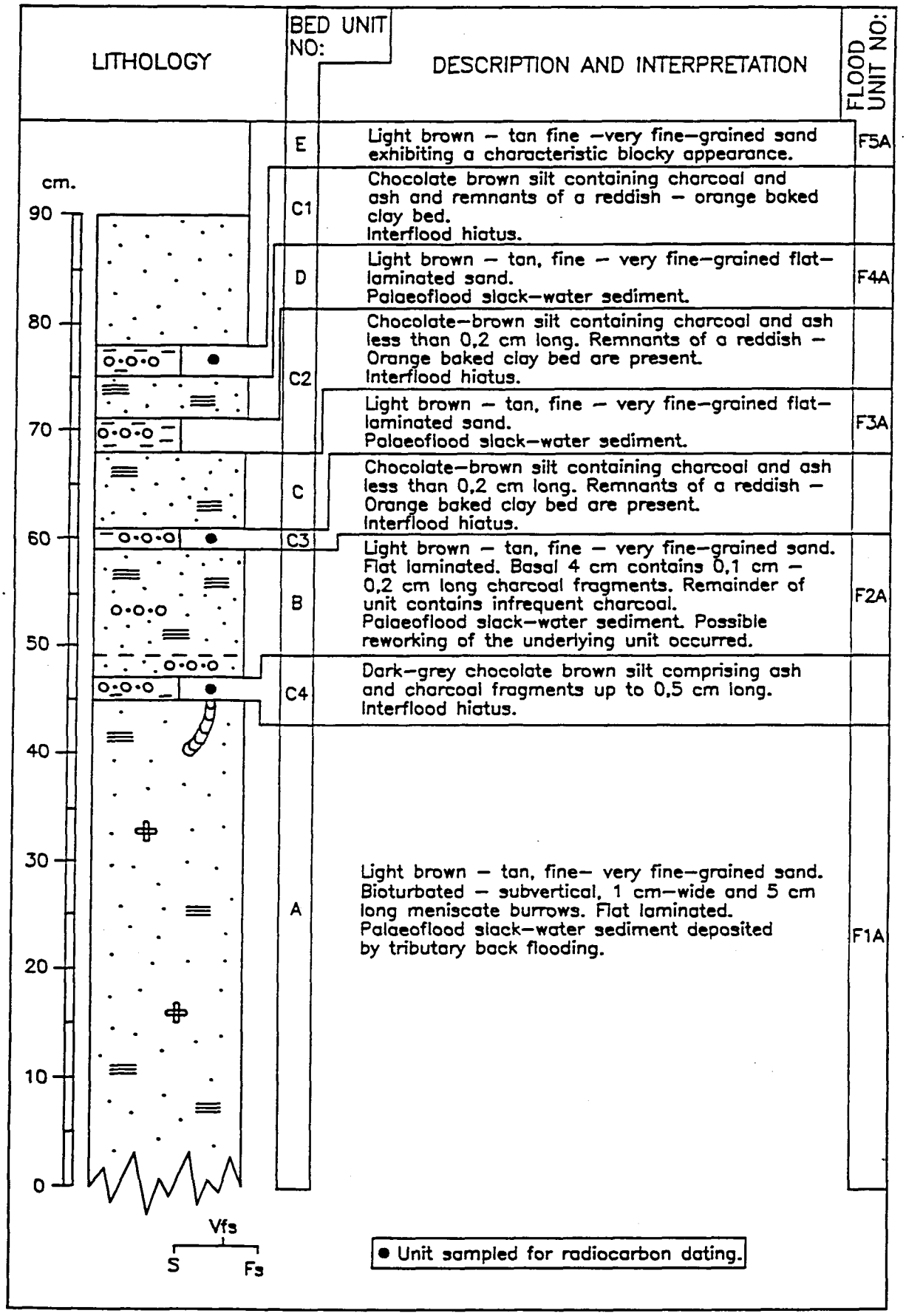

Fig. 3.47 - Lithological description and sedimentological interpretation of section 2 at lower Xobies of a sequence of 5 palaeoflood-deposited sediments interbedded with 4 non-palaeoflood charcoal- and ash-rich horizons.

after back-flooding, lush vegetation rapidly grew on the newly deposited slack-water sediments to later form the fuel for a bush or veld fire.

3.3.2 Bloeddrift palaeoflood site

3.3.2.1 Geological and geomorphological setting

The Bloeddrift palaeoflood site comprises a primary and a secondary site both of which are situated approximately 34 km downstream of the lower Xobies palaeoflood site at latitude 28°21'50" and longitude 16°48'37" on the 1:50 000 topocadastral sheet number 2816BD Khubus (Fig. 3.32). At low-flow conditions, the Orange River at Bloeddrift is single channeled, moderately sinuous and 130 m - 200 m wide comprising medial bars up to 3,4 m thick and side-attached longitudinal bars up to 2 km long. The eastern valley side or South African side of the Orange River comprises mainly moderately dipping blue-grey schist and thin arkose of the Kaigas Formation which is intruded by diabase dykes (Geological Map of the Richtersveld, 1958). The western or Namibian valley side of the Orange River, comprises a sparsely vegetated gravel point bar or terrace extending up to a height of 40 m.a.s.l.followed by prominent Miocene - lower Pleistocene diamondiferous gravel terraces of the Arriesdrift Gravel Formation similar to those at lower Xobies (Van Wyk and Pienaar, 1986). The banks of the Orange River are densely vegetated across a width of 10 m - 50 m decreasing rapidly to almost no vegetation.

The primary Bloeddrift palaeoflood site comprises a sequence of slack-water sediments located in a northerly flowing, low sinuosity, high-gradient, (0,1 m/m) bedrock-controlled tributary with a catchment area of less than 0,5 km^2 (Fig. 3.32). The tributary thalweg and sides exhibit no vegetation. The mouth of the tributary is blocked by the fine-grained sand bank of the Orange River up to a level of 15 m above water level. The secondary Bloeddrift site comprises a laterally continuous sequence of slack-water sediments which progressively thin and eventually pinchout approximately 500 m - 750 m upstream in the Annis River (Fig. 3.48).

3.3.2.2 Description and interpretation of the palaeoflood stratigraphy at Bloeddrift

The primary exposure at Bloeddrift comprises a 5 m - 7 m thick sequence of interbedded angular gravel with buff very fine-grained sand. Because the tributary thalweg is only 3 m - 5 m wide and is bordered by steeply dipping bedrock valley

sides, the differentiation between tributary-deposited and palaeoflood slack-water deposited sediment was straight forward. However, because the headwaters of the tributary were exceptionally steep (up to 45°), the maximum elevation of palaeoflood stage as indicated by the elevation of slack-water sediment pinchout, was considerably lower than that recorded in the Annis River. Therefore, the palaeoflood sediments in the Annis River, which although have infilled much of its thalweg, with subsequent incision being no greater than 2 m, was still recorded, successfully correlated with the primary Bloeddrift exposure and used to compile one composite palaeoflood stratigraphic profile (Fig. 3.49).

Fig. 3.48 - View of the Annis River at Bloeddrift exhibiting slack-water sediments that extend from the confluence with the Orange River (upper left of photograph) in an upstream direction (right of photograph) where they progressively thin and eventually pinchout at approximately 750 m from the Annis - Orange River confluence.

The basal 2.2 m of the Bloeddrift palaeoflood stratigraphy was examined using a series of relief peels. This, together with outcrop descriptions enabled the identification of six palaeoflood events and their hydrodynamic interpretation (Figs. 3.49 and 3.50 respectively) which is presented below.

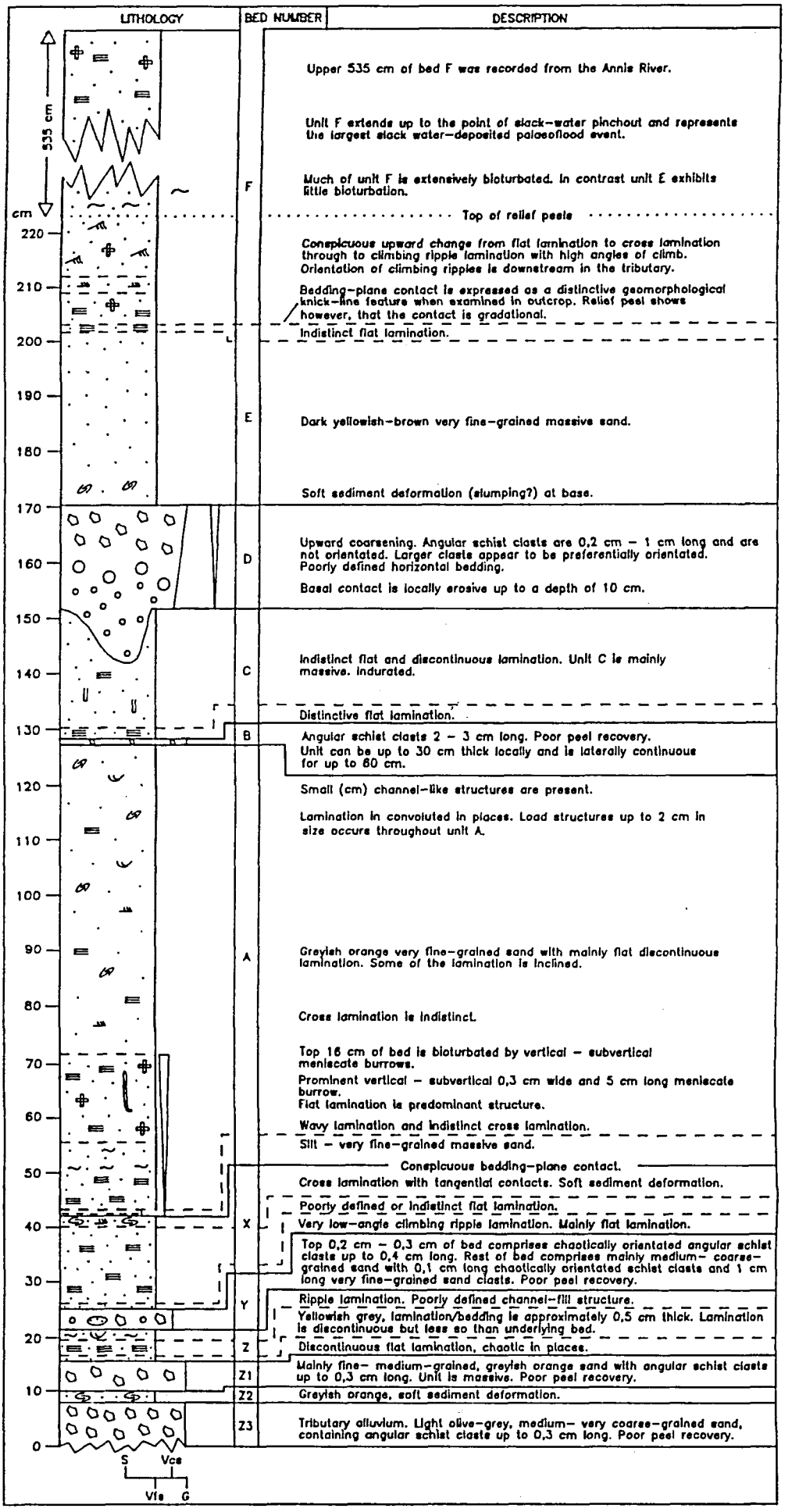

Fig. 3.49 - Lithological description of the palaeoflood stratigraphy at Bloeddrift (see legend on page 107).

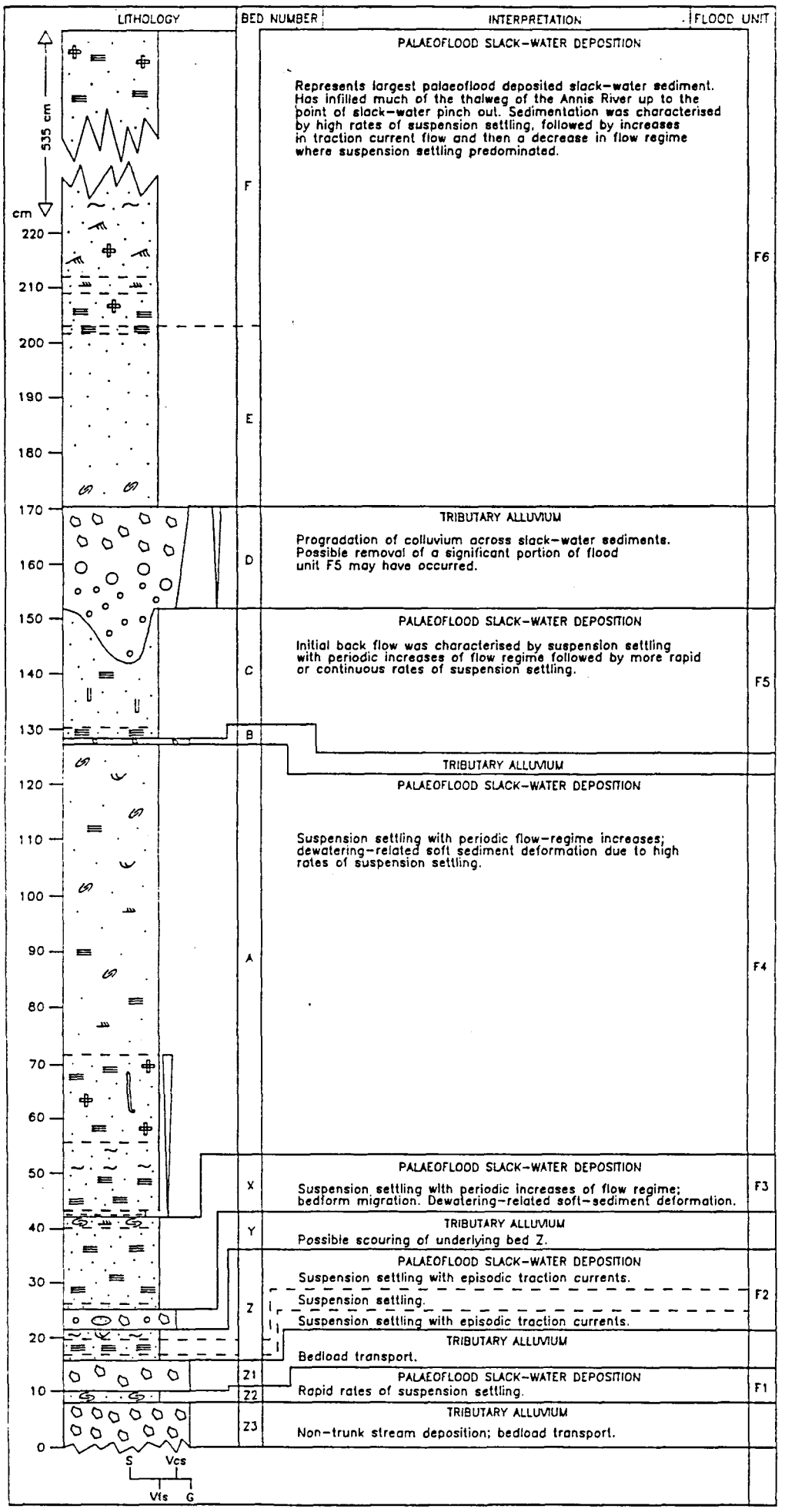

Fig. 3.50 - Sedimentological and hydrodynamic interpretation of the palaeoflood stratigraphy at Bloeddrift (see legend on page 107).

Flood unit F1 is a laterally continuous, 3 cm thick, indurated, flat laminated, greyish orange, light-grey very fine-grained sand (bed Z2; Fig. 3.49). A relief peel showed that bed Z2 contains convoluted and chaotically orientated lamination.

Bed Z2 is interpreted as a palaeoflood-deposited slack-water unit on account of its interbedded and contrasting lithology to the overlying and underlying angular gravel beds Z1 and Z3 respectively (Fig. 3.50). These beds represent tributary-deposited alluvium derived from the tributary catchment through periodic tributary flow (Fig. 3.50). The chaotic lamination may indicate dewatering-related soft-sediment deformation due to rapid rates of suspension settling during back flooding of the tributary.

Flood unit F2 is a laterally continuous 8 cm thick, indurated, mainly flat laminated, light grey very fine-grained sand (bed Z; Fig. 3.49). A relief peel shows that the basal unit of bed Z comprises discontinuous flat lamination that grades upwards into continuous lamination through to a ripple-laminated interval containing a channel-fill structure several centimetres wide (Fig. 3.49).

Flood unit F2 represents a slack-water sediment deposited by back flooding of the tributary during flooding of the Orange River (Fig. 3.50). This interpretation is justified on the basis of bed Z being interbedded between the gravel beds Z1 and Y which were deposited by non-palaeoflood tributary-related processes. Sedimentation during backflooding was mainly by suspension settling punctuated by slight changes of flow regime and less frequently by stronger traction currents competent enough to rework lamination which resulted in minor scouring (Fig. 3.50).

Flood unit F3 is a 14 cm - 16 cm thick mainly flat laminated, light-grey very fine-grained sand that passes upward into a cross-laminated sand with tangential laminae and convoluted and/or chaotic lamination (bed X; Fig. 3.49). A relief peel shows that the top of bed X is taken at a distinctive bedding plane which separates the sediments of bed X from the overlying darker and slightly coarser grained sediments of bed A (Fig. 3.49).

The interpretation of bed X as representing a palaeoflood slack-water sediment

is justified firstly, on its interbedded position between the underlying tributary-deposited gravel (bed Y; Fig. 3.49) and secondly, its position below a distinctive bedding plane and palaeoflood hiatus across which a conspicuous change of colour and grain size occurs (Fig. 3.50). Sedimentation was dominated by suspension settling which increased periodically leading to dewatering-related soft-sediment deformation. Suspension settling was interrupted by periodic increases of flow regime where traction transport resulted in the migration of small ripples (Fig. 3.50).

Flood unit F4 is a 115 cm thick, predominantly very fine-grained sand, exhibiting continuous or discontinuous flat lamination with infrequent convoluted lamination and weakly developed cross lamination (bed A; Fig. 3.49). The basal 30 cm coarsens upward from a massive silt to a bioturbated very fine-grained sand exhibiting subvertical meniscate burrows up to 5 cm long.

Bed A is interpreted as a palaeoflood slack-water sediment on account of its contrasting lithology and interbedded position between the overlying tributary-deposited gravel bed (bed B) and the underlying sharp bedding-plane contact described for flood unit F3 (Fig. 3.50). Furthermore, bed A does not contain any sharp contacts implying a constant sedimentation rate. Depositional conditions were dominated by suspension settling in quiet water conditions, punctuated by periodic increases of flow regime which resulted in the formation of wavy lamination and the partial reworking of flat lamination into discontinuous flat lamination. The convoluted lamination may indicate dewatering-related soft-sediment deformation probably as the result of high rates of suspension settling. The slight upward-coarsening trend present from the basal portion of flood unit F4 indicates a gradually increasing flood surge or pulse (Fig. 3.50).

Flood unit F5 is a 16 cm - 22 cm thick, very fine grained sand (bed C; Fig. 3.49). A relief peel shows that the bed is mainly massive with infrequent and indistinct flat lamination except for the basal 4 cm which exhibits conspicuous flat lamination (Fig. 3.49). Overlying bed C is a 12 cm - 15 cm thick upward-coarsening gravel containing angular clasts 0,2 cm - 10 cm long (bed D; Fig. 3.49). The larger gravel clasts show preferential orientation with the bed as a whole exhibiting weakly developed horizontal bedding. Underlying bed C is a 1 cm - 9 cm thick gravel

comprising angular clasts 2 cm - 3 cm long (bed B; Fig. 3.49).

The interbedded position of unit C and its contrasting finer-grained texture between the tributary-deposited gravel bed B and D indicates that it represents a palaeoflood slack-water sediment deposited during tributary back flooding (Fig. 3.50). Initial back flow was characterised by suspension settling with periodic slight increases of flow regime followed by more continuous or rapid rates of suspension settling which led to the massive appearance of bed C (Fig. 3.50). In contrast, the overlying and underlying gravel beds (beds D and B) were derived from the tributary catchment where periodic flow was sufficiently competent to entrain and partially imbricate the larger clasts. The overall upward increase in clast size noted from bed D indicates the progradation of an active colluvial source of sediment from the tributary valley sides across the slack-water sediments. Although much of unit D shows no channelisation and was therefore deposited by mainly unconfined sheet flow, its base is locally erosive (Fig. 3.49). This suggests that the slack-water sediment of unit C has been partially reworked and may therefore under estimate the palaeoflood stage.

Flood unit F6 is a 593 cm thick sequence of dark yellowish-brown very fine grained sand that can be traced continuously in an upstream direction up to its point of pinch out in the tributary and the Annis River. The basal 35 cm when examined in outcrop and with a relief peel indicates it is massive except for the basal 10 cm which exhibits contorted and chaotic lamination (bed E; Fig. 3.49). The top of bed E is marked by a conspicuous knick-point feature which can be observed through the entire back-flooded portion of both the tributary and the Annis River. It was initially thought that this weathering feature coincided with a bedding plane separating two palaeoflood slack-water units or intraflood pulses or surges. Macroscopic and microscopic examination of a relief peel of the interval showed however, that no sharp textural, mineralogical or structural feature exists, except for an upward gradation (10 cm - 15 cm thick) from massive sand to indistinct and discontinuous laminated sand through to an interval exhibiting distinctive and continuous flat-lamination. The remainder of flood unit F6 (bed F) comprises a distinctive motif of sedimentary structure from climbing ripple lamination to wavy lamination through to flat lamination which is the dominant structure for the uppermost 500 cm of bed F (Fig. 3.49). This motif is similar to that observed for the basal portion of flood unit F9 (bed P) at lower Xobies.

The interpretation of beds E and F as representing a palaeoflood slack-water sediment is based on their finer grained texture compared to the underlying gravel bed (bed D), their upstream thinning, draping and eventual pinch out against the valley side of both the tributary and the Annis River. Sedimentation was dominated by suspension settling of which the initial back-flood flow exhibited high rates of deposition during which dewatering related soft-sediment deformation occurred. The upward change from massive to flat lamination testifies to suspension settling but with periodic slight increases of flow regime. This was followed by an increase of flow regime during which migration of small ripples occurred under high rates of suspension settling to form climbing ripple lamination. Thereafter a drop of flow regime occurred, during which wavy lamination formed followed by a further decrease to form flat lamination where predominantly suspension settling in quiet-water conditions occurred.

3.3.3 Palaeoflood hydrology and dating of slack-water sediments from the lower Xobies and Bloeddrift sites

In order to calculate the palaeodischarge of a flood unit, requires the accurate determination of the elevation of the slack-water sediment above a datum and the cross-sectional area of the trunk stream using surveyed cross-sections at or close to the palaeoflood site. Cross sections of the Orange River were surveyed by the Department of Water Affairs and Forestry to an accuracy of ± 10 cm. The X and Y values were surveyed in relation to the South African co-ordinate system using total station theodolites. The elevation (Z value) was measured with respect to metres above sea level (m.a.s.l.).Although the water depth of the Orange River was relatively shallow (0,30 m - 2,5 m), the channel bottom was surveyed using a dinghy-mounted sonar.

Twenty-four samples from the lower Xobies and Bloeddrift palaeoflood stratigraphies were dated using radiocarbon and infra-red stimulated luminescence (IRSL) techniques, of which 13 were from lower Xobies and 11 from Bloeddrift. For radiocarbon dating, in-situ organic material that was deposited contemporaneously with the slack-water sediment was collected as well as from sediments that were deposited during palaeoflood hiatuses. Finding sufficient quantities of uncontaminated organic material required either extensive excavation or hand-picking charcoal blebs and/or sieving of the sediment. Despite this thorough sampling procedure, it was

possible to find sufficient organic material for only a few slack-water sediments. For IRSL dating, samples were taken from the same palaeoflood units for which organic material had been collected and from the major slack-water units. The samples for radiocarbon and infra-red luminescence samples were dated by the Quaternary Dating Research Unit (QUADRU) of the CSIR in Pretoria.

Lower Xobies. Two cross sections situated approximately 25 m (section 1) and 100 m (section 2) downstream of the Orange River - tributary confluence were surveyed (Figs 3.51 and 3.52 respectively). Little difference in shape exists between them except for section 1 being approximately 350 m wider. For each slack-water palaeoflood unit, a maximum elevation was surveyed, plotted on the cross sections (Figs 3.51 and 3.52) and converted to metres above channel base which was used in slope-area calculations to derive the corresponding discharge. In the following section, an account of the palaeodischarges and other hydraulic data for the various palaeoflood units (with increasing magnitude) at lower Xobies is given followed by a discussion of the radiocarbon and IRSL dates obtained for the slack-water sediments. This information is presented in Figs 3.53 - 3.55 and summarised in Table 3.5.

Palaeoflood unit F1 exhibits a flood stage of 17,56 m which corresponds to a minimum discharge of approximately 10 190 m^3/s (Fig. 3.53; Table 3.5). Placing these figures into perspective, the stage and discharge corresponding to bankfull flow is approximately 12,71 m and 5 580 m^3/s respectively (unit RB1) (Table 3.5). In addition, the largest discharge that was recorded by the nearest gauging stations to the lower Xobies site was 7 800 m^3/s in 1974 at Brandkaros and Rosh Pinah (located 56 km downstream and 22 km upstream respectively). Although unit F1 represents the basal palaeoflood unit of the main exposure at lower Xobies, it represents a flood event that was almost 25 % larger than the largest gauged lower Orange River flood.

Approximately 20 m - 40 m from the Orange River and extending across much of the mouth of the lower Xobies tributary is a dark, organic-rich slack-water sediment (flood unit - DSWS) exhibiting a maximum elevation of 38,67 m.a.s.l.(Table 3.5). This corresponds to a flood stage of 18,95 m and a discharge of 11 830 m^3/s.

Four palaeoflood units (F2 - F5) ranging in elevation from 38,94 m.a.s.l.- 39,76

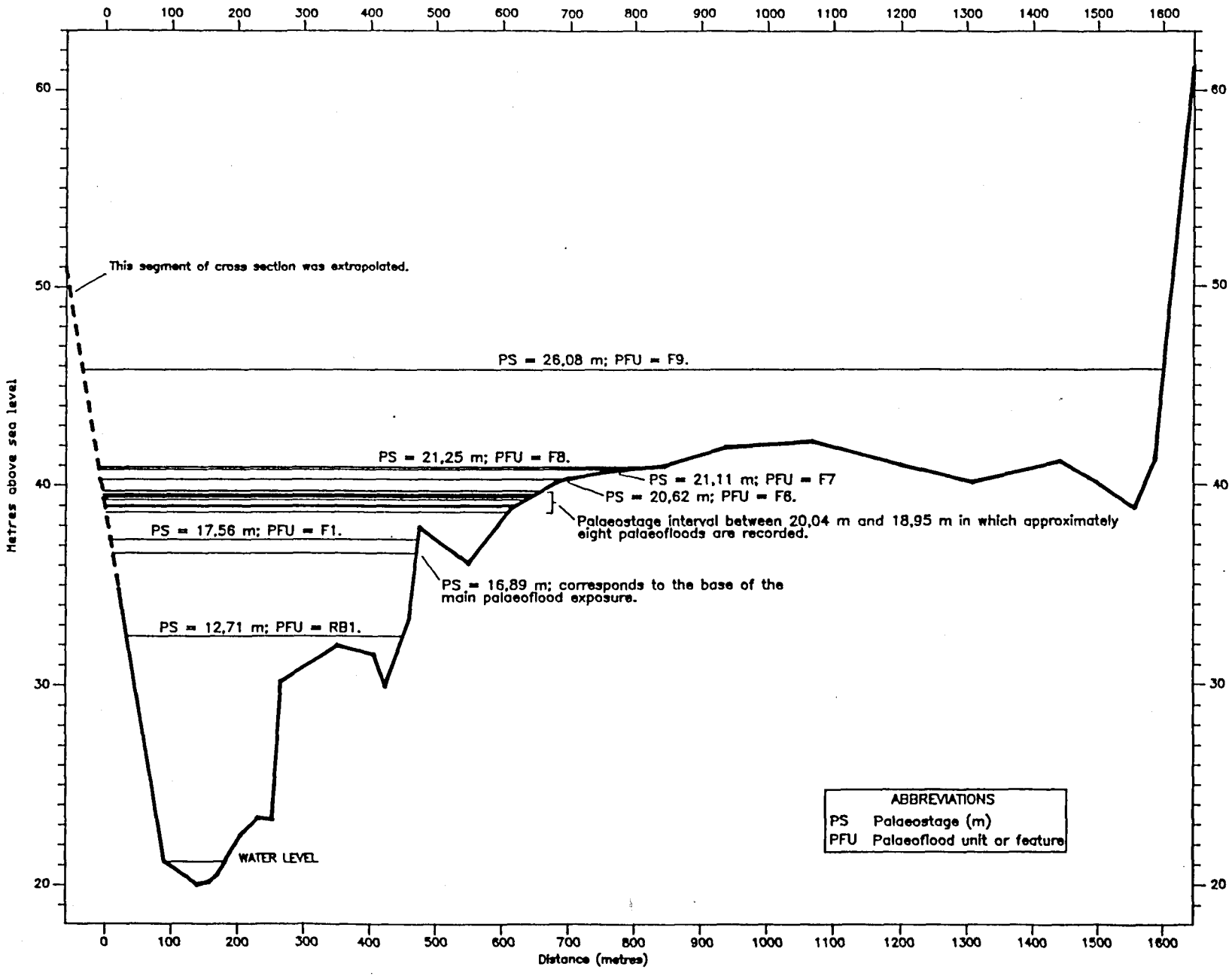

Fig. 3.51 - Cross-section 1 of the Orange River on which is plotted the palaeoflood stages based on the elevations of the slack-water sediments at lower Xobies (Table 3.5).

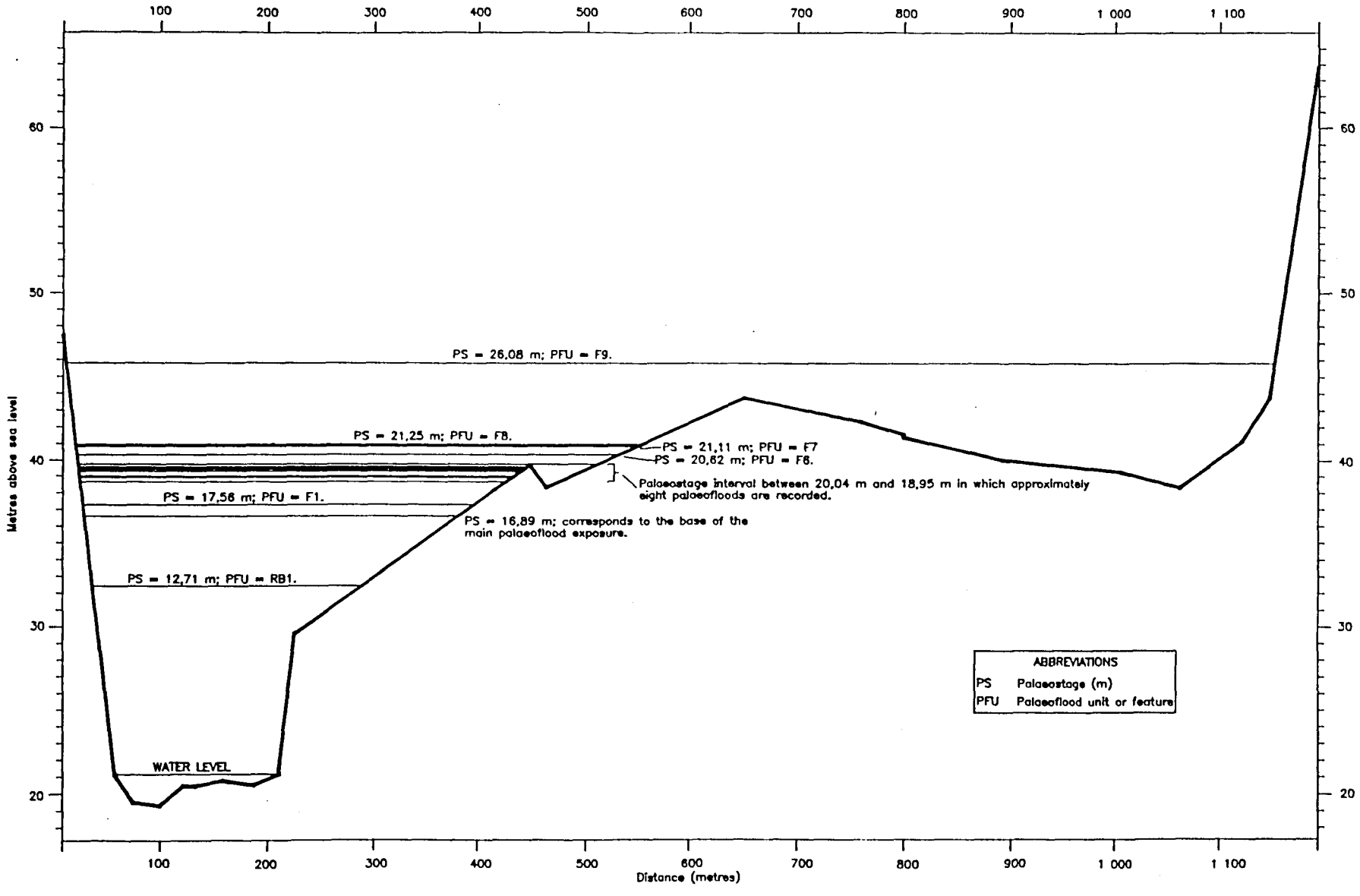

Fig. 3.52 - Cross-section 2 of the Orange River on which is plotted the palaeoflood stages based on the elevations of the slack-water sediments at lower Xobies (Table 3.5).

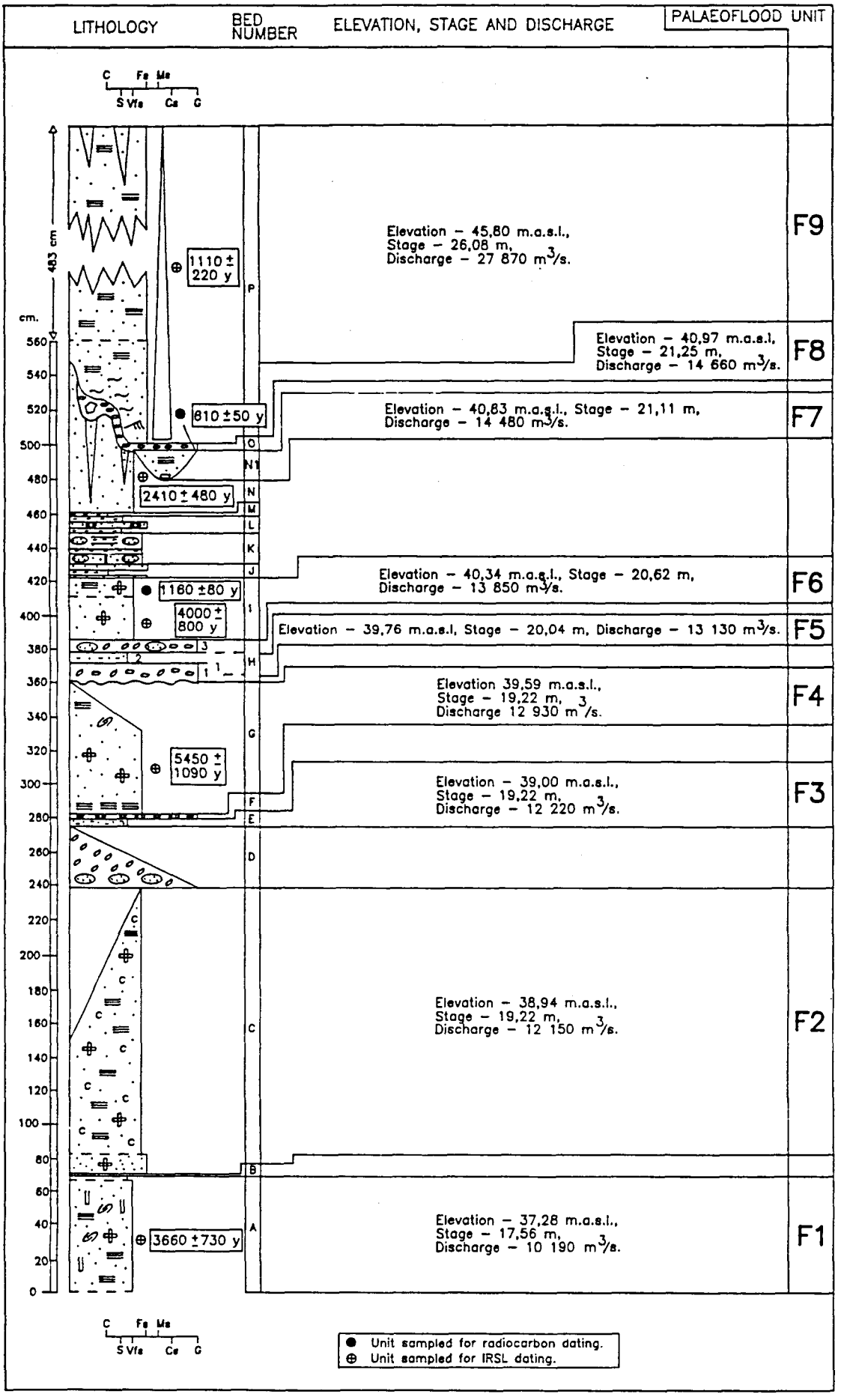

Fig. 3.53 - Elevation (m.a.s.l.),stage, palaeodischarge estimates and dating results (radiocarbon and IRSL) for the palaeoflood units F1 - F9 from the main exposure at lower Xobies.

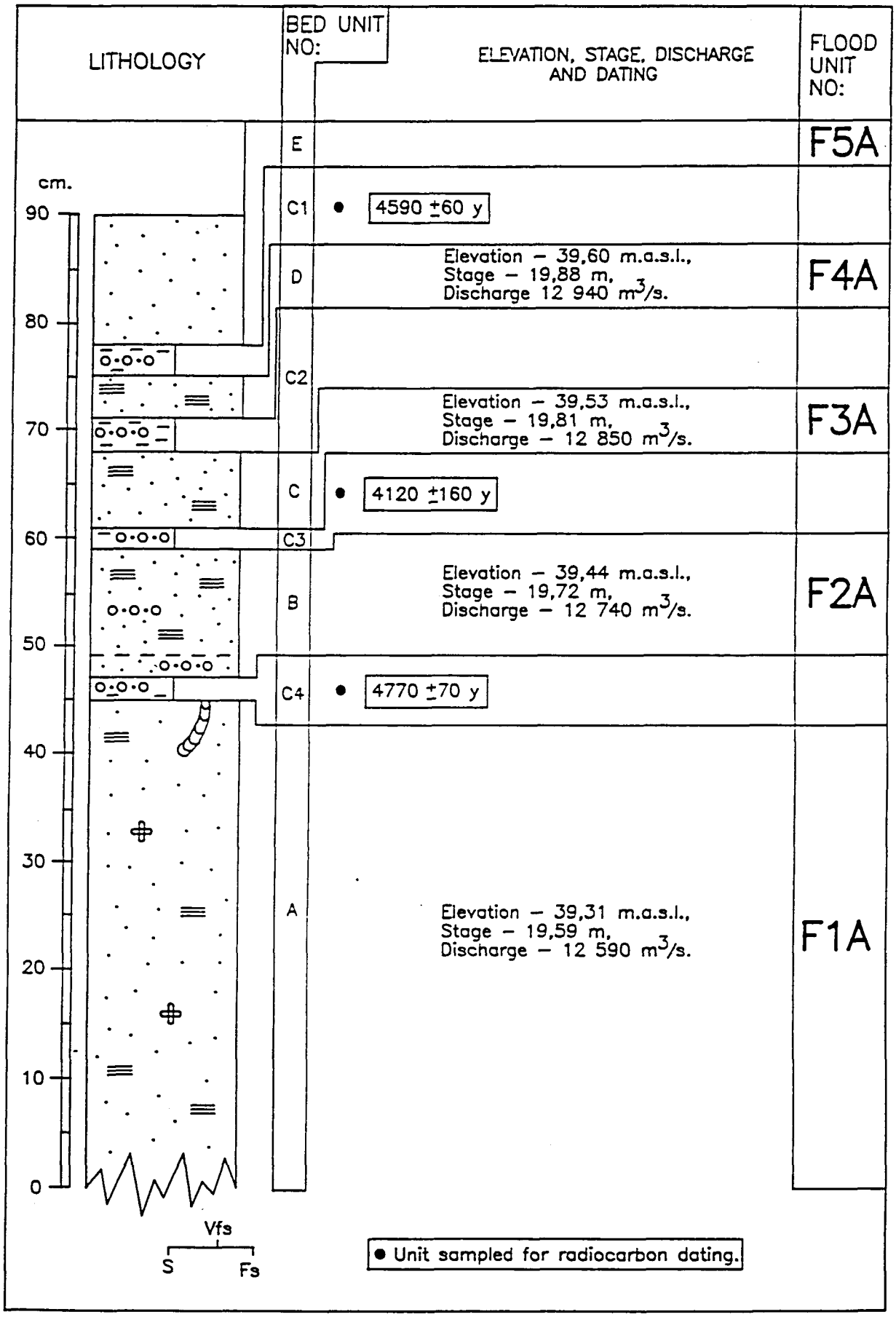

Fig. 3.54 - Elevation (m.a.s.l.),stage, palaeodischarge estimates and radiocarbon dating results for the palaeoflood units F1A - F5A from section 2 at lower Xobies.

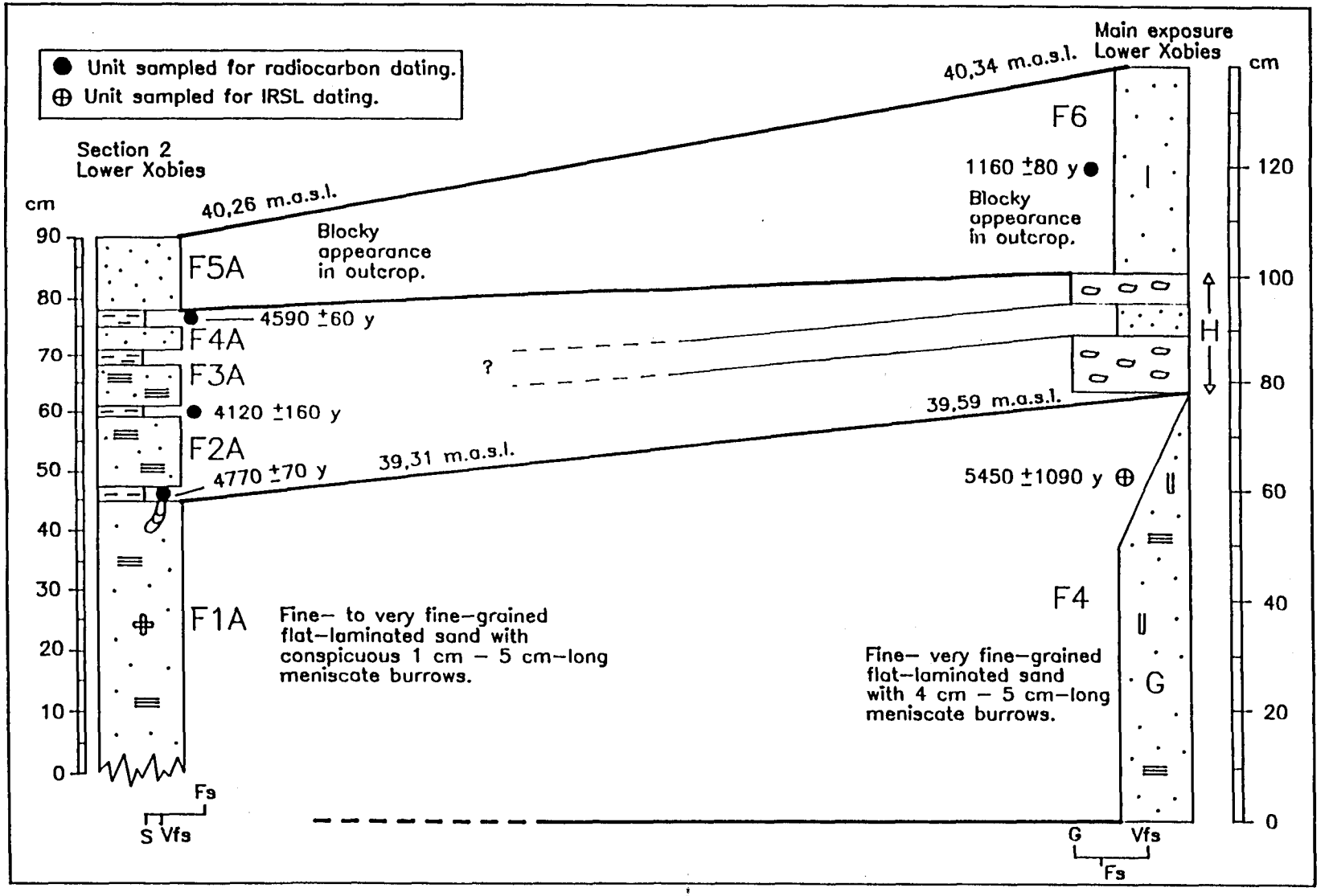

Fig. 3.55 - Correlation of palaeoflood stratigraphies between section 2 and the main exposure at lower Xobies. Note that because of similar elevations and lithological similarity between units F1A - G and F5A - I, flood units F2A, F3A and F4A are correlates of unit H.

Table 3.5 - Combined palaeoflood stratigraphy (main exposure and section 2) of the Orange River at lower Xobies comprising stage, palaeodischarge, radiocarbon and IRSL dating information arranged with increasing palaeoflood magnitude.

Palaeo-flood unit	Height m.a.s.l.	Palaeoflood stage in metres above Orange River channel base[a]	Palaeo-discharge (Q) m^3/s	Palaeo-velocity (v) m/s	Froude Number	Radio-carbon sample no.	Type of material dated	Radio-carbon age (years B.P.)[b] or ^{14}C content	Calibrated date[c]	IRSL sample no.	IRSL age (years)	Comments
F9 (Fig. 3.53)	45,80	26,08	27 870	3,1	0,2	Pta-6597	Ostrich egg shell from underlying bed O.	610 ±50	A.D. 1389(1405)1421; 1317-1347	Pta-5348	1110 ±220[d]	Radiocarbon date was obtained from bed immediately underlying F9. Therefore F9 is younger than 610 ±50 years B.P. IRSL dating reflects young age of F9 but is older than radiocarbon age.
F8 (Fig. 3.53)	40,97	21,25	14 660	2,7	0,2	-	-	-	-	Pta-5510	2410 ±480[d] 4020 ±800[e]	F8 is between 1160 ±80 years B.P. - 650 ±50 years B.P. based on radiocarbon dating of units F9 and F6. IRSL date is therefore anomalous.
F7 (Fig. 3.53)	40,83	21,11	14 480	2,7	0,2	-	-	-	-	-	-	F7 is between 1160 ±80 years B.P. - 650 ±50 years B.P. based on radiocarbon dating of units F9 and F6 but younger than F8.
F6 (Fig. 3.53)	40,34	20,62	13 850	2,7	0,2	Pta-6645	Bone fragments of Zebra jaw.	1160 ±80	A.D. 867(961) 1007	Pta-5511	4000 ±800[d] 4040 ±810[e]	Radiocarbon age is the more reliable figure. IRSL age is anomalously old and therefore inaccurate.
TOP OF PALAEOFLOOD STRATIGRAPHY AT SECTION 2 (Fig. 3.54)												
F5A (Fig. 3.54)	39,76	20,04	13 130	3,0	0,2	Pta-6602	Organic material in palaeosol underlying F5A.	4590 ±60	-	-	-	Represents maximum age for F5A. Considered to be chronstratigraphically equivalent age for F6 from main exposure (Fig. 3.54).
F4A (Fig. 3.54)	39,60	19,88	12 940	3,0	0,2	-	-	-	-	-	-	F4A underlies bed C1 and is therefore younger than 4590 ±60 years B.P. (Fig. 3.54).
F3A (Fig. 3.54)	39,53	19,81	12 850	3,0	0,2	Pta-6608	Organic material and charcoal in palaeosol underlying F3A.	4120 ±160	-	_	-	Although the age is similar to those obtained from F5A and F1A, it is anomalous with respect to its stratigraphic position (Fig. 3.54).
F2A (Fig. 3.54)	39,44	19,72	12 740	3,0	0,2	Pta-6601	Organic material in palaeosol underlying F2A.	4770 ±70	-	_	-	Age is probably younger than 4770 ±70 years B.P. but older than 4120 ±160 years B.P. (Fig. 3.54).
F1A (Fig. 3.54)	39,31	19,59	12 590	3,0	0,2	Pta-6601	Organic material in palaeosol overlying F1A.	4770 ±70	-	-	-	Represents a minimum age for F1A. F1A is correlated with F4 from the main exposure (Fig. 3.55) with its date confirming the IRSL date of 5450 ±1090 years for F4.
BOTTOM OF PALAEOFLOOD STRATIGRAPHY AT SECTION 2 (Fig. 3.54)												

Palaeo-flood unit	Height m.a.s.l.	Palaeoflood stage in metres above Orange River channel base[a]	Palaeo-discharge (Q) m^3/s	Palaeo-velocity (v) m/s	Froude Number	Radio-carbon sample no.	Type of material dated	Radio-carbon age (years B.P.)[b] or ^{14}C content	Calibrated date[c]	IRSL sample no.	IRSL age (years)	Comments
F5 (Fig. 3.53)	39,76	20,04	13 130	3,0	0,2	-	-	-	-	-	-	F5 underlies F6 and is therefore older than 1160 ±80 years B.P. Furthermore, F5 is part of bed unit H (Fig. 3.53) which is correlated with flood units F2A - F4A at section 2 (Fig. 3.55). Therefore the age of F5 is close to the mean age at section 2 of 4490 years B.P.
F4 (Fig. 3.53)	39,59	19,87	12 930	3,0	0,2	-	-	-	-	Pta-5349	5450 ±1090[d]	Age agrees with the minimum age obtained for F1A of 4770 ±70 years from section 2.
F3 (Fig. 3.53)	39,00	19,28	12 220	3,0	0,2	-	-	-	-	-	-	Likely to be older than 5450 ±1090 years.
F2 (Fig. 3.53)	38,94	19,22	12 140	3,0	0,2	-	-	-	-	-	-	Likely to be older than 5450 ±1090 years.
DSWS	38,67	18,95	11 830	3,0	0,2	Pta-6603	Organic material from an abandoned termitarium.	102,5 ±0,3%	A.D. 1956/1957	-	-	Date is anomalously young because the gauged record shows no floods of this magnitude occurring about this time. Formation of termitarium post dates the deposition of flood unit DSWS.
F1 (Fig. 3.53)	37,28	17,56	10 190	2,9	0,2	-	-	-	-	Pta-5350	3660 ±730[d]	Age of F1 is anomalously young in terms of its stratigraphic position and the overlying IRSL and correlated radiocarbon ages of 5450 ±1090 years and 4770 ±70 years respectively.
XO Upper Xobies site	35,11	15,01	7 550	2,8	0,2	Pta-6379	Plant material and sheep and/or goat droppings.	109,1 ±0,5%	A.D. 1958	-	-	Date and discharge corresponds to the 6 317 m^3/s flood recorded in 1957 at Vioolsdrift. The 16 % overestimation in discharge is attributed to cross-sectional differences between the Lower and Upper Xobies sites.
RB1	32,43	12,71	5 580	2,7	0,2	Pta-6600	Wood, twigs and bark from bed at top of Orange River bank.	210 ±50	A.D. 1666(1680) 1698; 1721(1780) 1820; 1852-1867; 1929-1950.	-	-	The 1929-1950calibrated age partially correlates with known floods recorded at Vioolsdrif listed in decreasing priority (1) 1936/1937; Q = 5 445 m^3/s, (2) 1933/1934; Q = 5 128 m^3/s, (3) 1943/1944; Q = 5 071 m^3/s.

[a] The base of the Orange River channel was surveyed to an elevation of 20,10 m a.s.l. at section 1 and 19,33 m a.s.l. at section 2. A median value of 19,72 m a.s.l. was therefore used in the calculation of the palaeflood stage and discharge.
[b] Radiocarbon years is expressed as years before present i.e. before A.D. 1950. Ages are corrected for variations in isotopic fractionation.
[c] Age calibrated for the southern hemisphere based on data presented by Stuiver and Pearson (1993). The 1 sigma range(s) is given with the most probable calendar date(s) in brackets. Note that an age range without an indication of the most probable calendar date is regarded as being an equally significant calibrated age.
[d] Additive method of age determination.
[e] Regenerative method of age determination.

Table 3.5 - Combined palaeoflood stratigraphy (main exposure and section 2) of the Orange River at lower Xobies comprising stage, palaeodischarge, radiocarbon and IRSL dating information arranged with increasing palaeoflood magnitude (continued).

m.a.s.l.with palaeoflood stages of 19,22 m - 20,04 m above the Orange River thalweg were surveyed from the main exposure at lower Xobies (Fig. 3.53; Table 3.1). This corresponds to a range of minimum palaeodischarges of 12 150 m^3/s - 13 130 m^3/s and corresponding trunk-stream palaeovelocities of approximately 3 m/s. The pattern of four palaeofloods exhibiting a restricted range of stage and palaeodischarge is similar to section 2 where the palaeoflood units F1A - F5A exhibit a range of palaeostages from 19,59 m - 20,04 m with a corresponding range of palaeodischarges of 12 590 m^3/s - 13 130 m^3/s (Fig. 3.54; Table 3.5). Although insufficient outcrop precluded the tracing of the palaeoflood units from section 2 upstream to the main exposure, it is suggested that the flood units F1A - F5A are correlatable with unit H from the main exposure (Fig. 3.55). This correlation is justified on the basis that the top of section 2 (unit F5A) has a conspicuous blocky appearance in outcrop similar to bed I (F5) from the main exposure, together with similar elevations obtained for flood units F5A and F5 (40,26 m.a.s.l.and 40,34 m.a.s.l.respectively) (Fig. 3.55). In addition, the basal flood unit F1A comprises a fine- to very fine-grained, flat-laminated sand with subvertical meniscate burrows which is similar to bed G (flood unit F4) from the main exposure. This, together with similar elevations for the top of unit F1A (39,31 m.a.s.l.) and unit F4 (39,59 m.a.s.l.), indicates that units F1A and F4 are correlatable (Fig. 3.55). The correlation of the palaeoflood stratigraphy between section 2 and the main exposure indicates that only one palaeoflood unit in bed H is recorded, in contrast to three flood units at section 2 (Fig. 3.55). This is ascribed to the main exposure being located in a proximal position with respect to colluvial sedimentation associated with the tributary valley side. This led to the removal of palaeoflood sediments by sheet-wash scour. In contrast, section 2 being distal to active colluvial sedimentation was largely unaffected by sheet-wash scour which led to the preservation of relatively thin slack-water sediments. An alternative explanation is that because flood units F2A - F4A are comparatively thin with the main exposure being close to their point of pinchout, no deposition of the slack-water units F2A - F4A occurred at the main exposure.

Surveying of flood units F6 - F8 showed that their elevations range from 40,34 m.a.s.l.- 40,97 m.a.s.l.(Table 3.5). The palaeoflood stages range from 20,62 m - 21,25 m for which flow modelling yielded the range of discharges from 13 850 m^3/s - 14 660 m^3/s (Fig. 3.53; Table 3.5).

Flood unit F9 represents the largest palaeoflood at lower Xobies attaining an elevation at its point of pinch out in the tributary of 45,80 m.a.s.l. This represents a minimum flood-stage height above the Orange River thalweg of 26,08 m and a corresponding minimum palaeodischarge of 27 870 m^3/s. To put this figure into perspective the largest historically recorded lower Orange River flood was gauged at Vioolsdrift (approximately 200 km upstream of lower Xobies) to be 8 331 m^3/s in 1974 according to Van Bladeren (1995). Other notable floods recorded at Vioolsdrift were those in 1937 (5 445 m^3/s), 1955 (5 370 m^3/s), 1967 (6 030 m^3/s) and 1988 (7 700 m^3/s) (Van Bladeren, 1995). In terms of discharge, the palaeoflood represented by unit F9 was over three times larger than any historically recorded lower Orange River flood. On this basis, this flood can be described as being of catastrophic magnitude.

Eleven dates were obtained from the palaeoflood succession at lower Xobies of which 6 were radio-carbon dated and 5 IRSL dated (Table 3.5 and Figs 3.53 - 3.55). Because IRSL dating is a comparatively new technique, especially with respect to the methodology and interpreting dating results of fine- very fine-grained fluvial slack-water sediments, the radio-carbon dating results are presented first. The results from IRSL dating are then included to firstly corroborate the radiocarbon dates, and secondly, to identify and differentiate the IRSL dates that are meaningful from those that are anomalous. This was done in partial consultation with J. Vogel who heads the luminescence dating laboratory of the CSIR.

The radiocarbon dates at lower Xobies are significant for two reasons. Firstly, the radiocarbon age corresponds to the lithostratigraphy. For example, the radio-carbon dates from progressively older sediments are as follows: 610 ±50 years B.P. (bed O; Fig. 3.53), 1160 ±80 years B.P. (bed I; Figs 3.53 and 3.55) and 4120 ±160 years B.P. - 4770 ±70 years B.P. (beds C - C4, section 2, correlated with bed H of the main exposure; Figs 3.53 - 3.55). Secondly, the dating of ostrich egg shell fragments from bed O indicates that the catastrophic flood represented by flood unit F9 was deposited less than 610 ±50 years B.P. ago (Fig. 3.53 and Table 3.5). Calibration of the radiocarbon age indicates that the flood post dates either A.D. 1405 or A.D. 1317 - 1347 (Table 3.5).

Radiocarbon dating of a part of a lower jaw identified as belonging to a Zebra (pers comm. Plug, Transvaal Museum) which was found at the base of unit I, gave a radiocarbon age of 1160 ±80 years B.P. and a calibrated date of A.D. 961 (Fig. 3.53 and Table 3.5). This indicates that not only is the palaeoflood represented by unit F6 approximately 1100 years old but also the palaeofloods represented by units F7 and F8, are between 1160 ±80 years B.P. - 610 ±50 years B.P. with unit F7 being the older palaeoflood (Table 3.5). In terms of calibrated dates, palaeofloods F7 and F8 occurred between A.D. 961 and A.D. 1405 or A.D. 1317-1347 (Table 3.5). This indicates that a maximum period of 550 years existed between palaeofloods F6 and the deposition of the gravel bed (bed O) underlying palaeoflood F9, during which, the two largest lower Orange River floods had discharges of approximately 14 550 m^3/s (Table 3.5).

Radiocarbon dating of the charcoal-rich units (C1, C3 and C4) from section 2 at lower Xobies gave radiocarbon ages of 4590 ±60 years B.P., 4120 ±160 years B.P. and 4770 ±70 years respectively (Table 3.5 and Fig. 3.54). Although the date for unit C3 is anomalous with respect to its stratigraphic position and dates obtained for the underlying and overlying units (Fig. 3.54), the dates at section 2 are similar exhibiting a mean age of 4490 years B.P. This indicates that during the period 4770 ±70 years B.P. - 4120 ±160 years B.P. (duration 650 years) the three largest lower Orange River floods were in the range of 12 740 m^3/s - 12 940 m^3/s (Fig. 3.54).

Because the palaeoflood units F2A - F4A are correlates of unit H from the main exposure (Fig. 3.55), this indicates that for the period 4770 ±70 years B.P. - 1160 ±80 years B.P. (duration 3610 years or 3330 years if the mean age at section 2 is used), the largest lower Orange River floods (4 floods, represented by units F2A - F5A; Figs. 3.54 and 3.55) were in the range of 12 740 m^3/s - 13 130 m^3/s. Alternatively, between the deposition of flood unit F4A which has a maximum age of 4590 ±60 years B.P. and the deposition of unit I (1160 ±80 years B.P.), only one palaeoflood event was recorded (unit F5A) with a discharge of 13 130 m^3/s (Figs 3.54 and 3.55 and Table 3.5).

Radiocarbon dating of organic material from an abandoned termite nest on palaeoflood unit DSWS gave an ultramodern radiocarbon age with a calibrated age of A.D. 1956/1957. This date is considered to be anomalously young because the

gauged Orange River floods about this time (1955 - 5 370 m^3/s, 1956 - 2 214 m^3/s, 1957 - 2 585 m^3/s, 1958 - 6318 m^3/s; gauged at Vioolsdrift) although comparatively large for the lower Orange River, are on average nearly 3 times smaller than the palaeodischarge indicated by the pinch out elevation of unit DSWS (11 830 m^3/s). It is therefore likely that the palaeoflood sediments of DSWS were deposited by an earlier flood. Although the termitarium is associated and comprises reworked slack-water sediments of unit DSWS, there is no reason to suppose that it formed immediately after deposition of DSWS. The anomalously young date records therefore, the formation of the termitarium and not the deposition of flood unit DSWS. Because the termite mound has not been scoured by flooding, the A.D. 1956/1957 date confirms the flood record that since 1955, no flood discharges came close to the 11 830 m^3/s discharge of the DSWS palaeoflood (Table 3.5). The largest floods during this period were in 1974 and 1988 with discharges of 8 331 m^3/s and 7 705 m^3/s respectively.

A further radiocarbon date was obtained from an organic-rich unit comprising leaf and mainly sheep and/or goat droppings overlying slack-water sediments at the upper Xobies site which is situated approximately 750 m upstream of lower Xobies (unit XO) (Fig. 3.32). The elevation of the top of flood unit XO was surveyed to 35,11 m.a.s.l.which corresponds to a flood stage of 15,01 m (the channel base of the Orange River was taken to be 20,01 m.a.s.l.from section 1 which is the nearest cross-section to this site) and a discharge of 7 550 m^3/s (Table 3.5). Radiocarbon dating yielded a calibrated date of A.D. 1958 (Table 3.5). The date and discharge derived from flood unit XO agrees with the gauging record for the lower Orange River at Vioolsdrift that documents a 6 317 m^3/s flood in 1957. The approximately 16 % overestimation in discharge of unit XO is ascribed to the differing channel geometry of the Orange River at upper Xobies that is not reflected in cross-section 1 at lower Xobies.

Interpretation of the IRSL results from lower Xobies is less clear than the radiocarbon dating for two reasons. Firstly, although the IRSL dates broadly follows the lithostratigraphy, several ages are possibly anomalous (Table 3.5 and Fig. 3.53). Secondly, the dates for some of the palaeoflood units are older than that indicated by the radiocarbon dating.

IRSL dating of the catastrophic flood unit F9 gave an age of 1110 ±220 years (Table 3.5 and Fig. 3.53). This date is almost twice the age of the maximum radiocarbon of 610 ±50 years B.P. for flood unit F9 (Table 3.5 and Fig. 3.53). Although the IRSL date for unit F9 appears too old, it is considered reliable for two reasons. Firstly, a similar date of 1040 ±210 years was obtained for the same palaeoflood unit at Bloeddrift and secondly, the date when examined with the other IRSL dates at lower Xobies agrees with the younger age for flood unit F9 as indicated by its stratigraphic position and radiocarbon age (Fig. 3.53). The older IRSL age compared to the radiocarbon age is ascribed to residual luminescence existing in the feldspars due to insufficient exposure of the sediment to the sunlight during flood conditions. An alternative but related explanation is the source of the slack-water sediments was close to lower Xobies which also resulted in a limited time for exposure to sunlight and zeroing of the luminescence signal. A likely reason for insufficient exposure to the sunlight is the high turbidity of the flood waters due to the high concentration of very fine-grained suspended load (the 4 μm - 11 μm fraction was used for IRSL dating).

Two IRSL ages were obtained for flood unit F8 using two differing techniques. Where the additive method was employed an age of 2410 ±480 years was obtained whereas 4020 ±800 years was obtained using the regenerative method. The difference between the two methods indicates that the sample is probably anomalous (pers comm. Vogel). In addition, neither of the ages are similar to the interpolated age for flood units F7 and F8 (between 1160 ±80 years B.P. - 650 ±50 years B.P.) based on radiocarbon dating of flood units F6 and the palaeoflood hiatus underlying flood unit F9 (Fig. 3.53). The IRSL age for flood unit F7 is therefore considered to be anomalous and has no chronostratigraphic significance.

IRSL dating of flood unit F6 using the additive and regenerative methods of age determination gave values of 4000 ±800 years and 4040 ±800 years respectively (Table 3.5 and Fig. 3.53). Although the difference in age between the two methods is acceptable, the median age is much older than the radiocarbon date of 1160 ±80 years B.P. obtained for in-situ bone from unit F6. The IRSL date for flood unit F6 is anomalously old and therefore inaccurate. As noted from IRSL dating of flood unit F9, this is ascribed to non-zeroing of the luminescence signal due to insufficient

exposure to the sunlight because of high turbidity.

Although no radiocarbon dating was done for flood unit F4, it is expected to be older than the median age of 4490 years B.P. obtained at section 2 and correlated with unit H from the main exposure because unit F4 (bed G) is a correlate of the basal slack-water unit of section 2 (Fig. 3.55). IRSL dating of flood unit F4 using the additive method of age determination confirmed this interpretation giving an age of 5450 ±1090 years (Table 3.5 and Figs 3.53 and 3.55). However, IRSL dating (additive method) of the basal flood unit at lower Xobies (unit F1) yielded an age of 3660 ±730 years which is anomalously young in terms of its stratigraphic position and the overlying IRSL date for flood unit F4 (Table 3.5 and Fig. 3.53). It is therefore suggested that the age of the flood units F3, F2 and F1 are older than approximately 5450 ±1090 years. This conclusion should be qualified with the observation that the IRSL dates at lower Xobies are generally older than the radiocarbon dates for the same flood units. It is therefore possible that the basal flood units may be younger than 5450 ±1090 years but probably older than the mean radiocarbon age of 4490 years B.P. obtained from section 2. This observation partially agrees with IRSL dating at Bloeddrift, where an age of 1800 ±360 years was obtained for the lowest dated flood unit (F4). This indicates that the underlying flood units (F3, F2 and F1) have a minimum age of approximately 1800 years.

The results of IRSL dating slack-water sediments at lower Xobies is generally disappointing. Several dates are anomalous with regard to their stratigraphic position and are inaccurate when compared against the more reliable radiocarbon dates. Specifically the dates are considerably older than the radiocarbon dates for the same flood unit. In general though, the IRSL dates have given an approximation of the period for which the palaeoflood stratigraphy at lower Xobies covers. The interflood chronostratigraphy is less clear, however. This indicates that IRSL dating of slack-water sediments and the interpretation of results thereof, should be done in conjunction with a more tested and reliable dating technique such as radiocarbon dating.

Bloeddrift. Three cross sections situated approximately 400 m (section 1), 950 m (section 2) and 2 125 m (section 3) downstream of the Orange River - tributary

confluence at Bloeddrift were surveyed (Figs 3.56 and 3.57). Cross-sections 1 and 2 are similar in shape whereas cross-section 3 is 500 m - 600 m shorter (Figs 3.56 and 3.57). As with lower Xobies, for each slack-water palaeoflood unit, a maximum elevation was surveyed, plotted on the cross sections (Figs 3.56 and 3.57) and converted to metres above channel base which was used in slope-area calculations to derive the corresponding discharge. In the following section, an account of the palaeodischarges and other hydraulic data for the various palaeoflood units (with increasing magnitude) at the main exposure at Bloeddrift is presented, followed by a discussion of the radiocarbon and IRSL dates obtained for the slack-water sediments. This information is illustrated in Fig. 3.58 and summarised in Table 3.6.

The mouth of the tributary is partially blocked by a prominent fine- to very fine-grained sand terrace which extends upstream along the Orange River (approximately 425 m) to the Annis River where it is steeply incised. The top of this feature (T1) represents approximately bankfull conditions (Figs 3.56). It has an elevation of 22,85 m.a.s.l. which corresponds to a stage of 12,40 m and a discharge of 5 780 m^3/s which is similar to the value obtained for RB1 at lower Xobies (5 580 m^3/s; Table 3.5). As noted from lower Xobies, this discharge corresponds approximately to a common flood discharge gauged for the lower Orange River during the period 1929 - 1950 at Vioolsdrift (1936 - 5 445 m^3/s; 1944 - 5 108 m^3/s; 1948 - 5 071 m^3/s; 1955 - 5 371 m^3/s; 1967 - 6 027 m^3/s).

A perched outcrop of fluvially transported organic debris comprising twigs, leaves and fine-grained organic fragments (T2) located approximately 50 m upstream of the Orange River - tributary confluence, was surveyed to an elevation of 24,47 m.a.s.l. (Table 3.6). This corresponds to a palaeostage and palaeodischarge of 14,02 m and 7 530 m^3/s respectively. This discharge approximates the two largest gauged lower Orange River floods of 8 331 m^3/s in 1974 and 7 705 m^3/s in 1988 for the period 1935 - present recorded at Vioolsdrift.

Three palaeoflood units (F1 - F3) ranging in stage from 15,77 m - 16,33 m with a corresponding range of discharge from 9 530 m^3/s - 10 260 m^3/s were surveyed at Bloeddrift (Fig. 3.58 and Table 3.6). The larger discharge exceeds the largest gauged flood discharge recorded in 1974 at Vioolsdrift by almost 19 %.

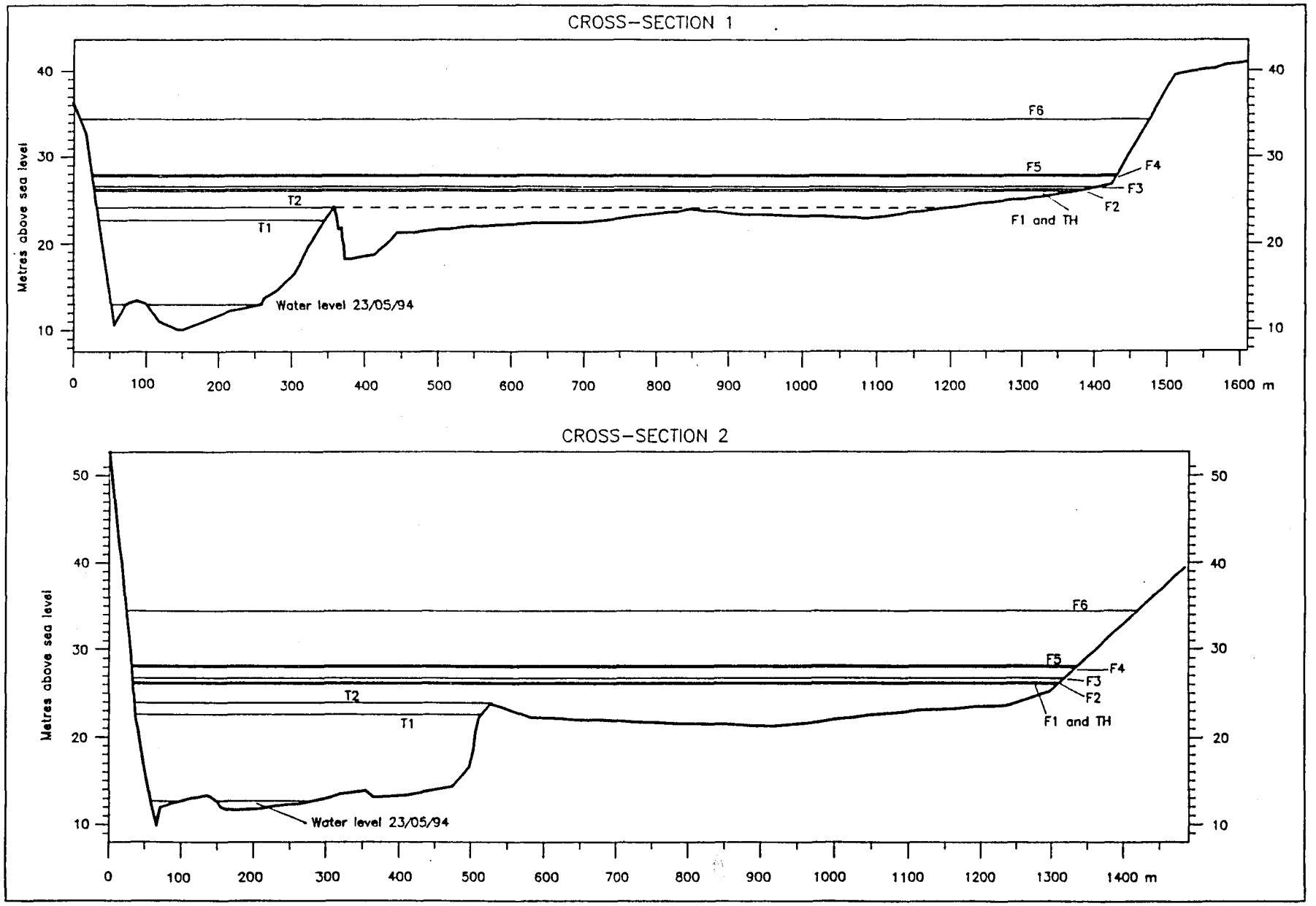

Fig. 3.56 - Cross-sections 1 and 2 of the Orange River which are located approximately 400 m and 950 m downstream of the Orange River - tributary confluence at Bloeddrift. The stages of the palaeoflood slack-water sediments at Bloeddrift are plotted with respect to the mean elevation of the Orange River channel base being 10,45 m.a.s.l. based on cross-sections 1 - 3).

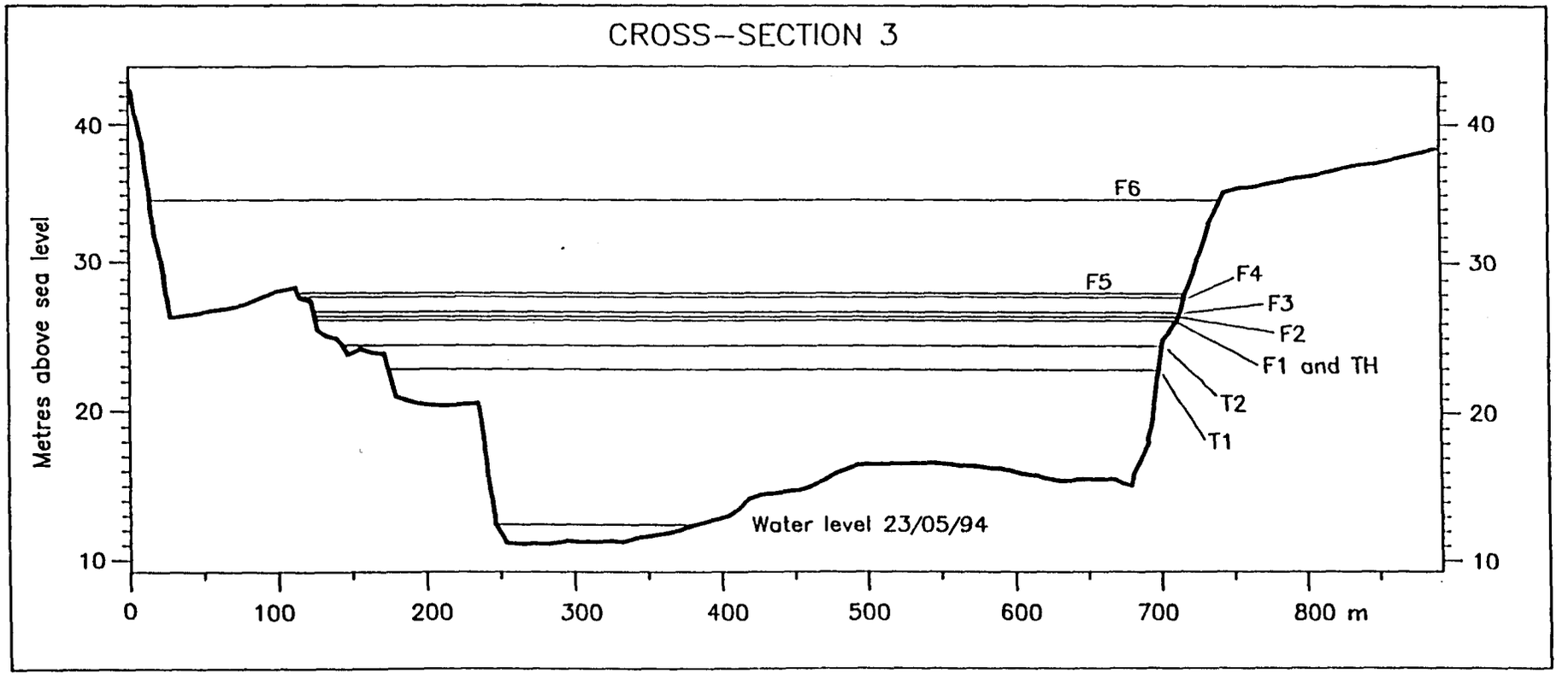

Fig. 3.57 - Cross-section 3 of the Orange River located approximately 2 125 m downstream of the Orange River - tributary confluence at Bloeddrift. The stages of the palaeoflood slack-water sediments at Bloeddrift are plotted with respect to the mean elevation of the Orange River channel base being 10,45 m.a.s.l.(based on cross-sections 1 - 3).

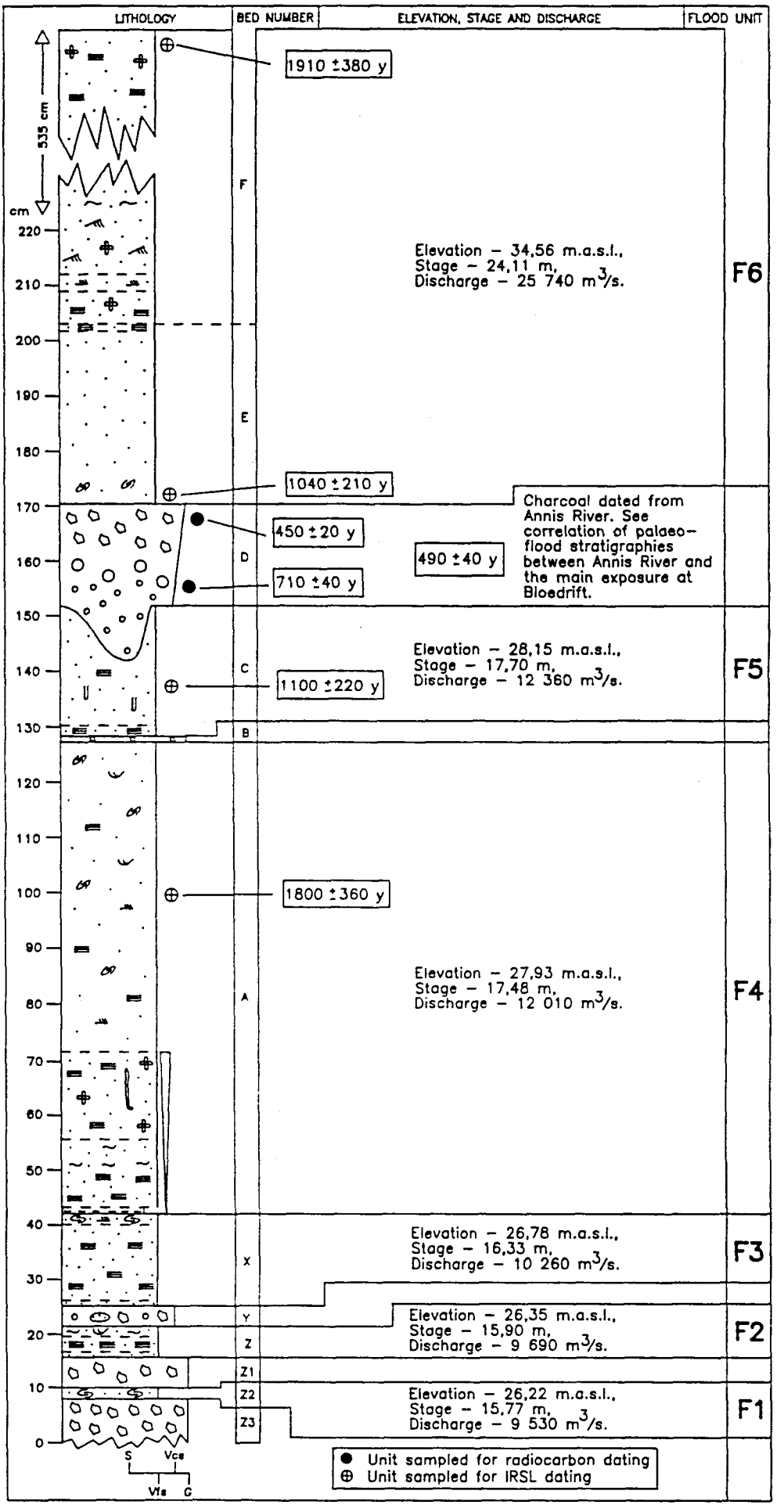

Fig. 3.58 - Elevation (m.a.s.l.),stage, palaeodischarge estimates and dating results (radiocarbon and IRSL) of the palaeoflood units F1 - F6 at Bloeddrift.

Table 3.6 - Palaeoflood stratigraphy of the Orange River at Bloeddrift (main exposure and Annis River) comprising stage, palaeodischarge, radiocarbon and IRSL dating information arranged with increasing palaeoflood magnitude.

Palaeo-flood unit	Height m.a.s.l.	Palaeoflood stage in metres above Orange River channel base[a]	Palaeo-discharge (Q) m^3/s	Palaeo-velocity (v) m/s	Froude Number	Radio-carbon sample no.	Type of material dated	Radio-carbon age (years B.P.)[b] or ^{14}C content	Calibrated date[c]	IRSL sample no.	IRSL age (years)	Comments
F6 (Fig. 3.58)	34,56	24,11	25 740	1,8	0,1	Pta-6385 --- Pta-6380 --- Pta-6358	Burnt root stock from underlying bed D. --- Charcoal from underlying flood hiatus in Annis River (see Fig. 26). --- Ostrich egg shell from underlying bed D.	450 ±20 --- 490 ±40 --- 710 ±40	A.D. 1452(1462) 1476 --- A.D. 1430(1444) 1462 --- A.D. 1289(1299) 1312; 1354-1384	Top of unit F6. Pta-5508 --- Base of unit F6. Pta-5345	1910 ±380[d] 1980 ±400[e] --- 1040 ±210[d]	Radiocarbon dating indicates that flood unit has a maximum age of 710 ±40 years B.P. and probably post dates 450 - 490 years B.P. Radiocarbon age is similar to age obtained for unit F9 from Lower Xobies. In terms of calibrated dates, unit F6 was deposited by a flood that occurred after the period A.D. 1444 - A.D. 1462. Upper IRSL age is anomalously old. Lower IRSL age reflects younger age of unit F6 (see IRSL ages for flood units F4 and F5) but is twice the expected age than that indicated by radiocarbon dating.
F5 (Fig. 3.58)	28,15	17,70	12 360	1,8	0,1	-	-	-	-	Pta-5346	1100 ±220[d]	Radiocarbon dating of overlying bed D indicates that the minimum age of unit F5 is 710 ±40 years B.P. IRSL age for unit F5 confirms this.
F4 (Fig. 3.58)	27,93	17,48	12 010	1,6	0,1	-	-	-	-	Pta-5347	1800 ±360[d]	Radiocarbon dating of overlying bed D indicates that the minimum age of unit F4 is 710 ±40 years B.P. and older than the IRSL age for unit F5. IRSL age for unit F4 confirms this.
F3 (Fig. 3.58)	26,78	16,33	10 260	1,6	0,1	-	-	-	-	Pta-5509	4360 ±870[d] 4480 ±900[e]	IRSL dating of overlying flood units F4 and F5 indicates that F3 is older than 1800 ±360 years. This is confirmed with correlation and IRSL dating of a basal slack-water unit from the Annis River which suggests that unit F3 could be as old as 4360 ±870 years B.P. (Fig. 3.59).
F2 (Fig. 3.58)	26,35	15,90	9 690	1,6	0,1	-	-	-	-	Pta-5509	4360 ±870[d] 4480 ±900[e]	
F1 (Fig. 3.58)	26,22	15,77	9 530	1,6	0,1	-	-	-	-	Pta-5509	4360 ±870[d] 4480 ±900[e]	

Palaeo-flood unit	Height m.a.s.l.	Palaeoflood stage in metres above Orange River channel base[a]	Palaeo-discharge (Q) m^3/s	Palaeo-velocity (v) m/s	Froude Number	Radio-carbon sample no.	Type of material dated	Radio-carbon age (years B.P.)[b] or ^{14}C content	Calibrated date[c]	IRSL sample no.	IRSL age (years)	Comments
TH (termite hill on SWS surface)	26,23	15,78	9 545	1,6	0,1	Pta-6604	Organic material from abandoned termite hill on slack-water sediment surface.	220 ±50	A.D. 1663(1677) 1693; 1727(1785) 1816; 1929-1950.	-	-	All three radiocarbon ages overlap and are therefore treated as being the same age. No gauged floods close to 9 545 m^3/s occurred during the period 1929-1950. Therefore this date is rejected. Because of the comparatively fresh nature of organics from T1 and T2, the younger calibrated date of A.D. 1785 is selected as the most likely date of deposition. Since approximately A.D. 1785 all Orange River floods were less than approximately 9 500 m^3/s.
T2 (out-crop of organic-rich bed)	24,47	14,02	7 530	1,5	0,1	Pta-6598	Comparatively fresh leaves and twigs.	270 ±50	A.D. 1648(1663) 1677; 1768-1801.	-	-	
T1 (top of prominent sandy terrace)	22,85	12,40	5 780	1,5	0,1	Pta-6600	Comparatively fresh wood, twigs and bark.	210 ±50	A.D. 1666(1680) 1698; 1721(1780) 1820; 1852-1867.	-	-	

[a] The base of the Orange River channel was surveyed to an elevation of 10,17 m a s l at cross-section 1, 10,00 m a s l at cross-section 2 and 11,19 m a s l at cross-section 3. A mean value of 10,45 m a s l was therefore used in the calculation of the palaeoflood stage and discharge

[b] Radiocarbon years is expressed as years before present i e. before A D 1950 Ages are corrected for variations in isotopic fractionation.

[c] Age calibrated for the southern hemisphere based on data presented by Stuiver and Pearson (1993). The 1 sigma range(s) is given with the most probable calendar date(s) in brackets. Note that an age range without an indication of the most probable calendar date is regarded as being an equally significant calibrated age.

[d] Additive method of age determination.

[e] Regenerative method of age determination.

Table 3.6 - Palaeoflood stratigraphy of the Orange River at Bloeddrift (main exposure and Annis River) comprising stage, palaeodischarge, radiocarbon and IRSL dating information arranged with increasing palaeoflood magnitude (continued).

Palaeoflood units F4 and F5 were surveyed to an elevation of 27,93 m.a.s.l.and 28,15 m.a.s.l.respectively (Table 3.6 and Fig. 3.58). This represents flood stages of 17,48 m and 17,70 m respectively, and corresponding palaeodischarges of 12 010 m^3/s and 12 360 m^3/s respectively (Fig. 3.58 and Table 3.6). To place these figures into perspective, the larger palaeodischarge for flood unit F5 is over 32 % larger than the largest gauged Orange River flood in 1974 (8 331 m^3/s).

Flood unit F6 represents the largest palaeoflood recorded at Bloeddrift attaining an elevation of 34,56 m.a.s.l.which corresponds to a flood stage of 24,11 m and a minimum discharge of 25 740 m^3/s (Fig. 3.58 and Table 3.6). This flood is over three times larger than the largest historically recorded flood for the lower Orange River (8 331 m^3/s - 1974) and is therefore described as being catastrophic in magnitude. This conclusion is supported by the similarity in discharge between flood unit F6 at Bloeddrift and flood unit F9 at lower Xobies (27 870 m^3/s; Table 3.5 and Fig. 3.53). Although the difference between the discharges is over 2 100 m^3/s, the percentage difference is less than 8 % which is considered an acceptable error for a flood of this magnitude.

Ten dates were obtained from the palaeoflood succession at Bloeddrift of which 5 were radiocarbon dated and 5 IRSL dated (Fig. 3.58 and Table 3.6). As with the lower Xobies site, the radiocarbon dates are presented and interpreted first, followed by an account of the IRSL dating obtained from the Bloeddrift slack-water sediments.

Radiocarbon dating of ostrich egg shell fragments from the base of the gravel bed D that underlies flood unit F6 gave a date of 710 ±40 years B.P. (Fig. 3.58 and Table 3.6). This age is similar to the date of 610 ±50 years B.P. obtained from unit O that underlies flood unit F9 at lower Xobies. Calibration of the age of flood unit F6 indicates that it post dates either A.D. 1299 or A.D. 1354 - A.D. 1384 (Table 3.6). A further date of a burnt root stock sampled from the top of unit D gave an age of 450 ±20 years B.P. Calibration of this age indicates that flood unit F6 post dates A.D. 1462 which is similar to the calibrated date of A.D. 1405 obtained from the gravel bed (bed O) underlying the catastrophic flood unit F9 at lower Xobies (Tables 3.5 and 3.6). A similar age and date was also obtained from a charcoal-rich horizon from the Annis River which was correlated with unit D from the main palaeoflood exposure at

Bloeddrift situated approximately 600 m away. Correlating the palaeoflood stratigraphies between the Annis River and the tributary was straightforward, since bed F of flood unit F6 exhibits a distinctive sedimentary motif and a conspicuous break-in-slope feature that occurs at the junction of beds E and F which can be traced throughout the Bloeddrift palaeoflood site (Fig. 3.59). The Annis River radiocarbon date gave an age of 490 ±40 years B.P. (Fig. 3.59 and Table 3.6) and a calibrated date of A.D. 1444 which is not only similar to the calibrated date of the root stock from unit D, but also to the date for unit O that underlies flood unit F9 at lower Xobies (Tables 3.5 and 3.6).

It is clear that the maximum age of flood unit F6 varies from 710 ±40 years B.P. - 450 ±20 years B.P. However, since the two dates obtained from the charcoal-rich horizon from the Annis River (Fig. 3.59) and the root stock from unit D are identical in terms of radiocarbon age, it is concluded that flood unit F6 post dates 450 - 490 years B.P. In terms of calibrated dates, the catastrophic flood represented by flood unit F6 occurred after the period A.D. 1444 - A.D. 1462.

Three further radiocarbon ages were obtained from lower elevation slack-water sediments with flood stages varying from 12,40 m - 15,78 m (Table 3.6). Their ages are 210 ±50 years B.P. (T1 feature), 270 ±50 years B.P. (T2 feature) and 220 ±50 years B.P. which was obtained for organic material from an abandoned termitarium located on a slack-water sediment surface (unit TH) (Table 3.6). In terms of their ages and associated 1 sigma standard deviation, no difference in age exists between the samples (Table 3.6). Calibration of the radiocarbon ages results in a wide range of calender dates varying from A.D. 1663 - A.D. 1929 - 1950 making the selection of the most likely date difficult (Table 3.6). However, the 1929 - 1950 calibrated date is not considered likely since the gauged record for this period does not indicate a flood with a discharge of 9 545 m^3/s (discharge corresponding to a 15,78 m stage) (Table 3.6). In fact, the largest recorded flood during this period was only 5 445 m^3/s in 1936 at Vioolsdrift. Because the three radiocarbon ages are the same with the organic material (leaf and twigs) collected from slack-water unit T2 appearing comparatively fresh, the younger calibrated date of A.D. 1785 is regarded as the most likely date of deposition for flood unit T2 (Table 3.6).

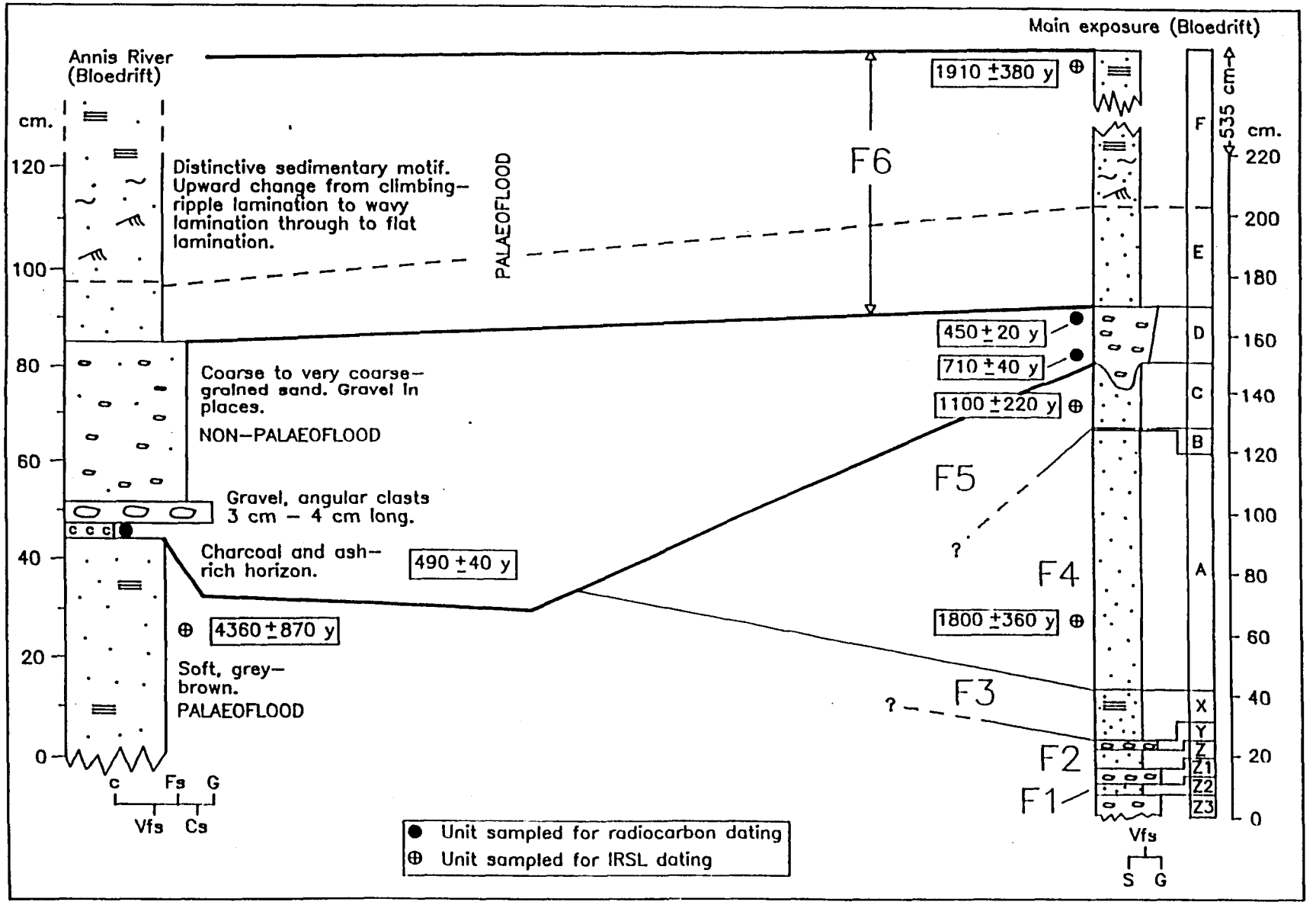

Fig. 3.59 - Correlation of the main exposure and Annis River palaeoflood stratigraphies at Bloeddrift. Note the correlation of flood unit F6 based on lithology and radiocarbon dating. The 4360 ±870 years IRSL age from the Annis River, suggests that one of the flood units F1 - F3 occurred approximately 4400 years ago.

Since no slack-water sediments containing abundant and relatively fresh organic material are present above the flood stage 15,78 m (26,23 m.a.s.l.), with the observation that the organic material of flood unit F2 has not been scoured due to flooding, indicates that the largest Orange River flood since approximately 233 years B.P. (mean radiocarbon age for flood units T1, T2 and TH) was 9 545 m^3/s. Alternatively stated, since approximately A.D. 1790 all Orange river floods were less than approximately 9 500 m^3/s. This observation coincides with the historical and modern flood record of the lower Orange River where the mean of the largest lower Orange River flood above 3 000 m^3/s is 4 938 m^3/s at Vioolsdrift, 5 844 m^3/s at Brandkaros and 6 372 m^3/s at Rosh Pinah (Table 3.7).

Four IRSL dates were obtained from palaeoflood units at the main exposure at Bloeddrift (Fig. 3.58) and one from the base of the sequence measured in the Annis River (Fig. 3.59). The results from the main exposure shows an increase in age with stratigraphy from the base of flood unit F6 - F4 (Fig. 3.58). However, the IRSL age of 1910 ±380 years (additive method) and 1980 ±400 years (regenerative method) from the top of flood unit F6 is anomalously old (Fig. 3.58 and Table 3.6) since a series of younger ages were obtained from the underlying IRSL dated flood units (Fig. 3.58). In addition, the radiocarbon dates for unit D from the main exposure and the Annis River indicate that flood unit F6 has a maximum age of 710 ±40 years B.P. This, together with the difference in ages obtained using the additive and regenerative is further evidence that the IRSL date from the top of unit F6 is anomalous (pers comm. Vogel).

Radiocarbon dating of unit D from the main exposure and its correlate in the Annis River shows that the overlying flood unit is younger than 450 - 490 years B.P. (Fig. 3.59). In contrast, IRSL dating of the base of flood unit F6 yielded an age of 1040 ±210 years which is similar to the age of 1110 ±220 years obtained for flood unit F9 from lower Xobies (Table 3.5). Although the IRSL age for flood unit F6 reflects its younger age when compared to the underlying IRSL ages of 1100 ±220 years and 1800 ±360 years, it is still twice the expected age than that indicated by the radiocarbon dating. As with the older IRSL date for flood unit F9 at lower Xobies, the older than expected age for flood unit F6 is ascribed to residual luminescence due to insufficient exposure of the sediment to sunlight because of the high suspended load

and associated turbidity during flood conditions. This is considered unlikely since flood units F9 (lower Xobies) and F6 (Bloeddrift) were deposited by a flood of catastrophic magnitude which was likely to have exhibited extremely high concentrations of suspended load.

Year of flood	Discharge recorded at the Brandkaros gauging station (located approximately 22 km downstream of Bloeddrift) in m^3/s. Period of continuous record 1971 - 1988.	Discharge recorded at the Rosh Pinah gauging station (located approximately 56 km upstream of Bloedrift) in m^3/s. Period of continuous record 1971 - 1987.	Discharge recorded at the Vioolsdrift gauging station (located approximately 234 km upstream of Bloedrift) in m^3/s. Period of continuous record 1935 - present.
1925	-	-	6 636
1936	-	-	5 445
1938	-	-	3 067
1941	-	-	3 121
1942	-	-	3 717
1943	-	-	3 396
1944	-	-	5 108
1948	-	-	5 071
1955	-	-	5 371
1957	-	-	6 318
1958	-	-	3 013
1961	-	-	4 447
1963	-	-	3 697
1966	-	-	3 471
1967	5 646	-	6 027
1972	3 630	-	-
1974	7 799	7 821	8 331
1976	4 947	4 924	-
1988	7 200	-	7 705
Mean discharge	**5 844**	**6 372**	**4 938**

Table 3.7 - Lower Orange River flood discharges above 3 000 m^3/s for the period 1935 - present recorded at the Brandkaros, Rosh Pinah and Vioolsdrift gauging stations (Van Bladeren, 1995). Note the relatively low mean-flood discharges.

The IRSL dates of 1100 ±220 years and 1800 ±360 years obtained from flood units F5 and F4 respectively, are in keeping with the stratigraphy since these flood units exhibit a minimum age of 710 ±40 years B.P. (Fig. 3.58 and Table 3.6). The accuracy of these dates remain in question however, as it was not possible to collect sufficient organic material from flood units F5 - F1 to verify and substantiate their age based on radiocarbon dating. An attempt was therefore made to correlate the palaeoflood stratigraphies underlying flood unit F6 between the main exposure and the Annis River by incorporating an additional IRSL date. This date was obtained

from a palaeoflood unit that underlies a radiocarbon dated palaeoflood hiatus which yielded an age of 490 ±40 years B.P. (Fig. 3.59). Although the IRSL age of 4360 ±870 years (additive method) and 4480 ±900 years (regenerative method) is in keeping with the radiocarbon dated stratigraphy of the Annis River, it does not correlate with the IRSL dates from the main exposure. This indicates that possibly one of the flood units F3 - F1 is chronostratigraphically correlatable with the age of 4360 ±870 years (Fig. 3.59). A broadly similar IRSL age was obtained from the basal palaeoflood unit F1 at lower Xobies which yielded an age of 3660 ±730 years. This suggests that the main palaeoflood stratigraphies at lower Xobies and Bloeddrift cover a period of approximately 4000 years (Figs 3.53 and 3.59). The 4360 ±870 age from the Annis River and its correlation to the main exposure indicates that flood units F5 and F4 are missing from the Annis River palaeoflood stratigraphy (Fig. 3.59).

3.3.3.1 Correlation of the lower Xobies and Bloeddrift palaeoflood stratigraphies

Correlation of the lower Xobies and Bloeddrift palaeoflood sequences was partially successful with only four palaeoflood units being correlated of which three are considered as tentative (Fig. 3.60).

The sequence comprising flood units F6 and F9 and the underlying non-palaeoflood deposited bed is correlated from the Annis River to the main exposure at Bloeddrift through to lower Xobies (Fig. 3.60). The correlation is based on an identical motif of sedimentary structure, similar palaeodischarges, thickness of flood unit and radiocarbon ages (Bloeddrift radiocarbon ages for the bed underlying unit F6 yielded 710 ±40 years B.P., 450 ±20 years B.P. and 490 ±40 years; lower Xobies radiocarbon age for a bed underlying unit F9 yielded an age of 610 ±50 years B.P.) exhibited by the two flood units (Fig. 3.60).

Flood unit F5 can be tentatively correlated from the main exposure at Bloeddrift to the main exposure at lower Xobies (flood unit F6) through to section 2 at lower Xobies (flood unit F5A) (Fig. 3.60). The correlation is based on the similarity in age between the IRSL age of 1100 ±220 years at Bloeddrift and the radiocarbon age of 1160 ±80 years B.P. for flood unit F6 at lower Xobies and the previously established correlation between the main exposure and section 2 at lower Xobies (see Fig. 3.55 for an explanation of the correlation between the two sections at lower

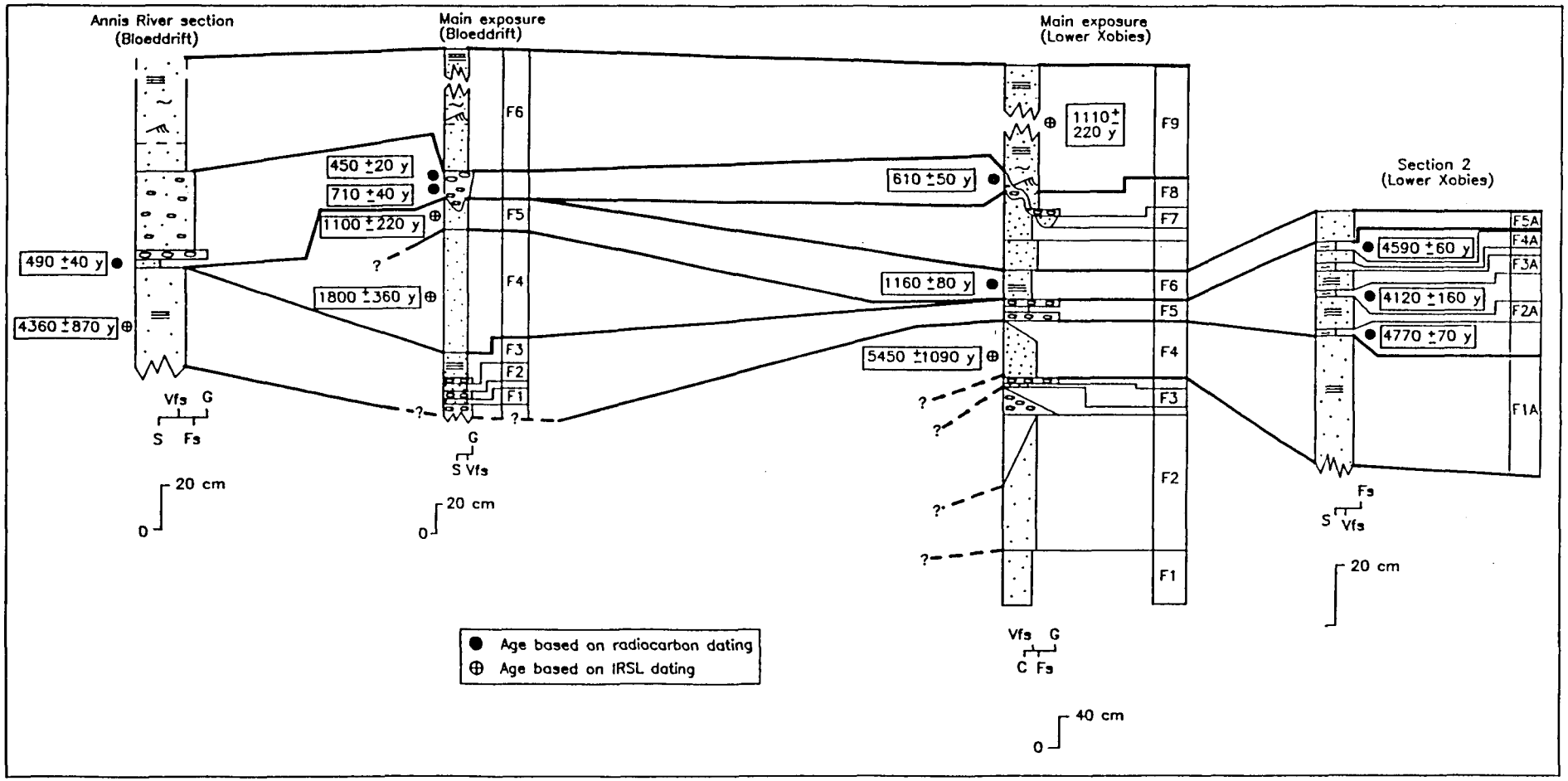

Fig. 3.60 - Correlation of the lower Xobies and Bloeddrift palaeoflood stratigraphies.

Xobies) (Fig. 3.60). It is noted however, that because the IRSL dates are older than expected, the IRSL age of unit F5 at Bloeddrift is likely to be younger and may not be correlatable with unit F6 from lower Xobies. However, in accepting the above correlation, neither of flood units F7 and F8 at lower Xobies are present at Bloeddrift (Fig. 3.60).

A further correlation between flood unit F5 and units F2A - F4A at the main exposure and section 2 of lower Xobies respectively, is tentatively extended to include the basal flood unit at the Annis River section (Fig. 3.60). This correlation is based on the previously established one existing between the main exposure and section 2 at lower Xobies (Fig. 3.55) and the similar IRSL age of 4360 ±870 years obtained for the basal flood unit from the Annis River (Fig. 60). This correlation indicates that either of flood units F1, F2 or F3 at Bloeddrift is a correlate of unit F5 from lower Xobies (Fig. 3.60).

Although the correlation of flood unit F4 with unit F1A between the main exposure and section 2 at lower Xobies is reasonably certain (Fig. 3.55), its extension to either of the palaeoflood sequences at Bloeddrift could not be established (Fig. 3.60). This indicates that the palaeoflood stratigraphy at the main exposure at lower Xobies contains a more comprehensive palaeoflood catalogue that extends for a longer period of time than that at Bloeddrift.

Although it is important to correlate and combine palaeoflood sequences at multiple sites in order to construct a comprehensive flood catalogue and thereby improving the accuracy of peak-discharge estimates (Kochel and Baker, 1988; Baker et al., 1983), correlation of the lower Xobies and Bloeddrift palaeoflood sequences has shown that correlating palaeoflood stratigraphies is not straight forward. This is despite the excellent outcrop and preservation of the palaeoflood sediments. Similarly, the reconnaissance investigation of many palaeoflood sites (Zawada and Hattingh, 1993) showed that correlating palaeoflood sediments from even adjacent back-flooded tributaries was problematic. The difficulty in correlating palaeoflood stratigraphies is attributed to the following reasons:

(1) the erosion of slack-water sediments by a combination of back-flood and

tributary-flow related scour which varies from site to site resulting in markedly different palaeoflood sequences. For example, the lower Xobies palaeoflood stratigraphy contains more palaeoflood events over a longer period than at Bloeddrift (Fig. 3.60).

(2) The homogeneity of slack-water sediments and the subtle lithological differences between slack-water sediments makes their correlation between sites difficult. This problem was partially overcome by using relief peels.

(3) The lack of datable quantities of organic material from slack-water sediments precludes their chronostratigraphic correlation to multiple sites. For example, only 5 flood units at lower Xobies and 6 from Bloeddrift out of a total of 24 palaeoflood units could be radiocarbon dated. Consequently, several chronostratigraphic "gaps"exist in the lower Xobies and Bloeddrift palaeoflood sequences. Although IRSL dating is an important innovation for dating slack-water sediments because it overcomes the problem of insufficient organic material, the IRSL ages of the slack-water sediments are older than that indicated by radiocarbon dating with a number of dates being anomalously old. Furthermore, the precision of the IRSL age as expressed by the plus/minus 1 sigma standard deviation value is relatively low being approximately 20 % of the age. This is in contrast to radiocarbon dating where the percentage error of the age is less than 5 %. IRSL dating of slack-water sediments should therefore be done in conjunction with more tested and reliable dating procedures such as radiocarbon dating. Until IRSL dating of slack-water sediments is shown to be a reliable dating tool, the dating of slack-water sediments will still be subject to the problem of collecting sufficient quantities of organic material for radiocarbon dating.

In conclusion, any palaeoflood investigation using slack-water sediments should attempt to correlate the palaeoflood sequences across multiple sites. However, even where detailed lithostratigraphic sections have been done with accurate dating being available, it is likely that only partial correlations of palaeofloods across multiple sites can be established.

3.4 Flood-frequency analysis of the lower Orange River

In evaluating the effect of incorporating the palaeoflood record in flood-frequency analysis of the lower Orange River, three flood-frequency analyses were completed. The first analysis used the systematic gauge record at Vioolsdrift for the period 1933 - 1992 (DWAF gauge station D8H003) which is the longest flow record for the lower Orange River. The second analysis incorporated the systematic record and the palaeoflood discharge estimate and date obtained for flood unit F9 (27 870 m^3/s) observed at lower Xobies and Bloeddrift. The third analysis incorporated the systematic record and the nine palaeoflood palaeodischarge estimates and dates for flood units F1 - F9; Table 3.5). For all three analyses, the Log Normal (LN), the Log Pearson Type 3 (LP3) and the General Extreme Value Probability Weighted Moments (GEV/PWM) probability distributions functions were selected as they are the most commonly applied ones in flood-frequency analysis in South Africa (Van Bladeren, pers comm.). The flood-frequency analysis was done by the flood studies section of the Department of Water Affairs and Forestry using the "REGFLOOD" computer programme written by Alexander (1990). The flow-gauge data and palaeoflood data on which this analysis was based, together with the statistical properties and characteristics associated with the flood-frequency analyses, are included in Appendix A.

Flood-frequency analysis using the systematic record for the period 1933 - 1992 indicates that the return period for the catastrophic flood (flood unit F9) varies widely depending on the probability distribution function used. For example, the GEV/PWM distribution yielded a return period in excess of 1 in 10 000 years. In contrast, extrapolation of the LN and LP3 distributions gave return periods of approximately 1 in 200 years and 1 in 1 000 years respectively (Fig. 3.61; Appendix A). Although all three distributions exhibit acceptable coincidence with the systematic flow record especially in the range of discharge 600 m^3/s - 6 000 m^3/s, considerable divergence between the different probability functions and therefore return periods exist with discharges in excess of approximately 10 000 m^3/s (Fig. 3.61). This indicates that estimating the return period of flood unit F9 based on the systematic record alone by extrapolation of the probability distributions does not yield return periods that are either consistent or meaningful.

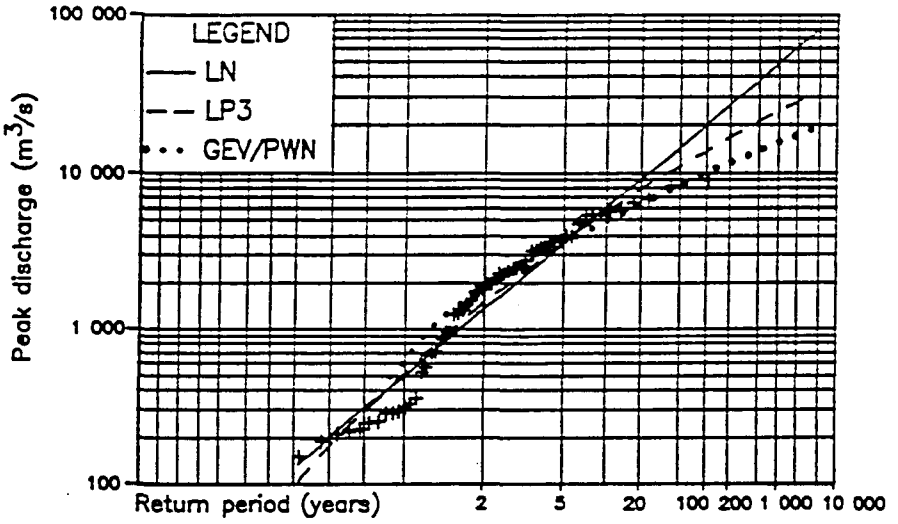

Fig. 3.61 - Flood-frequency analysis of the lower Orange River using the systematic flow-gauge record for the period 1933 - 1992.

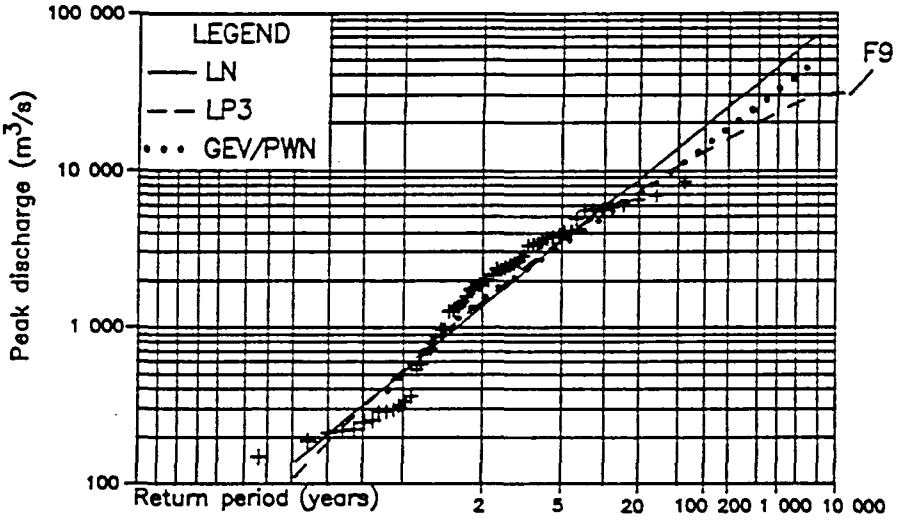

Fig. 3.62 - Flood-frequency analysis of the lower Orange River using the systematic flow-gauge record for the period 1933 - 1992 and the palaeoflood discharge and dates for flood unit F9.

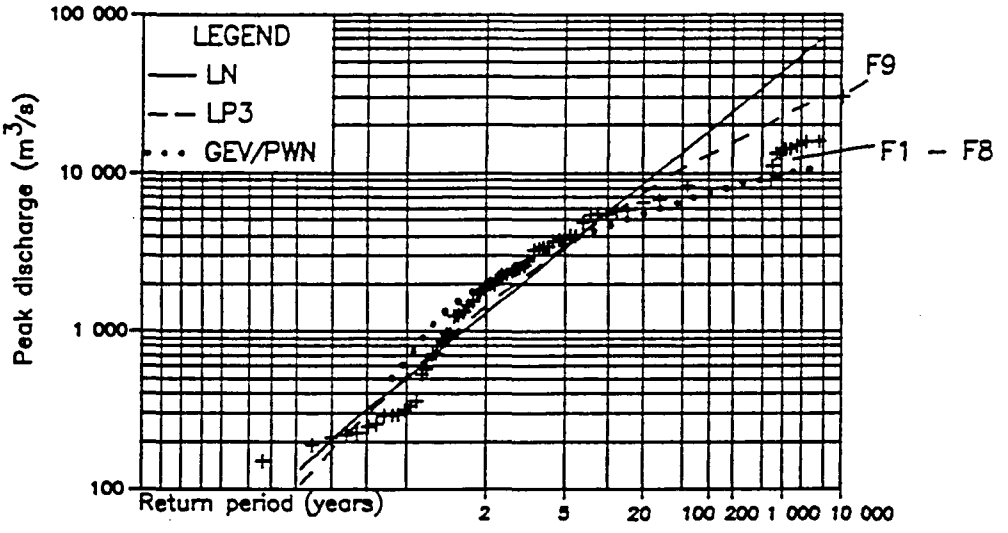

Fig. 3.63 - Flood-frequency analysis of the lower Orange River using the systematic flow-gauge record for the period 1933 - 1992 and the palaeoflood discharges and dates for flood units F1 - F9.

Note - Results are plotted on logarithmic - normal probability scale using the cunane plotting positions.

Flood-frequency analysis based on the systematic record and incorporating the palaeodischarge estimate of flood unit F9 yields more consistent and acceptable return periods for all three probability distribution functions. For example, the GEV/PWM distribution gives a return period of approximately 1 in 500 years. The LN and LP3 distributions yield return periods of approximately 1 in 200 years and 1 in 1 000 years which are similar to the results obtained from flood-frequency analysis using only the systematic flow record (Fig. 3.62; Appendix A). The LP3 distribution seems to fit the systematic and palaeoflood data better than either the LN or GEV/PWM distributions. In addition, the inclusion of flood unit F9 as an outlier appears to reduce the divergence between the three probability distribution functions for discharges in excess of 10 000 m^3/s compared to the frequency analysis based on the systematic record alone. The results of employing frequency analysis based upon the systematic record and a single palaeoflood-derived discharge indicates that the inclusion of even one flood outlier results in more consistent and possibly meaningful return periods for especially large floods in excess of 10 000 m^3/s. For example, the return period for flood unit F9 lies in a range of 1 in 200 - 1 in 1 000 years, of which the 1 in 1 000 year return period yielded by the LP3 distribution is considered the more accurate estimate.

A flood-frequency analysis using the systematic flow record with the palaeoflood record of flood units F1 - F9 at lower Xobies yielded return periods for flood unit F9 of approximately 1 in 200 years and 1 in 1 000 years using the LN and LP3 probability distribution functions respectively (Fig. 3.63; Appendix A). In contrast the GEV/PWM distribution yielded a return period of far in excess of 1 in 10 000 years (Fig. 3.63; Appendix A) and is therefore not considered to be meaningful. The LP3 distribution is considered to yield more accurate results as it fits both the systematic and palaeoflood data better than either of the LN and GEV/PWM distributions.

In conclusion, flood-frequency analysis of the lower Orange River using systematic flow gauge and palaeoflood data has indicated that the discharge represented by flood unit F9 has a return period of between 1 in 200 - 1 in 1 000 years. Because the LP3 distribution consistently fits both the gauging and palaeoflood record better than the LN and GEV/PWM probability distributions, the return period of 1 in 1 000 years is considered the more accurate estimate. This observation

highlights the value of including palaeoflood data in flood-frequency analysis in order to assess and identify the most appropriate probability distribution function. For example, the GEV/PWM distribution is overly sensitive to the inclusion of palaeoflood data because of changes to the skewness of the untransformed data and is therefore not recommended in this flood-frequency analysis. Similarly, the LN distribution which is used only with log-transformed data exhibiting zero skewness is not considered in this analysis because the systematic and palaeoflood records exhibits marked negative skewness (Appendix A).

The minimal effect of incorporating the palaeoflood record to the return period of flood unit F9 using the LP3 distribution, indicates that the systematic record for the lower Orange River is probably a representative record in terms of recorded discharges and the time span over which flow gauging occurred. This observation highlights the role of palaeoflood hydrology in verifying the representativeness and accuracy of flood-frequency analysis that is based only on the systematic flow gauge record. A further conclusion arising from this flood-frequency analysis is that the inclusion of the palaeoflood discharges for flood units F1 - F8 have not appreciably influenced the return period of flood unit F9 using the LP3 distribution. This indicates that although flood units F1 - F8 represent floods that were larger than any gauged or historically recorded flood for the lower Orange River, they have a relatively minor affect on the return periods of large floods compared to the influence of the catastrophic flood outlier represented by flood unit F9. This implies that even in the worst case situation of a fragmentary palaeoflood record, a knowledge of the largest palaeoflood in terms of discharge and date of occurrence still has an important role in verifying conventional flood-frequency estimates.

3.5 Lower Orange River palaeoflood periods and the southern African palaeoclimate record

A critical factor in preserving a palaeoflood slack-water sediment is the position of the slack-water sediments in relation to post-flood fluvial erosion. Alternatively stated, slack-water sediments that are perched above the stage associated with the frequent flow of the river, exhibit a high potential for long-term preservation. This implies that a sequence of palaeoflood slack-water sediments for a given geometry and thalweg elevation of the main channel, comprises a series of perched positions or

threshold stages/discharges during which the magnitude of the frequent flows were smaller. Deposition of sediments above this threshold can only occur where a flood exceeds the previous threshold (assuming a constant geometry and thalweg elevation of the main channel). It is important to note therefore, that a palaeoflood sequence such as lower Xobies and Bloeddrift does not represent a catalogue of the smallest to the largest flows of the river, but is a record of the changing maximum flood thresholds though time for the lower Orange River. One method of expressing the nature of threshold change is by calculating the difference in discharge between adjacent palaeoflood units as a percentage of the total difference in discharge exhibited by the smallest to the largest palaeoflood unit (F1 - F9 at lower Xobies and F1 - F6 at Bloeddrift) (Table 3.8). Of significance is that the percentage difference between palaeoflood units F8 - F9 at lower Xobies and F5 - F6 at Bloeddrift is 75,5 % and 82,5 % respectively, whereas the difference for the palaeoflood sequence F1 - F8 at lower Xobies and F1 - F5 at Bloeddrift is 3,6% and 4,4 % respectively (Table 3.8).

Interpreting the palaeoflood slack-water sediment record as a series of exceeded flood thresholds is a useful concept as it can be applied to investigate the relationship between climate and flood hydrology. Conversely, hydroclimatic inferences can be made when periods of non-exceedance of a threshold discharge are identified. Although it is simplistic to suggest that a proportional relationship exists between flood magnitude and climate change (Baker, 1993), a dated record of changed palaeoflood thresholds is likely to reflect broad changes in the palaeohydroclimate of a river. For example, Knox (1993) in a study of overbank sedimentation for the past 7 000 years from tributaries of the upper Mississippi River, found that large increases in flood magnitude occurred in response to relatively small changes of climate. The climate changes exhibited a mean annual temperature change of 1° - 2° and a change in the mean annual precipitation of ≤10% - 20 %. An indication of possible hydroclimatic change for the lower Orange River is observed in Table 3.8 which documents the percentage change between palaeoflood units at lower Xobies and Bloeddrift. For example, the dramatic difference between the largest and second largest palaeoflood is in contrast to the underlying palaeoflood sequence whose increase in discharge between flood units varies between 3,6% - 4,4 %. This suggests a sudden change of hydroclimate at or close to the time of deposition of flood unit F9.

The relationship between climate and flood regime is complex and operates on a spatial and temporal scale (Hirschboeck, 1988). This complexity leads to uncertainty in calibrating flood magnitude thresholds to climatic indices such as temperature and precipitation. However, the palaeoflood record can be used as an independent method in verifying current Holocene palaeoclimate change models for Southern Africa proposed by Partridge et al. (1990), Talma and Vogel (1992), Tyson and Lindesay (1992) and Tyson (1993). Accordingly, the following account attempts to place the palaeoflood record of the lower Orange River in a palaeoclimatic context for the latter half of the Holocene.

LOWER XOBIES		BLOEDDRIFT	
Palaeoflood unit change of adjacent palaeofloods.	**Percentage change in discharge as a proportion of the total difference in discharge between units F1 and F9.**	**Palaeoflood unit change of adjacent palaeofloods.**	**Percentage change in discharge as a proportion of the total difference in discharge between units F1 and F9.**
F8 to F9	75,5	F5 to F6	82,5
F7 to F8	1	F4 to F5	2
F6 to F7	3,5	F3 to F4	11
F5 to F6	4	F2 to F3	3,5
F4 to F5	1	F1 to F2	1
F3 to F4	4		
F2 to F3	0,5		
F1 to F2	11		

Table 3.8 - Percentage difference in discharge as a proportion of the total difference in discharge between adjacent palaeoflood units at lower Xobies and Bloeddrift. Note the similar difference in discharge between the largest and second largest palaeoflood at both sites.

Plotting discharge as an index of magnitude against age for the lower Xobies and Bloeddrift palaeoflood units together with the annual peak-flow series gauged at Vioolsdrift, shows that the lower Orange River flood record can be extended to approximately 5 500 years B.P. (Fig. 3.64). The record can also be subdivided into 4 palaeoflood periods each characterised by a threshold discharge value (Fig. 3.64).

Period 1 comprises 5 dated palaeoflood events over a period of approximately 3650 years from an IRSL age of 1800 ±360 years to at least 5450 ±1090 years during

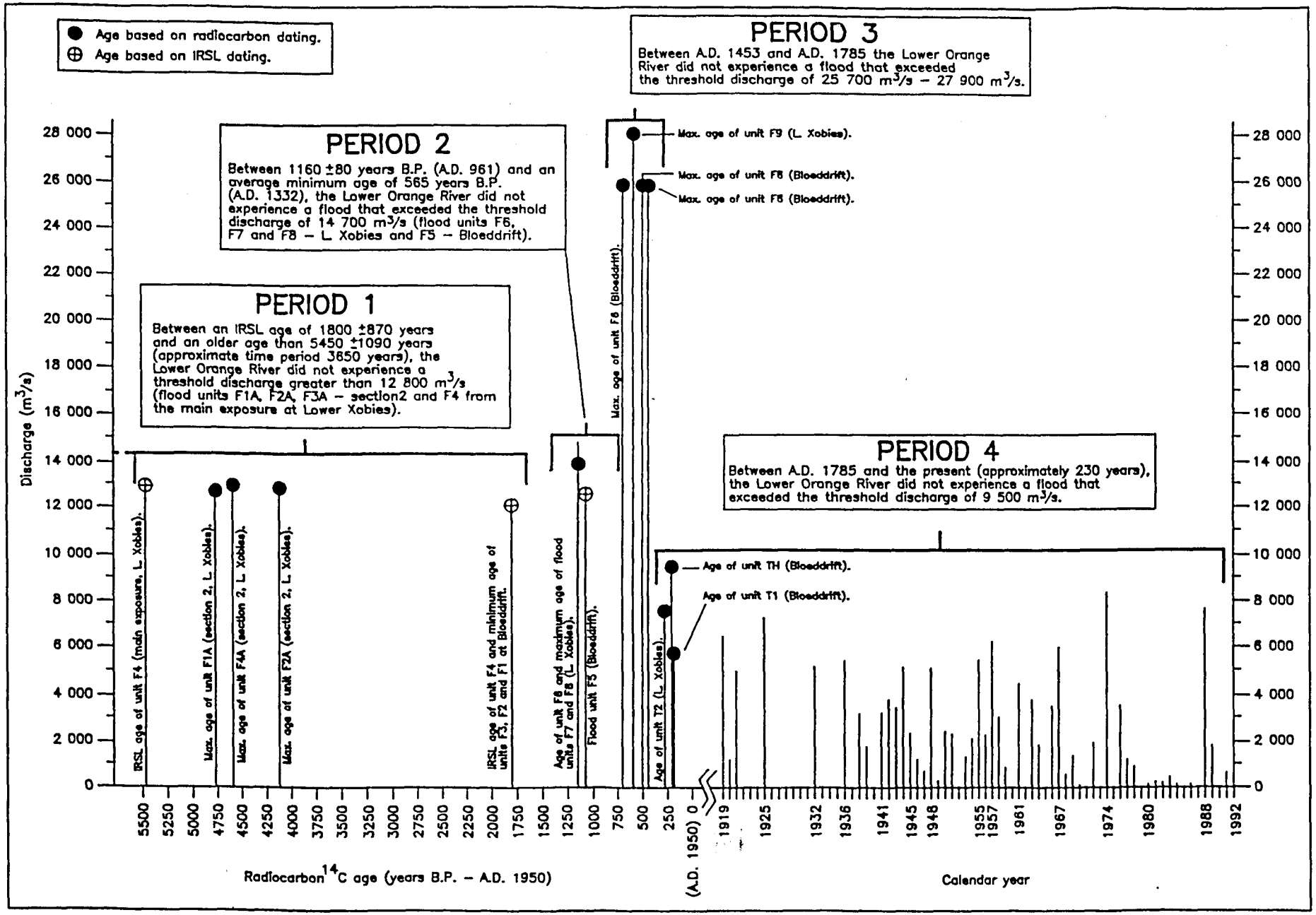

Fig. 3.64 - Compilation of the palaeoflood records of lower Xobies and Bloeddrift with the annual peak-flow series gauged at Vioolsdrift for the period 1919 - 1992 (Van Bladeren, 1995). The palaeoflood record is subdivided into 4 palaeoflood periods characterised by a threshold discharge value. This information has extended the modern flood record by approximately 5500 years.

which the lower Orange River did not experience a flood that exceeded the threshold discharge of 12 800 m^3/s (Fig. 3.64). Of further palaeoclimatic significance, is the occurrence of three floods (F1A, F2A and F3A) at lower Xobies that occurred in relatively quick succession over a period of 650 years from 4770 ±70 years B.P. - 4120 ±160 years B.P. (Fig. 3.64). The period between approximately 4120 ±160 years B.P. and 1800 ±360 years may also be palaeoclimatically significant since no palaeofloods are recorded. This may indicate that the Orange River for a period of approximately 2300 years experienced a flood regime well below the flood stage associated with a 12 800 m^3/s discharge.

Period 2 comprises 4 palaeoflood events (flood units F6, F7 and F8 from lower Xobies and F5 from Bloeddrift) occurring over a period of approximately 400 years from A.D. 961 - to the median date of A.D. 1332 for the period A.D. 1317 - A.D. 1347. During this time the maximum flood discharge for the lower Orange River did not exceed the threshold discharge of approximately 14 700 m^3/s (Fig. 3.64).

Period 3 comprises the catastrophic flood represented by flood units F9 and F6 at lower Xobies and Bloeddrift respectively, exhibiting a palaeodischarge between approximately 25 700 m^3/s - 27 900 m^3/s. Four radiocarbon dates of the non-palaeoflood bed underlying units F9 and F6 indicates that the flood occurred between the median date of A.D. 1453 for the period A.D. 1444 - A.D. 1462 and A.D. 1785 (Fig. 3.64). The younger limiting date was selected on the basis of three radiocarbon dates obtained for organic-rich slack-water sediments TH, T2 and T1 which yielded calibrated dates of around A.D. 1785 (Table 3.6). The catastrophic flood predates A.D. 1785 because the organic-rich beds of flood units TH, T2 and T1 are well preserved and are unlikely to have survived the effects of such a flood had they been deposited prior to A.D. 1785. In addition, no stratigraphic evidence was found of flood units F9 or F6 directly overlying either of the flood units TH, T2 and T1.

Period 4 extends from A.D. 1785 till the present. The organic-rich slack-water sediments of units TH, T2 and T1 are preserved and were not scoured out by floods with a discharge greater than approximately 9 500 m^3/s. This indicates that for a period of 210 years, the maximum flood experienced by the lower Orange River did not exceed the threshold discharge of 9 500 m^3/s. This conclusion is partially

supported by the gauge record which shows that between 1919 and 1992 the three largest lower Orange River floods were 8 330 m^3/s in 1974, 7 700 m^3/s in 1988 and 7 200 m^3/s in 1925 (Van Bladeren, 1995) (Fig. 3.64).

In placing the paleoflood periods 1 - 4 in a palaeoclimatic context, a palaeoclimate trend of relative temperature and wetness for the past 5500 years in Southern Africa was compiled using data presented by Tyson and Lindesay (1992) and Tyson (1993a, 1993b) covering the last 2000 years, and Partridge et al. (1990) for the period 2000 years B.P - 5500 years B.P. (Fig. 3.65). The palaeoclimate trends presented by Partridge et al. (1990) and Tyson (1993a, 1993b) represent the best accounts of climate change during the Holocene for Southern Africa as they are based on a synthesis of numerous palaeoclimate studies involving oxygen isotope analyses of a cave speleothem and mollusc remains in shell middens, foraminiferal studies, tree-ring analysis, palynology, micromammalian research and sedimentary records such as palaeosols and geomorphic features.

In accounting for the palaeoclimatic trends for the past 2 000 years, Tyson and Lindesay (1992), Tyson (1993a, 1993b) proposed a model that was originally designed to account for the modern-day 18 year wet and dry cycles experienced in Southern Africa. The model proposes that increased disturbance of tropically-induced circulation patterns forced by a strengthening of tropical easterlies leads to wet spells. In contrast, an increase in the occurrence of westerly disturbances leads to dry spells. This results in the summer rainfall regions of southern Africa receiving increased precipitation with a decrease in winter rainfall areas during wet spells, whereas in dry spells, the summer and winter rainfall regions experienced a decrease and increase in rainfall respectively. This model was extended back to the early Holocene, by Tyson and Lindesay (1992) and Tyson (1993a, 1993b) in which it was stated that the Little Ice Age which existed between A.D. 1300 - A.D. 1850 was cooler and drier in the summer rainfall region than at present. Furthermore, the model states that due to adjustments in the tropical circulation over the subcontinent, a reduction of rainfall in the interior was associated with lower temperatures. Conversely, an increase in temperature resulted in a higher summer rainfall. This conclusion is supported with palaeoclimatic data from the Kalahari and eastern regions (summer rainfall region) of southern Africa during the period 2 000 years B.P. - 8 000 years B.P. showing that increased

temperature is associated with increased rainfall (Partridge et al., 1990).

Relating the palaeoflood periods to the palaeoclimate trends proposed by Partridge et al. (1990) and Tyson (1993a, 1993b) it is significant that the median date of A.D. 1619 for the catastrophic flood of palaeoflood period 3 (A.D. 1453 - A.D. 1785), coincides with the date of A.D. 1550 for the peak of the warming episode in the Little Ice Age (Fig. 3.65). Although the Little Ice Age was generally cooler and drier than present, a sudden warming episode occurred between A.D. 1500 - A.D. 1675 which occurred over much of southern Africa (Tyson, 1993a, 1993b) (Fig. 3.65). The warming was associated with increased rainfall in the summer rainfall region. This, together with its sudden onset, (occurred over a period of only approximately 125 years, Tyson, 1993a, 1993b), could have resulted in a dramatic hydrological response in the Orange River catchment which led to the catastrophic flooding observed in the lower Orange River. Further indications of a wetter climate at around the deposition of the catastrophic flood is the relatively thick non-palaeoflood colluvialy-deposited gravel underlying the slack-water flood units F6 and F9 (bed O at lower Xobies and bed D at Bloeddrift, Figs 3.53 and 3.58). Furthermore, this deposition occurred on a dissected palaeoflood surface of flood unit F8 at lower Xobies (Figs. 3.41). The incision is ascribed to channelised flow originating from the tributary valley side and the headwaters of the tributary in response to a wetter and more vigorous hydrological regime.

Further corroboration of increased flooding being associated with wetter periods in the Holocene is palaeoflood period 2 which extends from A.D. 961 - to an average minimum age of 565 years B.P. (A.D. 1332). This period coincides with the Medieval Warm Epoch that existed from A.D. 900 - A.D. 1300 (Fig. 3.65). Although the Medieval Warm Epoch was variable, it was generally warmer which according to the model of Tyson and Lindesay (1992) and Tyson (1993a, 1993b), experienced an increased rainfall in the summer rainfall region and the Orange River catchment. This could account for the occurrence of 4 large palaeofloods in period 2 with an average discharge of over 13 800 m^3/s (Fig. 3.65).

Period 1 and particularly the interval between 4120 years B.P and 4770 years B.P. with a possible extension to 5450 years B.P., shows that a cluster of four large

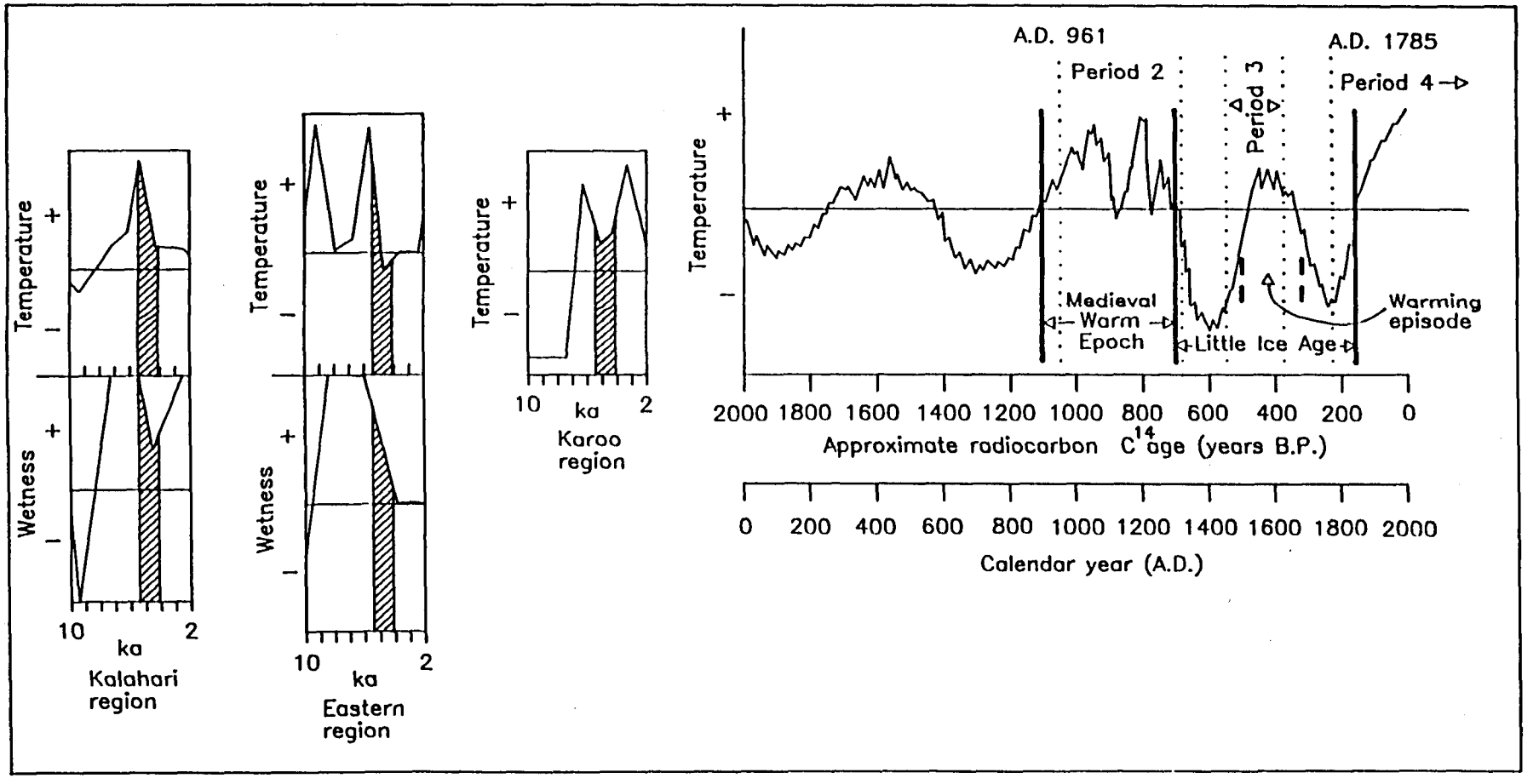

Fig. 3.65 - Inferred palaeoclimatic trend during the Holocene for Southern Africa based on palaeoclimatic compilations of Partridge et al., (1990) (2000 - 8000 years B.P.) and Tyson (1993) (0 - 2000 years B.P.) on which are plotted the palaeoflood periods 1 - 4 of the lower Orange River. Note that the palaeoflood periods 5450 - 4120 years B.P. of period 1 (hatched area) and periods 2, 3 and 4, are associated with warming episodes in the Holocene.

palaeofloods occurred (Fig. 3.65). For example, the interval between 4120 years B.P. and 4770 years B.P. (approximately 650 years) indicates that the floods F1A, F2A and F3A occurred on average every 200 years. Of significance is that during this period, the threshold showed negligible change, indicating a stable hydroclimatic regime. Furthermore, this interval coincides with the end of the Holocene hypsithermal that extended from approximately 4000 - 8000 years B.P. in Europe (Gates, 1993) and approximately 5000 - 8000 years B.P. in Southern Africa (Partridge, 1993a, 1993b). Specifically, the interval coincides with an increase in relative temperature and wetness inferred from sites in the eastern and Kalahari regions of Southern Africa with an increase in wetness for the Karoo region of the central interior (Partridge et al., 1990). Since these areas represents over 75 % of the Orange River's catchment, it is likely that their relative increase in wetness between 4120 years B.P - 5450 years led to a series of large palaeofloods with discharges of approximately 12 900 m^3/s (Fig. 3.65).

Period 4 of the palaeoflood record illustrated in Fig. 3.64 extends from A.D. 1785 to the present. Of significance is that the threshold discharge for the lower Orange River was set at approximately 9 500 m^3/s at around A.D. 1785. This date corresponds with oxygen isotope, foraminiferal and dendrological studies quoted by Tyson and Lindesay (1992), that at about A.D. 1800, a change to warmer and wetter conditions occurred during the transition from the Little Ice Age to the present warming phase (Fig. 3.65). Further evidence of wetter conditions was provided by Nicholson (1981) stating that the period A.D. 1790 - A.D. 1810 was generally wetter than the present, which together with studies presented by Tyson and Lindesay (1992), may account for the large floods recorded at around the 1800's. The modern flood record for the lower Orange does not show floods approximating the threshold discharge for period 1 (largest historically recorded flood was approximately 8 300 m^3/s in 1974). This could indicate that the Orange River since the floods of around A.D. 1785 has entered a differing hydroclimatic regime. However, no palaeoclimatic evidence exists for this except that a gradual warming has been occurring since the 1800's due to natural and possibly anthropogenic factors. In addition, the modern flood record for the lower Orange River is only 57 years long which may be too short to document the recurrence of floods that approximate the period 1 threshold discharge.

The lower Orange River palaeoflood periods can also be partially correlated

with the neoglacial episodes documented in southern South America (Jerardino, 1995). These events occurred in the latter part of the Holocene between 4 500 - 4 000 years B.P., between 3 000 - 2 000 years B.P. and during the last 1 000 years (Jerardino, 1995) during which a decrease of 1° - 3° C and an increase in precipitation was experienced. Jerardino (1995) correlated these episodes with also a decrease in temperature from the winter rainfall region of southern Africa and with evidence indicating increased humidity in the Kalahari summer rainfall region. Of these neoglacial episodes, palaeoflood period 1 is contemporaneous with the 4 500 - 4 000 years B.P. episode, and the last 1 000 year neoglacial advance correlates well with the period covered by the paleoflood periods 2, 3 and 4 (Fig. 3.65). The neoglacial episode between 3 000 - 2 000 years B.P is not reflected in the palaeoflood record (Fig. 3.65). This correlation supports the conclusion of Jerardino (1995) that the humid episodes in the Kalahari region were contemporary with the neoglacial advances recorded in southern South America. Although, Jerardino (1995) did not propose a specific meteorological mechanism to account for the increased precipitation in the summer rainfall region, she suggested that during the neoglacial episodes, cyclonic frontal systems might have penetrated more regularly and as far northward as the central and southern Kalahari. It is proposed that these frontal systems would have traversed much of the Orange River catchment resulting in increased precipitation and runoff to possibly produce the large floods and catastrophic flood documented in the palaeoflood record of the lower Orange River.

3.5.1 Can the catastrophic flood recorded from the lower Orange River recur in the present hydroclimatic regime?

Although palaeoflood hydrology of the lower Xobies and Bloeddrift sites shows that a flood of catastrophic magnitude with a discharge in the range of 25 700 m^3/s - 27 900 m^3/s occurred in the lower Orange River, this does not necessarily imply that a flood of a comparable magnitude can recur or is likely in the present hydroclimatic regime. However, assessing the possibility of recurrence of such a flood is difficult for two reasons. Firstly, a flood of this magnitude is the result of the interaction of a number of complex variables of which many are difficult to reconstruct or are unknown. For example, it is likely that such a flood is due partially to the coincidence of flood generating storm(s) over the larger tributary catchments such as the Fish River and/or the Molopo River with the flood flow of the Orange River. Secondly, the gauge record is of little help in assessing the recurrence of a flood of this magnitude

since no flood with a comparable discharge of 25 700 m^3/s - 27 900 m^3/s has occurred (Fig. 3.64). For example, the largest flood discharge ever recorded was over three times smaller.

For the reasons stated above, assessing the possibility that a catastrophic flood of such a magnitude can recur is likely to be partially speculative. However, three lines of evidence are presented that support the view that a flood with a discharge of approximately 27 000 m^3/s can occur in the present hydroclimatic regime of the Orange River.

The first line of evidence refers to the empirical method of Francou and Rodier (1967) which relates peak-flood discharge to the effective catchment area. This method was first applied to Southern Africa by Kovács (1980) and later revised (Kovács 1988). Although a more detailed account of the method is presented in section 1.2.3, two aspects that are important to the question of catastrophic flood recurrence are presented. The first is, that the method uses a peak-flood database that contains 519 flood peaks of which 354 were recorded in South Africa and 165 in other southern African countries (Kovács, 1988). The method is therefore independent of an unverifiable probabilistic or stochastic model. Secondly, the flood-peak database is obtained from gauging records, and therefore is a reflection for the period concerned, of the hydroclimatic regime. By plotting the K value using the Francou-Rodier equation (K value is a regional coefficient applicable to a hydrologically homogenous region) with its geographic position, Kovács (1988) not only compiled a map denoting regional maximum flood peak regions (RMF), but also a map that reflects the current hydroclimatic regions of Southern Africa (Fig. 1.4). Using this method to ascertain the RMF value of the lower Orange River, the lower Xobies and Bloeddrift sites yielded RMF discharges of 23 000 m^3/s (Boshoff et al., 1993) and 31 000 m^3/s using an effective catchment area of 524 000 km^2 and K-values 2,8 and 3,4 respectively, which were obtained from the regional maximum flood peak region map of Kovács (1980) (Fig. 1.4). Note that these discharges (median RMF discharge is approximately 27 000 m^3/s) are similar to the palaeoflood discharges of 25 700 m^3/s - 27 900 m^3/s recorded at lower Xobies and Bloeddrift. This indicates that not only does the palaeoflood information support the accuracy of the RMF K-values recorded for the lower Orange River, but also that the current hydroclimatic regime is able to generate a flood in the

range of 27 000 m^3/s.

The second line of evidence refers to the flood-frequency analysis of the lower Orange River discussed in section 3.3.3.2.Incorporating the palaeoflood data with the systematic gauge record for the period 1933 - 1992 indicates that the return period of flood unit F9 varies between 1 in 200 years - 1 - 1 000 years using the Log Normal (LN) and Log Pearson Type 3 (LP3) probability distribution functions respectively. Because, the LP3 probability distribution function fits the gauged and palaeoflood data better than the LN distribution, the 1 in 1 000 year return period is regarded as the more accurate estimate. Although this return period is relatively long with an annual probability of exceedance being comparatively low (0,1 % probability of recurrence in any one year), it represents nonetheless, a significant risk under certain circumstances. For example, it may be significant for certain high-risk projects such as nuclear power plants or very large dams where failure would have catastrophic effects.

The third line of evidence refers to the catastrophic flood occurring relatively recently during the period A.D. 1453 - A.D. 1785 (Fig. 3.64). Although these dates implies a similar hydroclimate between then and the present day, it should be noted that the floods occurred during the Little Ice Age climatic period during which cooler temperatures were experienced for most if not all of the earth (Grove, 1988). The effect of cooling during the Little Ice Age on the hydroclimate in southern Africa is uncertain. However, at higher latitudes such as Europe, glaciation increased volumetrically together with increased precipitation during the late 1500's - early 1600's which led to increased and occasionally catastrophic flooding (Grove, 1988). It is therefore likely that such a marked change of climate may have had significant and possibly dramatic hydroclimatic effects for the lower Orange River. This leads to the conclusion that because the post Little Ice Age climate since A.D. 1850 has been progressively warming, current climatic conditions are not favourable for generating large or catastrophic floods similar to those that occurred during A.D. 1453 - A.D. 1785. However, increased palaeoflooding in terms of discharge as represented by paleoflood periods 1 - 4 (Fig. 3.65) for the lower Orange River, coincide with the major warming episodes during the past 5000 years which has been documented for southern African in numerous palaeoclimatic studies compiled by Partridge et al. (1990) Tyson and Lindesay (1992), Tyson (1993a, 1993b) into Holocene palaeoclimate

change models. In particular, the catastrophic flood recorded in the lower Orange River occurred during the warming episode of the Little Ice Age during the period A.D. 1500 - A.D. 1675. The observation that increased flood thresholds occurred during Holocene warming episodes, with the warming currently experienced since A.D. 1850, together with the young age of the catastrophic floods, may indicate that the present hydroclimate could generate a flood with discharge in the range of 27 000 m^3/s.

3.6 Mineralogy of the Orange River slack-water sediments

3.6.1 Aims and objectives

A preliminary mineralogical study of the Orange River slack-water sediments from the Prieska and Richtersveld sites was done to achieve the following objectives:

(1) to establish if mineralogical differences exist between the Prieska and Richtersveld slack-water sediments. This information, together with a knowledge of the geology of the subcatchment regions of the Orange River system could give an indication of the relative contribution of sediment from these regions during flood conditions.

(2) To establish if the mineralogy of the catastrophic flood represented by flood unit F9 at lower Xobies differs from that of the smaller palaeoflood units at lower Xobies and Bloeddrift. A significant mineralogical difference could be correlated with the geology of the major subcatchments of the Orange River such as the Fish River, Molopo River and the Hartebees River. This information would give a qualitative indication of the relative contribution of flood discharge and sediment from these regions that resulted in the Richtersveld catastrophic flood.

3.6.2 Results

Forty one samples from all of the Orange River palaeoflood sites were analysed using X-Ray Diffraction (XRD) by the laboratory of the Council for Geoscience in Pretoria. The results are presented in Appendix B. For the Prieska sites, 12 samples were obtained from site 9 (sections 1 and 2) of which 10 represent slack-water sediments and two non-palaeoflood deposited sediments, 10 samples from site 14

(sections 1 and 2) of which all represent slack-water sediments and 7 samples were obtained from site 19 of which 4 represent slack-water sediments and 3 non-palaeoflood deposited sediments. For the Richtersveld sites, 12 samples were obtained from slack-water sediments of which 7 were from the lower Xobies site and 5 from the Bloeddrift site.

The mineralogy of the Orange River slack-water sediments comprises quartz (mean 57,0 %), plagioclase (mean 19,9 %), smectite (mean 18,8 %), illite (mean 2,9 %) and minor kaolinite (mean 0,7 %). Goethite, hematite, magnetite and microcline is restricted to the coarser grained non-palaeoflood deposited sediments (Appendix B). Comparison of the slack-water sediment mineralogy between the Prieska and Richtersveld palaeoflood sites indicates that in general little difference exists between the sites (Table 3.9; Fig. 3.66). However, the Richtersveld slack-water sediments contain almost 5 times more illite than the Prieska slack-water sediments (Table 3.9). This may indicate the introduction of a differing sediment composition between Prieska and the Richtersveld. However, in relation to the rest of the mineralogy, the change is small and not significant in terms of possible provenance changes. Site 14 exhibits higher quartz and lower plagioclase and total clay values (Table 3.9). In addition, the slack-water sediments at site 14 display on average, a higher quartz/(plagioclase + clay) ratio which is an approximate indicator of compositional maturity (Pettijohn, 1975) (Table 3.9 and Fig. 3.67). The higher detrital fraction of the slack-water sediments at site 14 is ascribed to their generally coarser-grained nature and the associated higher flow-regime during back flooding rather than differences in provenance.

In assessing possible mineralogical differences between slack-water flood units and especially between the catastrophic flood F9 at lower Xobies and the smaller flood units F1 - F7, their mineralogical compositions were plotted and illustrated in Fig. 3.68. The following observations and conclusions are made:

(1) no mineralogical difference exists between flood unit F9 and the underlying smaller palaeoflood units. A possible reason to account for this is that other flood-producing catchments such as the Fish River did not significantly contribute in terms of sediment load during the flooding represented by flood

unit F9. Alternatively, if there was a contribution in terms of discharge and sediment load, it was diluted by the greater volume sediment carried by the Orange River during flooding.

(2) No significant trend in their mineralogy exists with decreasing age. This indicates that for a period of over 5 500 years, the mineralogical composition of slack-water sediments has not appreciably changed. It should be noted, however that slack-water sediments are mainly transported in suspension in areas removed from the Orange River thalweg and associated bed load transport. Consequently, slack-water sediments may not accurately reflect the change of the total load transported during flood conditions by the Orange River. Alternatively, the XRD analysis is insufficiently insensitive in recording sediment compositional changes due to differing subcatchment contributions of sediment in time.

	PRIESKA PALAEOFLOODSITES			RICHTERSVELD PALAEOFLOODSITES	
	SITE 9 Mean (Sta.Dev. %)	SITE 14 Mean (Sta. Dev. %)	SITE 19 Mean (Sta. Dev. %)	XOBIES (L) Mean (Sta.Dev. %)	BLOEDDRIFT Mean (Sta. Dev. %)
Plagioclase	21,4(2,1)	15,4(5,7)	22,2(9,0)	20,28(4,75)	20,4(2,07)
Quartz	53,4(9,2)	74,4(9,9)	50,2(9,2)	48,0(6,90)	59,2(6,18)
Smectite	24,8(9,0)	8,0(4,8)	23,5(5,9)	23,57(9,01)	14,2(5,45)
Illite	0,4(0,97)	2,3(1,4)	0,75(0,95)	5,57(0,97)	5,6(1,52)
Kaolinite	0(0)	0(0)	0,4(0,89)	2,57(2,44)	0,6(1,34)
Q/(Plag.+clay)	1,24(0,5)	3,5(1,96)	1,19(0,6)	0,95(0,26)	1,50(0,40)
Total clay	25,10(8,54)	10,30(5,50)	25,03(4,92)	31,54(9,58)	20,33(6,84)

Table 3.9 - Mineralogical composition of slack-water sediments from the Prieska and Richtersveld palaeoflood sites.

(3) A co-variance exists between quartz and total clay (smectite, illite and kaolinite). This is attributed to hydrodynamic differences between back-flooding episodes and probably does not reflect differing subcatchment contributions through time.

(4) A comparison of the clay mineralogy between the Richtersveld slack-water

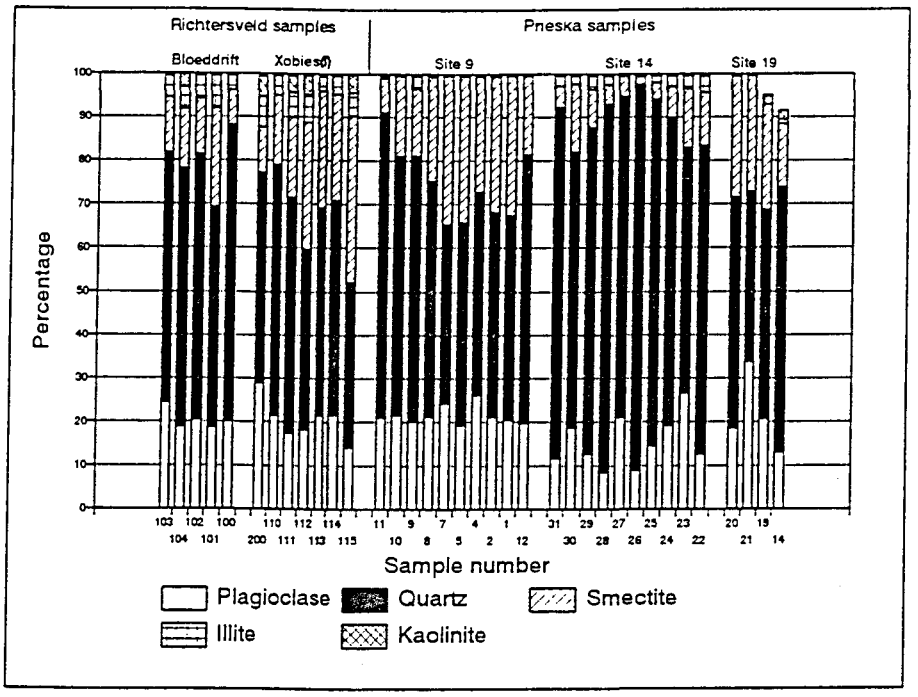

Fig. 3.66 - Mineralogical composition of the Orange River slack-water sediments from Prieska and the Richtersveld.

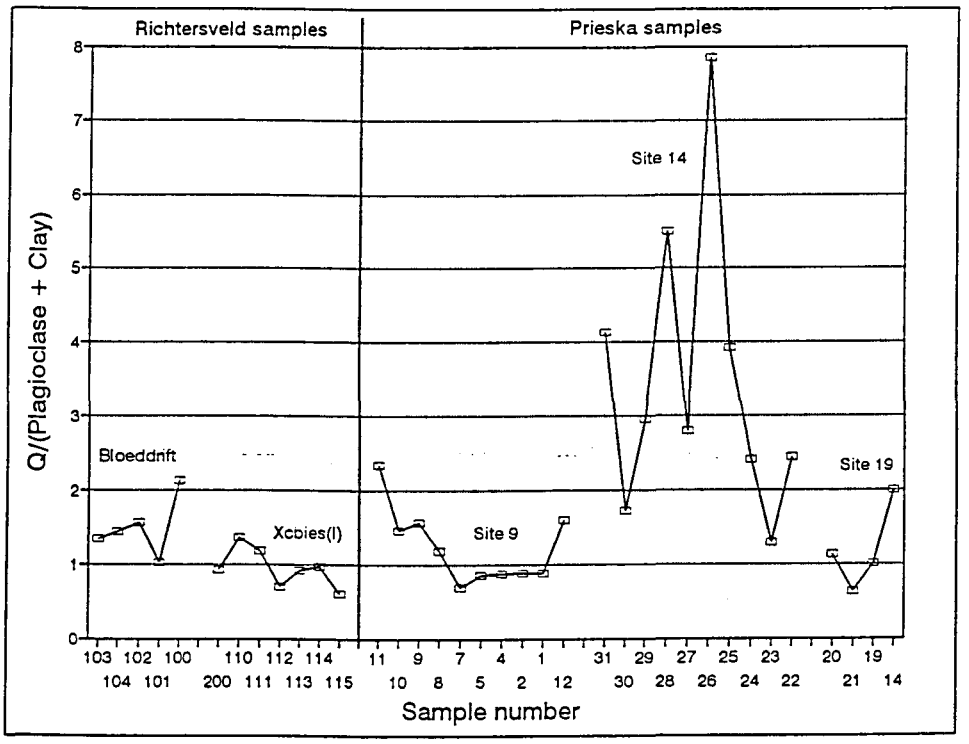

Fig. 3.67 - Maturity index (modified after Pettijohn, 1975) of the Orange River slack-water sediments from Prieska and the Richtersveld.

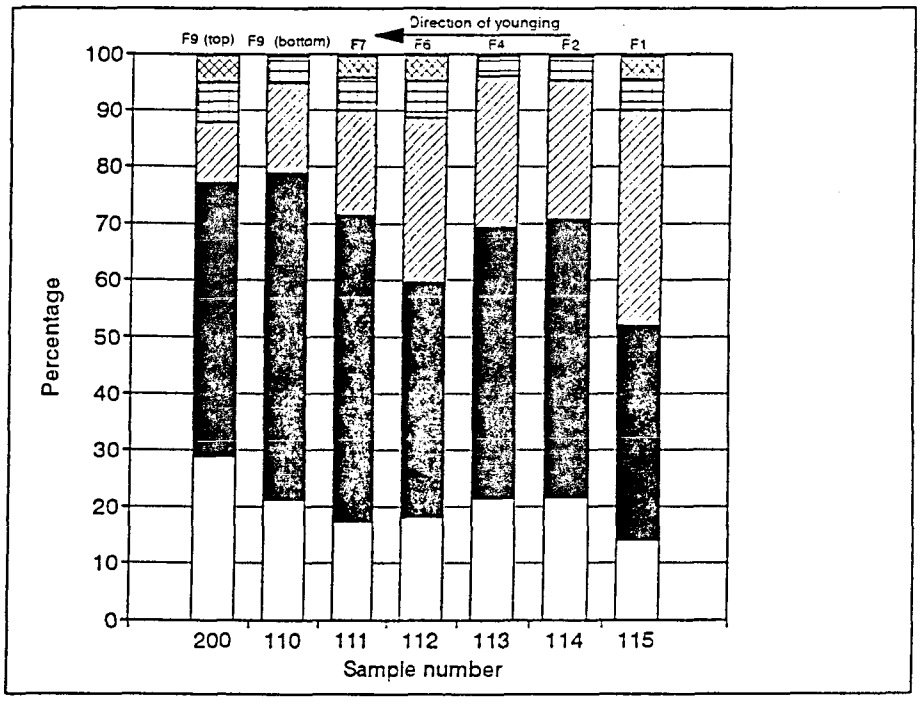

Fig. 3.68 - Mineralogical composition of the slack-water sediments of flood units F1 -F9 at lower Xobies (see legend in Fig. 3.66).

sediments and suspended sediment samples from the 1988 Orange River floods at the mouth of the Orange River by Bremner et al. (1990) reveals several significant differences. Bremner et al. (1990) reported that illite was the dominant clay mineral of the clay fraction but montmorillonite (clay type belonging to the smectite group of clay minerals) which was derived from the Drakensberg Basalts increased in abundance during the Bloemfontein and Kroonstad flood pulses. In contrast, low montmorillonite was recorded during the Fish River flood pulse. The Richtersveld slack-water sediments on the other hand contain relatively low amounts of illite as a proportion of the total clay with the major clay type being smectite (Table 3.9). It is therefore clear that the slack-water sediments for the past 5 000 years differs to that of the modern day mineralogy as recorded during the 1988 Orange River floods. A further conclusion is that the high amounts of smectite in the slack-water sediments were derived mainly from the weathering of volcanic lithologies in the upper catchment of the Orange River. This implies that the large floods recorded in the Richtersveld palaeoflood sediments may have been generated in the upper and middle portions of the Orange River catchment with a minor contribution in runoff from the lower reaches (downstream of Augrabies) of the Orange River. This conclusion is supported with reference to the kaolinite abundances of the Prieska and Richtersveld slack-water sediments (Table 3.9). The palaeoflood sediments at Prieska contain little or no kaolinite (Table 3.9). This is ascribed to the relatively small granitic terraine over which the Orange River flows up to Prieska. In contrast, an increase in kaolinite is observed from the Richtersveld slack-water sediments (Table 3.9) which reflects firstly, the presence of granitic lithologies in the lower Orange River catchment and secondly, a contribution in runoff although relatively minor, from the lower portion of the Orange River catchment.

Although the conclusions arising from the mineralogical analysis of the Orange River slack-water sediments are preliminary, the study indicates that the palaeoflood-deposited slack-water sediments are compositionally similar at a site, between sites and between the middle and lower reaches of the Orange River. This compositional homogeneity may be apparent and needs to be verified using more sensitive provenance indicators such as heavy mineral assemblages (Pettijohn et al., 1987).

4. DISCUSSION AND CONCLUSIONS

This chapter represents the substantive findings documented in this study followed by a list of the promising areas for future palaeoflood hydrological research.

The development and evolution of palaeoflood hydrology from a research-based technique to that of an applied one has occurred mainly in the United States (Baker et al., 1988) over a period of nearly 20 years. In contrast, South Africa's geologists, geomorphologists and hydrologists have largely ignored this technique neither appreciating its applied value in flood forecasting, nor its application to fluvial sedimentology, geomorphology and palaeoclimatology for the southern African region as a whole. In recognising the need to develop palaeoflood hydrological expertise in southern Africa with the objective of establishing it as a complementary applied tool in the important field of water resource management, a three-fold approach has been adopted in this study. Firstly, the study has focused on establishing an inventory of the types and characteristics of the palaeoflood evidence that exist from differing climatic regions of the country in order to show that certain regions of South and southern Africa are well suited to applying palaeoflood hydrology. Secondly, a detailed palaeoflood hydrological analysis was done for the Orange River in order to demonstrate that the technique yields information on the flood history of a river which would otherwise either be overlooked or inaccessible during conventional hydrological investigations. Thirdly, this study has attempted to show that southern African Holocene palaeoflood records represent an important source of proxy palaeoclimatic data that can be used to verify and refine the palaeoclimate change models for southern Africa.

A reconnaisance investigation of 67 potential palaeoflood sites for 8 major rivers in different climatic regions of South Africa has shown that the main types of palaeoflood hydrological evidence that exist in the country are terraces, knick-line features cut into bedrock, large in-channel boulders and slack-water sediments in back-flooded tributaries. Since experience in the United States has shown that slack-water sediments represent the most accurate palaeostage indicators (Baker et al., 1990a), the investigation focused on identifying promising flood-related slack-water sequences in bedrock-controlled reaches. Although 49 sites were located and documented, their value in constructing palaeoflood records was variable depending mainly on their state

of preservation and, more critically, their degree of biogenic reworking by plants growing on the sediments. Biogenic reworking of slack-water sediments was the most important factor impeding the collection of sufficient quantities of uncontaminated organic material for accurate radiocarbon dating results. The issue of accurate radiocarbon dating is of fundamental importance to palaeoflood hydrological analysis because it provides a chronostratigraphy to the slack-water sequence. This enables firstly, the correlation of flood events between sites, and secondly, it permits the incorporation of palaeoflood records into the systematic flow-gauge record and lastly, it permits the incorporation of palaeoflood records into Holocene palaeoclimatological models.

The preservation status of slack-water sediments is controlled by the degree of biogenic reworking which is a function of mean annual rainfall. This observation resulted in the identification of two regions in South Africa that are most suited for palaeoflood hydrological investigations. The first region covers much of the central interior of the country, namely the Orange Free State and the Cape Province north of the Cape Fold Mountains. This region experiences a mean annual rainfall gradient from approximately 800 mm in Lesotho to 100 mm - 200 mm along the west coast, Namaqualand and the Richtersveld. Accordingly, the region exhibits well preserved slack-water sediments with excellent examples occurring in the central and western portions of the region. This is an important finding as the region has the lowest density of flow-gauge records in the country and would therefore benefit from palaeoflood information in its water management of water resources. The second region includes the southern branch of the Cape Fold Mountains from Port Elizabeth westward to Cape Town and the western branch northward to approximately latitude 33° south. This area experiences a mean annual rainfall of 600 mm - 800 mm. Although the area exhibits a high vegetation density, it is variable and is largely controlled by orographic rainfall. Well-preserved slack-water sediments with a moderate to high potential for radiocarbon dating exists in the area. In addition, the region has numerous bedrock-controlled reaches since most of the rivers flow southwards breaching the Cape Fold Mountains.

The regions of the country that are least suited to palaeoflood hydrological analysis using slack-water sediments are the subtropical portions of Natal which

experience a mean annual rainfall of 800 mm - 1 000 mm and the northern Transvaal extending from Pretoria northwards and eastwards to the borders of Zimbabwe and Mozambique. The slack-water sediments in these regions are frequently poorly preserved due to extensive biogenic reworking exhibiting a low potential for radiocarbon dating. In addition, the high density of vegetation in these regions leads to masking of the sediments which makes them difficult to recognise.

Although the reconnaisance investigation did not report on all the major rivers in South Africa, it represents a valuable source of information on a large number of potential palaeoflood sites which should help to focus and guide palaeoflood investigations in South Africa in the foreseeable future.

Detailed palaeoflood hydrological analysis has focused on recording and constructing dated and flow-modelled palaeoflood catalogues for the middle (Prieska region) and lower reaches (Richtersveld region) of the Orange River. This was done using 5 bedrock-controlled reaches where slack-water sediments occurred in back-flooded tributaries. Detailed sedimentological descriptions and interpretations of the palaeoflood and non-palaeoflood sediments at each site using outcrop descriptions and 50 relief peels (represents a thickness of 25 m) permitted the identification of 43 palaeoflood-deposited flood units. For each of the three Prieska sites 6 flood units are on average present whereas 16 and 9 flood units occur at the two Richtersveld sites. Palaeodischarge estimates based on the maximum elevation of the flood units indicate that the palaeoflood sequences of the middle and lower Orange Rivers represent two ranges of palaeodischarge. At Prieska the range varies from 2 660 m^3/s - 13 080 m^3/s whereas the Richtersveld sites record a range of 5 580 m^3/s - 27 870 m^3/s. A total of 39 age determinations (15 ages refer to the Prieska sites and 24 refer to the Richtersveld sites) of mainly slack-water sediments and several interbedded non-palaeoflood sediments using a combination of radiocarbon TL and IRSL were obtained (18 of these dates were radiocarbon dated, 16 were IRSL dated and 5 were TL dated). The dating results also indicate that the palaeoflood sequences of the middle and lower Orange River cover two age ranges. The Prieska sites exhibit a range from 12 400 ±2 480 years (IRSL date) - 120 ±15 years B.P. (radiocarbon date), whereas the Richtersveld sites exhibit an age range from 5 440 ±1 090 years (IRSL date) - 210 ±50 years B.P. (radiocarbon date). It is clear that in terms of the number

of palaeoflood units identified, their respective palaeodischarges and ages, the palaeoflood sequences of the middle reach of the Orange River are markedly different to those of the lower Orange River.

Palaeoflood hydrological analysis of the lower Orange River has indicated that the Orange River has experienced 13 floods with discharges in the range of approximately 10 200 m^3/s - 14 660 m^3/s during the last 5 500 years. In addition, slack-water sediments representing a catastrophic flood with a discharge of approximately 28 000 m^3/s was recorded at both sites in the lower Orange River. Three radiocarbon dates indicates that this flood occurred after the period A.D. 1444 - A.D. 1462. The palaeoflood sequence of the lower Orange River records therefore a series of flood events that were all larger than the largest historically documented or gauged discharge of 8 331 m^3/s in 1974 at Vioolsdrift. The catastrophic flood was over three times the discharge of the largest historically recorded or gauged flood.

Flood-frequency analysis of the lower Orange River using the systematic gauge record for the period 1933 - 1992 indicates that the return period for the catastrophic flood varies between 1 in 200 years - greater than 1 in 10 000 years depending on which probability distribution function is employed. However, flood-frequency analysis using the systematic record and the discharge and date of occurrence of the catastrophic flood yields more consistent and acceptable return periods of approximately 1 in 500 years, 1 in 200 years and 1 in 1 000 years using the General Extreme Value Probability Weighted Moments (GEV/PWN), Log Normal (LN) and Log Pearson Type 3 (LP3) probability distribution functions respectively. Similarly, the incorporation of the palaeoflood record that comprises nine palaeofloods with the systematic record yielded return periods of 1 in 200 years and 1 in 1 000 years using the LN and LP3 distributions respectively. The LP3 distribution consistently yielded a return period of 1 in 1 000 years for the catastrophic flood and is therefore regarded as the most accurate estimate. The minimal effect of incorporating the palaeoflood record with the systematic record on the return period of the catastrophic flood indicates that the systematic record for the lower Orange River is a representative record in terms of discharges and the time span over which flow gauging occurred. A further conclusion arising from the flood-frequency analysis is that the inclusion of the smaller palaeofloods did not appreciably influence the return period of the

catastrophic flood using the LP3 distribution. This would indicate that a knowledge of only the largest palaeoflood can still have an important role in verifying conventional flood-frequency estimates. Flood-frequency analysis of the lower Orange River has also indicated that the inclusion of only the largest palaeoflood is valuable for assessing and identifying the most appropriate probability distribution function.

The palaeoflood record of the lower Orange River has been interpreted as a series of exceeded thresholds or changing maximum flood thresholds through time. Although it is simplistic to suggest that a proportional relationship exists between flood magnitude and climate change, a dated record of changed palaeoflood thresholds is likely to reflect broad changes in the palaeohydroclimate of a river. Plotting discharge as an index of magnitude against age of the palaeoflood units indicates that the palaeoflood record of the lower Orange River can be subdivided into 4 palaeoflood periods, each being characterised by a threshold discharge value. Period 1 comprises 5 dated palaeofloods over a period of approximately 3 650 years from 1 800 ±360 years B.P. - 5 450 ±1 090 years B.P. during which the lower Orange River did not experience a flood that exceeded the threshold discharge of 12 800 m^3/s. Of further significance is the occurrence of three floods that occurred in relatively quick succession over a period of 650 years from 4 770 ±70 years B.P. - 4 120 ±160 years B.P. Period 2 comprises 4 palaeofloods that occurred over a period of 400 years from A.D. 961 - A.D. 1332 during which the lower Orange River did not exceed the threshold discharge of approximately 14 700 m^3/s. Period 3 comprises the catastrophic flood with a discharge of approximately 28 000 m^3/s. During the period A.D. 1453 - A.D. 1785, the lower Orange River did not exceed the maximum threshold discharge of approximately 28 000 m^3/s. Period 4 extends from A.D. 1785 till the present during which the lower Orange River did not exceed the threshold discharge of 9 500 m^3/s.

In placing the palaeoflood periods 1 - 4 into a palaeoclimatic context, they were plotted on to a relative palaeotemperature and palaeowetness (inferred rainfall) trend covering the last 5 500 years for southern Africa. This trend was obtained from a synthesis of numerous palaeoclimate studies involving oxygen-isotope analyses of a cave speleothem and mollusc remains in shell middens, foraminiferal studies, tree-ring analysis, palynology, micromammalian research and sedimentary records such as palaeosols and geomorphic features. It was found that periods of increased flooding

in terms of discharge correlate well with periods of increased temperature. In accounting for this correlation, the palaeoclimatic model of Tyson (1993a; 1993b), indicates that periodic adjustments of the tropical circulation system over the subcontinent resulted in decreased rainfall being associated with lower temperatures. Conversely, an increase in temperature resulted in a higher summer rainfall. Periods of increased flooding in terms of magnitude are also partially correlatable with the neoglacial episodes documented in southern South America. In particular palaeoflood period 1 is contemporaneous with the 4500 - 4000 years B.P episode, with the last neoglacial advance correlating well with the period covered by the palaeoflood periods 2, 3 and 4. The neoglacial episode between 3 000 - 2 000 B.P. is not reflected in the palaeoflood record. This correlation supports the conclusion of Jerardino (1995) that the humid episodes in the Kalahari and the summer rainfall regions of southern Africa were contemporary with the neoglacial advances recorded in southern South America. A possible mechanism to account for the correlation between the palaeoflood periods and the neoglacial episodes is the development of cyclonic frontal systems that may have penetrated more regularly and as far northward as the central and southern Kalahari. These frontal systems would have traversed much of the Orange River catchment resulting in increased precipitation and runoff to possibly produce the large floods and catastrophic flood documented in the palaeoflood record of the lower Orange River.

Although the development and penetration of cyclonic frontal systems over the summer rainfall region may explain the occurrence of the catastrophic flood, it does not adequately explain the high co-variance that exists between the palaeoflood periods and the relatively small amplitude changes of increased temperature and inferred rainfall for the last 1 500 years. However, Tyson's (1993) model of periodic adjustments of the tropical circulation system over the subcontinent accounts better for the observed covariance between the palaeoflood periods and increased temperature and inferred rainfall for the past 1 500 years.

It is suggested that the lower Orange River could, in the present hydroclimatic regime, experience a flood with a discharge of approximately 28 000 m^3/s. This conclusion was based on three lines of evidence. Firstly, a discharge of this magnitude is similar to the discharges of 23 000 m^3/s and 31 000 m^3/s obtained using the

Francou-Rodier K-values of 2,8 and 3,4 respectively. Because the Francou-Rodier method of regional maximum flood (RMF) estimation is based on 519 historically and/or gauged flood peaks, the RMF estimates are a reflection of the present hydroclimatic regime. This indicates that not only does the palaeoflood information support the accuracy of the RMF K-values recorded for the Orange River, but also that the present hydroclimate is able to generate a flood of approximately 28 000 m^3/s. The second line of evidence refers to the flood-frequency analysis of the lower Orange River. Three flood-frequency analyses using a combination of systematic flood data and systematic plus palaeoflood data has consistently yielded a return period of approximately 1 in 1 000 years using the LP3 probability distribution function. Although this return period is relatively long with an annual probability of exceedance being comparatively low (0,1 % probability of recurrence in any one year), it represents a significant risk for high-risk projects such as nuclear power plants or very large dams where failure would have catastrophic consequences. The third line of evidence refers to the correlation between increased flooding and increased temperature during the past 5 500 years. Extrapolating this relationship into the future with the observation that since the end of the Little Ice Age (A.D. 1850) there has been gradual warming, it is possible that the present hydroclimatic is approaching or has attained conditions that could result in the lower Orange River experiencing a flood with a 28 000 m^3/s discharge.

Palaeoflood hydrological analyses of the Prieska sites has been generally disappointing for two main reasons. Firstly, despite a broad similarity of lithostratigraphy between the sites, the correlation of individual flood units between sites remains tentative. Secondly, because difficulty was experienced in collecting sufficient quantities of organic material for radiocarbon dating only 4 radiocarbon dates were obtained from the three sites. IRSL and TL dating of the slack-water sediments was therefore done to augment the radiocarbon dates in order to date further flood units. However, the luminescence dating yielded conflicting results which served to further complicate the chronostratigraphic interpretation of the palaeoflood sequences.

Palaeodischarge modelling of the flood units at Prieska yielded a range of discharges from approximately 2 660 m^3/s - 13 080 m^3/s. However, at any one site the

ranges differed from 3 040 m^3/s - 11 260 m^3/s at site 19, 2 480 m^3/s - 13 080 m^3/s at site 9 and 2 760 m^3/s - 9 000 m^3/s at site 14. Consequently, using discharge alone to correlate between sites was not possible. Combining the discharge estimates with the observation that a broad lithostratigraphic similarity exists between the basal and upper portions of the palaeoflood sequences did permit partial correlation. It was found for example, that applying a correction factor of subtracting 31 % from each discharge estimate at site 9 resulted in a high correlation of the basal flood units F1 - F5 between sites 9 and 14. Although the application of a correction factor is considered doubtful, it does suggest that a systematic error in the palaeodischarge estimates exists at either site 9 or site 14. The most likely reason for this is that the cross sections selected for calculating the discharge were not hydraulically representative. In contrast, application of a correction factor to site 19 resulted in only a slight improvement in the correlation between sites 9 and 19. This is attributed to the absence of several flood units and evidence of extensive reworking found in several of the basal flood units at site 19.

Chronostratigraphic correlation between the three sites indicates that the basal portion of the palaeoflood sequences that extends to the top of the uppermost non-palaeoflood deposited gravel ranges in age from approximately 12 500 years (IRSL date) - 7 000 years B.P. (radiocarbon date). The correlation of the upper portion of the palaeoflood sequences is less clear. For example, although similar radiocarbon ages of 150 ±45 years B.P and 120 ±15 years B.P. was obtained for the uppermost slack-water unit (flood unit F7) at sites 9 and 14 respectively, their respective corrected discharges were 4 510 m^3/s and 9 000 m^3/s. A tentative correlation suggests that either flood unit F5 or F6 at site 19, flood unit F6 at site 9 and the uppermost portion of F7 are correlatable and deposited between A.D. 1850 - A.D. 1440.

The difficulty in correlating the palaeoflood sequences between the three sites due to chronostratigraphic uncertainty and possible discharge estimate errors resulted in difficulties in relating the palaeoflood record to the systematic and historical record that exists for the middle reach of the Orange River. For example, the maximum palaeoflood recorded at site 9 corresponds to an uncorrected discharge of 13 080 m^3/s which could be correlated with either the 1804 flood (12 470 m^3/s) or the 1873 flood (13 970 m^3/s). However, the IRSL date of 6 610 ±1 320 years is clearly a conflicting

result. In a further example, calibration of the radiocarbon age for flood unit F7 at site 14 indicates that a flood with a discharge of approximately 9 000 m^3/s occurred in 1900. The gauge record shows however, that no notable floods occurred about this time.

Although the palaeoflood record has not recorded the effect of relatively large floods even those that were historically recorded, the following conclusions regarding the smaller palaeofloods can be made. (1) The basal portion of the palaeoflood stratigraphy at the three Prieska sites indicate that the Orange River experienced a series of floods with discharges of between approximately 2 500 m^3/s - 4 000 m^3/s. Radiocarbon and IRSL dating indicates that these floods occurred between approximately 7 000 years B.P. - 12 500 years B.P. (2) A flood with a discharge of approximately 4 440 m^3/s occurred 500 ±90 years B.P. which corresponds to the most probable calibrated age of A.D. 1440 (flood unit F4, site 19). This indicates that the overlying palaeoflood units F5 and F6 with respective discharges of 5 050 m^3/s and 9 030 m^3/s were deposited after A.D. 1440.

Flood-frequency analysis using the systematic flow-gauge record and the palaeoflood record was not done at Prieska for two reasons. Firstly, the palaeoflood record does not contain evidence of floods with magnitudes greater than those recorded in the historical and flow-gauge record. Consequently, the palaeoflood record would not have a significant influence on the flood-frequency analysis. Secondly, the gauge record covers the period 1910 - 1989 with 4 historical peaks that extends the Prieska flood record back to 1804. The inclusion of the relatively small magnitude palaeoflood events in a historical and gauge record that is 185 years long would have a negligible effect if any on the flood-frequency analysis.

A common problem experienced at the Prieska and Richtersveld sites and one common to palaeoflood analysis using slack-water sediments is the collection of sufficient quantities of organic material for radiocarbon dating. Most of the palaeoflood units did not contain organic material and rarely was there suitable material in the interbedded non-palaeoflood units. IRSL and TL dating (Prieska only) was therefore applied to augment the radiocarbon dating in order to improve the chronostratigraphic interpretation of the palaeoflood sequences. Because TL and IRSL

dating of very fine-grained fluvial sediments is a relatively new technique, together with the recent development of a luminescence dating laboratory in South Africa, the TL and IRSL results were considered significant only where comparison or verification with radiocarbon results was done. Thermoluminescence dating of slack-water sediments at Prieska yielded dates that were in stratigraphic order but were consistently older than the radiocarbon date. For example, a radiocarbon age of 150 ±45 years B.P. was obtained for flood unit F7 at site 9. In contrast a TL age of 6 030 ±1 210 years was obtained for the same unit. This is ascribed to insufficient bleaching or partial emptying of the electron traps that leads to a residual luminescence signal because of insufficient exposure to sunlight under turbid conditions. TL dating is therefore not expected to yield accurate age estimates of very fine-grained slack-water sediments and should not be applied without verification using radiocarbon dating.

Infra-red stimulated luminescence dating of palaeoflood units was done to obtain more realistic ages. This technique is theoretically advantageous to TL dating because the "easy-to-bleach" electron traps are sampled which largely overcomes the problem of a residual luminescence signal. This is important for water-deposited sediments that experience brief exposure to sunlight. The IRSL results at Prieska and the Richtersveld appear more reliable as they are in stratigraphic order and reflect an age closer to the radiocarbon age. For example, an IRSL date of 2 760 ±550 years was obtained compared to the TL date of 6 030 ±1 210 years for flood unit F7 at site 9. The IRSL date is still however, much older than the radiocarbon age of 150 ±45 years B.P. A similar observation was made at the Bloeddrift site where a radiocarbon age of 710 ±40 years B.P. was obtained for the non-palaeoflood unit underlying flood unit F6. In contrast, IRSL dating of flood unit F6 yielded an age of 1 910 ±380 years.

Although IRSL dating has yielded more accurate results than TL dating of slack-water sediments, the technique still yields much older ages compared to those obtained by radiocarbon dating. This indicates that problems still exist with residual luminescence due to the grains receiving insufficient exposure to the sunlight during transport and deposition. Insufficient leaching may be related to the very-fine-grained texture and the relatively high proportion of clay (10 % - 32 %) comprising the Orange River slack-water sediments. This may lead to flocculation of grains during transport and deposition and consequently partial bleaching or resetting of the

luminescence signal. This implies that more accurate IRSL results could be obtained from coarser-grained slack-water sediments.

Although it is acknowledged that the construction of a comprehensive and accurate palaeoflood catalogue requires the correlation of multiple sites, correlation of the Orange River palaeoflood stratigraphies between even closely spaced sites indicates that this is not straight forward. This is despite the excellent outcrop and preservation of the sequences. The difficulty in correlating palaeoflood sequences is attributed to the following reasons:

(1) the lack of datable quantities of organic material from slack-water sediments leads to several chronostratigraphic "gaps"and therefore hinders the correlation of flood units to multiple sites. Although IRSL dating is an important innovation for dating slack-water sediments because it overcomes the problem of insufficient organic material, the IRSL technique consistently over estimates the true age. IRSL dating of slack-water sediments should therefore be done in conjunction with more tested and reliable dating procedures such as radiocarbon dating. Furthermore, until IRSL dating is shown to be a reliable dating tool of especially fine-grained fluvial sediments, the dating and correlation of slack-water sediments to multiple sites will still be subject to the problem of collecting sufficient quantities of uncontaminated organic material for radiocarbon dating.

(2) The erosion of slack-water sediments by a combination of back-flood and tributary-flow related scour which varies from site to site results in markedly different palaeoflood sequences and therefore creates difficulties in multiple-site correlation.

(3) The homogeneity of slack-water sediments and the subtle lithological differences between slack-water sediments makes their correlation between sites difficult. This problem was partially overcome by using relief peels.

An attempt should be made to correlate slack-water sequences across multiple sites in a palaeoflood investigation. However, even where detailed lithostratigraphic

sections exist with accurate dating being available, it is likely that the palaeflood units can only be partially correlated across multiple sites.

A preliminary mineralogical analysis of slack-water sediments using X-Ray diffraction from the five sites has shown the following:

(1) that no mineralogical difference exists between the catastrophic flood unit F9 and the underlying smaller palaeoflood units. A possible reason to account for this is that other flood-producing catchments such as the Fish River did not significantly contribute in terms of sediment load during the flooding represented by flood unit F9. Alternatively, if there was a contribution in terms of sediment load, it was diluted by the greater sediment transported by the Orange River during flooding.

(2) No significant mineralogical trend exists with decreasing age at any of the 5 sites examined. This indicates that for a period of over 5 500 years in the lower Orange River and over 12 000 years in the middle reach of the Orange River, the mineralogical composition of slack-water sediments has remained constant. It should be noted, however that slack-water sediments are mainly transported in suspension in areas removed from the Orange River thalweg and associated bed load transport. Consequently, slack-water sediments may not accurately reflect possible changes in the total load transported during flood conditions by the Orange River.

(3) A co-variance exists between quartz and total clay (smectite, illite and kaolinite). This is attributed to hydrodynamic differences between back-flooding episodes and probably does not reflect differing subcatchment contributions through time.

(4) A difference in illite and smectite abundances between the 1988 Orange River flood and the slack-water sediments of the lower Orange River indicates that for the past 5 000 years, the large palaeofloods were generated in the upper and middle reaches of the Orange River catchment. A relatively minor contribution in runoff was generated in the lower reaches of the Orange River

catchment.

Although the conclusions arising from the mineralogical analysis of the Orange River slack-water sediments are preliminary, the study does indicate that the palaeoflood-deposited slack-water sediments are compositionally similar at a site, between sites and between the middle and lower reaches of the Orange River. This compositional homogeneity may be apparent and needs to be verified using more sensitive provenance indicators such as heavy mineral assemblages (Pettijohn et al., 1987).

5. RECOMMENDATIONS FOR FUTURE WORK

Although this study is the first of its kind in southern Africa and Africa, it is hoped that it will stimulate further research in the palaeoflood hydrology of rivers. The following represents a list of rivers where palaeoflood hydrology is required as part of South Africa's ongoing development of its water resources.

(1) The completion of detailed palaeoflood hydrological investigations for the major rivers in Kwa-Zulu/Natal such as the Mzimvubu, Mzimkulu, Mkomazi, Umvoti, Tugela, Mgeni, Mfolozi, Mkuze and the Pongola Rivers.

(2) Completion of detailed palaeoflood hydrological analysis of other major rivers in South Africa such as the Limpopo, the Orange River at proposed dam sites at Vioolsdrift, Boegoeberg and Pella and the larger rivers in the lowveld such as the Komati, Letaba and the Olifants River.

Other promising areas of research using palaeoflood hydrology include the following:

(1) Established and in some cases tentative observations indicate that the El Niño Southern Oscillation that occurs in the Pacific Ocean off the coast of South America has teleconnections with portions of the southern African subcontinent. Palaeoflood records can be used to examine the effect that the El Niño phenomenon has had on the hydroclimate of certain rivers during the latter part of the Holocene.

(2) A portion of this study has focused on using palaeoflood records to verify summer rainfall temperatures and inferred rainfall changes for the past 5 000 years in the summer rainfall region. A need exists to apply a similar approach to the winter rainfall region of southern Africa.

(3) Although this study has focused on the semi-arid regions of South Africa, a need exists to construct palaeoflood records for the eastern sub-tropical regions of South Africa. These areas are rapidly developing with an increasing

demand for water resources. Future water management policies that may prescribe the construction of dams will therefore require palaeoflood information in these regions.

(4) An important field of research that will widen the applicability of palaeoflood hydrology for the subcontinent is refining the IRSL dating of slack-water sediments. This would largely overcome the problem of finding sufficient quantities of uncontaminated organic material in slack-water sediments from especially sub-tropical regions. Although this study has shown that IRSL dating has promise for dating flood-deposited sediments, uncertainty still exists as to the degree that resetting of the luminescence signal occurs during transportation of the sediment in turbid flood conditions. This observation may be applicable to only very-fine grained slack-water sediments. Attention should therefore be given to assessing the accuracy of IRSL dating for other types of slack-water sediments.

Palaeoflood hydrology is a multidisciplinary approach involving sedimentology, geomorphology, hydrology and specialist dating techniques. The interdisciplinary nature of palaeoflood hydrology has resulted in this approach not being extensively applied especially in the field of water resource management. This study has shown that, by its very multidisciplinary nature, palaeoflood hydrology offers insights and valuable flood information that would otherwise, not have been obtained. This study has also shown that palaeoflood hydrology not only represents a research tool but an important applied technique that is of particular value in southern Africa where an increasing demand is made on planners to develop water resources in the region. The increasing demand for water will more than likely increase the threat to the environment. It is therefore suggested that the multidisciplinary nature of palaeoflood hydrology should be extended even further to include water resource planners, civil engineers and environmentalists specialising in the field of fluvial or fresh-water ecology.

REFERENCES

Adamson, P.T. (1975). Problems in assessing the quality of input models. Symposium on control theory, University of the Witwatersrand, Johannesburg.

Aitken, M.J. (1992). Optical dating. Quaternary Science Reviews, v. 11, p. 127-131.

Alexander, W.J.R. (1988). Flood hydrology: Are we addressing the real issues? *In* Floods in perspective. CSIR conference organised by the South African Institution of Civil Engineers. Pretoria.

_____ (1990a). Flood hydrology for southern Africa. South African National Committee on Large Dams (SANCOLD), Pretoria.

_____ (1990b). Flood hydrology: empiricism, logic and science. *In* Course on practical flood risk analysis. University of Pretoria.

Alexander, W.J.R. and Kovacs, Z.P. (1988). Lessons learnt from exceptional floods in southern Africa. *In* Sixteenth congress of the International Commission Of Large Dams (ICOLD), San Francisco, p. 1 223-1238.

American Meteorological Society (1978). Flash floods - a national problem. Bull. Amer. Met. Soc., v. 59, p. 585-586.

Ashley, G.M., Southard, J.B. and Boothroyd, J.C. (1982). Deposition of climbing-ripple beds: a flume simulation. Sedimentology, v. 29, p. 67-79.

Baker, V.R. (1987). Palaeoflood hydrology and hydroclimatic change. *In* The influence of climate change and climatic variability on the hydrological regime and water resources. Proceedings Vancouver Symposium, JAHS Publ. No. 168, p. 123-131.

_____ (1993). Learning from the past. Nature, v. 361, p. 402-403.

Baker, V.R., Ely, L.L. and O'Connor, J.E. (1990a). Palaeoflood hydrology and design decision for high-risk projects. *In* Hydraulic engineering, proceedings of the 1990 National Conference, H.H. Chang and J.C. Hill (editors). American Society of Civil Engineers, New York, p. 433-438.

Baker, V.R., Ely, L.L., O'Connor, J.E. and Partridge, J.B. (1987). Paleoflood hydrology and design applications. *In* Regional flood frequency analysis. Proceedings of the international symposium on flood frequency and risk analyses, Louisiana State University, Baton Rouge, U.S.A. V.P. Singh (editor). D. Reidel Publishing Company, Dordrecht, p. 339-353.

Baker, V.R., Kochel, R.C. and Patton, P.C. (1988). Paleofloods. *In* Flood geomorphology, V.R. Baker, R.C. Kochel and P.C. Patton (editors). John Wiley & Sons, New York, p. 317-320.

Baker, V.R., Kochel, R.C., Patton, P.C. and Pickup, G. (1983). Palaeohydrologic analysis of Holocene flood slackwater sediments. International Association of Sedimentologists Special Publication, v. 6, p. 229-239.

Barron, E.J., Hay, W.W. and Thompson, S. (1989). The hydrologic cycle; a major variable during Earth history. Palaeogeography Palaeoclimatology Palaeoecology, v. 75, p. 157-174.

Beaumont, P. and Morris, D. (1990). Guide to archaeological sites in the northern Cape. South African Association of Archaeologists post-conference excursion 9th -13th September 1990. 61pp.

Bingham, A. (1989). Floods of aid for Bangladesh. New Scientist, no. 1693, p. 42-46.

Boshoff, P., Kovács, Z., Van Bladeren, D. and Zawada, P.K. (1993). Potential benefits from palaeoflood investigations in South Africa. J. South African Institution of Civil Engineers, v. 35, p. 25-26.

Bremner, J.M., Rogers, J. and Willis, J.P. (1990). Sedimentological aspects of the 1988 Orange River floods. Transactions of the Royal Society of South Africa, v. 47, p. 247-294.

Church, M.A., McLean, D.G. and Wolcott, J.F. (1987). River bed gravels: sampling and analysis. *In* Sediment transport in gravel-bed rivers. Eds C.R. Thorne, J.C. Bathurst and R.D. Hey. John Wiley & Sons, Chichester, p. 43-79.

Costa, J.E. (1978a). Holocene stratigraphy in flood frequency analysis. Water Resources Research, v. 14, p. 626-632.

_____ (1986). A history of paleoflood hydrology in the United States, 1800-1970. Eos (Transactions of the American Geophysical Union), v. 67, p. 425-430.

Costa, J.E. and Baker, V.R. (1981). Surficial geology. Building with the earth. John Wiley & Sons, New York, 498pp.

De Wit, M.C.J. (1993). Cainozoic evolution of drainage systems in the north-western Cape. PhD thesis (unpubl.), University of Cape Town, 371pp.

Enzel, Y., Ely, L.L., Kyle House, P., Baker, V.R. and Webb, R.H. (1993). Paleoflood evidence for a natural upper bound to flood magnitudes in the Colorado River basin. Water Resources Research, v. 29, p. 2 287-2 297.

Forman, S.L. and Ennis, G. (1992). Limitations of thermoluminescence to date waterlain sediments from glaciated fiord environments of western Spitsbergen, Svalbard. Quaternary Science Reviews, v. 11, p. 61-70.

Fourie, L.W. (1990). Impact of floods. *In* Course on practical flood risk analysis. University of Pretoria.

Francou, J. and Rodier, J.A. (1967). Essai de classification des crues maximales. Proceedings of the Leningrad Symposium on floods and their computation. UNESCO.

Frank, N.L. and Husain, S.A. (1971). The deadliest tropical cyclone in history? Bull. Amer. Met. Soc., v. 52, p. 438-445.

Frostick, L.E., Lucas, P.M. and Reid, I. (1984). The infiltration of fine matrices into coarse-grained alluvial sediments and it's implications for stratigraphical interpretation. J. geol. Soc. Lond., v. 141, p. 955-965.

Gates, D.M. (1993). Climate change and its biological consequences. Sinauer Associates, Sunderland, 280pp.

Geological map of the Republics of South Africa, Transkei, Bophuthatswana, Venda and Ciskei and the kingdoms of Lesotho and Swaziland (1984). 1:1 000 000 scale map published by the Geological Survey of South Africa.

Geological map of the Richtersveld (1958). Geological Survey of the Union of South Africa, Pretoria, (2 maps).

Grove, J.M. (1988). The Little Ice Age. Methuen & Co., London, 498pp.

Hirschboeck, K.K. (1988). Flood hydroclimatology. *In* Flood geomorphology, V.R. Baker, R.C. Kochel and P.C. Patton (editors). John Wiley & Sons, New York, p. 27-49.

Jerardino, A. (1995). Late Holocene neoglacial episodes in southern South America and southern Africa: a comparison. The Holocene, v. 5, p. 361-368.

Klemeš, V. (1988). The improbable probabilities of extreme floods and droughts. Proceedings of the technical conference of the World Meteorological Organization, Geneva. James & James, London, 319pp.

Knox, J.C. (1993). Large increases in flood magnitude in response to modest changes in climate. Nature, v. 361, p. 430-432.

Kochel, R.C. (1980). Interpretation of flood-paleohydrology using slackwater deposits, Lower Pecos and Devils Rivers, southwestern Texas. Ph.D thesis (unpubl.), University of Texas, Austin, 364pp.

Kochel, R.C. and Baker, V.R. (1988). Paleoflood analysis using slackwater deposits. *In* Flood geomorphology, V.R. Baker, R.C. Kochel and P.C. Patton (editors). John Wiley & Sons, New York, p. 357-376.

Kokot, D.F. (1965). Oranjerivier. Tegnikon, v. 14, p. 7-9.

Kovács, Z. (1980). Maximum flood peak discharges in South Africa: An empirical approach. Department of Water Affairs and Forestry Technical Report, TR 105.

_____ (1988). Regional maximum flood peaks in Southern Africa. Department of Water Affairs and Forestry Technical Report, TR 137, 25pp.

_____ (1990). Regional maximum flood peaks in Southern Africa. *In* Course on practical flood risk analysis. University of Pretoria.

Lang, A. and Wagner, G.A. (1995). Optical- and infrared-stimulated luminescence dating of late glacial and Holocene sediments. International Union for Quaternary Research (INQUA), XIV International Congress, Abstracts, Berlin, p. 153.

Lundgren, L. (1986). Environmental geology. Prentice-Hall Ltd, London, 576pp.

Marais, G.F. (1981). Day of the Buffalo. G.F. Marais, Strand, 99pp.

Muller, A.M.M. (1978). Die beplanning van 'n optimale riviervloeimeetstasienetwerk vir Suid Afrika. MSc. thesis (unpubl.), University of Pretoria.

Noble, R.G. and Hemens, J. (1978). Inland water ecosystems in South Africa - a review of research needs. Report of the South African Natural Scientific Programme, v. 34, p. 1-150.

Nutalaya, P. (1989). Flooding and land subsidence in Asia. Episodes, v. 12, p. 239-248.

Partridge, T.C. (1993a). Warming phases in southern Africa during the last 150,000 years: an overview. Palaeogeography, Palaeoclimatology, Palaeoecology, v. 101, p. 237-244.

_____ (1993b). The evidence for Cainozoic aridification in southern Africa. Quaternary International, v. 17, p. 105-110.

Partridge, T.C. and Brink, A.B.A. (1967). Gravels and terraces of the lower Vaal river basin. South African Geographical Journal, v. 49, p. 21-38.

Partridge, T.C., Avery, D.M., Botha, G.A., Brink, J.S., Deacon, J., Herbert, R.S., M aud, R.R., Scholtz, A., Scott, L., Talma, A.S. and Vogel, J.C. (1990). Late Pleistocene and Holocene climatic change in Southern Africa. South African Journal of Science, v. 86, p. 302-306.

Perry, J. (1988). Basic physical geography/hydro data for 'estuaries' of the western Cape (CW 1-32). Data Report, N.R.I.O..,C.S.I.R.,D8802, p. 1-6.

Pettijohn, F.J. (1975). Sedimentray rocks (third edition). Harper & Row, Publishers, New York, 628pp.

Pettijohn, F.J., Potter, P.E., Siever, R. (1987). Sand and sandstone (second edition). Springer-Verlag, New York, 553pp.

Platt, R.H. (1979). Options to improve federal non-structural response to floods. U.S. Water Resources Council, Washington, D.C., 102pp.

Prieska Geological Map (in press). 1:250 000 scale Prieska geological map published by the Geological Survey of South Africa.

Reck, K.W. (1994). Tracks and trails of the Richtersveld. K.W. Reck, 53pp.

Shah, B.V. (1983). Natural disaster reduction: how meteorological services can help. World Meteorological Organization, no. 722.

Smith, A.M. (1991). Extreme palaeofloods: their climatic significance and the chances of floods of similar magnitude recurring. South African Journal of Science, v. 87, p. 219-220.

_____ (1992a). Palaeoflood hydrology of the lower Umgeni River from a reach south of the Inanda Dam, Natal. South African Geographical Journal, v. 74, p. 63-68.

_____ (1992b). Holocene palaeoclimatic trends from palaeoflood analysis. Palaeogeography, Palaeoclimatology, Palaeoecology (Global and Planetary Change Section), v. 97, p. 235-240.

Smith, A.M. and Zawada, P.K. (1990). Palaeoflood hydrology: a tool for South Africa? - An example from the Crocodile River near Brits, Transvaal, South Africa. Water SA, v. 16, p. 195-200.

Smith, G.A. (1993). Missoula flood dynamics and magnitudes inferred from sedimentology of slack-water deposits on the Columbia Plateau, Washington. Geol. Soc. Amer. Bull., v. 105, p. 77-100.

Snell, E.F.A. (1990). Control of development along water courses towards the development of a national flood plain policy. *In* Course on practical flood risk analysis. University of Pretoria.

Stedinger, J.R. and Baker, V.R. (1987). Surface water hydrology: historical and paleoflood information. Reviews of Geophysics, v. 25, p. 119-124.

Stuiver, M. and Pearson, G.W. (1993). High-precision bidecadal calibration of the radiocarbon time scale, AD 1950-500 BC and 2500-6000 BC. Radiocarbon, v. 35, p. 1-23.

Talma, A.S. and Vogel, J.C. (1992). Late Quaternary paleotemperatures derived from a speleothem from Cango Caves, Cape Province, South Africa. Quaternary Research, v. 37, p. 203-213.

Tankard, A.J., Jackson, M.P.A., Eriksson, K.A., Hobday, D.K., Hunter, D.R. and Minter, W.E.L. (1982). Crustal evolution of southern Africa - 3.8 billion years of earth history. Springer-Verlag, New York, 523pp.

Tyson, P.D. (1993). Recent developments in the modelling of the future climate of southern Africa. South African Journal of Science, v. 89, p. 494-505.

_____ (1993a). Recent developments in modelling climatic change in Southern Africa. Thirtieth Raymond Dart Memorial Lecture, Witwatersrand University Press, 33pp.

Tyson, P.D. and Lindesay, J.A. (1992). The climate of the last 2000 years in southern Africa. The Holocene, v. 2, p. 271-278.

U.S. Water Resources Council. (1976). Guidelines for determining the flood flow frequency. Hydrology Committee, Bull. 17, 134pp.

Van Bladeren, D. (1995). Documentation of historical floods in South Africa. Department of Water Affairs and Forestry Technical Report No., TR 152.

Van Heerden, J. (1990). Flood producing rainfall events. *In* Course on practical flood risk analysis. University of Pretoria.

Van Wyk, N.J., Keuris, H. and Du Plessis, D.B. (1990). Flood peak measurement in South Africa. *In* Course on practical flood risk analysis. University of Pretoria.

Van Wyk, J.P. and Pienaar, L.F. (1986). Diamondiferous gravels of the lower Orange River, Namaqualand. *In* Mineral deposits of Southern Africa. Vols I & II. Eds C.R. Anhaeusser and S. Maske. Geol. Soc. S. Afr., Johannesburg, p. 2 309-2 321.

Water Science and Technology Board (1988). Estimating probabilities of extreme floods. Methods and recommended research. Committee on techniques for estimating probabilities of extreme floods. National Research Council. National Academy Press, Washington, D.C., 141pp.

_____ (1958). The evolution of the Orange River basin: some outstanding problems. South African Geographical Journal, v. 40, p. 3-30.

Zawada, P.K. (1991). Palaeofloods and the climatic record. South African Journal of Science, v. 87, p. 362.

Zawada, P.K. and Hattingh, J. (1993). Reconnaissance study of palaeoflood sites of South Africa. 1993 progress report for the Water Research Commission in connection with research on the palaeoflood hydrological analysis for selected South African Rivers, 197pp.

_____ (1994). Studies on the palaeoflood hydrology of South African Rivers. South African Journal of Science, v. 90, p. 567-568.

Zawada, P.K. and Smith, A.M. (1991). The 1988 Orange River flood, Upington region, northwestern Cape Province, RSA. Terra Nova, v. 3, p. 317-324.

APPENDIX A

1. PALAEOFLOOD AND SYSTEMATIC FLOW-GAUGE RECORD DATA USED IN THE FLOOD-FREQUENCY ANALYSIS OF THE LOWER ORANGE RIVER.

2. STATISTICAL CHARACTERISTICS AND PROPERTIES OF THE FLOOD-FREQUENCY ANALYSIS OF THE LOWER ORANGE RIVER

PALAEOFLOOD AND SYSTEMATIC FLOW-GAUGE DATA USED IN THE FLOOD-FREQUENCY ANALYSIS OF THE LOWER ORANGE RIVER.

VIOOLSDRIFT (DWAF gauge station number D8H003) Latitude: 28°45'39",Longitude: 17°43'49",Catchment area: 850 530 km²/s			
Hydrological year	**Q (m³/s)**	**Date**	**Notes**
	10 190	Post 3500 B.C.	Palaeoflood data from lower Xobies and Bloeddrift.
	12 150	Post 3500 B.C.	
	12 220	Post 3500 B.C.	
	12 930	circa 3500 B.C.	
	13 130	2540 B.C.	
	13 850	961 A.D.	
	14 480	1260 A.D.	
	14 660	1340 A.D.	
	27 870	1453 A.D.	
1933/34	8 009	--/01/1934	
1934/35			
1935/36	1 604	05/06/1936	Open 01/11/1935
1936/37	5 445	28/11/1936	GH(25/02/1937)=3.944m & Q=5346m³/s
1937/38	3 067	24/02/1938	
1938/39			No record
1939/40	1 729	20/11/1939	
1940/41	3 121	04/02/1941	
1941/42	3 717	13/03/1972	
1942/43	3 396	20/05/1943	
1943/44	5 108	21/02/1944	
1944/45	2 328	15/03/1945	
1945/46	1 238	11/04/1946	
1946/47	793	19/02/1947	
1947/48	5 071	26/03/1948	
1948/49	309	21/03/1949	
1949/50	2 406	17/04/1950	
1950/51	2 271	09/01/1951	
1951/52	1 651	04/11/1951	
1952/53	1 336	06/03/1953	
1953/54	2 102	02/04/1954	
1954/55	5 371	15/02/1955	
1955/56	2 214	06/03/1956	
1956/57	2 585	04/01/1957	
1957/58	6 318	10/10/1957	
1958/59	3 013	18/11/1958	
1959/60	887	15/12/1959	
1960/61	2 102	04/04/1961	
1961/62	4 447	06/12/1961	
1962/63	3 697	01/02/1963	
1963/64	1 156	25/11/1963	
1964/65	1 826	26/10/1964	
1965/66	3 471	28/01/1966	
1966/67	6 027	08/02/1967	
1967/68	531	27/05/1968	
1968/69	1 423	18/03/1969	

VIOOLSDRIFT (DWAF gauge station number D8H003) Latitude: 28°45'39",Longitude: 17°43'49",Catchment area: 850 530 km²/s			
Hydrological year	**Q (m^3/s)**	**Date**	**Notes**
1969/70	659	06/11/1969	
1970/71	204	30/10/1970	
1971/72	1 958	01/04/1972	
1972/73	292	25/11/1972	
1973/74	8 331	09/03/1974	
1974/75	1 438	08/02/1975	
1975/76	2 465	22/02/1976	Gap March
1976/77	1 183	14/02/1977	
1977/78	887	07/02/1978	
1978/79	269	11/11/1978	
1979/80	178	28/06/1980	
1980/81	269	20/04/1981	
1981/82	239	21/05/1982	
1982/83	491	08/04/1983	
1983/84	197	29/10/1983	
1984/85	141	12/11/1984	
1985/86	211	18/02/1986	
1986/87	232	04/12/1986	
1987/88	7 705	01/03/1988	
1988/89	1 826	24/02/1989	
1989/90	277	28/12/1989	
1990/91	670	27/03/1991	
1991/92	333	04/11/1991	
1992/93	51	27/02/1993	

PALAEOFLOOD AND SYSTEMATIC FLOW-GAUGE DATA USED IN THE FLOOD-FREQUENCY ANALYSIS OF THE LOWER ORANGE RIVER (CONTINUED).

FLOOD-FREQUENCY ANALYSIS OF LOWER ORANGE RIVER BASED ON VIOOLSDRIFT SYSTEMATIC RECORD (1933 - 1992)

High threshold		8 331 m³/s
GAUGED PERIOD		
Record length (years)		57
Peaks greater than or equal to high threshold		1
Peaks between thresholds excluding missing data		56
Non-zero peaks below low threshold		0
Zero flows		0
Missing data		0
ADDITIONAL HISTORICAL RECORDS		
Additional record length		0
Peaks greater than or equal to high threshold		0
Missing data		0
TOTALS USED IN THIS ANALYSIS		
Total time span	YT =	57
Observed peaks greater than or equal to high threshold	NA =	1
Observed peaks between thresholds	NB =	56
Censored data (missing, low and zero flows)	NC =	0
(Note: YT = NA + NB + NC)		
Observed flows below threshold including zero flows	LW =	0
Zero flows	ZR =	0

Calculations based on this station's moments only:

Period of gauged observations	57
Plus historical highs	0
Excluded low outliers	0
Excluded zero flows	0
Excluded missing flows	0
Balance used in this analysis	57

Statistical properties: natural data (m³/s):

Median annual peak	1826
Mean annual peak	2283
Standard deviation	2044
Coefficient of variation	0,90
Skewness coefficient	1,09

Statistical properties: log 10 transformed data:

Mean annual peak	3,132 (1356 m³/s)
Standard deviation	0,503
Coefficient of variation	0,161
Skewness coefficient	-0,429

EV parameters:

	EV1/MM	LEV1/MM	GEV/MM	GEV/PWM
a	0,70	0,13	0,72	0,61
u	0,60	0,93	0,58	0,57
k			0,01	-0,11

WAK/PWM parameters:

m = 0,000 a = 0,000 b = 0,000 c = 0,000 d = 0,000

Single station historically adjusted LP3/MM parameters:

Weight	Mean	Std. Dev	Skew
1,000	3,132	0,503	-0,429

ESTIMATED MAXIMA BASED ON THIS STATION'S MOMENTS ONLY

UNTRANSFORMED DATA

Return period	EV1/MM	GEV/MM	GEV/PWM	WAK/PWM
2	1947	1954	1829	0
10	4950	5017	4870	0
20	6097	6172	6211	0
50	7583	7655	8114	0
100	8696	8756	9674	0
200	9805	9846	11354	0
500	11268	11272	13779	0
1000	12373	12341	15783	0
10000	16044	15836	23659	0

LOG-TRANSFORMED DATA

Return period	LN/MM	LP3/MM	LEV1/MM
2	1356	1473	1121
10	5977	5618	6150
20	9071	7842	11784
50	14588	11142	27348
100	20180	13885	51394
200	26962	16845	96360
500	38171	21029	220827
1000	48688	24417	413281
10000	101039	36636	3310579

FLOOD-FREQUENCY ANALYSIS OF LOWER ORANGE RIVER BASED ON VIOOLSDRIFT SYSTEMATIC RECORD (1933 - 1992) AND PALAEOFLOOD DISCHARGE FOR F9 (3491 B.C.- 1992)

High threshold 8 331 m^3/s

GAUGED PERIOD

Record length (years)	57
Peaks greater than or equal to high threshold	1
Peaks between thresholds excluding missing data	56
Non-zero peaks below low threshold	0
Zero flows	0
Missing data	0

ADDITIONAL HISTORICAL RECORDS

Additional record length	5483
Peaks greater than or equal to high threshold	1
Missing data	5482

TOTALS USED IN THIS ANALYSIS

Total time span	YT =	5540
Observed peaks greater than or equal to high threshold	NA =	2
Observed peaks between thresholds	NB =	56
Censored data (missing, low and zero flows)	NC =	5482
(Note: YT = NA + NB + NC)		
Observed flows below threshold including zero flows	LW =	0
Zero flows	ZR =	0

Calculations based on this station's moments only:

Period of gauged observations	57
Plus historical highs	1
Excluded low outliers	0
Excluded zero flows	0
Excluded missing flows	0
Balance used in this analysis	58

Statistical properties: natural data (m^3/s):

Median annual peak	1826
Mean annual peak	2181
Standard deviation	1908
Coefficient of variation	0,88
Skewness coefficient	1,33

Statistical properties: log 10 transformed data:

Mean annual peak	3,119 (1314 m^3/s)
Standard deviation	0,492
Coefficient of variation	0,158
Skewness coefficient	-0,428

EV parameters:

	EV1/MM	LEV1/MM	GEV/MM	GEV/PWM
a	0,68	0,12	0,67	0,50
u	0,61	0,93	0,62	0,45
k			-0,02	-0,34

WAK/PWM parameters:

m = 0,000 a = 0,000 b = 0,000 c = 0,000 d = 0,000

Single station historically adjusted LP3/MM parameters:

Weight	Mean	Std. Dev	Skew
98,893	3,119	0,492	-0,428

ESTIMATED MAXIMA BASED ON THIS STATION'S MOMENTS ONLY

UNTRANSFORMED DATA

Return period	EV1/MM	GEV/MM	GEV/PWM	WAK/PWM
2	1867	1839	1416	0
10	4670	4666	4720	0
20	5741	5782	6668	0
50	7127	7255	10026	0
100	8165	8382	13351	0
200	9200	9524	17563	0
500	10566	11060	24913	0
1000	11598	12245	32233	0
10000	15023	16325	73931	0

LOG-TRANSFORMED DATA

Return period	LN/MM	LP3/MM	LEV1/MM
2	1314	1425	1091
10	5607	5278	5766
20	8433	7317	10894
50	13423	10319	24822
100	18438	12800	46010
200	24478	15467	85093
500	34394	19222	191518
1000	43639	22251	353571
10000	891339	33113	2706844

FLOOD-FREQUENCY ANALYSIS OF LOWER ORANGE RIVER BASED ON VIOOLSDRIFT SYSTEMATICRECORD (1933 - 1992) AND 9 PALAEOFLOODDISCHARGESFOR F1 - F9 (3491 B.C. - 1992)

High threshold 8 331 m^3/s

GAUGED PERIOD

Record length (years)	57
Peaks greater than or equal to high threshold	1
Peaks between thresholds excluding missing data	56
Non-zero peaks below low threshold	0
Zero flows	0
Missing data	0

ADDITIONAL HISTORICAL RECORDS

Additional record length	5483
Peaks greater than or equal to high threshold	9
Missing data	5474

TOTALS USED IN THIS ANALYSIS

Total time span	YT = 5540
Observed peaks greater than or equal to high threshold	NA = 10
Observed peaks between thresholds	NB = 56
Censored data (missing, low and zero flows)	NC = 5474
(Note: YT = NA + NB + NC)	
Observed flows below threshold including zero flows	LW = 0
Zero flows	ZR = 0

Calculations based on this station's moments only:

Period of gauged observations	57
Plus historical highs	9
Excluded low outliers	0
Excluded zero flows	0
Excluded missing flows	0
Balance used in this analysis	66

Statistical properties: natural data (m^3/s):

Median annual peak	2214
Mean annual peak	2182
Standard deviation	1900
Coefficient of variation	0,87
Skewness coefficient	1,05

Statistical properties: log 10 transformed data:

Mean annual peak	3,118 (1313 m^3/s)
Standard deviation	0,493
Coefficient of variation	0,158
Skewness coefficient	-0,426

EV parameters:

	EV1/MM	LEV1/MM	GEV/MM	GEV/PWM
a	0,68	0,12	0,71	0,68
u	0,61	0,93	0,59	0,65
k			0,02	0,07

WAK/PWM parameters:

m = 0,000 a = 0,000 b = 0,000 c = 0,000 d = 0,000

Single station historically adjusted LP3/MM parameters:

Weight	Mean	Std. Dev	Skew
98,750	3,118	0,493	-0,426

ESTIMATED MAXIMA BASED ON THIS STATION'S MOMENTS ONLY

UNTRANSFORMED DATA

Return period	EV1/MM	GEV/MM	GEV/PWM	WAK/PWM
2	1870	1887	1953	0
10	4661	4724	4534	0
20	5728	5780	5440	0
50	7108	7124	6550	0
100	8143	8116	7338	0
200	9174	9090	8089	0
500	10534	10354	9029	0
1000	11561	11294	9702	0
10000	14974	14323	11732	0

LOG-TRANSFORMED DATA

Return period	LN/MM	LP3/MM	LEV1/MM
2	1313	1424	1090
10	5616	5288	5775
20	8451	7337	10921
50	13461	10359	24915
100	18499	12859	46226
200	24570	15550	85571
500	34540	19341	192827
1000	43840	22403	356316
10000	89639	33405	2736183

APPENDIX B

XRD RESULTS OF PALAEOFLOOD-DEPOSITED SLACK-WATER SEDIMENTS FOR THE ORANGE RIVER

Sample no:	Site name	Region	Bed unit no:	Flood unit no:	MINERALOGICALCOMPOSITION (%)										Comments
					Smectite	Illite	Kaolinite	Quartz	Plagioclase	Microcline	Calcite	Goethite	Hematite	Magnetite	
PKZ.103	Bloeddrift	Richtersveld	F	F6	13	5	0	57	24	0	0	0	0	0	Top of flood unit F6
PKZ.104	Bloeddrift	Richtersveld	F	F6	14	5	3	59	19	0	0	0	0	0	Base of flood unit F6
PKZ.102	Bloeddrift	Richtersveld	E	F6	13	6	0	61	20	0	0	0	0	0	Base of flood unit F6
PKZ.101	Bloeddrift	Richtersveld	C	F5	23	8	0	51	19	0	0	0	0	0	
PKZ.100	Bloeddrift	Richtersveld	A	F4	8	4	0	68	20	0	0	0	0	0	
PKZ.110	L. Xobies	Richtersveld	P	F9	16	5	0	58	21	0	0	0	0	0	Base of flood unit F9
PKZ.200	L. Xobies	Richtersveld	P	F9	11	7	5	48	29	0	0	0	0	0	Top of flood unit F9 (close to pinch-out position)
PKZ.111	L. Xobies	Richtersveld	N	F7	19	6	4	54	17	0	0	0	0	0	
PKZ.112	L. Xobies	Richtersveld	I	F6	29	6	5	41	18	0	0	0	0	0	
PKZ.113	L. Xobies	Richtersveld	G	F4	27	4	0	48	21	0	0	0	0	0	
PKZ.114	L. Xobies	Richtersveld	C	F2	25	5	0	49	22	0	0	0	0	0	
PKZ.115	L. Xobies	Richtersveld	A	F1	38	6	4	38	14	0	0	0	0	0	
PKZ.011	Site 9 sec 2	Prieska	U2	F6(U)	8	1	0	70	21	0	0	0	0	0	Top of flood unit F6
PKZ.010	Site 9 sec 2	Prieska	T	F6(U)	19	0	0	59	22	0	0	0	0	0	Top of flood unit F6
PKZ.009	Site 9 sec 2	Prieska	R	F6(L)	16	3	0	61	20	0	0	0	0	0	Base of flood unit F6
PKZ.008	Site 9 sec 2	Prieska	P	F6(L)	25	0	0	54	21	0	0	0	0	0	Base of flood unit F6
PKZ.007	Site 9 sec 2	Prieska	N	F5	35	0	0	41	24	0	0	0	0	0	
PKZ.006	Site 9 sec 2	Prieska	L		14	3	0	65	10	8	0	0	0	0	Coarser grained, non-palaeoflood deposited
PKZ.005	Site 9 sec 2	Prieska	J	F4	34	0	0	46	19	0	0	0	0	0	
PKZ.004	Site 9 sec 2	Prieska	G	F3	27	0	0	47	26	0	0	0	0	0	
PKZ.003	Site 9 sec 2	Prieska	E		14	4	0	70	10	2	0	0	0	0	Coarser grained, non-palaeoflood deposited
PKZ.002	Site 9 sec 2	Prieska	D	F2	32	0	0	47	21	0	0	0	0	0	
PKZ.001	Site 9 sec 2	Prieska	B	F1	33	0	0	47	20	0	0	0	0	0	
PKZ.012	Site 9 sec 1	Prieska	B	F7	19	0	0	62	20	0	0	0	0	0	Composite sample from flood unit F7
PKZ.031	Site 14 sec 1	Prieska	Z	F7	5	3	0	80	12	0	0	0	0	0	
PKZ.030	Site 14 sec 1	Prieska	Q	F5	16	2	0	63	19	0	0	0	0	0	
PKZ.029	Site 14 sec 1	Prieska	O	F4	9	4	0	75	13	0	0	0	0	0	
PKZ.028	Site 14 sec 1	Prieska	M	F3	5	2	0	85	8	0	0	0	0	0	Sampled from a coarser grained bed of flood unit F3
PKZ.027	Site 14 sec 1	Prieska	I	F2	5	0	0	74	21	0	0	0	0	0	
PKZ.026	Site 14 sec 1	Prieska	D	F1	2	0	0	89	9	0	0	0	0	0	
PKZ.025	Site 14 sec 2	Prieska	L	F2	4	2	0	80	14	0	0	0	0	0	Middle portion of flood unit F2
PKZ.024	Site 14 sec 2	Prieska	G	F2	7	3	0	71	19	0	0	0	0	0	Bottom of flood unit F2

Sample no:	Site name	Region	Bed unit no:	Flood unit no:	MINERALOGICALCOMPOSITION (%)										Comments
					Smectite	Illite	Kaolinite	Quartz	Plagioclase	Microcline	Calcite	Goethite	Hematite	Magnetite	
PKZ.023	Site 14 sec 2	Prieska	B	F1	14	3	0	56	26	0	0	0	0	0	Top of flood unit F1
PKZ.022	Site 14 sec 2	Prieska	A	F1	13	4	0	71	13	0	0	0	0	0	Bottom of flood unit F1
PKZ.020	Site 19	Prieska	L2	F5	28	0	0	53	18	0	0	0	0	0	
PKZ.021	Site 19	Prieska	L1	F4	27	0	0	39	34	0	0	0	0	0	
PKZ.019	Site 19	Prieska	J	F3	24	2	0	48	21	5	0	0	0	0	Unit has been partially reworked
PKZ.017	Site 19	Prieska	G		0	3	0	57	6	8	0	6	11	10	Coarser grained reddish brown non-palaeoflood unit
PKZ.015	Site 19	Prieska	E		8	2	1	78	10	0	0	0	0	0	Coarser grained reddish brown non-palaeoflood unit
PKZ.014	Site 19	Prieska	C	F1	15	1	2	61	13	0	9	0	0	0	Unit has been partially reworked
PKZ.013	Site 19	Prieska	B		5	0	3	85	7	0	0	0	0	0	Coarser grained reddish brown non-palaeoflood unit

APPENDIX C

PUBLICATIONS AND REPORTS RESULTING FROM THIS STUDY

(1) Hattingh, P.K. and Zawada, P.K. (1995). Palaeoflood hydrology of the Gamtoos and Sundays Rivers in the Eastern Cape. Southern African Society for Quaternary Research (SASQUA), XII Biennial Conference, Abstracts, p. 14.

(2) Hattingh, J. and Zawada, P.K. (in press). Relief peels in the study of palaeoflood slack-water sediments. Geomorphology.

(3) Zawada, P.K. (1995). Palaeoflood hydrology of South African Rivers: evidence for Holocene catastrophic flooding in the lower Orange River valley. International Union for Quaternary research (INQUA), XIV International Congress, Abstracts, Berlin, p. 310.

(4) Zawada, P.K. (1995). Evidence for Holocene catastrophic flooding in the lower Orange River valley. Southern African Society for Quaternary Research (SASQUA), XII Biennial Conference, Abstracts, p. 14.

(5) Zawada, P.K. (1995). How big can an orange river flood be? The geological evidence and its palaeoclimatic implications. Joburg/Geotalks Series, Wits University.

(6) Zawada, P.K. Palaeoflood hydrology of selected South African Rivers. PhD thesis, University of Port Elizabeth. (Submitted for examination).

(7) Zawada, P.K. and Hattingh, J. (1993). Reconnaissance study of palaeoflood sites of South Africa. 1993 progress report for the Water Research Commission in connection with research on the palaeoflood hydrological analysis for selected South African Rivers, 197pp.

(8) Zawada, P.K. and Hattingh, J. (1994). Studies on the palaeoflood hydrology of South African Rivers. South African Journal of Science, v. 90, p. 567-568.

(9) Zawada, P.K. and Hattingh, J. (1994) Progress report for the period January - December 1994 for the Water Research Commission project: Palaeoflood hydrological analysis of selected South African Rivers. WRC report, 22pp.

APPENDIX D

METHODOLOGY USED IN THE IRSL AND TL DATING OF THE PRIESKA AND RICHTERSVELD SLACK-WATER SEDIMENTS

By

J.C. Vogel
(QUADRU, CSIR, PO Box 395, Pretoria 0001)

1. LUMINESCENCE DATING OF FLOOD DEPOSITS OF THE ORANGE RIVER IN THE PRIESKA AREA

The ages of seven sediment samples from terraces along the Orange River in the Prieska area were determined using both the thermoluminescence (TL) technique and the Infra Red Stimulated Luminescence (IRSL) technique.

The analyses were performed on coarse fractions (75-150μ or 15-300μ). The material was leached with concentrated hydrochloric acid and separated into size fractions by dry sieving. The selected fraction was then passed through a magnetic separator to remove heavy minerals.

The total environmental radiation doses (ED) were determined by the regeneration technique after bleaching in the sun and regenerating the signal by gamma radiation from a cobalt source. All samples were pre-heated at 150° for 16 hours before measurement.

The radioactive dose rates were calculated from the potassium contents and thick source alpha particle measurements on crushed raw material.

The results of both the TL and the IRSL analyses are given in Tables 1 and 2. The TL dates are consistently about double the ages obtained by the IRSL method. This can be explained by assuming that the grains of these flood deposits were not exposed to sunlight for long enough immediately before deposition. To effectively destroy any previously accumulated TL signal, the grains need to be exposed to full sunlight for several days, while the IRSL signal is removed within minutes of exposure. The TL dates thus do not actually date the floods, while the IRSL ages can be expected to give a more accurate estimate of these events.

Sample	ED (Gy)	K%	α activity (dpm/g)	Dose rate (αGy/a)	TL age (a)
5245 IRSL.PKZ 2	13,05	0,86	2,24±0,18	2166	6030
5248 IRSL.PKZ 1	29,38	0;80	1,29±0,23	1650	17800
5249 IRSL.PKZ 3	21,46	0,82	1,26±0,12	1655	12900
5246 IRSL.PKZ 4	22,12	0,90	1,78±0,10	2021	10900
5250 IRSL.PKZ 6	41,19	0,77	1,76±0,09	1831	22500
5247 IRSL.PKZ 7	44,24	0,76	1,87±0,15	1872	23600

Table 1 - Results of the TL dating of Orange River terraces in the Prieska area (the error margin of these results is mainly due to the uncertainty in the constancy of the dose rate over time and is considered to be less than 20%).

Sample	ED (Gy)	K%	α activity (dpm/g)	Dose rate (αGy/a)	IRSL age (a)
5245 IRSL.PKZ 2	6,62	0,86	2,24±0,18	2396	2760
5248 IRSL.PKZ 1	11,68	0,80	1,29±0,23	1768	6610
5246 IRSL.PKZ 4	14,24	0,90	1,78±0,10	2251	6330
5212 IRSL.PKZ 5	12,08	1,49	1,69±0,10	2595	8400
5250 IRSL.PKZ 6	24,04	0,77	1,76±0,09	1950	12300
5247 IRSL.PKZ 7	24,73	0,76	1,87±0,15	1990	12400

Table 2 - Results of the IRSL dating of Orange River terraces in the Prieska area (the error margin of these results is mainly due to the uncertainty in the constancy of the dose rate over time and is considered to be less than 20%).

2. LUMINESCENCE DATING OF SILT DEPOSITS FROM THE LOWER ORANGE RIVER (RICHTERSVELD REGION)

The ages of ten silt samples from flood deposits along the lower Orange River were determined using the Infra Red Stimulated Luminescence (IRSL) of the fine grain fraction (4-11μ) of the silt.

The samples were leached with 3N hydrochloric acid before the 4-11μ fraction of the silts was separated by repeated suspension in 0,01N sodium oxalate. Finally, the cleaned fractions were treated with 30% hydrogen peroxide to remove organics.

The total environmental radiation dose (ED) was determined by using the single disc additive dose technique and in some cases, also the regenerative technique. All samples were preheated at 150° for 16 hours before measurement.

The radioactive dose rate was calculated from the potassium content and the thick source alpha particle measurement on crushed raw material.

The results are summarized in Table 3. The general correspondence of the ages obtained using the additive and regenerative dose techniques (A & R) adds credence to the results although they may be slightly old due to insufficient zeroing of the original luminescence signal during transport in the flood waters.

Sample	ED (Gy)	K%	α activity (dpm/g)	Dose rate (αGy/a)	IRSL* age (a)
5508 IRSL PKZ 100	6,56 6,78	1,93	2,29±0,12	3433±197	1910±310 (A) 1980±400 (R)
5345 IRSL PKZ 101	2,70	1,00	2,40±0,15	2602±187	1040±210 (A)
5346 IRSL PKZ 102	3,30	0,93	3,16±0,14	3010±234	1100±220 (A)
5347 IRSL PKZ 103	4,43	0,81	2,46±0,15	2466±188	1800±210 (A)
5509 IRSL PKZ 104	14,26 14,66	1,82	1,74±0,12	3274±187	4423±450 (A) 4546±500 (R)
5348 IRSL PKZ 105	3,36	0,93	3,18±0,17	3022±237	1110±180 (A)
5510 IRSL PKZ 106	13,56	1,92	2,20±0,08	3369±189	4020±480 (A)
5511 IRSL PKZ 107	11,88 12,07	1,64	2,02±0,10	2987±173	3980±400 (A) 4040±420 (R)
5349 IRSL PKZ 108	12,20 16,53	0,73	2,23±0,12	2238±170	5450±600 (A) 6500±940 (R)
5350 IRSL PKZ 110	11,92 11,01	1,98	1,93±0,13	3259±178	3660±420 (A) 4010±440 (R)

* (A) - Additive dose technique
(B) - Regenerative dose technique

Table 3 - Results of the IRSL dating of silt deposits in the lower Orange River (Richtersveld region).